Programa de Doctorado en Tecnologías Industriales y Materiales

Escuela de Doctorado de la Universitat Jaume I

Identification of proteomic biomarkers for the prediction of implant biological responses

Memoria presentada por Francisco J Romero Gavilán para optar al grado de doctor/a por la Universitat Jaume I

Author:

Francisco J Romero Gavilán

Directed by:

Dr. Julio Suay Antón

Dra. Isabel Goñi Echave

Castellón de la Plana, September 2018

Financiación recibida

Las distintas instituciones que han financiado las investigaciones desarrolladas en este trabajo se detallan a continuación:

- A la Universitat Jaume I por la beca predoctoral para la formación de personal investigador (PREDOC/2014/25), así como por las dos ayudas para realizar estancias temporales en otros centros de investigación (E-2016-31 y E-2017-21) y los proyectos de investigación (P11B2014-19 y UJI-B2017-37).

- Al Ministerio de Economía y Competitividad (MINECO) por la financiación concedida en los proyectos MAT2014-51918-C2-2-R y MAT2017-86043-R.

- Al País Vasco por su apoyo a través del proyecto IT611/56 y a la Universidad del País Vasco por el proyecto UFI11/56.

- Al Aveiro Institute of Materials – CICECO de la Universidad de Aveiro (Aveiro, Portugal), lugar en el que se realizó una estancia de investigación.

- Al Department of Biomaterials, University of Oslo (Oslo, Noruega), donde se realizó una estancia de investigación.

- A la empresa Ilerimplant S.L. por su apoyo a esta investigación.

A mi madre….

ACKNOWLEDGEMENTS

En primer lugar, me gustaría agradecer a mis directores de tesis, Isabel Goñi y Julio Suay la oportunidad de llevar a cabo esta tesis doctoral, así como la confianza y apoyo mostrado durante todo su desarrollo. Gracias por todo lo que me habéis enseñado durante estos años y por haberme acompañado durante este proceso de crecimiento personal y profesional.

A los coautores de las publicaciones que forman parte de esta tesis, me gustaría agradecerles el esfuerzo realizado en el desarrollo de las mismas, así como el haberme permitido realizar la tesis por compendio de artículos.

Del mismo modo, me gustaría dar las gracias a las personas que han sido parte del grupo de investigación PIMA durante estos años. He tenido la suerte de estar rodeado de grandes compañeros y haber contado con su apoyo y ayuda.

Así mismo, gracias a todos los compañeros con los que he tenido la oportunidad de compartir laboratorios y despacho, por vuestro apoyo y voluntad de ayudar: Sara, Irene, Montse, Javi, María José, Estefanía, Jenni, Adrià, Lourdes, Braulio, Ximo, Patricia, Aziz, Nuno…

En este sentido, gracias Sara por ser una gran maestra y amiga, por cuidarme y guiar mis primeros pasos en el mundo de la investigación. A ti Jenni, gracias por tu amistad y apoyo incondicional en los peores momentos, por escucharme y darme fuerzas para seguir adelante. Estefania, gracias por estar siempre ahí como una buena amiga, ha sido un placer procrastinar contigo. Nuno, a ti gracias por haber sido un buen compañero, esto no habría sido posible sin ti.

A Raquel Oliver y José Ortega os agradezco vuestra ayuda y vuestros consejos desde el primer instante que pisé los laboratorios del Área de Materiales. El saber que estabais ahí, dispuestos a ayudar en todo momento tiene un valor incalculable.

Agradezco a Jorge García, Raúl Izquierdo, José Gámez, Luis Cabedo su ayuda, tanto en docencia como en investigación, cada vez que los he necesitado.

Por otro lado, me gustaría agradecer la disposición mostrada por los técnicos del SCIC para ayudarme en la preparación y estudio de muestras.

En cuanto a las colaboraciones científicas realizadas con otros centros de investigación, me gustaría hacer un especial agradecimiento al Grupo de investigación en Ciencia de Polímeros de la Universidad del País Vasco. Gracias Bea, María e Iñaki, y en especial Mariló Gurruchaga e Isabel Goñi por vuestra ayuda, ha sido un placer trabajar con vosotros durante este tiempo.

Del mismo modo, me gustaría agradecer a la Plataforma de Proteómica del cicBIOGUNE su disposición a ayudar; Félix, Iñaki e Ibón, este trabajo no habría sido posible sin vosotros.

Gracias también a los miembros del Departamento de Medicina de la Universitat Jaume I, de modo especial a Ana Sánchez y Cristina Martínez, gracias por vuestra ayuda y vuestra paciencia con este ingeniero.

Relativamente aos estágios levados a cabo durante o trabalho experimental desenvolvido nestes últimos 3 anos, gostaria agradecer aos membros do Departamento de Engenharia de Materiais e Cerâmica e do CICECO da Universidade de Aveiro, em Portugal por terem-me recebido nas suas instalações. Muito obrigado ás professoras Maria Helena e Isabel pela oportunidade de pertencer ao vosso grupo, e obrigado José Carlos e Erika pela vossa disponibilidade e ajuda, assim como por tudo o que aprendi com voçês. Este estágio permitiu-me ganhar uma nova perspectiva acerca dos materiais sol-gel e suas múltiplas aplicações, e entender um pouco mais da sua lógica graças a uma "mente sol-gel" como a do José Carlos.

Regarding my temporary-stay carried out in Oslo, I would like thank to Professor Håvard to give me the opportunity to work in the Department of Biomaterials (Institute of Clinical Dentistry, University of Oslo, Norway). Despite the -17 ºC, I found a charming and multicultural lab environment. "Takk" Hanna, Hao, Florian, Liebert, Mousumi, Sonny, María, Aman, Anne, Elisabeth, Manu, Pawel, Saffiye, Aina, Catherine, Duarte, Javier and Alejandro for your hospitality and making me feel one more of your group. I learnt a lot about the QCM-D technique and its application in the biomaterial field, in this sense, thank Alejandro for your teachings. My stay in Oslo was a wonderful experience: Hao, Liebert, Fernanda thank you for sharing with me the Norwegian

experiences and dinners; Hanna, Florian, Aina, for showing me Norwegian traditions and special places and experiences in Oslo.

En el terreno más personal, quisiera agradecer a toda mi familia y amigos por el apoyo recibido. Habéis sido una pieza clave durante este proceso, siempre habéis estado ahí apoyándome y animándome para superar todos los retos a los que me he enfrentado. A pesar de haber estado ausente en algunas ocasiones, por las estancias y la falta de tiempo; siempre os he tenido en mente. Espero conseguir que os sintáis orgullosos.

ABSTRACT

Given the growing need in dental implantology field to develop new biomaterials with better and better properties, the production and characterization optimization is crucial. Thus, the poor correlation shown between *in vitro* testing and subsequent *in vivo* experimentation compromises the efficiency of this process, giving rise to the need to developing new *in vitro* methodologies that enable the prediction of biomaterial behaviour in a more efficient way.

After the material implantation in the organism, it comes into contact with tissues and body fluids such as blood, and this interaction results in the formation of a protein layer on its surface. This protein layer plays a key role in the biological processes triggered as a response to the implant presence in the body, leading to its success or failure.

Considering the important role of these proteins in the implantation outcome, this doctoral thesis focuses on the proteomic characterization of serum protein adsorption onto distinct biomaterials by the use of liquid chromatography-tandem mass spectrometry. Hence, biomaterials with different properties are systematically designed to control their biological response. These materials were characterized by proteomics, *in vitro* and *in vivo* assays. This information enabled the correlation between the movements detected in the protein patterns and the material biological response, obtaining biomarkers that could predict the *in vivo* response of new biomaterials.

This methodology has allowed to identify as biomarkers a cluster of proteins related to biocompatibility problems. This cluster could be associated with an acute immune reaction, which may suppose an excessive inflammatory response and provoke the implant failure. In parallel, the study of different materials with specific biological effects, positively associated with the implant osseointegration capacity, has allowed to identify movements in protein patterns linked to these biological responses. In this sense, a common affinity pattern has been detected for the proteins vitronectin and apolipoprotein E, which role on tissue regenerative processes is well-known and described in literature.

Therefore, the work presented in this doctoral thesis has allowed an improvement on the understanding of both biomaterial-protein and protein-tissue response interactions, as well as to

identify biomarkers associated with different biological responses, which could form the basis for the development of new *in vitro* methodologies based in proteomics.

RESUMEN

Dada la creciente necesidad en el campo de la implantologia dental de desarrollar nuevos biomateriales con cada vez mejores propiedades, resulta crucial la optimización de su producción y caracterización. Así, la poca correlación mostrada entre la caracterización *in vitro* y su posterior ensayo *in vivo* compromete la eficiencia de este proceso dando lugar a la necesidad de desarrollar nuevas metodologías *in vitro* que permitan predecir el comportamiento real de los biomateriales de un modo más eficaz.

Tras la implantación de un material en el cuerpo, éste entra en contacto con tejidos y fluidos corporales como la sangre, y esta interacción da lugar a la formación de una capa de proteínas en su superficie. Esta capa de proteínas desempeña un papel clave en los procesos biológicos que se desencadenan como respuesta a la presencia del implante, pudiendo llegar a disponer su éxito o fracaso.

De esta manera, considerando la importante función de estas proteínas en el resultado de la implantación, esta tesis doctoral se centra en la caracterización proteómica de la adsorción de proteínas séricas sobre distintos biomateriales mediante el uso de cromatografía liquida acoplada a espectrometría de masas en tándem. Así, biomateriales con distintas propiedades son sistemáticamente diseñados para controlar su respuesta biológica. Estos materiales son caracterizados mediante proteómica, ensayos *in vitro* e *in vivo*. Esta información hace posible la correlación entre los movimientos detectados en los patrones de proteínas y la respuesta biológica del material, obteniendo biomarcadores que podrían predecir la respuesta *in vivo* de futuros biomateriales.

Esta metodología ha permitido identificar como biomarcadores un clúster de proteínas que podrían estar asociadas a problemas de biocompatibilidad. Este clúster estaría relacionado con una reacción inmune aguda que podría suponer una excesiva respuesta inflamatoria, culminando en el fallo del implante. En paralelo, el estudio de distintos materiales con efectos biológicos específicos, asociados positivamente a la capacidad de osteointegración de un implante, ha permitido identificar movimientos en patrones de proteínas ligados a estas respuestas biológicas. En este

sentido, se ha detectado un patrón común de afinidad hacía las proteínas vitronectina y apolipoproteína E, cuyo papel clave en la regeneración tisular se encuentra descrito en la literatura.

Por tanto, el trabajo expuesto en esta tesis doctoral ha permitido mejorar la comprensión de las interacciones biomaterial-proteína y proteína-respuesta tisular, así como identificar biomarcadores asociados a distintas respuestas biológicas, que constituirían las bases para el desarrollo de nuevas metodologías *in vitro* basadas en proteómica.

RESUM

Donada la creixent necessitat en el camp de la implantologia dental de desenrotllar nous biomaterials amb cada vegada millors propietats, resulta crucial l'optimització de la seua producció i caracterització. Així, la poca correlació mostrada entre la caracterització *in vitro* i el seu posterior assaig *in vivo* compromet l'eficiència d'este procés donant lloc a la necessitat de desenrotllar noves metodologies *in vitro* que permeten predir el comportament real dels biomaterials d'una manera més eficaç.

Després de la implantació d'un material en el cos, este entra en contacte amb teixits i fluids corporals com la sang, i esta interacció dóna lloc a la formació d'una capa de proteïnes en la seua superfície. Esta capa de proteïnes exerceix un paper clau en els processos biològics que es desencadenen com a resposta a la presència de l'implant, podent arribar a disposar el seu èxit o fracàs. D'esta manera, considerant la important funció d'estes proteïnes en el resultat de la implantació, esta tesi doctoral es centra en la caracterització proteòmica de l'adsorció de proteïnes sèriques sobre distints biomaterials per mitjà de l'ús de cromatografia liquida acoblada a espectrometria de masses en tàndem. Així, biomaterials amb distintes propietats són sistemàticament dissenyats per a controlar la seua resposta biològica. Estos materials són caracteritzats per mitjà de proteòmica, assajos *in vitro* i *in vivo*. Esta informació fa possible la correlació entre els moviments detectats en els patrons de proteïnes i la resposta biològica del material, obtenint biomarcadors que podrien predir la resposta *in vivo* de futurs biomaterials.

Aquesta metodologia ha permès identificar com biomarcadors un clúster de proteïnes que podrien estar associades a problemes de biocompatibilitat. Aquest clúster estaria relacionat amb una reacció immune aguda que podria suposar una excessiva resposta inflamatòria, culminant en la fallada de l'implant. En paral·lel, l'estudi de distints materials amb efectes biològics específics, associats positivament a la capacitat d'osteointegració d'un implant, ha permès identificar moviments en patrons de proteïnes lligats a aquestes respostes biològiques. En aquest sentit, s'ha detectat un patró comú d'afinitat a les proteïnes vitronectina i apolipoproteïna E, estant descrit en la literatura el seu paper clau en la regeneració tissular.

Per tant, el treball exposat en esta tesi doctoral ha permès millorar la comprensió de les interaccions biomaterial-proteïna i proteïna-resposta tissular, així com identificar biomarcadors associats a distintes respostes biològiques, que constituirien les bases per al desenvolupament de noves metodologies *in vitro* basades en proteòmica.

Graphical Abstract

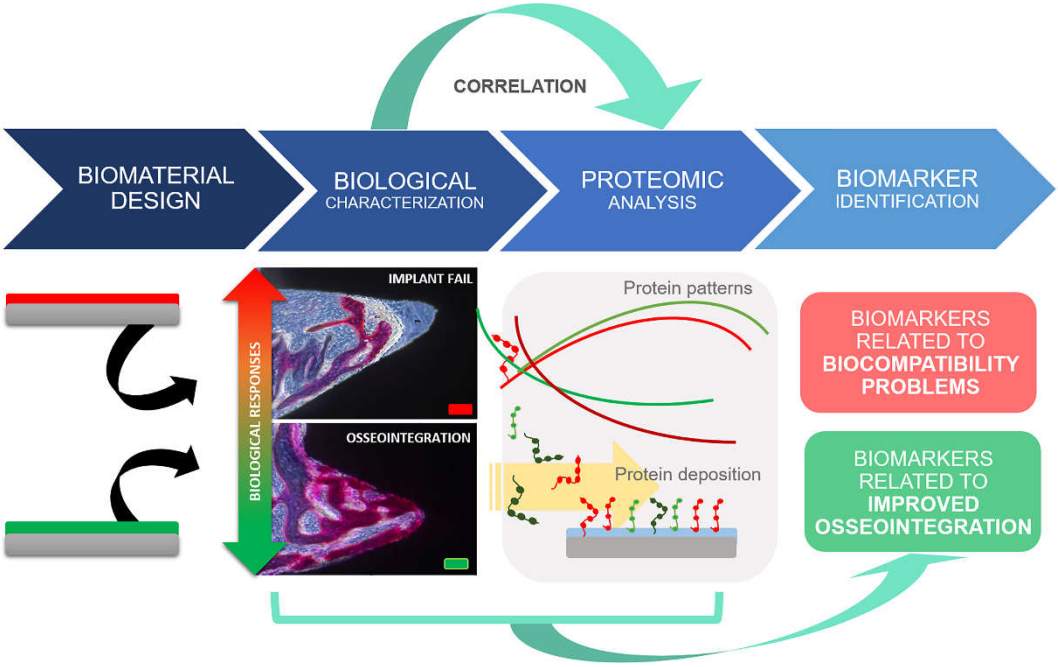

INDEX

Identification of proteomic biomarkers for the prediction of implant biological responses 1
ACKNOWLEDGEMENTS 7
ABSTRACT 11
RESUMEN 13
RESUM 15
Graphical Abstract 17
INDEX 19
1. INTRODUCTION 27
1.1. Motivation 29
1.2. Theoretical framework 35
1.2.1. Bone tissue 35
1.2.2. Bone regeneration around implants and osseointegration concept 36
1.2.3. Protein adsorption phenomena at biomaterials 39
1.2.4. Factors controlling protein adsorption 41
1.2.5. Protein layer composition – Biological implications 43
1.2.6. Coagulation system: proteomic point of view 44
1.2.7. Fibrinolytic system 46
1.2.8. Angiogenesis 48
1.2.9. Immune reaction: Complement system 49
1.2.10. Osteogenesis 51
1.2.11. Biomaterial protein layer characterization 53
1.2.12. Dental implants and its surface modification 56
1.2.13. Silica hybrid sol-gel coatings 56
1.2.14. Hybrids as delivery vehicles: Osteogenic role of Ca and Sr 58
1.3. Objectives 61
1.4. Research strategy 63
1.5. Statement of significance 67
REFERENCES 69

2. CHAPTER 1 87
Control of the degradation of silica sol-gel hybrid coatings for metal implants prepared by the triple combination of alkoxysilanes 87
ABSTRACT 91
Graphical abstract 93
2.1. Introduction 95
2.2. Materials and methods 97
2.2.1. Sol-gel synthesis 97
2.2.2. Coating preparation 97
2.2.3. Chemical characterization 98
2.2.4. Physico-chemical characterization 99
2.3. Results 100
2.3.1. Chemical characterization 100
2.3.2. Contact angle 102
2.3.3. Morphological characterization 103
2.3.4. EIS 105
2.3.5. Hydrolytic degradation 110
2.4. Discussion 112
2.5. Conclusions 114
ACKNOWLEDGEMENTS 114
REFERENCES 114
3. CHAPTER 2 119
Proteomic analysis of silica hybrid sol-gel coatings: a potential tool for predicting biocompatibility of implants *in vivo* 119
ABSTRACT 123
Graphical abstarct 125
3.1. Introduction 127
3.2. Materials and methods 128
3.2.1. Titanium discs 128
3.2.2. Sol-gel synthesis and sample preparation 129
3.2.3. Physicochemical characterisation of coated titanium discs 129
3.2.4. *In vitro* assays 130
3.2.4.1. Cell culture 130

3.2.4.2. Cytotoxicity 130
3.2.4.3. ALP activity 130
3.2.5. *In vivo* assay 131
3.2.5.1. *In vivo* experimentation 131
3.2.5.2. Histological quantification 132
3.2.6. Statistical analysis 132
3.2.7. Adsorbed protein layer 132
3.2.8. Proteomic analysis 133
3.3. Results 134
3.3.1. Synthesis and physicochemical characterisation 134
3.3.2. *In vitro* assays 136
3.3.3. *In vivo* assays 137
3.3.4. Proteomic analysis 139
3.4. Discussion 144
3.5. Conclusions 148
ACKNOWLEDGEMENTS 148
REFERENCES 149
4. CHAPTER 3 155
Proteome analysis of human serum proteins adsorbed onto different titanium surfaces used in dental implants 155
ABSTRACT 159
Graphical abstract 161
4.1. Introduction 163
4.2. Materials and methods 165
4.2.1. Surface disc preparation 165
4.2.2. Physico-chemical characterisation of titanium discs 165
4.2.3. *In vitro* assays 166
4.2.3.1. Cell culture 166
4.2.3.2. Cell proliferation 166
4.2.3.3. ALP activity 166
4.2.3.4. Total protein 167
4.2.4. Statistical analysis 167
4.2.5. Formation of the protein layer 167

4.2.6. Proteomic analysis 168
4.3. Results 169
4.3.1. Physico-chemical characterisation of Ti discs 169
4.3.2. *In vitro* cultures 172
4.3.3. Proteomic analysis 173
4.3.3.1. Identification of proteins adsorbed onto the SAE-Ti and smooth Ti 173
4.3.3.2. Gene ontology analysis of the identified proteins 175
4.3.3.3. Specifically enriched proteins 177
4.4. Discussion 178
4.5. Conclusions 181
ACKNOWLEDGEMENTS 181
REFERENCES 182
5. CHAPTER 4 191
Bioactive potential of silica coatings and its effect on the adhesion of proteins to titanium implant 191
ABSTRACT 195
Graphical abstract 197
5.1. Introduction 199
5.2. Materials and methods 200
5.2.1. Titanium discs 200
5.2.2. Sol-gel synthesis and sample preparation 200
5.2.3. Physico-chemical characterisation of coated titanium discs 201
5.2.4. *In vitro* assays 201
5.2.4.1. Cell culture 201
5.2.4.2. Cytotoxicity 202
5.2.4.3. Cell Proliferation 202
5.2.4.4. ALP activity 202
5.2.4.5. RNA isolation and cDNA synthesis 203
5.2.4.6. Quantitative Real-time PCR 203
5.2.5. Statistical analysis 204
5.2.6. *In vivo* experimentation 204
5.2.7. Adsorbed protein layer 205
5.2.8. Proteomic analysis 205

5.3. Results 206
5.3.1. Synthesis and physicochemical characterisation 206
5.3.2. *In vitro* assays 208
5.3.2.1. Cell cytotoxicity, proliferation and ALP activity 208
5.3.2.2. mRNA expression levels 208
5.3.3. *In vivo* experimentation 209
5.3.4. Proteomic analysis 211
5.4. Discussion 215
5.5. Conclusion 218
ACKNOWLEDGEMENTS 218
REFERENCES 219
6. CHAPTER 5 225
The effect of strontium incorporation into sol-gel biomaterials on their protein adsorption and cell interactions 225
ABSTRACT 229
Graphical abstract 231
6.1. Introduction 233
6.2. Materials and methods 235
6.2.1. Substrate 235
6.2.2. Sol-gel synthesis and coating preparation 235
6.2.3. Physico-chemical characterisation 236
6.2.4. *In vitro* Assays 236
6.2.4.1. Cell culture 236
6.2.4.2. RNA isolation and cDNA synthesis 237
6.2.4.3. Quantitative Real-time PCR 237
6.2.5. Adsorbed protein layer 238
6.2.6. Proteomic analysis 238
6.2.7. Statistical analysis 238
6.3. Results 239
6.3.1. Synthesis and physico-chemical characterisation 239
6.3.2. *In vitro* assay - mRNA expression levels 241
6.3.3. Proteomic analysis 242
6.4. Discussion 246

6.5. Conclusion 249
ACKNOWLEDGEMENTS 250
REFERENCES 250
7. CHAPTER 6 257
Proteomic analysis of calcium enriched sol-gel biomaterials 257
ABSTRACT 261
Graphical abstract 263
7.1. Introduction 265
7.2. Materials and methods 267
7.2.1. Substrate 267
7.2.2. Sol-gel synthesis and coating preparation 267
7.2.3. Physico-chemical characterisation 268
7.2.4. *In vitro* assays 269
7.2.4.1. Cell culture 269
7.2.4.2. RNA isolation and cDNA synthesis 269
7.2.4.3. Quantitative Real-time PCR 270
7.2.5. Adsorbed protein layer 270
7.2.6. Proteomic analysis 271
7.2.7. Statistical analysis 271
7.3. Results 271
7.3.1. Synthesis and physicochemical characterisation 271
7.3.2. *In vitro* assay - mRNA expression levels 273
7.3.3. Proteomic analysis 274
7.4. Discussion 281
7.5. Conclusion 285
ACKNOWLEDGEMENTS 286
REFERENCES 286
8. GENERAL DISCUSSION 291
9. CONCLUSIONS 299
10. FUTURE LINES OF RESEARCH 311
11. ANNEXES 317
11.1. List of publications 319
11.2. First page of the published articles presented as thesis results 321

Chapter 1 321
Chapter 2 322
Chapter 3 323
Chapter 4 324
11.3. Works presented at national and international conferences 325
11.4. List of abbreviations and acronyms..... 329
General 329
Protein abbreviations 331
11.5. List of figures 333
Introduction 333
Chapter 1 333
Chapter 2 334
Chapter 3 335
Chapter 4 336
Chapter 5 337
Chapter 6 338
11.6. List of tables 341
Introduction 341
Chapter 1 341
Chapter 2 341
Chapter 3 342
Chapter 4 342
Chapter 5 342
Chapter 6 343

1. INTRODUCTION

1. Introduction

1.1. **Motivation**

Our society is experiencing an aging process. According to the United Nations practically every country in the world is experiencing growth in the number and proportion of older persons in their population. In fact, Europe presents the highest percentage of population over 60 years of age. This ageing is considered to become one of the most important social transformation of twenty-first century, having wide impacts in nearly all sectors of society [1]. New challenges arise as a result of this problem.

In this sense, the Horizon 2020 program establishes as one of its strategic objectives to investigate the major issues affecting European citizens in terms of health, demographic change and wellbeing. One of the challenges to achieve is the active aging, that is, finding solutions that allow the aging population to lead active daily life for as long as possible [2].

The development of new biomaterials with better and better performance that allow to recover or substitute biological functions that have been lost in the body can improve human's quality of life, being that essential to support persons to be healthy and active, ensuring their wellbeing.

From a board point of view, a biomaterial is a material, which is set to interact with biological system in order to assess, increase, restore or heal altered tissues, organs or functions [3].

However, the biomaterial concept has evolved as its field of research has advanced, developing new systems and technologies. In 1987, the European Society of Biomaterials defined that a biomaterial was a material used in a medical device, intended to interact with biological systems [4]. Later, in 2009, Williams refined the biomaterial concept as ''a substance that has been engineered to take a form which, alone or as part of a complex system, is used to direct, by control of interactions with components of living systems, the course of any therapeutic or diagnostic procedure, in human or veterinary medicine" [5].

1. Introduction

Until now, several biomaterial generations have been developed, being the first materials for biomedical application used to replace lost and damage tissues. During this generation, the goal was achieving materials with an inert behaviour, avoiding carcinogenicity effects, toxicity, allergy and inflammatory reactions. Nevertheless, the advances in the field allowed the development of bioactive materials, designed to promote specific responses by the surrounding tissues, which constitute a second biomaterial generation. The third biomaterial generation are now created to promote an appropriate response for a given application, e.g. being able to stimulate the tissue regeneration [6].

One of the main biomaterial characteristics is its biocompatibility, property that has evolved in parallel to the biomaterial field development. By the 1970s, this concept was associated to toxicology, stablishing that a biomaterial must be no toxic and not does any harm to the biological system. In this line, biocompatibility was defined as the ability of a material to perform with an appropriate host response in a specific application [4]. Williams proposed a more accurate version of this definition, describing the biocompatibility as the biomaterial ability to perform its desired function with respect to a medical therapy, without eliciting any undesirable local or systemic effects in the recipient or beneficiary of that therapy, but generating the most appropriate beneficial cellular or tissue response in that specific situation, and optimizing the clinically relevant performance of that therapy [7]. However, in 2011, Ratner offered a new definition, considering that biocompatibility is the material ability to locally trigger and guide non-fibrotic wound healing, reconstruction and tissue integration; which differs from the term biotolerability, defined as the material ability to reside in the body for long periods of time with only low degrees of inflammatory reaction [8].

During the last years, technological advances have allowed a high level of development and selection of the most suitable biomaterials with specific biological responses for each application, promoted by the increasing necessity of these materials as consequence of population aging.

Specifically, this research arises within the existing need in dental field to improve the present implant systems for the replacement of missing tooth. Despite the good results obtained with the current titanium implants, with a reported percentage of failure varying from 3 % - 5 % for healthy persons and reaching up to 10 % for patients with risk factors [9], there is a continuous demand to

improve these figures and reduce the recovering times. This issue is especially relevant in risk patients with poor bone quality, either due to their age or systemic pathologies which impair bone metabolism (e.g. osteoporosis, diabetes). Consequently, the development of bioactive implants that favour the bone regeneration process and display better success rates results crucial. Taking in account that around 800.000 dental implants are placed in Spain, technological advances in this field can have a great impact on society. In fact, global dental implant market was valued at $3.4 billion in 2011, and is expected to be $6.6 billion in this 2018 [10].

Thus, great efforts are made in the design and development of new materials for its application in dental implantology. The development of these new biomaterials is based on a complex screening process in which after ensuring adequate physicochemical properties, the biological evaluation establishes their efficiency in the corresponding application. This iterative process allows the development of materials with better properties, each time more secure and with more precise functions. However, it needs a large investment of both time and money [11].

The biomaterial biological evaluation is carried out through its *in vitro, in vivo* and clinical studies. The international organization of standards details in ISO 10993 the steps to follow for the biological evaluation of a biomaterial. In this way, *in vitro* experimentation is used as an initial screening method to characterize the material biosecurity and biofunctionality. This characterization aims to test the cell viability, proliferation and differentiation potential of a certain cell line through its direct or indirect contact with the evaluated material [12]. *In vitro* studies indicate which materials would show a greater biological potential and then the materials with better *in vitro* performance would be tested in an *in vivo* model, observing their behaviour in a real biological system.

However, cell cultures are relatively simple compared to the complexity of living tissues. As a consequence, unfortunately, correlation problems are evidenced between the results obtained in the *in vitro* evaluation and the subsequent *in vivo*. In recent years, this traditional methodology has proved not to be efficient enough.

Despite the enormous effort that is being made to improve dental implants and the implementation of a large number of trials associated with this process, in a significant number of cases the final results are contradictory and a material that has shown excellent *in vitro* qualities

can result in a disastrous *in vivo* outcome. This low efficiency supposes a great wastage of the resources, both economic and time. Additionally, the scientific use of animals supposes ethical problems in society, detecting a growing social demand towards its reduction or even its total prohibition [13]. In fact, the European law that regulates animal experimentation according to directive 2010/63/EU establishes as a principle the *in vivo* tests substitution by *in vitro* experimentation or computer simulations whenever possible, aiming the use of animals in research reduction to the minimum [14].

This problem is shown more clearly when the type of material to be tested is intended for bone tissue regeneration, resulting from the special complexity of this system. These *in vitro* tests tend to focus on the ability of bone formation, forgetting other vital aspects in the bone healing process and remodelling that would occur *in vivo*, such as for example, the interaction of bone cells with cells associated to the immune system [15]. Hulsart-Billström *et al*. [16] evaluated the correlation between *in vitro* and *in vivo* results in a multi-center study involving 8 different universities and compared the results of 93 different materials, finding a surprisingly poor *in vitro-in vivo* correlation of 58 %. These data show the current *in vitro* test deficiencies and the need to develop new methodologies, which allow to test biomaterials with greater reliability and thus reduce the *in vivo* studies need. On the other hand, although *in vivo* tests are considered the "gold standard" to establish the real implant behaviour in the body, its use is limited by ethical issues and its high economic cost, in addition to the increasing social pressure to reduce the use of animals in this type of research [17]. Additionally, some authors also point out the *in vivo* experimentation limitations and the problems that it would be found in their subsequent correlation with clinical studies. This fact reinforces the need to develop new *in vitro* methodologies, which allow to obtain a greater knowledge of how a biomaterial will behave when it is implanted in the human body [18].

Then, these facts highlight the need to stablish new methodologies for the development of biomaterials based on new *in vitro* studies that allow a greater knowledge of how the material will behave in a living system and thus be able to face *in vivo* experimentation with greater safety and efficiency [19].

In this sense, different measures are being taken to try to solve these limitations of the traditional *in vitro* testing. Most are based on increasing the design complexity of existing *in vitro* cell cultures

with the aim of obtaining more representative systems that can reproduce the biological response of the human body to a biomaterial with greater accuracy. Proposals in this line of research are the development of co-cultures [15] and 3D cell cultures [20,21], which perform a more realistic biomechanical and biochemical environment.

Alternative approaches to this problem are based on carrying out further characterizations to biomaterials in order to acquire additional information. In this sense, many efforts are being made in understand the material-protein-cell interactions since the body's response to the biomaterials are determined largely by the extent and nature of the initial protein adsorption [22,23].

The study of protein-biomaterial interactions could improve the knowledge about the events which are triggered after implantation. This better comprehension of phenomena happening on this material-tissue interfaces can be helpful for future biomaterial designs.

Although great efforts are being made in the biomaterial field to understand the material interaction with proteins, in most cases the followed research lines are based on studies between a variety of materials and model monoprotein solutions (e.g. fibronectin, fibrinogen, albumin, immunoglobulin) or as much, mixtures of a small number of these proteins. These systems are too simplistic to reproduce the complex mechanisms on which the protein adsorption process onto surfaces is based, in which hundreds of these proteins participate.

1.2. **Theoretical framework**

1.2.1. Bone tissue

Aiming a better understanding about complex interactions between biomaterials in field of bone tissue regeneration and this biological system, a brief description of this organ is going to be exposed.

Bone is the major structural element of the skeleton, providing locomotor support and protection, but also a dynamic mineral and protein reservoir. Two phases, a mineral and another organic constitute this highly dynamic form of connective tissue. This hybrid composition gives bone rigidity, but at the same time mechanical strength and flexibility [24]. The inorganic part constitutes 60-70 % of this tissue, being formed by a set of inorganic mineral salts and ions such as phosphates, carbonates, Ca^{2+}, Mg^{2+} or F^{-1}, which are distributed in a hydroxyapatite nanocrystal matrix (Ca10(PO4)6(OH2)). On the another hand, the organic part is formed by collagen fibers, mainly type I (90 %), as well as other types of proteins such as growth factors, osteocalcin, osteopontin or bone morphogenetic proteins. Additionally, this tissue contains different types of cells such as pre-osteoblasts, osteoblasts and osteocytes, which are derived from the differentiation of mesenchymal cells, and osteoclasts which are polynucleated cells, derived from hematopoietic precursors supplied by the bone marrow and blood vessels [3]. Bone system is being continuously repaired and renewed, through a remodelling process based on a dynamic equilibrium of resorption and tissue formation, being osteoblasts and osteoclasts the main cells involved in this process as is exposed in Figure 1.1. Osteoclasts degrade the bone matrix in two-phase process: the hydrochloric acid secretion dissolves the mineral part, while proteolytic enzymes degrade the organic one. Osteoblasts are responsible for bone tissue formation, synthesizing collagen fibers and, subsequently, carrying out its mineralization based on the deposition of inorganic salts. During this process, the osteoblasts remain enclosed in the extracellular matrix, differentiating into osteocytes. These cells are responsible for detecting the effects of mechanical loads to which the system is subjected and, thus, regulate their homeostasis depending on their functional demand, allowing bone to maintain its correct architecture [15].

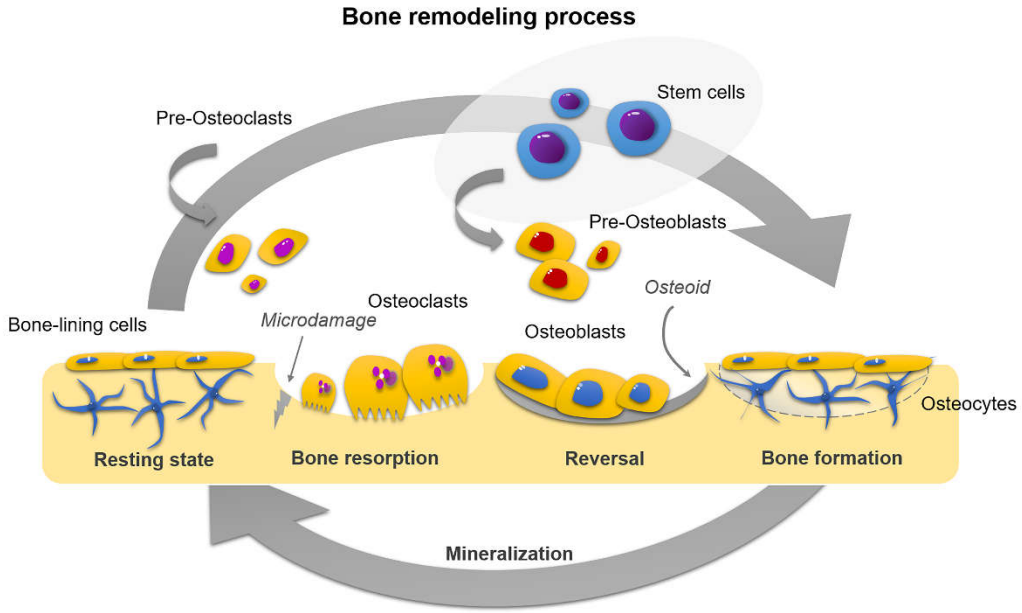

Figure 1.1. Bone remodelling process.

In addition, mainly two types of structures form bone: cortical and trabecular. The cortical tissue forms a homogeneous and compact structure, being composed of bone lamellae that can be arranged in a parallel or concentric way around channels, named Haversian Canals, through which blood vessels and nerves provide the necessary nutrients to cells. On the other hand, the trabecular bone has a spongy structure with lower density and greater surface area, as it is constituted by a network of interconnected bone segments, which generate large empty space, inside of which is the bone marrow [25].

1.2.2. Bone regeneration around implants and osseointegration concept

When a biomaterial is implanted in bone, such as a dental prosthesis, as a consequence of surgical intervention, different tissues and blood vessels are damaged. This trauma, together with the biomaterial presence, provoke multiple stimuli in the system, which give rise to a series of events with the aim of achieving the damaged tissue healing.

In dental implantology field, the success of this process is measured in terms of osseointegration, concept which was used for first time in 1985 by Brånemark to define the structural and functional intimate connection between ordered and live bone and the load-bearing implant [26]. Nevertheless, Brånemark subsequently modified his own definition, establishing that the implant osseointegration is a continuing structural and functional coexistence, possibly in a symbolic manner, between differentiated, adequately remodelling, biologic tissues and strictly defined and controlled synthetic components providing lasting specific clinical functions without initiating rejection mechanism [27].

The bone regeneration process carried out around implants is similar to fracture healing. In both cases, the immune system response, the neovascularization process and the osteoprogenitor cell recruitment are observed. However, during the bone fracture healing these cells differentiate into both chondrocytes and osteoblasts carrying out an endochondral ossification; whereas when regeneration occurs around an implant, progenitor cells differentiate into osteoblasts, carrying out intramembranous ossification. Likely, this different mechanism is due to the biomaterial influence on molecular and cellular responses [28].

Below the bone-implant interactions during the healing process are going to be explained, always starting from the premise that the surgical intervention has been carried out correctly, achieving and adequate primary mechanical implant stability (direct contact between the implant and bone walls), which does not prevent reaching a good osseointegration level [29].

Immediately after implantation, the biomaterial comes in contact with different body fluids such as blood, consequently proteins and biomolecules adsorb on its surface, activating a cascade of complex physiological mechanisms with the aim of achieving implant osseointegration [30].

The first host response to the biomaterial is the formation of hematoma and the activation of the immune system. When the trauma is made, the stage of haemostasis begins with the objective of stopping the haemorrhage associated with the surgical intervention. This stage can last from minutes to hours. Both, the presence of platelets and the coagulation cascade activation lead to fibrin polymerization and the consequent blood clot formation, which serves as a support for neoangiogenesis, the extracellular matrix deposition and the reception of osteoprogenitor cells [31].

Likewise, after the first implantation minutes, an inflammatory phase is generated, which may last for several days. Inflammatory mediators such as interleukin-1 (IL-1), IL-6, IL-11, IL-18 and tumor necrosis factor-α (TNF-α) are activated to initiate the tissue healing, setting up a microenvironment, which promotes cell recruitment. Inflammatory cells (lymphocytes, polymorphonuclear leukocytes or macrophages), growth factors (transforming growth factor- β (TGF-β) and platelet-derived growth factor (PDGF)) and progenitor cells move to the healing place [15]. Inflammatory cells, neutrophils and monocytes, allows the necrotic tissue and pathogens removal. Moreover, the monocytes differentiate into macrophages, which release fibroblast growth factor (FGF) and epidermal growth factor (EGF), to mediate the growth of fibroblasts and new blood vessels [32]. The biomaterial characteristics could influence the behaviour of immune cells, marking the intensity of this immune reaction. Depending on the development of this process the regeneration could achieve a properly bone formation and matrix vascularization or leading to a fibrotic body reaction [33].

Then a proliferative phase begins, characterized by the formation of extracellular matrix and angiogenesis. At the same time, the fibrinolytic system ensures the fibrin clot degradation allowing the tissue remodelling.

In the early stage, large part of repairing tissue is composed of soft callus derived from fibroblast. The formation of blood vessels allows the arrival of necessary nutrients during the regenerative process. The progenitor cells at the injured tissue periphery attach to extracellular matrix proteins via integrin. Then, they differentiate into osteoblasts, beginning the formation of new bone with the secretion of a collagen matrix. The mineralization during this first stage is a rapid process, but at the same time unorganized [34]. This new formed bone is named woven bone and it may grow directly from the bony walls, process known as osteoconduction, or from isolated areas within the regenerating area (osteoinduction) [35]. Additionally, during this stage, there could be periods in which both new bone and soft connective tissue are present. During the remodelling phase, this woven bone is retired by osteoclast, replacing it by structured lamellar bone. This process could take 6 months or longer [31].

1.2.3. Protein adsorption phenomena at biomaterials

First step after the biomaterial / prosthesis implantation in a living organism is the adsorption of protein on its surface. In addition, it is widely accepted that these proteins have the ability to catalyse, mediate or moderate the subsequent biochemical reactions that determine the success or failure of implantation [36]. Therefore, understanding the interaction that takes place between the complex multicomponent mixtures that are the biological fluids and the biomaterial surfaces is essential to be able to design new biomaterials with better performances [37].

Blood plasma contains many hundreds of proteins with a variety of biological functions and activities, which are present in distinct concentrations [38]. Proteins are complex biopolymers whose primary chemical structure is based on a central sequence of amino acids, which can present large variations between different molecules, and possible additional side chains such as phosphates, oligosaccharides or lipids. This structural and functional complexity makes it difficult to establish simple hypotheses about its adsorption processes [39].

This protein adsorption is a thermodynamic process that occurs spontaneously whenever protein-containing aqueous solutions contact solid surfaces. Once the biomaterial comes into contact with blood and interstitial fluids, its surface hydration instantaneously occurs, as a consequence of the water molecules anchoring through hydrogen bonding; then the proteins diffuse into this new interface creating the protein layer. During its formation process, a decrease in its volume is observed, associated with the expulsion of water molecules and/or proteins initially adsorbed. The water molecules expulsion during the process is due to the fact that the adsorption of each protein is associated with a water previously adsorbed displacement equivalent to the protein volume [40].

Therefore, this protein adsorption will depend on surface-water-protein interactions, which may favour or hinder the phenomena. This process is based on the dehydration of the proteins and the surface, the redistribution of charges in the interface and the conformational changes of the proteins [41]. Thus, the interfacial water displacement requires a certain amount of energy depending on chemistry and energy characteristics of the surface on which the process is carried out, so that the more hydrophilic the material, the higher the energy cost required for this dehydration [42].

On the other hand, in this first stage the adsorption increases with time and protein concentration, at least until reaching the surface coverage. Thus, the adsorption rate decreases as fewer binding positions are available, being the process increasingly dependent on the affinity between the protein and the material [41].

In addition, the composition of the layer could change with time as a consequence of the displacement of proteins associated with different degrees of affinity with the biomaterial. The proteins with the greatest number of anchoring positions have a greater potential for adsorption on the biomaterial surface. However, in complex mixtures of proteins, such as blood, the proteins of smaller size and with a greater concentration have a higher diffusion speed and, therefore, reach first the biomaterial surface. Then, they are displaced by higher molecular weight proteins with higher affinity. This competitive phenomenon is known as Vroman effect; which, still is not completely understood, despite having been widely investigated [43].

The simultaneous and potentially nonlinear development of microscopic processes in terms of adsorption, desorption, diffusion or conformational changes, represents a challenge when mechanism models to explain this competitive diffusion process at the biomaterial - biological fluid interface are proposed [44]. In this sense, the Langmuir adsorption isotherm theory, which describes the adsorption of gas molecules to surfaces, could serve as starting point for the development of theoretical descriptions of protein adsorption, even though this theory is too simple to match the high-complex protein behaviour [45].

Several exchange processes were identified as partial interpretation of this phenomenon. On the one hand, desorption / adsorption model supposes that adsorbed proteins naturally desorb into the bulk solution and leaves available space on the surface, where a distinct protein could be adsorbed. Nevertheless, this model is not consistent with the fact that protein exchange is also detected in surfaces exposed to single protein solution, which is strongly adsorbed to prevent the desorption, consequently this phenomenon could not explain by itself the Vroman effect. The time constant for the protein exchange was only consistent with the desorption time constant at long time scales, suggesting that the exchange observed on the shorter time scales could be because of competing displacement process, which supposes that protein with higher surface affinity could displace other earlier-adsorbed proteins. However, the displacement mechanism of this process is

still understand, although it may occur via a “transient complex” protein exchange based in three steps: the adsorption of the initial layer and the subsequent adhesion of a new protein layer on the initial one, forming a protein multilayer. Thus, a rotary movement would expose the initial layer to the solution, enhancing its desorption and obtaining as a result a final layer enriched in the second adsorption proteins [46].

1.2.4. Factors controlling protein adsorption

The protein layer formation depends on multiple factors associated to the external solution characteristics, the surface properties, as well as the characteristics of the deposited proteins themselves. In this way, the conditions in which the adsorption process is carried out will influence the final layer conformation.

The main external factors associated to the protein solution are temperature, pH, ionic strength, and buffer composition. Temperature can affect both the protein adsorption kinetics and its final equilibrium, since a higher temperature is related to faster protein diffusivity and, consequently, increased adsorption rates. Therefore, a temperature increase could suppose a higher amount of adsorbed proteins on the biomaterial surface [47]. The pH establishes the protein charge depending on its isoelectric point. For pH equal to isoelectric point, the protein shows a neutral state since positive and negative charges are balanced. When the pH decreases or increases with respect to the isoelectric point, proteins have positive or negative charge, respectively. Then, depending on pH, the electrostatics forces could affect the final layer packing density, being that at the isoelectric point, the lower repulsions allow higher density conformations. On the other hand, the ionic strength conditions the Debye length, related to the damping distance of the electric potential of a fixed charge in an electrolyte. Then, charged proteins adsorption is hampered in oppositely charged substrates, whereas the adsorption to like-charged substrates is enhanced [39].

As expected, proteins characteristics such size, net charge or its structure have high influence during the protein layer deposition. Depending on which proteins constitute the layer, both protein-protein and protein-material interactions could display different affinities, resulting in distinct protein packing, orientations and water contents [39].

Many studies establish arbitrary values regarding parameters related to physiological medium properties as well as its proteomic composition. However, these properties are fixed in a living system during the implantation of a prosthesis, being the optimization of the physical-chemical biomaterial properties the main strategy to achieve controlling the protein layer deposition process.

The surface properties can mark the protein layer features since surface chemistry, wettability, charge and morphology are important parameters affecting protein adsorption (Figure 1.2). Surface chemistry and functional groups can mark some surface properties such as wettability and charge, and affect to protein adsorption, denaturation, and functional activity [48,49].

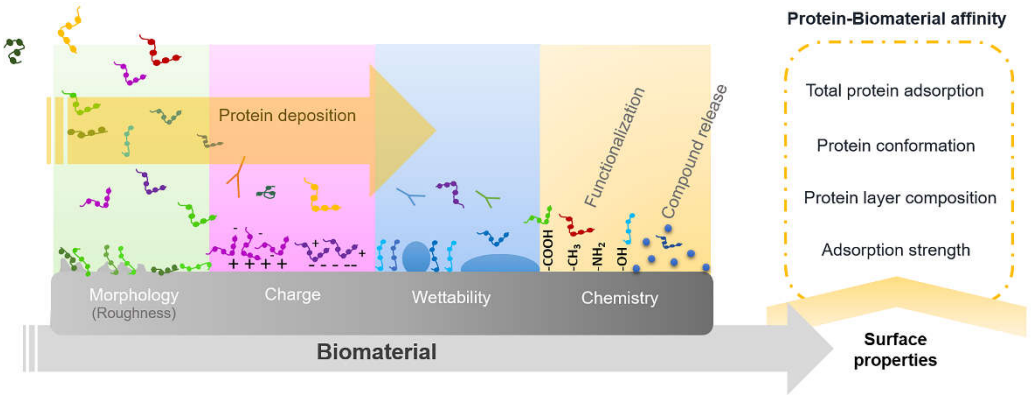

Figure 1.2. Biomaterial properties affecting protein adsorption.

Surface wettability is a key parameter, which determines the adsorption kinetics and the amount of attached proteins on the material [50]. In hydrophilic surfaces, the stronger interaction between the surface and water difficult the protein-material interaction, fact that could increase protein desorption. Therefore, generally the affinity of proteins to biomaterial increases on hydrophobic surfaces and decreases on hydrophilic surfaces [51]. Otherwise, proteins tend to adsorb more strongly to charged materials than to uncharged ones [39,52] and the surface charge can condition the protein orientation at the solid interface [53]. Biomaterial topography might influence the way that proteins interact with the surface, allowing the control of total protein adsorption levels and influencing the ratio of different proteins, the spatial distribution, protein conformation, and surface binding affinity [54]. As protein size are on the nanometer range, nanoscale topographies

are thought to affect more protein adsorption, than micro-topographies. Then morphology factors in term of roughness, geometry or porosity on the nanoscale could allow controlling the protein layer properties, regarding both composition and conformation [43]. It was found that surface nano-topography influence the amount of attached proteins, showing increased saturation uptake. Moreover, the surface geometry could display important effects on protein orientation, which determines which part of the protein interact with the material and which part is exposed [55].

1.2.5. Protein layer composition – Biological implications

An appropriate biological response to implanted materials is essential for tissue regeneration and integration. It has been exposed that the surface characteristics could determine the protein binding onto the biomaterials, being this process described as the first step after implantation. Consequently, actually the cells would not directly interact with the material surface at all, but instead only see the layer of proteins adsorbed on it [56]. In this sense, Lim *et al.* [57] found that cell adhesion was unaffected by nanotopography when the assay was performed in the absence of serum, whereas this effect was observed in the presence of proteins. This result is an example how the adsorbed proteins are to which cells initially respond, rather than the surface itself [43]. Therefore, the attached proteins on the biomaterial could have a pivotal role controlling the subsequent events required for tissue repair, apart from the influence of the material.

As it was explained in point 1.2.2, the implant osseointegration success requires the proper initiation and development of coagulation, angiogenesis, immune response, fibrinolysis and osteogenesis processes (Figure 1.3).

Hence, depending on the protein layer composition, these events could be positive stimulated, favouring the tissue regeneration, or in the opposite way, the erroneous or disproportionate protein signalling could suppose the development of a fibrous capsule or even the material rejection by the biological system.

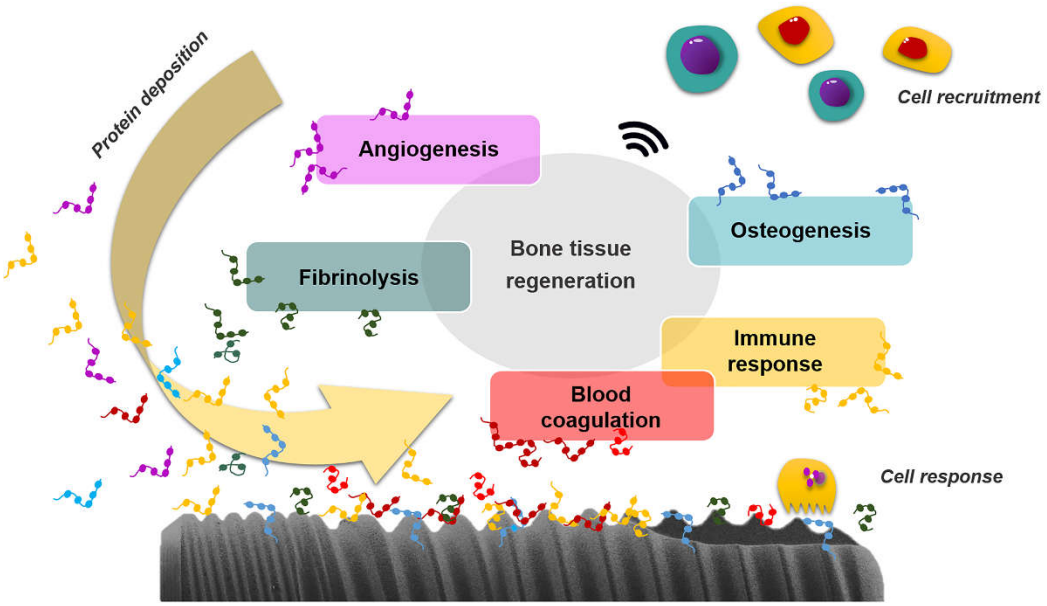

Figure 1.3. Biological implication of the protein layer formed onto implants during the osseointegration process.

In the following points, it is going to be developed in greater profundity the most important proteins involved in coagulation, angiogenesis, immune, fibrinolysis and osteogenesis events.

1.2.6. Coagulation system: proteomic point of view

In a similar way to the process occurring after blood vessel injury, biomaterial surfaces can induce the coagulation of contacting blood. Then, after implantation, one of the first step in bone healing process is the blot clot formation and how the clots are formed can influence the subsequent steps during bone regeneration [58].

The coagulation process involves a series of zyminogen-enzime conversions, which can be activated through intrinsic and extrinsic pathways as is shown in Figure 1.4. Both converge in the activation of factor X to Xa, resulting in a common pathway. Following injury, the extrinsic pathway is initiated by tissue factor protein (TF) secreted by cells surrounding the damage area, which binds

to the active serine protease factor VIIa (FVIIa), resulting from the circulating factor VII conversion, and forms the extrinsic tenase TF-FVIIa complex [59].

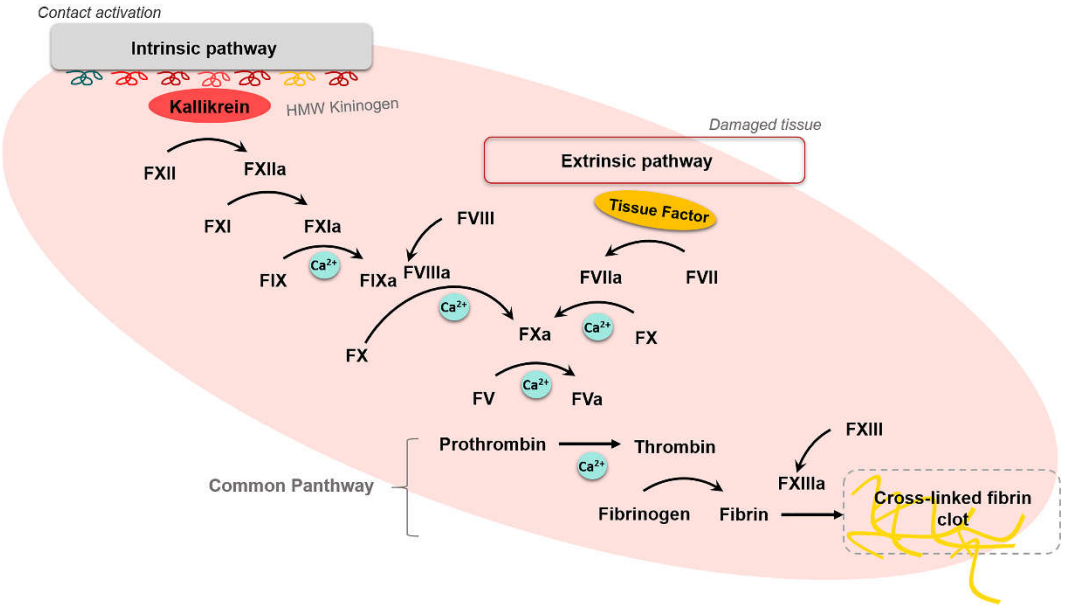

Figure 1.4. Coagulation cascade diagram.

In parallel, the intrinsic pathway is initiated by the proteins prekallikrein, high molecular weight kininogen and factor XII contact surface activation. This cascade results in the intrinsic tenase complex formation, through the binding of factor IX to FVIIIa (FIX-FVIIIa). Then, both complexes can activate factor X, leading factor Xa, which binds to activated factor V (FVa) and forms the prothrombinase complex (FXa-FVa) [58]. This complex results in the conversion of prothrombin to small amounts of thrombin, which displays multiple procoagulant effects as the activation of factors V, VIII, XI and XIII and the activation of platelets, amplifying the reaction and forming most of the thrombin [60]. Thrombin cleaves fibrinogen to fibrin monomers leading the fibrin clot [61]. Despite the extrinsic pathway was related to the haemostatic control and the response to vascular injury, there is evidence that this cascade is involved in biomaterial associated coagulation as well [62]. Although, it is likely the intrinsic pathway the most important in this process around the implants, being known to trigger coagulation on artificial surfaces [63,64].

An adequate level of coagulation proteins is crucial to achieve a correct development of this process [65]. Additionally, to the obvious role of these proteins in the coagulation cascade, it is also remarkably its interaction with cells such bone cells [66] and platelets [64], which play key role during the blood clotting process. The preferential biomaterial adhesion of proteins such vitronectin and fibrinogen can bind to platelets via membrane protein GPIIbIIIa, promoting platelet adhesion and formation of stable platelet aggregates [64,67]. These platelets contain growth factors, such as PDGF, vascular endothelial growth factor (VEGF) and FGF, which are known to support revascularization and osseointegration [68]. Therefore, the superior osseointegrating properties of some biomaterials could be consequence of its thrombogenicity behaviour [69].

On the other hand, the coagulation mediators activate the production of cytokines, chemokines, growth factors and other proinflammatory compounds. The interaction between the immune system and the coagulation cascade supposes that an excessive coagulation could contribute to inflammatory events [62,70].

The coagulation pathway is regulated to avoid a disproportionate clot formation. Then, the adsorption of anticoagulant proteins takes part in the control of this cascade activation and ensures its correct development. An adequate balance between activator and inhibitor proteins of this complex process is pivotal to obtain a proper clot architecture which expedites the healing process. Specific regulators of the coagulation system are proteins as antithrombin, vitamin K-dependent proteins C and S, tissue factor pathway inhibitor, heparin cofactor II, α2-macroglobulin, α2-antiplasmin, protein C inhibitor or corn trypsin inhibitor [71–73].

1.2.7. Fibrinolytic system

Bone healing process after biomaterial implantation is associated to the extravascular deposits of a fibrin-rich matrix, being this fibrin the primary product of the coagulation cascade. Fibrinolysis is the process through which fibrin clots are degraded to form fibrin monomers and other fibrin degradation products [74]. The biochemical mechanism of this system is centered around protein plasminogen, an inactive proenzyme, which can be activated to plasmin. The plasminogen system plays a relevant role during the regeneration of oral tissues, which in addition to fibrinolysis include

extracellular matrix degradation, inflammation, immune response, angiogenesis, tissue remodelling, cell migration and wound healing [75]. In fact, reduced levels of plasminogen was observed in chronic wounds of diabetic patients, which could be associated to its defective healing [76].

As is shown in Figure 1.5, plasmin is generated from plasminogen when it is activated by plasminogen activators, being tissue-type plasminogen activator (t-PA) and urokinase-type plasminogen activator (u-PA) the most important [77]. t-PA is synthesized and released by endothelial cells, while u-PA is produced by monocytes, macrophages, and urinary epithelium [78]. Plasmin presents a crucial role in wound healing due to its role in the extracellular matrix degradation, promoting cell migration and tissue remodelling [79]. In this line, loss of plasmin was related to impaired hard tissue callus formation and heterotopic ossification during bone healing, indeed plasmin seems to be key for achieving a proper endochondral-mediated vascularization of fracture callus, as well as, the soft tissue callus remodellation to newly woven bone [80].

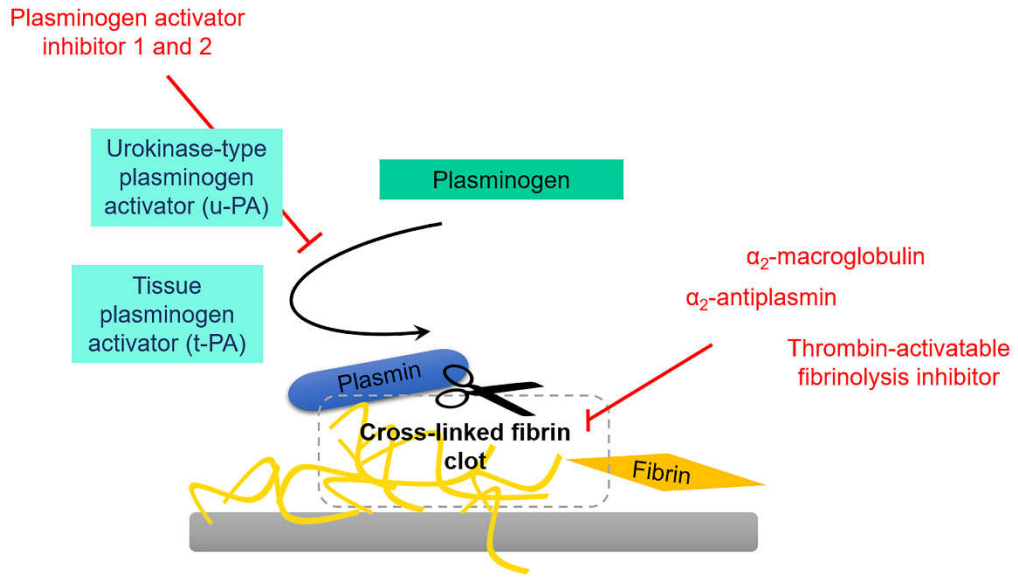

Figure 1.5. Scheme of the fibrinolysis process. Red items represent the inhibitory mechanism of this system.

Similar to the coagulation, the fibrinolytic system is highly regulated in order to restrict the fibrinolysis to the clot site. The inhibition of this process may occur during the plasminogen activation, mainly by plasminogen activator inhibitor 1 and 2 (PAI-1, PAI-2) or by thrombin-activatable fibrinolysis inhibitor (TAFI); and at the level of plasmin by α_2-antiplasmin (A2AP). Others plasmin inhibitors are α2-macroglobulin, C1-esterase inhibitor, and compounds related to the coagulation contact pathway, which can also contribute in plasmin inhibition [74].

1.2.8. Angiogenesis

Angiogenesis is a fundamental process by which new blood capillaries arise from pre-existing vessels. In this process, the endothelial cells, which form the blood vessels, proliferate and migrate forming new canals. This angiogenic trial is essential during the bone tissue regeneration, since it involves the construction of new vessels to ensure the supply of nutrients, energy and signals that the process requires [81].

The oxygen deficiency, due to the destruction of blood vessels as a result of trauma, activates the hypoxia-inducible program driven by hypoxia inducible factor 1-α protein (HIF-1α). This program provokes endothelial cells response to angiogenic signals. As consequence of integrin signalling, endothelial cells migrate to the healing site. Proteases liberate angiogenic molecules such as VEGFs and FGFs, creating an environment conducive to angiogenesis [82]. The vessel growth is based in two endothelial cell behaviours. First, so-called tip cells spearhead new sprouts and probe the environment for guidance cues. Then, following tip cells, stalk cells extend establish a lumen and proliferate to support sprout elongation [83]. Thus, signals such as platelet-derived growth factor B (PDGF-B), angiopoietin-1 (ANG-1), TGF-β, ephrin-B2 and NOTCH, as well as protease inhibitors such as tissue inhibitors of metalloproteinases and PAI-1, regulate the correct formation of new functional vessels [84,85].

1.2.9. Immune reaction: Complement system

The complement system has a key role in the initial host recognition of the implanted biomaterial, being essential in the subsequent immune and inflammatory reactions [86]. This system comprises numerous plasma and membrane-bound proteins and regulators, as it can be seen in Figure 1.6. These complement proteins collaborate as a cascade, being initiated by pattern recognition molecules or by the direct bonding of complement components to nonself surfaces [87]. The cascade can be initiated via three distinct pathways: the classical pathway, the lectin pathway and the alternative pathway, each conducting to a common terminal pathway [88].

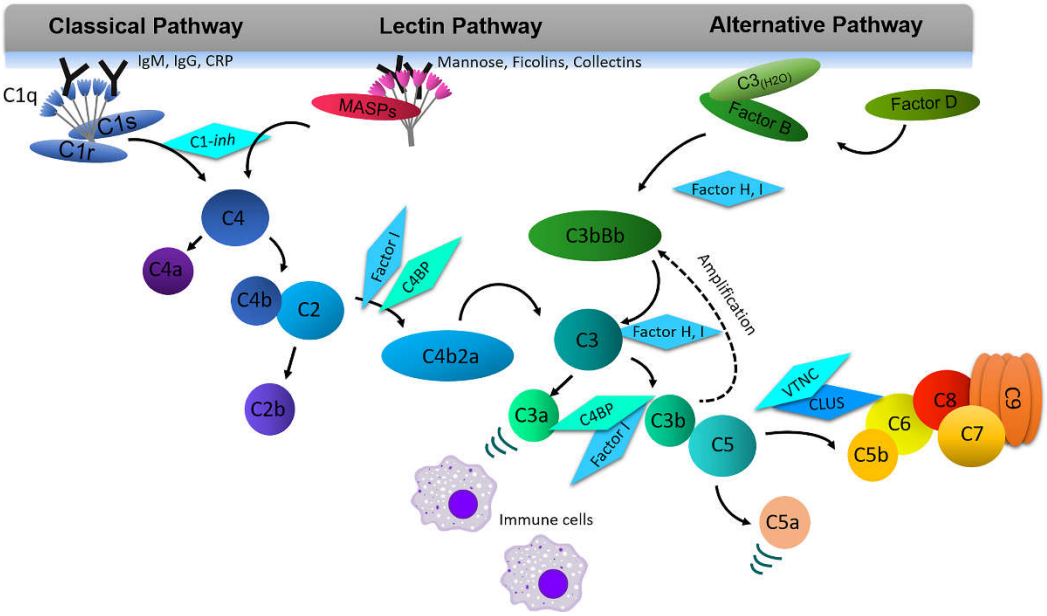

Figure 1.6. Complement system activation mechanisms. Diamonds display the inhibitory proteins, which belong to this system, in their possible action sites.

The molecular mechanisms which conduct the initiation and development of this cascade have been widely described in different reviews [88,89]. Briefly, respective pathway is activated through different recognition molecules. Complement component C1q activates the classical pathway by its binding to ligands as immunoglobulins (IgM and IgG) or pentraxins (C-reactive protein (CRP) and pentraxin-3), while the lectin pathway is initiated by mannose-binding lectin, ficolins-1, 2 and 3 and collectins. The alternative pathway can be triggered directly by foreign surfaces such as

biomaterials. The cascade initiation results in the formation of C3 convertases. In the classical pathway the C1q complex formation activates the C1r and C1s proteases. C1s cleaves complement component C4 into C4a and C4b, then C4b bound C2 into C2a and C2b. These reactions generate C4b2a convertase. Otherwise, the recognition lectin pathway molecules convene with the serine proteases associated to mannose binding lectins, activating C2 and C4 in turn and obtaining C4b2a convertase, similarly to classical pathway. In parallel, the alternative pathway allows the generation of C3bBb convertase by spontaneous activation of C3, by hydrolysis ($C3H_2O$) and binding to Factor B via Factor D or by C3b binding to properdin [90]. This C3 convertases activate C3, being this protein the central component of the complement system, into C3a and C3b. The resulting C3b is deposited, leading the formation of more alternative pathway complexes C3bBb, amplifying the response. C3b activates the cleavage of C5 into C5a and C5b, initiating the terminal phase. C5b interacts with C6, C7, C8 and C9 which ultimately forms the C5b-9 complex [91]. The generated C3a and C5a act as potent chemoattractants, recruiting immune cells such as monocytes and macrophages to the biomaterial site [92].

The complement system is strictly controlled to avoid a disproportionate immune response. Plasma proteins such as C1-inhibitor, anaphylotoxin inhibitor, factors H and I, C4b-binding protein (C4BP), clusterin (CLUS), vitronectin (VTNC) and several complement receptors restrict the cascade enzymatic reactions avoiding the host tissue damage [93,94]. These regulators can recognize specific surface patters, supporting the complement inhibition on surfaces [95].

The layer of proteins immediately and spontaneously adsorbed onto the biomaterial surface could trigger this cascade. The type, concentration and conformation of complement proteins presents in the protein layer play an important role in the initiation and intensity of this system, determining wound healing and foreign body reaction. In this line, some studies tried to stablish correlations between the adsorption of complement proteins onto biomaterials and its subsequent biological response. In this line, some studies suggest the binding of protein C3 on artificial surfaces as biocompatibility indicator [96,97]. Similarly, Engberg *et al.* [98] proposed the C4/C4BP binding ratio as a predictor of the biomaterial inflammatory response. These adsorbed complement proteins could interact with the biological system surrounding the implant, modelling the inflammatory response and the recruitment of immune cells [86]. Therefore, the adsorption of this proteins can trigger the production of different cytokines and chemokines via integrin-ligand interactions [99].

The severity of the immune reaction will mark the production of this activating and inhibiting substances able to modulate macrophage activity and consequently its polarization into pro-inflammatory (M1) or pro-regenerative phenotypes (M2) [100]. These macrophage phenotypes modulate the balance between the tissue repair and the chronic inflammation, thus playing a key role in the implant failure or success [101,102].

Additionally, to the complement proteins, the presence of adsorbed proteins such as albumin, fibrinogen or fibronectin can modulate the host inflammatory cell response [103].

In fact, the complement activation and its impact in the biomaterial outcome reaches a high complexity as consequence of the interconnection existing between this system and both fibrinolytic and coagulation cascades [104].

1.2.10. Osteogenesis

Osteogenesis consists in the development of new bone tissue, in which bone cells play a pivotal role [105]. This process is highly regulated by important signalling pathways such as Wnt/β-caterin, Notch, BMP/TGF-β, PI3K/Akt/mTOR, mitogen-activated protein kinase (MAPK), PDGF, insulin-like growth factor (IGF), FGF and Ca^{2+}, which result crucial for bone regeneration. The functions of these signalling pathways in osteogenesis is widely described in literature, intervening in their activation and molecular mechanism development a wide range of proteins [106–108]. These proteins (i.e. bone morphogenetic proteins (BMPs), PDGFs and IGFs) act as signalling molecules and are involved in cell proliferation, differentiation and maturation, regulating directly the osteoblast activity and then bone repair [107].

BMP/ TGF-β pathways are the main cascades responsible for osteogenesis. Both BMPs and TGF- βs belong to the same superfamily of proteins, which are greatly abundant in bone tissue. They have the ability to induce new bone formation, promoting osteoblast differentiation and reducing osteoclastogenesis [109–111]. Wtn/ β-caterin pathway is formed by Wnt, a family of glycoproteins, which activate the pathway central player, β-caterin. This pathway promotes osteoblastogenesis, having a key role in skeletal development and bone mass maintenance and remodelling [112,113].

IGFs and insulin growth factor binding proteins take part in IGF signalling pathway, being important regulators of bone [114]. Similarly, PI3K/Akt [115], Ca^{2+} [116], PDFG [117] and MAPK [118] pathways play vital roles in the regulation of numerous cell functions in bone, promoting its formation and remodelling. Notch pathway displays a direct osteinductive effect on osteoblasts, resulting in the alkaline-phosphatase (ALP) and bone sialoprotein osteoblast gene expression increases [119]. Some FGF proteins also have pivotal functions in osteogenesis, regulating the proliferation and differentiation of both osteoblasts and fibroblasts [120].

Otherwise, ample evidence relates the extracellular matrix (ECM) proteins to the promotion of osteogenesis. The interaction between bone cells and ECM proteins supposes the activation of integrin on the cell surface, originating different signals which might regulate cell adhesion, proliferation and mineralization. In that sense, proteins such as collagen and vitronectin are described to promote osteogenic differentiation of human mesenchymal stem cells (MSCs) [121]. In fact, the presence of collagen onto titanium implant surfaces was found to enhance the *in vivo* osseointegration rates compared to non-collagen coated Ti [122]. Collagen integrin receptors are said to regulate osteoblast differentiation, through activation of BMP pathway [123]. On the other hand, osteogenic differentiation of MSCs as a consequence of the presence of vitronectin was related to an enhanced focal adhesion formation, and to a lower activation of MAPK and PI3K pathways [124]. Another ECM protein, fibronectin, it is a glycoprotein which has a key role not only in blood clotting, but also as a regulator of cell functions during tissue repair [125]. In fact, a study refers that fibronectin can be related with the osteogenic differentiation of MSCs, in a density-dependent manner [126]. Similarly, fibrinogen is documented to promote osteogenic development of stem cells via runt-related transcription factor 2 activation (RUNX2) [127]. Moreover, other proteins such as apolipoprotein E [128] and vitamin D [129], which are present in blood plasma, can display osteogenic potential by their positive effect on osteoblastogenesis.

Additionally, it is necessary take in account the interplay between osteogenesis and the others key processes in bone regeneration (i.e. coagulation and immune reaction), since their signalling molecules can show important regulatory effects in bone cells. In this sense, during last years the osteoimmunology field is studying the complicated interactions between immune and skeletal systems [130]. Immune cells (i.e. macrophages and T and B cells) arrive at the healing site and release different immunomodulatory molecules such as cytokines and chemokines, which finally

affect to the bone healing process [131]. An optimum immune environment could ensure the proper release of factors to achieve a favourable osteoblast and osteoclast regulation [132,133]. Thus, the adhesion of proteins such as complement proteins onto the biomaterial could affect to the material osteogenic properties and then, to their osseointegration capability [134].

1.2.11. Biomaterial protein layer characterization

Variety of methods have been employed to study the protein behaviour on biomaterials, including atomic force microscopy, ellipsometry, quartz crystal microbalance, Western blot, immunoassays and ELISA. However, these techniques were limited in scope since they were suitable only for analyse a restricted number of proteins/samples, being difficult to get a wider picture of protein-biomaterial interactions [22].

Proteomics is defined as the large scale analysis of proteins [135]. During the past years, the progress in proteomic technologies, in terms of resolution, mass accuracy and speed, enabled the sensitive and specific identification and quantification of proteins in complexes mixtures, achieving its global analysis. This situation has turned proteomics into a powerful tool to investigate protein profiles. Techniques such protein microarrays, gel electrophoresis, chromatography and mass spectrometry (MS) are allowing the proteomic comparative and quantitative composition analysis, which results are potentially interesting for biomaterial researches [19,136].

Proteomic based on mass spectrometry have demonstrated its power in a large-scale study of proteins as consequence of the high resolution detecting proteins displayed by current MS equipment. Mass spectrometers are based on an ionizing source, being matrix assisted laser desorption ionization (MALDI) and electrospray ionization (ESI) the most commonly used; and one or more analysers. Time-of-flight (TOF), ion trap, quadruple, Orbitrap and Fourier transform ion cyclotron resonance (FTICR) are the five types of analysers, which are usually used in tandem (MS/MS) to obtain a higher degree of ion separation and identification [137].

The use of MS as proteomic technique in the biomaterial field is growing and new measurement strategies are adopted to obtain improving sensitivity, reproducibility and to be able to analyse

more complex samples [138]. In this sense, Griesser et al. reviewed the use of MALDI-TOF MS to study protein-biomaterial interactions [139]. More recent studies have opted for the combination of MS/MS with liquid chromatography (LC) as a separation method. This particular LC-MS/MS combination has turned in a powerful technique in the proteomic field, being able to detect even proteins present in small amounts with high reproducibility [22,140]. Due to this potential investigating proteomic profiling, this technique was widely employed to discover biomarkers related to pathologic diseases as osteoporosis, osteoarthritis or bone tumours [36].

Otherwise, LC-MS/MS has been applied in biomaterial research in different ways. Some authors made use of LC-MS/MS to study the expressed protein profiles of cells cultured on new materials [141,142]. Although is followed by limited number of studies, another LC-MS/MS approach focus on the comparative analysis of proteomic profiles expressed during the *in vivo* bone regeneration around biomaterials [143]. On the other hand, LC-MS/MS proteomic studies were performed to characterize protein adsorption onto biomaterials. This type of works is mainly focused on the protein attachment on nanoparticle surfaces and the evaluation of their nanotoxicity [136,144,145]. Some authors have also applied LC-MS/MS to characterize the protein adsorption onto biomaterials used in implantology. The limited studies focusing on this specific approach are shown in Table 1.1.

Table 1.1. LC-MS/MS proteomic studies focusing on the characterization of protein adsorption onto biomaterials used in implantology.

Protein source	Technology	Biomaterial	Detected proteins	Reference
Human blood plasma	LC-MS/MS	Rough Ti	25	[146]
Platelet rich plasma	LC-MS/MS	PolyNaSS/Ti	29	[147]
Rat serum	LC-MS/MS	OCP/HA	138	[148]
Pig bone proteins	LC-MS/MS	TiO_2	151	[149]
MatrigelTM	LC-ESI-MS/MS	alginate, Ti, PHEMA, nylon 6, nylon 12, PMMA and PDLLA	149	[150]
FBS	LC-MS/MS	PEG-hydrogel	391	[151]

Dodo *et al*. [146] characterized the protein layer adsorbed to a rough Ti surface, after being incubated with blood plasma. LC-MS/MS analysis revealed that this layer was mainly composed of proteins related to cell adhesion, molecular transportation and coagulation. Otherwise, the differential analysis of the proteins attached onto poly sodium styrene sulfonate (PolyNaSS) showed a higher level of protein adsorption on this surface than on the un-grafted titanium after being incubated with platelet rich plasma [147]. Kaneko *et al.* [148] determined which rat serum proteins were differentially adsorbed onto two bone substitute materials, octacalcium phosphate (OCP) and hydroxyapatite (HA) crystals. Similarly, Sugimoto *et al*. [149] investigate the specific bone-related proteins adhered on the titanium dioxide surface (TiO_2) after their incubation with proteins extracted from pig bone. The attached proteins were analysed through both sodium dodecyl sulfate polyacrylamide gel electrophoresis (SDS-PAGE) and LC-MS/MS, resulting in the identification of extracellular matrix components, enzymes, growth factors and some proteins with mineralization capacity. On the other hand, Abdallah *et al.* [150] studied the adsorption of proteins from MatrigelTM on distinct material surfaces: alginate, Ti, poly (2-hydroxyethyl methacrylate) (PHEMA), nylon 6, nylon12, polycaprolactone (PCL), poly (methyl methacrylate) (PMMA) and poly (D,L-lactic acid) (PDLLA). The proteomic analysis showed that biomaterial surface chemistry determines the surface proteomic profile and due to this fact PMMA and PDLLA surfaces promoted the selective adsorption of key basal lamina proteins and consequently also displayed greater interactions with epithelial cells. Swartzlander *et al.* [151] studied the protein adsorption of fetal bovine serum (FBS) proteins onto distinct poly (ethylene glycol) (PEG) hydrogels using LC-MS/MS, founding that the majority of detected proteins were related to an acute inflammatory response. These results were concordant with the *in vivo* foreign body response triggered by these materials.

Overall, these studies demonstrate the high potential of LC-MS/MS as proteomic technique to perform a large-scale characterization of the proteins adsorbed onto biomaterial surfaces.

1.2.12. Dental implants and its surface modification

A dental implant is defined as an artificial tooth root that is placed into mandible aiming to hold a replacement tooth [152]. In 1965, the Per-Ingvar Brånemark's titanium screw implant system supposed the beginning of the modern oral implantology [26]. Since then, titanium has emerged as the gold standard material in implant dentistry. The choice of titanium and its alloys for dental implants is based on its favourable characteristics such as good mechanical properties, chemical stability and excellent biocompatibility. However, titanium and its alloys are defined as inert materials [153]. For this reason, a variety of surface treatments, including physico-chemical, morphological and biochemical approaches, have been developed to bioactivate the titanium implant surfaces, aiming their clinical performance enhancement. These surface modifications are widely described in literature (for more information see reviews [154–162]).

Nowadays, the application of silica hybrid coatings to dental implants is a promising research line to achieve a proper surface functionalization, providing beneficial characteristics that allow obtaining a desirable biological response for bone healing implants.

1.2.13. Silica hybrid sol-gel coatings

Since Larry Hench developed the first bioactive glass for being used in tissue engineering applications in 1969, novel silica materials with improved features such hybrid sol-gel compounds have been appeared providing new possibilities in the field [163].

The sol-gel route is based in two type reactions, which can occur simultaneously. Both hydrolysis and condensation of alkoxysilanes give rise to a solid silicate network, as it is shown in Figure 1.7. In the first step, the alkoxysilane precursor is hydrolysed via its reaction with water to form silanol groups. Then, during condensation a silanol group come into contact with another silanol group or a not hydrolysed alkoxy (-OR), crosslinking the silicon atoms through siloxane bonds (Si-O-Si), and forming silica nanoparticles (Reaction 1.1) [164].

$$\mathbf{Si(OR)_4} + \boldsymbol{nH_2O} \rightarrow \boldsymbol{Si(OR)_{4-n}(OH)n} + \boldsymbol{nR(OH)}$$

$$\mathbf{R_3SiOH} + \boldsymbol{HOSiR'_3} \rightarrow \boldsymbol{R_3Si - O - SiR'_3} + \boldsymbol{H_2O}$$

$$\boldsymbol{R_3SiOH} + \boldsymbol{ROSiR'_3} \rightarrow \boldsymbol{R_3Si - O - SiR'_3} + \boldsymbol{R(OH)}$$

Reaction 1.1. Hydrolysis-condensation reactions of sol-gel process.

Gelation occurs when siloxane links are generated between the scattered colloid particles forming a three-dimensional structure that encloses the liquid phase. Finally, these materials can be synthetized with heat treatments at low temperatures [165].

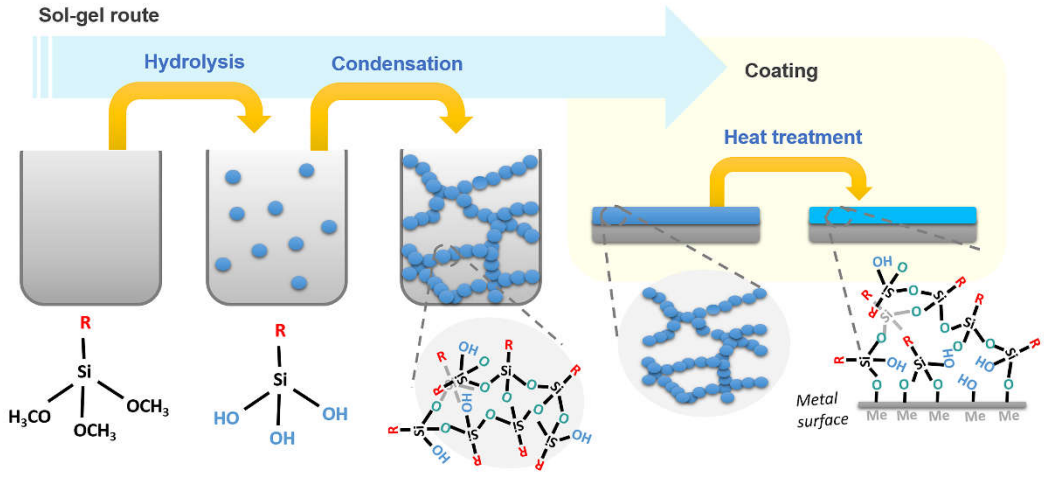

Figure 1.7. Sol-gel route scheme: chemical reactions and coating formation.

The sol-gel processing allows the use of organically modified alkoxysilanes, being possible the incorporation of functional groups in the network achieving hybrid compounds [166]. Another advantage of this technique is its versatility designing materials. Networks with different attributes in term of hydrophilicity, morphology, porosity, chemistry or degradability can be developed controlling preparation parameters such the precursor nature, the degree of functionalization, temperature, pH, H_2O:Si ratio and the type of solvent [167].

Additionally, hybrids have been proved to be biocompatible compounds with great potential in biomedical applications [168]. Silica sol-gel networks showed promising results for bone regeneration since these materials support osteoblast attachment, proliferation and

differentiation boosting the expression of multiple genes which lead osteogenesis [169]. In this sense, such materials can be applied as a coating on prosthesis (Figure 1.7), in the scope of implant bioactivation [170]. These coatings, during its degradation process, release silicon compounds in the $Si(OH)_4$ form, giving the implant osteoinductive properties [171]. Being that Si has a positive effect on bone metabolism by enhancing osteoblastogenesis [172,173]. The good performance of these organic-inorganic coatings when are applied on titanium dental implants have been described in literature [174,175]. In fact, in our group several hybrid compounds have been developed for this application [176–178].

Moreover, these hybrids can be used as delivery systems due to the possibility of controlling its biodegradability kinetic [179]. Therefore, these networks can be enriched with therapeutic compounds providing added values to the implant, since the coating not only bioactivates the titanium surface but also performs as a delivery vehicle supplying agents with specific functions (i.e. antibacterial, anti-inflammatory, osteogenic) to the healing site [180]. In this sense, several authors worked in the incorporation of osteogenic compound to these sol-gel biomaterials, aiming the increase their positive effects during bone tissue healing [181,182].

1.2.14. Hybrids as delivery vehicles: Osteogenic role of Ca and Sr

The sol-gel networks allow the superficial modification of dental implants, being able to achieve that these prostheses have the desired biological outcome due to the control of properties such their functionalization degree or the incorporation of bioactive compounds. For that reason, hybrids are a proper choice to design biomaterials to provoke different biological responses to perform the aim of this thesis.

In this sense, the incorporation of ions with recognized positive effects in bone tissue healing can be an interesting strategy to follow in order to obtain that these materials provide specific biological responses. Indeed, ions such as Ca^{2+} and Sr^{2+} are related to bone metabolism and play a physiological role in the growth and mineralization of bone tissues which makes their use attractive as therapeutic agents to stimulate regeneration [183].

Calcium is one of the main structural components of bone, playing a very important role in the formation and resorption of this tissue through its interaction with bone cells. In this sense, extracellular Ca have a stimulating effect on osteoblasts *in vitro* via the activation of CaR receptors that have the capacity to regulate the activity of osteoblasts and osteoclasts. Valerio *et al.* [184] observed Ca^{2+} increases the release of glutamate which is an important signal for bone mechanosensitivity, therefore Ca would act as a bone formation stimulator. Other authors observed that Ca^{2+} induces an increase in insulin pathway signalling via insulin growth factors I and II (IGF-I, IGF-II), which regulate osteoblasts proliferation [185]. *In vitro* studies have also revealed that the presence of Ca^{2+} supposed an overexpression of osteogenic markers such as type I collagen, alkaline phosphatase (ALP), bone morphogenetic protein 2 (BMP-2), osteopontin and osteocalcin [116,186]. Then, calcium ions display a positive effect on osteoblastic proliferation and mineralization, as well as on bone remodelling, which implies that the release of Ca ions from biomaterials can trigger bone healing [183,187]. However, it is important to take in consideration that these effects are dependent on the Ca concentration. In this sense, Maeno *et al.* [188] observed that low concentrations of Ca^{2+} (2-4 mM) were adequate for the survival and proliferation of osteoblasts, whereas higher concentrations (6-8 mM) favoured osteoblastic differentiation and mineralization. Nevertheless, concentrations over 10 mmol of Ca^{2+} were found cytotoxic. Additionally, to this osteogenic potential, Ca^{2+} also play an important role in blood clotting conditioning clot formation and its stability, fact that might finally affect to the tissue healing process [189].

Otherwise, strontium shows a positive effect on bone formation *in vivo* and is a promising agent for osteoporosis treatments [183]. This element plays a role in bone remodelling, decreasing bone resorption through both osteoclastogenesis inhibition and osteoblastic proliferation promotion. These effects are dose dependent, being observed that at low concentrations Sr increases osteoprogenitor cell differentiation, while at high concentrations it impairs osteoblastogenesis [190]. Indeed, optimal Sr^{2+} presence supposed an enhancement of *in vitro* osteoblast proliferation and mineralization [191]. This cation up-regulates osteogenic expression markers such as ALP, Runx2, type I collagen and osteocalcin [192]. Moreover, *in vivo* studies revealed the safety and effectiveness of Sr enriched biomaterials for stimulating bone growth and remodelling [193]. In fact, this element has been incorporated into different biomaterials in order to foster their bone

regeneration capabilities. Examples are its addition into hydroxyapatites [194], hydrogels [195], bioglasses [191,192] or hybrids [181,196]; reporting in all cases an improvement of osseointegration potential compared to controls without the presence of strontium. This osteogenic behaviour makes interesting the incorporation of these elements into the sol-gel networks, aiming the development of bioactive materials with specific functionalities.

1.3. **Objectives**

The main goal of this thesis is the proteomic analysis of serum protein deposition phenom on distinct biomaterials through liquid chromatography-tandem mass spectrometry (LC-MS/MS) in order to find correlations between protein deposition patterns onto biomaterials and their respective biological outcomes, to **establish protein biomarkers capable of anticipating the material *in vivo* response**.

The specific objectives to accomplish the above-cited goal are listed below:

I. The systematic development of different surface treatments to control different *in vitro* and *in vivo* biological responses.

II. The analysis of the specific biological outcome of previously designed treatments by performing *in vitro* and *in vivo* experimentation, as well as the differential proteomic characterization of serum proteins adsorbed onto these materials using liquid chromatography-tandem mass spectrometry (LC-MS/MS).

III. Correlation between the differential proteins and the biological results that could allow the identification of two types of proteomic biomarkers:

- Biomarkers capable of predicting more effectively biocompatibility problems in biomaterials.
- Biomarkers that could allow an improved material selection to be evaluated *in vivo* in terms of regenerative efficiency.

1.4. **Research strategy**

The approach to attain this objective is schematically presented in Figure 1.8.

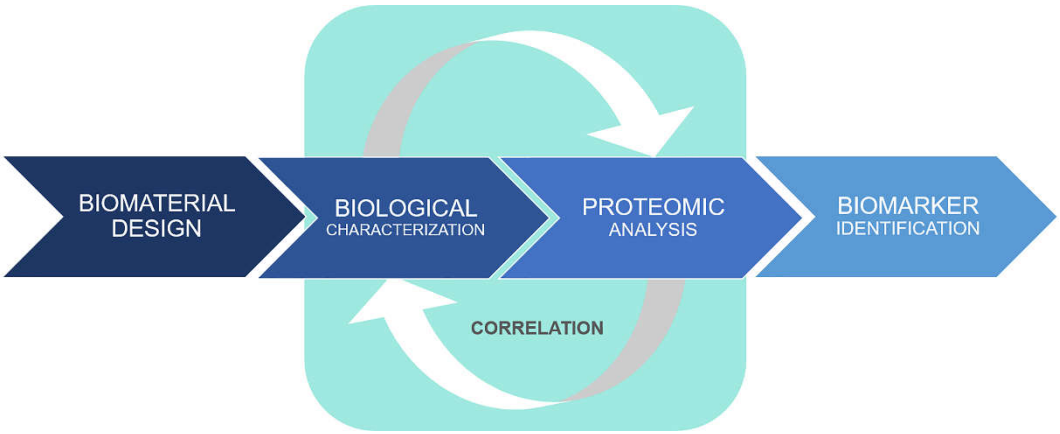

Figure 1.8. Thesis approach.

The first step to approach the final aim is the systematic development of different surface treatments based on hybrid sol-gel coatings and their physico-chemical characterization in order to optimize the employment of these networks as delivery vehicle of osteogenic compounds (**Chapter 1**).

Moreover, the strategy to achieve the identification of the different proteomic biomarkers is exposed below:

*Identification of proteomic biomarkers related to **biocompatibility problems** (Figure 1.9):*

- To achieve this goal, in **Chapter 2**, the first protein layer adsorbed on titanium pre-treated with four distinct hybrid silica sol-gel formulations is going to be characterized. Two of the formulations induce the formation of a fibrous connective tissue surrounding the implant (poor biocompatibility), whereas the other two show good osseointegration (good biocompatibility). Then, the comparative proteomic analysis between these two groups of biomaterials with distinct *in vivo* outcome could stablish the proteins related to this biocompatibility question.

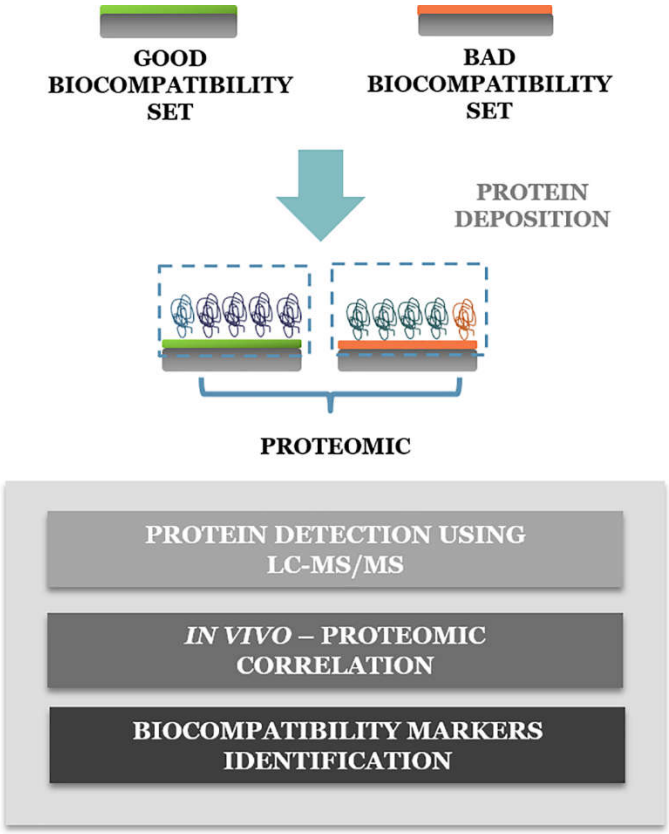

Figure 1.9. Approach for the identification of biomarkers related to biocompatibility problems.

*Identification of proteomic patterns related to a **more efficient osseointegration ability**:*

The followed strategy to detect biomaterial efficacy is based on trying to know how the protein patterns vary in various group of materials previously designed for it, trying to establish a common pattern of biocompatibility and effectiveness among them (Chapters 3, 4, 5 and 6). Then, systematic proteomic studies to different implant surface treatments are performed with the purpose of detect the common efficiency biomarkers (Figure 1.10).

- Characterization and comparison of the protein layers adsorbed onto two types of Ti surfaces, smooth Ti and sandblasted acid-etched Ti (SAE), currently used in commercial

dental implants, after their incubation in human serum, assessing the correlation between proteomic results and in vitro outcomes of these surfaces (**Chapter 3**).

- The proteomic characterization and comparison of sandblasted, acid-etched titanium and a hybrid silica sol-gel coating applied onto this substrate in order to bioactivate it. The correlations between proteomic results and both *in vitro* and *in vivo* behaviours (**Chapter 4**).

- The previous developed silica hybrid sol-gel composition enrichment with various amounts of an osteogenic compound such $SrCl_2$ to be applied onto titanium as coatings. The evaluation of Sr increasing content effects on the *in vitro* interactions with both osteoblasts and macrophages. Proteomic analysis to identify the protein patterns affected by Sr addition and the correlations between proteomic results and *in vitro* testing (**Chapter 5**).

- Incorporation of increasing $CaCl_2$ amounts in the silica hybrid sol-gel composition in order to obtain coatings with specific biological behaviours. The proteomic analysis of human serum protein deposited onto these Ca-enriched surfaces, with the aim of characterize the protein pattern movements between materials with distinct $CaCl_2$ concentrations. The correlation between these results and the *in vitro* characterization, regarding the biomaterial osteogenic potential and its interactions with immune cells (**Chapter 6**).

As has been mentioned above, the strategy followed in this doctoral thesis is based on the use of human serum as a protein medium. This fact allows achieving a greater real biological environment mimicry than monoprotein or few protein mixtures. In addition, it is a commercial product that can be acquired without problems. This fact would facilitate the standardization of a future *in vitro* methodology based on proteomics. The use of more complex protein resources such as human plasma, whose commercialization is not legal in Europe, would imply the need for donors and the consequent approval of ethics committees.

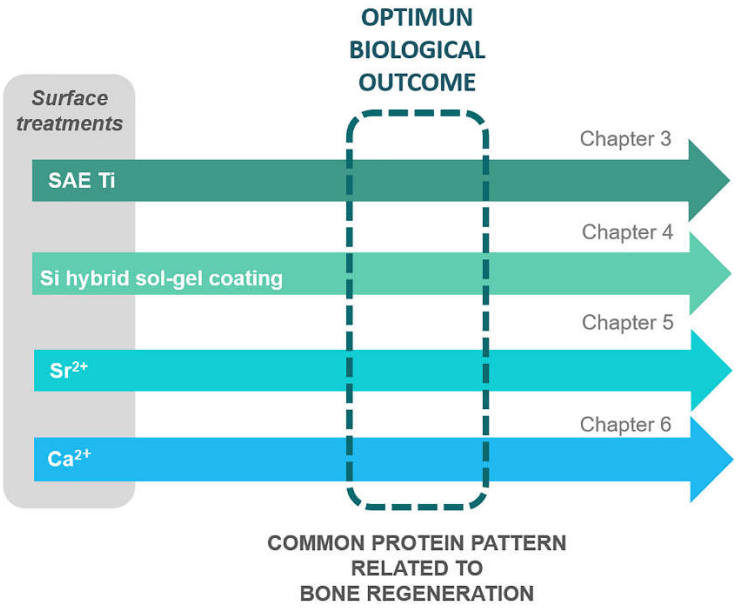

Figure 1.10. Approach for the identification of biomarkers related to regenerative efficiency.

The approach of this work would not have been possible without the collaboration of a multidisciplinary team with members specialized in different fields. For that, the experiments were performed at different places due to the availability of analysis instruments.

The required *in vitro* and *in vivo* characterization was carried out by biologists members of Department of Medicine at Universitat Jaume I, and histologists from Pathology Department at University of Valencia. The mass spectrometry analyses were performed by proteomic platform members at the CIC bioGUNE.

1.5. **Statement of significance**

This research work is part of a RETOS project entitled “Development of dental implants with osteogenic properties for the universalization of receptors. Determination of protein patterns of regenerative efficacy - PROTEODENT” with financial support provided by the Spanish Ministry of Economy and Competitiveness and by Universitat Jaume I, Universidad del País Vasco and an industrial partner Ilerimplant S.L.

Our research group has been working in the development of degradable coatings synthesized via sol-gel process to bioactivate dental implants for 10 years. Several theses about this issue have been presented during this period, thereby Miriam Hernández Escolano (2011), María Jesus Juan Díaz (2013), Irene Lara Sáez (2015), María Martínez Ibánez (2015) and Sara Maria Da Silva Barros (2016) worked on the development and characterization of different sol-gel compositions for this application. In an important number of cases, it was disappointing that after all the effort the *in vivo* results showed behaviours totally opposite to what was expected according to the rest of characterizations, showing the poor existing *in vitro* - *in vivo* correlation testing biomaterials for bone regeneration.

Taking into account this situation, our research group decided to start a new research line, which focus in the study of protein-biomaterial interactions in order to develop new tools to predict the *in vivo* outcome of future compositions.

This doctoral thesis develops an innovative strategy based on the proteomic characterization of systematically synthetized biomaterials, with different functionalities, and their correlation with the material biological behaviour, looking for the identification of biomarkers associated with their biological responses.

This research could contribute to improve the existing understanding in regard to the interaction of proteins with biomaterials and its consequent effect on their biological response, establishing the knowledge bases for the construction of a new methodology *in vitro* which could lead to a better prediction on *in vivo* response of new materials.

This greater efficacy would be associated with a reduction of *in vivo* experimentation, since proteomics would allow efficient discarding of a greater number of materials that would be considered suitable with the current *in vitro* trials, but then rejected *in vivo*. This fact could mean a significant reduction of both the number of animals destined for *in vivo* experimentation and its associated economic cost, assuring the highest safety standards for patients. This last point is of great interest as a result of the ethical problems related to this type of experimentation and the increasing social rejection against animal testing. Indeed, the development of this new *in vitro* methodology could contribute to the 3R principle applied in European laboratories that aims to reduce the number of animals used in research to the minimum strictly necessary following the 2010/63/EU directive instructions.

Additionally, the different formulations of silica hybrid sol-gel materials systematically designed to be applied as coatings in dental implants, trying to achieve their bioactivation, can result useful in dental implantology field, being able to suppose an advance in the development of this type of treatments. Moreover, the proteomic characterization carried out on these materials could aid to better understand their interaction with tissues and as these systems bioactivate implants

REFERENCES

[1] United Nation, Agein, (2018). http://www.un.org/en/sections/issues-depth/ageing/index.html (accessed May 10, 2018).

[2] European commission, Founding programmes: Horizon 2020, (2018). https://ec.europa.eu/programmes/horizon2020/en/h2020-section/health-demographic-change-and-wellbeing (accessed May 10, 2018).

[3] A.M. Collignon, J. Lesieur, C. Vacher, C. Chaussain, G.Y. Rochefort, Strategies developed to induce, direct, and potentiate bone healing, Front. Physiol. 8 (2017) 1–8. doi:10.3389/fphys.2017.00927.

[4] D.F. Williams, The Williams dictionary of biomaterials, Liverpool University Press, Liverpool, 1999.

[5] D.F. Williams, On the nature of biomaterials, Biomaterials. 30 (2009) 5897–5909. doi:10.1016/j.biomaterials.2009.07.027.

[6] R.J. Narayan, The next generation of biomaterial development, Philos. Trans. R. Soc. A Math. Phys. Eng. Sci. 368 (2010) 1831–1837. doi:10.1098/rsta.2010.0001.

[7] D.F. Williams, On the mechanisms of biocompatibility, Biomaterials. 29 (2008) 2941–2953. doi:10.1016/j.biomaterials.2008.04.023.

[8] B.D. Ratner, The biocompatibility manifesto: Biocompatibility for the twenty-first century, J. Cardiovasc. Transl. Res. 4 (2011) 523–527. doi:10.1007/s12265-011-9287-x.

[9] E.S. Corada, España es líder en implantologia a nivel mundial, La Razón. (2017). https://www.larazon.es/atusalud/salud/espana-es-lider-en-implantologia-a-nivel-mundial-NC15711936 (accessed May 20, 2018).

[10] Technological Advancements and Elderly Populations Lead to Increased Preference for Dental Implants, GBI Res. (2013). http://gbiresearch.com/media-center/press-releases/technological-advancements-and-elderly-populations-lead-to-increased-preference-for-dental-implants (accessed May 20, 2018).

[11] J. Henkel, M.A. Woodruff, D.R. Epari, R. Steck, V. Glatt, I.C. Dickinson, P.F.M. Choong, M.A. Schuetz, D.W. Hutmacher, Bone Regeneration Based on Tissue Engineering Conceptions — A 21st Century Perspective, Bone Res. 1 (2013) 216–248. doi:10.4248/BR201303002.

[12] N. Gurav, B. Buranawat, L. Di Silvio, Biological Characterization of Biomaterials: In-vitro Tests, in: L. Rimondini, C. Bianchi, E. Vernè (Eds.), Surf. Tailoring Inorg. Mater. Biomed.

Appl., Bentham Science Publishers, Naples, 2012: pp. 207–223.

[13] M. Ansede, La UE rechaza la petición ciudadana de prohibir la experimentación animal, El Pais. (2015). https://elpais.com/elpais/2015/06/03/ciencia/1433332057_271437.html.

[14] Legislation for the protection of animals used for scientific purposes, Eur. Comm. (2016). http://ec.europa.eu/environment/chemicals/lab_animals/legislation_en.htm (accessed May 20, 2018).

[15] N. Kohli, S. Ho, S.J. Brown, P. Sawadkar, V. Sharma, M. Snow, E. García-Gareta, Bone remodelling in vitro : Where are we headed?, Bone. 110 (2018) 38–46. doi:10.1016/j.bone.2018.01.015.

[16] G. Hulsart-Billström, J.I. Dawson, S. Hofmann, R. Müller, M.J. Stoddart, M. Alini, H. Redl, A. El Haj, R. Brown, V. Salih, J. Hilborn, S. Larsson, R.O.C. Oreffo, A surprisingly poor correlation between in vitro and in vivo testing of biomaterials for bone regeneration: Results of a multicentre analysis, Eur. Cells Mater. 31 (2016) 312–322. doi:10.22203/eCM.v031a20.

[17] M. Gasik, Understanding biomaterial-tissue interface quality: combined in vitro evaluation, Sci. Technol. Adv. Mater. 18 (2017) 550–562. doi:10.1080/14686996.2017.1348872.

[18] J. Bailey, M. Thew, M. Balls, An analysis of the use of animal models in predicting human toxicology and drug safety., Altern. to Lab. Anim. 42 (2014) 181–199.

[19] W.M. Gallagher, I. Lynch, L.T. Allen, I. Miller, S.C. Penney, D.P. O'Connor, S. Pennington, A.K. Keenan, K.A. Dawson, Molecular basis of cell-biomaterial interaction: Insights gained from transcriptomic and proteomic studies, Biomaterials. 27 (2006) 5871–5882. doi:10.1016/j.biomaterials.2006.07.040.

[20] K. Duval, H. Grover, L.-H. Han, Y. Mou, A.F. Pegoraro, J. Fredberg, Z. Chen, Modeling physiological events in 2D vs. 3D cell culture, Physiology. 32 (2017) 266–277. doi:10.1152/physiol.00036.2016.

[21] B.A. Justice, N.A. Badr, R.A. Felder, 3D cell culture opens new dimensions in cell-based assays, Drug Discov. Today. 14 (2009) 102–107. doi:10.1016/j.drudis.2008.11.006.

[22] Z. Othman, B. Cillero Pastor, S. van Rijt, P. Habibovic, Understanding interactions between biomaterials and biological systems using proteomics, Biomaterials. 167 (2018) 191–204. doi:10.1016/j.biomaterials.2018.03.020.

[23] L.T. Allen, M. Tosetto, I.S. Miller, D.P. O'Connor, S.C. Penney, I. Lynch, A.K. Keenan, S.R. Pennington, K.A. Dawson, W.M. Gallagher, Surface-induced changes in protein adsorption and implications for cellular phenotypic responses to surface interaction, Biomaterials. 27

(2006) 3096–3108. doi:10.1016/j.biomaterials.2006.01.019.

[24] S.H. Ralston, Bone structure and metabolism, Medicine. 45 (2017) 560–564. doi:10.1016/j.mpmed.2017.06.008.

[25] K.K. Nishiyama, S.K. Boyd, In vivo assessment of trabecular and cortical bone microstructure, Clin. Calcium. 21 (2011) 1011–1019. doi:CliCa110710111019.

[26] P.I. Brånemark, B.O. Hansson, R. Adell, U. Breine, J. Lindström, O. Hallén, A. Ohman, Osseointegrated implants in the treatment of the edentulous jaw. Experience from a 10-year period, Scand. J. Plast. Reconstr. Surg. Suppl. 16 (1977) 1–132.

[27] P.I. Branemark, Osseointegration and its experimental background, J. Prosthet. Dent. 50 (1983) 399–410. doi:10.1016/S0022-3913(83)80101-2.

[28] C. Colnot, D.M. Romero, S. Huang, J. Rahman, J.A. Currey, A. Nanci, J.B. Brunski, J.A. Helms, Molecular analysis of healing at a bone-implant interface, J. Dent. Res. 86 (2007) 862–867. doi:10.1177/154405910708600911.

[29] D.D. Bosshardt, V. Chappuis, D. Buser, Osseointegration of titanium, titanium alloy and zirconia dental implants: current knowledge and open questions, Periodontol. 2000. 73 (2017) 22–40. doi:10.1111/prd.12179.

[30] A. Barfeie, J. Wilson, J. Rees, Implant surface characteristics and their effect on osseointegration, Br. Dent. J. 218 (2015) 1–9. doi:10.1038/sj.bdj.2015.171.

[31] H. Terheyden, N.P. Lang, S. Bierbaum, B. Stadlinger, Osseointegration - communication of cells, Clin. Oral Implants Res. 23 (2012) 1127–1135. doi:10.1111/j.1600-0501.2011.02327.x.

[32] A. Chug, S. Shukla, L. Mahesh, S. Jadwani, Osseointegration-Molecular events at the bone-implant interface: A review, J. Oral Maxillofac. Surgery, Med. Pathol. 25 (2013) 1–4. doi:10.1016/j.ajoms.2012.01.008.

[33] N.A. Hotaling, L. Tang, D.J. Irvine, J.E. Babensee, Biomaterial Strategies for Immunomodulation, Annu. Rev. Biomed. Eng. 17 (2015) 317–349. doi:10.1146/annurev-bioeng-071813-104814.

[34] D.F. Willians, Review Tissue-biomaterial interactions, J. Mater. Sci. 22 (1987) 3421–3445. doi:10.1007/bf01161439.

[35] T. Albrektsson, C. Johansson, Osteoinduction, osteoconduction and osseointegration, Eur. Spine J. 10 (2001) S96–S101. doi:10.1007/s005860100282.

[36] E. Calciolari, N. Donos, The use of omics profiling to improve outcomes of bone regeneration and osseointegration. How far are we from personalized medicine in dentistry?, J. Proteomics. 18 (2018) 30048–4. doi:10.1016/j.jprot.2018.01.017.

[37] G. Raffaini, F. Ganazzoli, Understanding the performance of biomaterials through molecular modeling: Crossing the bridge between their intrinsic properties and the surface adsorption of proteins, Macromol. Biosci. 7 (2007) 552–566. doi:10.1002/mabi.200600278.

[38] I. Lynch, T. Cedervall, M. Lundqvist, C. Cabaleiro-Lago, S. Linse, K.A. Dawson, The nanoparticle-protein complex as a biological entity; a complex fluids and surface science challenge for the 21st century, Adv. Colloid Interface Sci. 134–135 (2007) 167–174. doi:10.1016/j.cis.2007.04.021.

[39] M. Rabe, D. Verdes, S. Seeger, Understanding protein adsorption phenomena at solid surfaces., Adv. Colloid Interface Sci. 162 (2011) 87–106. doi:10.1016/j.cis.2010.12.007.

[40] E.A. Vogler, Protein adsorption in three dimensions, Biomaterials. 33 (2012) 1201–1237. doi:10.1016/j.biomaterials.2011.10.059.

[41] C.J. Wilson, R.E. Clegg, D.I. Leavesley, M.J. Pearcy, Mediation of Biomaterial–Cell Interactions by Adsorbed Proteins: A Review, Tissue Eng. 11 (2005) 1–18. doi:10.1089/ten.2005.11.1.

[42] Q. Wei, T. Becherer, S. Angioletti-Uberti, J. Dzubiella, C. Wischke, A.T. Neffe, A. Lendlein, M. Ballauff, R. Haag, Protein interactions with polymer coatings and biomaterials, Angew. Chemie - Int. Ed. 53 (2014) 8004–8031. doi:10.1002/anie.201400546.

[43] I. Firkowska-Boden, X. Zhang, K.D. Jandt, Controlling Protein Adsorption through Nanostructured Polymeric Surfaces, Adv. Healthc. Mater. 7 (2018) 1–19. doi:10.1002/adhm.201700995.

[44] M. Kastantin, B.B. Langdon, D.K. Schwartz, A bottom-up approach to understanding protein layer formation at solid-liquid interfaces, Adv. Colloid Interface Sci. 207 (2014) 240–252. doi:10.1016/j.cis.2013.12.006.

[45] I. Langmuir, Vapor pressures, evaporation, condensation and adsorption, J. Am. Chem. Soc. 54 (1932) 2798–2832. doi:10.1021/ja01346a022.

[46] S.L. Hirsh, D.R. McKenzie, N.J. Nosworthy, J.A. Denman, O.U. Sezerman, M.M.M. Bilek, The Vroman effect: Competitive protein exchange with dynamic multilayer protein aggregates, Colloids Surfaces B Biointerfaces. 103 (2013) 395–404. doi:10.1016/j.colsurfb.2012.10.039.

[47] P. Koutsoukos, W. Norde, J. Lyklema, Protein adsorption on hematite (α-Fe2O3) surfaces, J. Colloid Interface Sci. 95 (1983) 385–397. doi:10.1016/0021-9797(83)90198-4.

[48] N. Afara, S. Omanovic, M. Asghari-Khiavi, Functionalization of a gold surface with fibronectin (FN) covalently bound to mixed alkanethiol self-assembled monolayers (SAMs): The influence of SAM composition on its physicochemical properties and FN surface secondary structure, Thin Solid Films. 522 (2012) 381–389. doi:10.1016/j.tsf.2012.08.025.

[49] K.M. Evans-Nguyen, L.R. Tolles, O. V. Gorkun, S.T. Lord, M.H. Schoenfisch, Interactions of thrombin with fibrinogen adsorbed on methyl-, hydroxyl-, amine-, and carboxyl-terminated self-assembled monolayers, Biochemistry. 44 (2005) 15561–15568. doi:10.1021/bi0514358.

[50] A. Quinn, H. Mantz, K. Jacobs, M. Bellion, L. Santen, Protein adsorption kinetics in different surface potentials, EPL. 81 (2008) 56003. doi:10.1209/0295-5075/81/56003.

[51] A. Sethuraman, M. Han, R.S. Kane, G. Belfort, Effect of surface wettability on the adhesion of proteins, Langmuir. 20 (2004) 7779–7788. doi:10.1021/la049454q.

[52] B.P. Frank, G. Belfort, Atomic force microscopy for low-adhesion surfaces: Thermodynamic criteria, critical surface tension, and intermolecular forces, Langmuir. 17 (2001) 1905–1912. doi:10.1021/la0011533.

[53] R.A. Hartvig, M. Van De Weert, J. ??stergaard, L. Jorgensen, H. Jensen, Protein adsorption at charged surfaces: The role of electrostatic interactions and interfacial charge regulation, Langmuir. 27 (2011) 2634–2643. doi:10.1021/la104720n.

[54] E. Luong-Van, I. Rodriguez, H.Y. Low, N. Elmouelhi, B. Lowenhaupt, S. Natarajan, C.T. Lim, R. Prajapati, M. Vyakarnam, K. Cooper, Review: Micro-and nanostructured surface engineering for biomedical applications, J. Mater. Res. 28 (2013) 165–174. doi:10.1557/jmr.2012.398.

[55] N. Giamblanco, E. Martines, G. Marletta, Laminin adsorption on nanostructures: Switching the molecular orientation by local curvature changes, Langmuir. 29 (2013) 8335–8342. doi:10.1021/la304644z.

[56] I. Lynch, Are there generic mechanisms governing interactions between nanoparticles and cells? Epitope mapping the outer layer of the protein-material interface, Phys. A Stat. Mech. Its Appl. 373 (2007) 511–520. doi:10.1016/j.physa.2006.06.008.

[57] J.Y. Lim, J.C. Hansen, C.A. Siedlecki, J. Runt, H.J. Donahue, Human foetal osteoblastic cell response to polymer-demixed nanotopographic interfaces, J. R. Soc. Interface. 2 (2005) 97–108. doi:10.1098/rsif.2004.0019.

[58] H.T. Shiu, B. Goss, C. Lutton, R. Crawford, Y. Xiao, Formation of blood clot on biomaterial implants influences bone healing, Tissue Eng. - Part B Rev. 20 (2014). doi:10.1089/ten.teb.2013.0709.

[59] G. Sidhu, G.A. Soff, The Coagulation System and Angiogenesis, in: D. Green, H.C. Kwaan (Eds.), Coagul. Cancer, Springer, Chicago, 2009: pp. 67–82.

[60] S.R. Coughlin, Thrombin signalling and protease-activated receptors, Nature. 407 (2000) 258–264. doi:10.1038/35025229.

[61] H.A. Scheraga, The thrombin-fibrinogen interaction, Biophys. Chem. 112 (2004) 117–130. doi:10.1016/j.bpc.2004.07.011.

[62] M. Hulander, J. Hong, M. Andersson, F. Gervén, M. Ohrlander, P. Tengvall, H. Elwing, Blood interactions with noble metals: Coagulation and immune complement activation, ACS Appl. Mater. Interfaces. 1 (2009) 1053–1062. doi:10.1021/am900028e.

[63] C. Sperling, M. Fischer, M.F. Maitz, C. Werner, Blood coagulation on biomaterials requires the combination of distinct activation processes, Biomaterials. 30 (2009) 4447–4456. doi:10.1016/j.biomaterials.2009.05.044.

[64] L.C. Xu, J.W. Bauer, C.A. Siedlecki, Proteins, platelets, and blood coagulation at biomaterial interfaces, Colloids Surfaces B Biointerfaces. 124 (2014) 49–68. doi:10.1016/j.colsurfb.2014.09.040.

[65] D.M. Monroe, M. Hoffman, What does it take to make the perfect clot?, Arterioscler. Thromb. Vasc. Biol. 26 (2006) 41–48. doi:10.1161/01.ATV.0000193624.28251.83.

[66] U.H. Lerner, Regulation of bone metabolism by the kallikrein-kinin system, the coagulation cascade, and the acute-phase reactants, Oral Surgery, Oral Med. Oral Pathol. 78 (1994) 481–493. doi:10.1016/0030-4220(94)90043-4.

[67] R.A.S. Ariëns, Novel mechanisms that regulate clot structure/function, Thromb. Res. 141S2 (2016) S25–S27. doi:10.1016/S0049-3848(16)30358-9.

[68] J. Hong, A. Azens, K.N. Ekdahl, C.G. Granqvist, B. Nilsson, Material-specific thrombin generation following contact between metal surfaces and whole blood, Biomaterials. 26 (2005) 1397–1403. doi:10.1016/j.biomaterials.2004.05.036.

[69] J. Hong, J. Andersson, K.N. Ekdahl, G. Elgue, N. Axén, R. Larsson, B. Nilsson, Titanium is a highly thrombogenic biomaterial: Possible implications for osteogenesis, Thromb. Haemost. 82 (1999) 58–64. doi:10.1055/s-0037-1614630.

[70] A.J. Chu, Blood coagulation as an intrinsic pathway for proinflammation: a mini review., Inflamm. Allergy Drug Targets. 9 (2010) 32–44. doi:10.2174/187152810791292890.

[71] K. Brummel-Ziedins, K.G. Mann, Molecular Basis of Blood Coagulation, in: Hematology, Seventh Ed, Elsevier Inc., 2018: p. 1885–1905.e8. doi:10.1016/B978-0-323-35762-3.00126-8.

[72] H. Weidmann, L. Heikaus, A.T. Long, C. Naudin, H. Schlüter, T. Renné, The plasma contact system, a protease cascade at the nexus of inflammation, coagulation and immunity, Biochim. Biophys. Acta - Mol. Cell Res. (2017). doi:10.1016/j.bbamcr.2017.07.009.

[73] J. Sánchez, P.B. Lundquist, G. Elgue, R. Larsson, P. Olsson, Measuring the degree of plasma contact activation induced by artificial materials, Thromb. Res. 105 (2002) 407–412. doi:10.1016/S0049-3848(02)00051-8.

[74] J. Konings, L.R. Hoving, R.S. Ariëns, E.L. Hethershaw, M. Ninivaggi, L.J. Hardy, B. De Laat, H. Ten Cate, H. Philippou, J.W.P. Govers-Riemslag, The role of activated coagulation factor XII in overall clot stability and fibrinolysis, Thromb. Res. 136 (2015) 474–480. doi:10.1016/j.thromres.2015.06.028.

[75] C. Wehner, K. Janjić, H. Agis, Relevance of the plasminogen system in physiology, pathology, and regeneration of oral tissues – From the perspective of dental specialties, Arch. Oral Biol. 74 (2017) 136–145. doi:10.1016/j.archoralbio.2016.09.014.

[76] Y. Shen, Y. Guo, P. Mikus, R. Sulniute, M. Wilczynska, T. Ny, J. Li, Plasminogen is a key proinflammatory regulator that accelerates the healing of acute and diabetic wounds, Blood. 119 (2012) 5879–5887. doi:10.1182/blood-2012-01-407825.

[77] D.C. Rijken, H.R. Lijnen, New insights into the molecular mechanisms of the fibrinolytic system, J. Thromb. Haemost. 7 (2009) 4–13. doi:10.1111/j.1538-7836.2008.03220.x.

[78] J.C. Chapin, K.A. Hajjar, Fibrinolysis and the control of blood coagulation, Blood Rev. 29 (2015) 17–24. doi:10.1016/j.blre.2014.09.003.

[79] D.F. Draxler, R.L. Medcalf, The fibrinolytic system-more than fibrinolysis?, Transfus. Med. Rev. 29 (2015) 102–109. doi:10.1016/j.tmrv.2014.09.006.

[80] M. Yuasa, N.A. Mignemi, J.S. Nyman, C.L. Duvall, H.S. Schwartz, A. Okawa, T. Yoshii, G. Bhattacharjee, C. Zhao, J.E. Bible, W.T. Obremskey, M.J. Flick, J.L. Degen, J. V. Barnett, J.M.M. Cates, J.G. Schoenecker, Fibrinolysis is essential for fracture repair and prevention of heterotopic ossification, J. Clin. Invest. 125 (2015) 3117–3131. doi:10.1172/JCI80313.

[81] J. Folkman, Y. Shing, Angiogenesis., J. Biol. Chem. 267 (1992) 10931–10934.

http://www.ncbi.nlm.nih.gov/pubmed/1375931.

[82] A.N.N. Hoeben, B. Landuyt, M.S.M. Highley, H. Wildiers, A.T.V.A.N. Oosterom, E.A.D.E. Bruijn, A.T. Van Oosterom, E.A. De Bruijn, Vascular endothelial growth factor and angiogenesis., Pharmacol. Rev. 56 (2004) 549–580. doi:10.1124/pr.56.4.3.549.

[83] M. Potente, H. Gerhardt, P. Carmeliet, Basic and therapeutic aspects of angiogenesis, Cell. 146 (2011) 873–887. doi:10.1016/j.cell.2011.08.039.

[84] P. Carmeliet, R.K. Jain, Molecular mechanisms and clinical applications of angiogenesis, Nature. 473 (2011) 298–307. doi:10.1038/nature10144.

[85] G.A. McMahon, E. Petitclerc, S. Stefansson, E. Smith, M.K.K. Wong, R.J. Westrick, D. Ginsburg, P.C. Brooks, D.A. Lawrence, Plasminogen Activator Inhibitor-1 Regulates Tumor Growth and Angiogenesis, J. Biol. Chem. 276 (2001) 33964–33968. doi:10.1074/jbc.M105980200.

[86] I. Kourtzelis, S. Rafail, R.A. DeAngelis, P.G. Foukas, D. Ricklin, J.D. Lambris, Inhibition of biomaterial-induced complement activation attenuates the inflammatory host response to implantation, FASEB J. 27 (2013) 2768–2776. doi:10.1096/fj.12-225888.

[87] R. Lubbers, M.F. van Essen, C. van Kooten, L.A. Trouw, Production of complement components by cells of the immune system, Clin. Exp. Immunol. 188 (2017) 183–194. doi:10.1111/cei.12952.

[88] N.S. Merle, S.E. Church, V. Fremeaux-Bacchi, L.T. Roumenina, Complement system part I - molecular mechanisms of activation and regulation, Front. Immunol. 6 (2015) 1–30. doi:10.3389/fimmu.2015.00262.

[89] K. Murphy, P. Travers, M. Walport, The complement system and innate immunity., Janeway's Immunobiol. 7 (2008) 61–81. doi:10.1086/596249.

[90] E. Hein, P. Garred, The Lectin Pathway of Complement and Biocompatibility, in: J.D. Lambris, K.N. Ekdahl, D. Ricklin, B. Nilsson (Eds.), Immune Responses to Biosurfaces, Springer International Publishing, Switzerland, 2015: pp. 77–92. doi:10.1007/978-3-319-18603-0.

[91] D. Ricklin, G. Hajishengallis, K. Yang, J.D. Lambris, Complement: a key system for immune surveillance and homeostasis., Nat. Immunol. 11 (2010) 785–97. doi:10.1038/ni.1923.

[92] K.N. Ekdahl, J.D. Lambris, H. Elwing, D. Ricklin, P.H. Nilsson, Y. Teramura, I.A. Nicholls, B. Nilsson, Innate immunity activation on biomaterial surfaces: A mechanistic model and coping strategies, Adv. Drug Deliv. Rev. 63 (2011) 1042–1050.

doi:10.1016/j.addr.2011.06.012.

[93] T.E. Mollnes, M. Kirschfink, Strategies of therapeutic complement inhibition, Mol. Immunol. 43 (2006) 107–121. doi:10.1016/j.molimm.2005.06.014.

[94] P.F. Zipfel, C. Skerka, Complement regulators and inhibitory proteins, Nat. Rev. Immunol. 9 (2009) 729–740. doi:10.1038/nri2620.

[95] Y.K. Kim, E.Y. Chen, W.F. Liu, Biomolecular strategies to modulate the macrophage response to implanted materials, J. Mater. Chem. B. 4 (2016) 1600–1609. doi:10.1039/C5TB01605C.

[96] K. Nilsson-Ekdahl, B. Nilsson, C.G. Gölander, H. Elwing, B. Lassen, U.R. Nilsson, C. Golander, Gustaf, C.G. Golander, Complement activation on radio frequency plasma modified polystyrene surfaces, J. Colloid Interface Sci. 158 (1993) 121–128. doi:10.1006/jcis.1993.1236.

[97] E. Allémann, P. Gravel, J.C. Leroux, L. Balant, R. Gurny, Kinetics of blood component adsorption on poly(D,L-lactic acid) nanoparticles: Evidence of complement C3 component involvement, J. Biomed. Mater. Res. 37 (1997) 229–234. doi:10.1002/(SICI)1097-4636(199711)37:2<229::AID-JBM12>3.0.CO;2-9.

[98] A.E. Engberg, P.H. Nilsson, S. Huang, K. Fromell, O.A. Hamad, T.E. Mollnes, J.P. Rosengren-Holmberg, K. Sandholm, Y. Teramura, I.A. Nicholls, B. Nilsson, K.N. Ekdahl, Prediction of inflammatory responses induced by biomaterials in contact with human blood using protein fingerprint from plasma, Biomaterials. 36 (2015) 55–65. doi:10.1016/j.biomaterials.2014.09.011.

[99] R. Sridharan, A.R. Cameron, D.J. Kelly, C.J. Kearney, F.J. O'Brien, Biomaterial based modulation of macrophage polarization: A review and suggested design principles, Mater. Today. 18 (2015) 313–325. doi:10.1016/j.mattod.2015.01.019.

[100] M. Shen, I. Garcia, R. V. Maier, T.A. Horbett, Effects of adsorbed proteins and surface chemistry on foreign body giant cell formation, tumor necrosis factor alpha release and procoagulant activity of monocytes, J. Biomed. Mater. Res. 70A (2004) 533–541. doi:10.1002/jbm.a.30069.

[101] S. Babaei, N. Fekete, C.A. Hoesli, P.L. Girard-Lauriault, Adhesion of human monocytes to oxygen- and nitrogen- containing plasma polymers: Effect of surface chemistry and protein adsorption, Colloids Surfaces B Biointerfaces. 162 (2018) 362–369. doi:10.1016/j.colsurfb.2017.12.003.

[102] J.M. Anderson, A. Rodriguez, D.T. Chang, Foreign body reaction to biomaterials, Semin.

Immunol. 20 (2008) 86–100. doi:10.1016/j.smim.2007.11.004.

[103] C.R. Jenney, J.M. Anderson, Adsorbed serum proteins responsible for surface dependent human macrophage behavior, J. Biomed. Mater. Res. 49 (2000) 435–447. doi:10.1002/(SICI)1097-4636(20000315)49:4<435::AID-JBM2>3.0.CO;2-Y.

[104] K. Oikonomopoulou, D. Ricklin, P.A. Ward, J.D. Lambris, Interactions between coagulation and complement - Their role in inflammation, Semin. Immunopathol. 34 (2012) 151–165. doi:10.1007/s00281-011-0280-x.

[105] J.T. Triffitt, C.J. Joyner, R.O.C. Oreffo, A.S. Virdi, Osteogenesis: Bone development from primitive progenitors, Biochem. Soc. Trans. 26 (1998) 21–27. doi:10.1042/bst0260021.

[106] M. Majidinia, A. Sadeghpour, B. Yousefi, The roles of signaling pathways in bone repair and regeneration, J. Cell. Physiol. (2017) 2937–2948. doi:10.1002/jcp.26042.

[107] A. Hayrapetyan, J.A. Jansen, J.J.J.P. van den Beucken, Signaling Pathways Involved in Osteogenesis and Their Application for Bone Regenerative Medicine, Tissue Eng. Part B Rev. 21 (2015) 75–87. doi:10.1089/ten.teb.2014.0119.

[108] K. Senarath-Yapa, S. Li, N.P. Meyer, M.T. Longaker, N. Quarto, Integration of multiple signaling pathways determines differences in the osteogenic potential and tissue regeneration of neural crest-derived and mesoderm-derived calvarial bones, Int. J. Mol. Sci. 14 (2013) 5978–5997. doi:10.3390/ijms14035978.

[109] F. Deschaseaux, L. Sensébé, D. Heymann, Mechanisms of bone repair and regeneration, Trends Mol. Med. 15 (2009) 417–429. doi:10.1016/j.molmed.2009.07.002.

[110] S. Maeda, M. Hayashi, S. Komiya, T. Imamura, K. Miyazono, Endogenous TGF-β signaling suppresses maturation of osteoblastic mesenchymal cells, EMBO J. 23 (2004) 552–563. doi:10.1038/sj.emboj.7600067.

[111] G.S. Anusuya, M. Kandasamy, S.A.J. Raja, S. Sabarinathan, P. Ravishankar, B. Kandhasamy, Bone morphogenetic proteins: Signaling periodontal bone regeneration and repair, J. Pharm. Bioallied Sci. 8 (2016) S39–S41. doi:10.4103/0975-7406.191964.

[112] Y. Chen, B.A. Alman, Wnt pathway, an essential role in bone regeneration, J. Cell. Biochem. 106 (2009) 353–362. doi:10.1002/jcb.22020.

[113] D.G. Monroe, M.E. McGee-Lawrence, M.J. Oursler, J.J. Westendorf, Update on Wnt signaling in bone cell biology and bone disease, Gene. 492 (2012) 1–18. doi:10.1016/j.gene.2011.10.044.

[114] C.A. Conover, Insulin-like growth factor-binding proteins and bone metabolism, Am. J. Physiol. - Endocrinol. Metab. 294 (2008) E10–E14. doi:10.1152/ajpendo.00648.2007.

[115] V. Ulici, K.D. Hoenselaar, H. Agoston, D.D. McErlain, J. Umoh, S. Chakrabarti, D.W. Holdsworth, F. Beier, The role of Akt1 in terminal stages of endochondral bone formation: Angiogenesis and ossification, Bone. 45 (2009) 1133–1145. doi:10.1016/j.bone.2009.08.003.

[116] A.M.C. Barradas, H.A.M. Fernandes, N. Groen, Y.C. Chai, J. Schrooten, J. van de Peppel, J.P.T.M. van Leeuwen, C.A. van Blitterswijk, J. de Boer, A calcium-induced signaling cascade leading to osteogenic differentiation of human bone marrow-derived mesenchymal stromal cells., Biomaterials. 33 (2012) 3205–15. doi:10.1016/j.biomaterials.2012.01.020.

[117] J.O. Hollinger, C.E. Hart, S.N. Hirsch, S. Lynch, G.E. Friedlaender, Recombinant human platelet-derived growth factor: Biology and clinical applications, J. Bone Jt. Surg. - Ser. A. 90 (2008) 48–54. doi:10.2106/JBJS.G.01231.

[118] X. Chen, J. Wang, Y. Chen, H. Cai, X. Yang, X. Zhu, Y. Fan, X. Zhang, Roles of calcium phosphate-mediated integrin expression and MAPK signaling pathways in the osteoblastic differentiation of mesenchymal stem cells, J. Mater. Chem. B. 4 (2016) 2280–2289. doi:10.1039/C6TB00349D.

[119] F. Zhu, M. t Sweetmyne, K.D. Hankerson, PKCd Is Required for Jagged-1 Induction of Human Mesenchymal Stem Cell Osteogenic Differentiation FENGCHANG, Stem Cells. 31 (2013) 1181–1192. doi:Doi 10.1002/Stem.1353.

[120] D.M. Ornitz, P.J. Marie, FGF signaling pathways in endochondral and intramembranous bone development and human genetic disease, Genes Dev. 16 (2002) 1446–1465. doi:10.1101/gad.990702.ized.

[121] R.M. Salasznyk, R.F. Klees, M.K. Hughlock, G.E. Plopper, ERK Signaling Pathways Regulate the Osteogenic Differentiation of Human Mesenchymal Stem Cells on Collagen I and Vitronectin, Cell Commun. Adhes. 11 (2004) 137–153. doi:10.1080/15419060500242836.

[122] M. Morra, C. Cassinelli, G. Cascardo, P. Cahalan, L. Cahalan, M. Fini, R. Giardino, Surface engineering of titanium by collagen immobilization. Surface characterization and in vitro and in vivo studies, Biomaterials. 24 (2003) 4639–4654. doi:10.1016/S0142-9612(03)00360-0.

[123] A. Jikko, S.E. Harris, D. Chen, D.L. Mendrick, C.H. Damsky, Collagen integrin receptors regulate early osteoblast differentiation induced by BMP-2, J. Bone Miner. Res. 14 (1999) 1075–1083. doi:10.1359/jbmr.1999.14.7.1075.

[124] A.K. Kundu, A.J. Putnam, Vitronectin and collagen I differentially regulate osteogenesis in mesenchymal stem cells., Biochem. Biophys. Res. Commun. 347 (2006) 347–57. doi:10.1016/j.bbrc.2006.06.110.

[125] W.S. To, K.S. Midwood, Plasma and cellular fibronectin: distinct and independent functions during tissue repair, Fibrogenesis Tissue Repair. 4 (2011) 21. doi:10.1186/1755-1536-4-21.

[126] A.B. Faia-Torres, T. Goren, T.O. Ihalainen, S. Guimond-Lischer, M. Charnley, M. Rottmar, K. Maniura-Weber, N.D. Spencer, R.L. Reis, M. Textor, N.M. Neves, Regulation of Human Mesenchymal Stem Cell Osteogenesis by Specific Surface Density of Fibronectin: a Gradient Study, ACS Appl. Mater. Interfaces. 7 (2015) 2367–2375. doi:10.1021/am506951c.

[127] F. Kidway, J. Edwards, L. Zou, D. Kaufman, Fibrinogen Induces RUNX2 Activity and Osteogenic Development from Human Pluripotent Stem Cells, Stem Cells. 34 (2016) 2079–2089. doi:http://dx.doi.org/ 10.1002/stem.2427.

[128] D. Bächner, D. Schröder, N. Betat, M. Ahrens, G. Gross, Apolipoprotein E (ApoE), a Bmp-2 (bone morphogenetic protein) upregulated gene in mesenchymal progenitors (C3H10T1/2), is highly expressed in murine embryonic development, BioFactors. 9 (1999) 11–17. doi:10.1002/biof.5520090103.

[129] F. Posa, A. Di Benedetto, E.A. Cavalcanti-Adam, G. Colaianni, C. Porro, T. Trotta, G. Brunetti, L. Lo Muzio, M. Grano, G. Mori, Vitamin D promotes MSC osteogenic differentiation stimulating cell adhesion and αVβ3 expression, Stem Cells Int. 2018 (2018). doi:10.1155/2018/6958713.

[130] V. Nicolin, D. De Iaco, R. Valentini, Osteoimmunology represents a link between skeletal and immune system, Ital. J. Anat. Embrylogy. 121 (2016) 37–42. doi:10.13128/IJAE-18342.

[131] T. Ono, H. Takayanagi, Osteoimmunology in Bone Fracture Healing, Curr. Osteoporos. Rep. 15 (2017) 367–375. doi:10.1007/s11914-017-0381-0.

[132] D.S. Amarasekara, H. Yun, S. Kim, N. Lee, H. Kim, J. Rho, Regulation of Osteoclast Differentiation by Cytokine Networks, Immune Netw. 18 (2018) 1–18. doi:10.4110/in.2018.18.e8.

[133] M.S. Nanes, Osteoimmunology and the Osteoblast, in: Osteoimmunology, Elsevier, 2016: pp. 71–81. doi:10.1016/B978-0-12-800571-2.00005-0.

[134] Z. Chen, T. Klein, R.Z. Murray, R. Crawford, J. Chang, C. Wu, Y. Xiao, Osteoimmunomodulation for the development of advanced bone biomaterials, Mater. Today. 19 (2016) 304–321. doi:10.1016/j.mattod.2015.11.004.

[135] N.L. Anderson, N.G. Anderson, Proteome and proteomics: new technologies, new concepts, and new words, Electrophoresis. 19 (1998) 1853–1861. doi:10.1002/elps.1150191103.

[136] Z.W. Lai, Y. Yan, F. Caruso, E.C. Nice, Emerging techniques in proteomics for probing nano-bio interactions, ACS Nano. 6 (2012) 10438–10448. doi:10.1021/nn3052499.

[137] E.C. Nice, J. Rothacker, J. Weinstock, L. Lim, B. Catimel, Use of multidimensional separation protocols for the purification of trace components in complex biological samples for proteomics analysis, J. Chromatogr. A. 1168 (2007) 190–210. doi:10.1016/j.chroma.2007.06.015.

[138] B. Domon, R. Aebersold, Mass spectrometry and protein analysis., Science. 312 (2006) 212–7. doi:10.1126/science.1124619.

[139] H.J. Griesser, P. Kingshott, S.L. McArthur, K.M. McLean, G.R. Kinsel, R.B. Timmons, Surface-MALDI mass spectrometry in biomaterials research, Biomaterials. 25 (2004) 4861–4875. doi:10.1016/j.biomaterials.2004.01.049.

[140] T. Fröhlich, G.J. Arnold, Proteome research based on modern liquid chromatography - Tandem mass spectrometry: Separation, identification and quantification, J. Neural Transm. 113 (2006) 973–994. doi:10.1007/s00702-006-0509-3.

[141] K.A. Power, K.T. Fitzgerald, W.M. Gallagher, Examination of cell-host-biomaterial interactions via high-throughput technologies: A re-appraisal, Biomaterials. 31 (2010) 6667–6674. doi:10.1016/j.biomaterials.2010.05.029.

[142] J. Xu, A.K. Khiam, J. Sui, J. Zhang, L.T. Tuan, N.C. Wei, Comparative proteomics profile of osteoblasts cultured on dissimilar hydroxyapatite biomaterials: An iTRAQ-coupled 2-D LC-MS/MS analysis, Proteomics. 8 (2008) 4249–4258. doi:10.1002/pmic.200800103.

[143] E. Calciolari, N. Mardas, X. Dereka, A.K. Anagnostopoulos, G.T. Tsangaris, N. Donos, Protein expression during early stages of bone regeneration under hydrophobic and hydrophilic titanium domes. A pilot study, J. Periodontal Res. 53 (2018) 174–187. doi:10.1111/jre.12498.

[144] V. Serpooshan, M. Mahmoudi, M. Zhao, K. Wei, S. Sivanesan, K. Motamedchaboki, A. V. Malkovskiy, A.B. Goldstone, J.E. Cohen, P.C. Yang, J. Rajadas, D. Bernstein, Y.J. Woo, P. Ruiz-Lozano, Protein Corona Influences Cell-Biomaterial Interactions in Nanostructured Tissue Engineering Scaffolds, Adv. Funct. Mater. 25 (2015) 4379–4389. doi:10.1002/adfm.201500875.

[145] E. Fröhlich, Role of omics techniques in the toxicity testing of nanoparticles, J.

Nanobiotechnology. 15 (2017) 1–22. doi:10.1186/s12951-017-0320-3.

[146] C.G. Dodo, P.M. Senna, W. Custodio, A.F. Paes Leme, A.A. Del Bel Cury, Proteome analysis of the plasma protein layer adsorbed to a rough titanium surface., Biofouling. 29 (2013) 549–57. doi:10.1080/08927014.2013.787416.

[147] S. Oughlis, S. Lessim, S. Changotade, F. Bollotte, F. Poirier, G. Helary, J.J. Lataillade, V. Migonney, D. Lutomski, Development of proteomic tools to study protein adsorption on a biomaterial, titanium grafted with poly(sodium styrene sulfonate), J. Chromatogr. B Anal. Technol. Biomed. Life Sci. 879 (2011) 3681–3687. doi:10.1016/j.jchromb.2011.10.006.

[148] H. Kaneko, J. Kamiie, H. Kawakami, T. Anada, Y. Honda, N. Shiraishi, S. Kamakura, T. Terasaki, H. Shimauchi, O. Suzuki, Proteome analysis of rat serum proteins adsorbed onto synthetic octacalcium phosphate crystals., Anal. Biochem. 418 (2011) 276–85. doi:10.1016/j.ab.2011.07.022.

[149] K. Sugimoto, S. Tsuchiya, M. Omori, R. Matsuda, M. Fujio, K. Kuroda, M. Okido, H. Hibi, Proteomic analysis of bone proteins adsorbed onto the surface of titanium dioxide, Biochem. Biophys. Reports. 7 (2016). doi:10.1016/j.bbrep.2016.07.007.

[150] M.N. Abdallah, S.D. Tran, G. Abughanam, M. Laurenti, D. Zuanazzi, M.A. Mezour, Y. Xiao, M. Cerruti, W.L. Siqueira, F. Tamimi, Biomaterial surface proteomic signature determines interaction with epithelial cells, Acta Biomater. 54 (2017) 150–163. doi:10.1016/j.actbio.2017.02.044.

[151] M.D. Swartzlander, C.A. Barnes, A.K. Blakney, J.L. Kaar, T.R. Kyriakides, S.J. Bryant, Linking the foreign body response and protein adsorption to PEG-based hydrogels using proteomics, Biomaterials. 41 (2015) 26–36. doi:10.1016/j.biomaterials.2014.11.026.

[152] D. Duraccio, F. Mussano, M.G. Faga, Biomaterials for dental implants: current and future trends, J. Mater. Sci. 50 (2015). doi:10.1007/s10853-015-9056-3.

[153] M.J. Jackson, J. Kopac, M. Balazic, D. Bombac, M. Brojan, F. Kosel, Titanium and titanium alloy applications in medicine, in: M. Jackson, A. Waqar (Eds.), Surf. Eng. Surg. Tools Med. Devices, Second edi, Springer, Boston, 2017: pp. 475–518. doi:10.1007/978-0-387-27028-9_15.

[154] T. Hanawa, A comprehensive review of techniques for biofunctionalization of titanium, J. Periodontal Implant Sci. 41 (2011) 263–272. doi:10.5051/jpis.2011.41.6.263.

[155] S. Anil, P.S. Anand, H. Alghamdi, J.A. Janse, Dental Implant Surface Enhancement and Osseointegration, Implant Dent. - A Rapidly Evol. Pract. (2011). doi:10.5772/16475.

[156] R. Junker, A. Dimakis, M. Thoneick, J.A. Jansen, Effects of implant surface coatings and composition on bone integration: A systematic review, Clin. Oral Implants Res. 20 (2009) 185–206. doi:10.1111/j.1600-0501.2009.01777.x.

[157] R. Smeets, B. Stadlinger, F. Schwarz, B. Beck-broichsitter, O. Jung, C. Precht, F. Kloss, A. Gröbe, M. Heiland, T. Ebker, Review Article Impact of Dental Implant Surface Modifications on Osseointegration, Biomed Res. Int. 2016 (2016) 1–16.

[158] A.A. John, S.K. Jaganathan, E. Supriyanto, A. Manikandan, Surface modification of titanium and its alloys for the enhancement of osseointegration in orthopaedics, Curr. Sci. 111 (2016) 1003–1015. doi:10.18520/cs/v111/i6/1003-1015.

[159] A. Jemat, M.J. Ghazali, M. Razali, Y. Otsuka, Surface modifications and their effects on titanium dental implants, Biomed Res. Int. 2015 (2015). doi:10.1155/2015/791725.

[160] L. Le Guéhennec, A. Soueidan, P. Layrolle, Y. Amouriq, Surface treatments of titanium dental implants for rapid osseointegration, Dent. Mater. (2007). doi:10.1016/j.dental.2006.06.025.

[161] A. Civantos, E. Martínez-Campos, V. Ramos, C. Elvira, A. Gallardo, A. Abarrategi, Titanium Coatings and Surface Modifications: Toward Clinically Useful Bioactive Implants, ACS Biomater. Sci. Eng. 3 (2017) 1245–1261. doi:10.1021/acsbiomaterials.6b00604.

[162] K. Subramani, Titanium Surface Modification Techniques for Implant Fabrication – From Microscale to the Nanoscale, J. Biomim. Biomater. Tissue Eng. 5 (2010) 39–56. doi:10.4028/www.scientific.net/JBBTE.5.39.

[163] J.R. Jones, Reprint of: Review of bioactive glass: From Hench to hybrids, Acta Biomater. 23 (2015) S53–S82. doi:10.1016/j.actbio.2015.07.019.

[164] H. Reuter, Sol-gel processes, Adv. Mater. 3 (1991) 258–259. doi:10.1002/adma.19910030510.

[165] C.J. Brinker, G.W. Scherer, Sol-gel Science - The Physics and Chemistry of Sol-gel Processing, Elsevier Academic Press, San Diego, 1990.

[166] G. Schottner, Hybrid sol-gel-derived polymers: Applications of multifunctional materials, Chem. Mater. 13 (2001) 3422–3435. doi:10.1021/cm011060m.

[167] G.J. Owens, R.K. Singh, F. Foroutan, M. Alqaysi, C.M. Han, C. Mahapatra, H.W. Kim, J.C. Knowles, Sol-gel based materials for biomedical applications, Prog. Mater. Sci. 77 (2016) 1–79. doi:10.1016/j.pmatsci.2015.12.001.

[168] K. Tsuru, Z. Robertson, B. Annaz, I.R. Gibson, S.M. Best, Y. Shirosaki, S. Hayakawa, A. Osaka, Sol-Gel Synthesis and In Vitro Cell Compatibility Analysis of Silicate-Containing Biodegradable Hybrid Gels, Key Eng. Mater. 361–363 (2008) 447–450. doi:10.4028/www.scientific.net/KEM.361-363.447.

[169] M. Łączka, K. Cholewa-Kowalska, A.M. Osyczka, Bioactivity and osteoinductivity of glasses and glassceramics and their material determinants, Ceram. Int. 42 (2016) 14313–14325. doi:10.1016/j.ceramint.2016.06.077.

[170] H. Podbielska, a Ulatowska-Jarza, Sol-gel technology for biomedical engineering, Bull. Polish Acad. Sci. 53 (2005) 261–271. doi:10.1.1.510.5860.

[171] D. Arcos, M. Vallet-Regí, Sol-gel silica-based biomaterials and bone tissue regeneration., Acta Biomater. 6 (2010) 2874–88. doi:10.1016/j.actbio.2010.02.012.

[172] E.-J. Kim, S.-Y. Bu, M.-K. Sung, M.-K. Choi, Effects of Silicon on Osteoblast Activity and Bone Mineralization of MC3T3-E1 Cells, Biol. Trace Elem. Res. 152 (2013) 105–112. doi:10.1007/s12011-012-9593-4.

[173] M. Wiens, X. Wang, H.C. Schröder, U. Kolb, U. Schloßmacher, H. Ushijima, W.E.G. Müller, The role of biosilica in the osteoprotegerin/RANKL ratio in human osteoblast-like cells, Biomaterials. 31 (2010) 7716–7725. doi:10.1016/j.biomaterials.2010.07.002.

[174] M. Catauro, F. Bollino, F. Papale, C. Ferrara, P. Mustarelli, Silica–polyethylene glycol hybrids synthesized by sol–gel: Biocompatibility improvement of titanium implants by coating, Mater. Sci. Eng. C. 55 (2015) 118–125. doi:10.1016/j.msec.2015.05.016.

[175] M. Catauro, F. Papale, F. Bollino, S. Piccolella, S. Marciano, P. Nocera, S. Pacifico, Silica/quercetin sol–gel hybrids as antioxidant dental implant materials, Sci. Technol. Adv. Mater. 16 (2015) 35001. doi:10.1088/1468-6996/16/3/035001.

[176] M. Hernández-Escolano, M.J. Juan-Díaz, M. Martinez-Ibáñez, J. Suay, I. Goñii, M. Gurruchaga, Synthesis of hybrid sol-gel materials and their biological evaluation with human mesenchymal stem cells, J. Mater. Sci. Mater. Med. 24 (2013) 1491–1499. doi:10.1007/s10856-013-4900-y.

[177] M.J. Juan-Dí-az, M. Martí-nez-Ibáñez, I. Lara-Sáez, S. da Silva, R. Izquierdo, M. Gurruchaga, I. Goñi, J. Suay, Development of hybrid sol–gel coatings for the improvement of metallic biomaterials performance, Prog. Org. Coatings. 96 (2015) 42–51. doi:10.1016/j.porgcoat.2016.01.019.

[178] M. Martínez-Ibáñez, M.J. Juan-Díaz, I. Lara-Saez, A. Coso, J. Franco, M. Gurruchaga, J. Suay Antón, I. Goñi, Biological characterization of a new silicon based coating developed for

dental implants., J. Mater. Sci. Mater. Med. 27 (2016) 80. doi:10.1007/s10856-016-5690-9.

[179] M.J. Juan-Díaz, M. Martínez-Ibáñez, M. Hernández-Escolano, L. Cabedo, R. Izquierdo, J. Suay, M. Gurruchaga, I. Goñi, Study of the degradation of hybrid sol–gel coatings in aqueous medium, Prog. Org. Coatings. 77 (2014) 1799–1806. doi:10.1016/j.porgcoat.2014.06.004.

[180] J. Oshiro Junior, M. Paiva Abuçafy, E. Berbel Manaia, B. Lallo da Silva, B. Chiari-Andréo, L. Aparecida Chiavacci, Drug Delivery Systems Obtained from Silica Based Organic-Inorganic Hybrids, Polymers (Basel). 8 (2016) 91. doi:10.3390/polym8040091.

[181] J.C. Almeida, A. Wacha, P.S. Gomes, L.C. Alves, M.H.V. Fernandes, I.M.M. Salvado, M.H.R. Fernandes, A biocompatible hybrid material with simultaneous calcium and strontium release capability for bone tissue repair, Mater. Sci. Eng. C. 62 (2016) 429–438. doi:10.1016/j.msec.2016.01.083.

[182] M. Martinez-Ibañez, I. Aldalur, F.J. Romero-Gavilán, J. Suay, I. Goñi, M. Gurruchaga, Design of nanostructured siloxane-gelatin coatings: Immobilization strategies and dissolution properties, J. Non. Cryst. Solids. 481 (2018) 368–374. doi:10.1016/j.jnoncrysol.2017.11.010.

[183] A. Hoppe, N.S. Güldal, A.R. Boccaccini, A review of the biological response to ionic dissolution products from bioactive glasses and glass-ceramics, Biomaterials. 32 (2011) 2757–2774. doi:10.1016/j.biomaterials.2011.01.004.

[184] P. Valerio, M.M. Pereira, A.M. Goes, M.F. Leite, Effects of extracellular calcium concentration on the glutamate release by bioactive glass (BG60S) preincubated osteoblasts., Biomed. Mater. 4 (2009) 45011. doi:10.1088/1748-6041/4/4/045011.

[185] P.J. Marie, The calcium-sensing receptor in bone cells: A potential therapeutic target in osteoporosis, Bone. 46 (2010) 571–576. doi:10.1016/j.bone.2009.07.082.

[186] M.M. Dvorak, D. Riccardi, Ca2+ as an extracellular signal in bone, Cell Calcium. 35 (2004) 249–255. doi:10.1016/j.ceca.2003.10.014.

[187] P. Habibovic, J.E. Barralet, Bioinorganics and biomaterials: bone repair., Acta Biomater. 7 (2011) 3013–26. doi:10.1016/j.actbio.2011.03.027.

[188] S. Maeno, Y. Niki, H. Matsumoto, H. Morioka, T. Yatabe, A. Funayama, Y. Toyama, T. Taguchi, J. Tanaka, The effect of calcium ion concentration on osteoblast viability, proliferation and differentiation in monolayer and 3D culture, Biomaterials. 26 (2005) 4847–4855. doi:10.1016/j.biomaterials.2005.01.006.

[189] J. Gessmann, D. Seybold, E. Peter, T.A. Schildhauer, M. Köller, Plasma clots gelled by different amounts of calcium for stem cell delivery, Langenbeck's Arch. Surg. 398 (2013) 161–167. doi:10.1007/s00423-012-1015-8.

[190] S.C. Verberckmoes, M.E. De Broe, P.C. D'Haese, Dose-dependent effects of strontium on osteoblast function and mineralization, Kidney Int. 64 (2003) 534–543. doi:10.1046/j.1523-1755.2003.00123.x.

[191] S. Hesaraki, M. Gholami, S. Vazehrad, S. Shahrabi, The effect of Sr concentration on bioactivity and biocompatibility of sol-gel derived glasses based on CaO-SrO-SiO2-P2O5quaternary system, Mater. Sci. Eng. C. 30 (2010) 383–390. doi:10.1016/j.msec.2009.12.001.

[192] J. Isaac, J. Nohra, J. Lao, E. Jallot, J.M. Nedelec, A. Berdal, J.M. Sautier, Effects of Strontium-Doped Bioactive Glass on the Differentiation of Cultured Osteogenic Cells, Eur. Cell. Mater. 21 (2011) 130–143. doi:10.22203/eCM.v021a11.

[193] N. Neves, D. Linhares, G. Costa, C.C. Ribeiro, M.A. Barbosa, In vivo and clinical application of strontium-enriched biomaterials for bone regeneration: A systematic review., Bone Joint Res. 6 (2017) 366–375. doi:10.1302/2046-3758.66.BJR-2016-0311.R1.

[194] Y. Li, Q. Li, S. Zhu, E. Luo, J. Li, G. Feng, Y. Liao, J. Hu, The effect of strontium-substituted hydroxyapatite coating on implant fixation in ovariectomized rats, Biomaterials. 31 (2010) 9006–9014. doi:10.1016/j.biomaterials.2010.07.112.

[195] W.-T. Su, W.-L. Chou, C.-M. Chou, Osteoblastic differentiation of stem cells from human exfoliated deciduous teeth induced by thermosensitive hydrogels with strontium phosphate, Mater. Sci. Eng. C. 52 (2015) 46–53. doi:10.1016/j.msec.2015.03.025.

[196] S. Omar, F. Repp, P.M. Desimone, R. Weinkamer, W. Wagermaier, S. Ceré, J. Ballarre, Sol-gel hybrid coatings with strontium-doped 45S5 glass particles for enhancing the performance of stainless steel implants: Electrochemical, bioactive and in vivo response, J. Non. Cryst. Solids. (2015). doi:10.1016/j.jnoncrysol.2015.05.024.

2. CHAPTER 1

Control of the degradation of silica sol-gel hybrid coatings for metal implants prepared by the triple combination of alkoxysilanes

2. Chapter 1

Control of the degradation of silica sol-gel hybrid coatings for metal implants prepared by the triple combination of alkoxysilanes.

F. Romero-Gavilán[1], S. Barros-Silva[1], J. García-Cañadas[1], B. Palla[2], R. Izquierdo[1], M. Gurruchaga[2], I. Goñi[2], J. Suay[1]

[1] Department of Industrial Systems and Design, Universitat Jaume I, Av. Vicent-Sos Baynat s/n. Castellón, 12071 Spain.

[2] Facultad de Ciencias Químicas. Universidad del País Vasco. P. M. de Lardizábal, 3. San Sebastián 20018. Spain.

Journal of Non-Crystalline Solids (2016)

ABSTRACT

Hybrid materials obtained by sol-gel process are able to degrade and release Si compounds that are useful in regenerative medicine due to their osteoinductive properties. The present work studies the behaviour of new organic-inorganic sol-gel coatings based on triple mixtures of alkoxysilanes in different molar ratios. The precursors employed are methyl-trimethoxysilane (MTMOS), 3-glycidoxypropyl-trimethoxysilane (GPTMS) and tetraethyl-orthosilicate (TEOS). After optimization of the synthesis conditions, the coatings were characterized using 29Si nuclear magnetic resonance (29Si-MNR), Fourier transform infrared spectrometry (FT-IR), contact angle measurements, hydrolytic degradation assays, electrochemical impedance spectroscopy (EIS) and mechanical profilometry. The degradation and EIS results show that by controlling the amount of TEOS precursor in the coating it is possible to tune its degradation by hydrolysis, while keeping properties such as wettability at their optimum values for biomaterials application. The corrosion properties of the new coatings were also evaluated when applied to stainless steel substrate. The coatings showed an improvement of the anticorrosive properties of the steel which is important to protect the metal implants at the early stages of the regeneration process.

Keywords: Si release, corrosion resistance, TEOS, biomaterials, coatings.

Graphical abstract

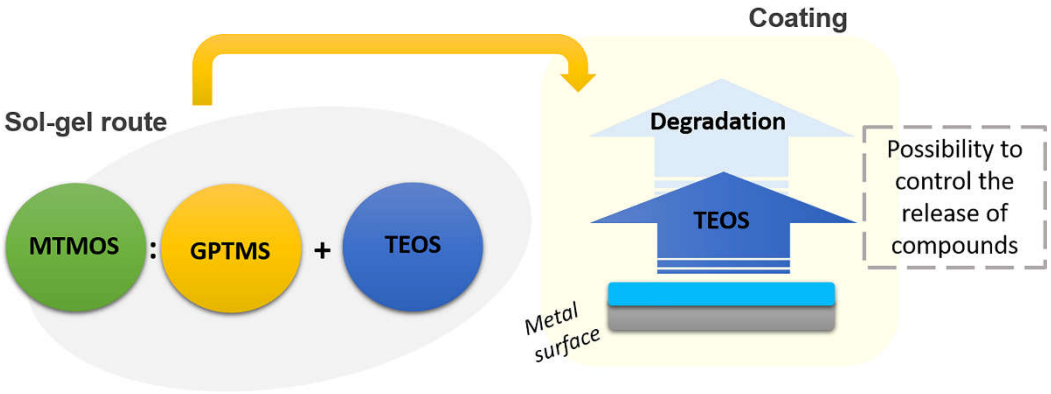

Figure 2.0. Graphical abstract of the work named "Control of the degradation of silica sol-gel hybrid coatings for metal implants prepared by the triple combination of alkoxysilanes".

2.1. Introduction

In implantology, metal implants are the most frequently used materials, being titanium and its alloys the most widely used. This is due to their low density, high resistance to corrosion, good mechanical properties and its biocompatibility [1]. However, these materials are bio-inert and damage in their protective oxide layer that provides their corrosion resistive properties, can produce implant failure. Studies about implants failure suggest that some of the faults may be due to the diffusion of corrosion products through the surrounding tissues as a result of the degradation of the titanium dioxide layer [2,3]. Another problem in the use of titanium as an implant is its high cost, which is the reason behind the still significant demand for surgical grade stainless steel implants in some countries. Stainless steel possesses worse properties and a higher risk of failure than titanium [4]. Both, the need to protect the metal to prevent the release of corrosion products and the functionalization of metal implants surface in order to improve their biological interaction are required for the development of new implant coatings.

The sol-gel technique allows developing coatings in a relatively inexpensive way which confers the implant surface the desired properties by means of an appropriate selection of precursors and the optimization of the synthesis parameters. These coatings are biocompatible, able to release Si compounds with osteoinductive properties, protecting the implant against corrosion, and enable the functionalization of the metal surface to achieve the desired cellular response to improve tissue regeneration [5–9].

Within the sol-gel materials, there is a growing interest in organic-inorganic silicon materials synthesized via sol-gel [10]. For this reason, this work focuses on the implant surface bioactivation via hybrid sol-gel coatings from alkoxysilanes, which are used due to their possibility to more easily regulate key properties such as the hydrophilic behaviour and degradability [11]. These materials have already been used in biomedical applications due to their osteoinductive capabilities [12,13], as delivery vehicles of drugs [14,15], or as antibacterial agents to enhance the strength of implants to yeast infections [16,17].

This osteoinductive capability of the hybrid sol-gel materials is attributed to their ability to release silicon compounds during the hydrolytic degradation of the sol-gel network [7,18]. Silicon is an

essential element for the metabolic processes associated with the formation and calcification of bone [19]. It develops a biological crosslinking agent role, which contributes to the resistance architecture and connective tissues [20]. In addition, the presence of Si in the $Si(OH)_4$ form promotes the synthesis of collagen type I and enhances osteoblastic differentiation [20,21]. Consequently, the degradation control is a way to regulate the bioactivity degree of coatings.

Ballarre *et al.* developed hybrid sol-gel coatings based on the combination of several layers on surgical grade stainless steel to enhance their anticorrosive properties, demonstrating their protective capabilities [22]. Catauro *et al.* succeeded in improving the bioactivity and biocompatibility of grade 4 titanium dental implants by employing sol-gel hybrid coatings synthesized from polyethylene glycol (PEG) and TEOS in different ratios [13]. Juan-Diaz *et al.* developed hybrid sol-gel coatings, using methyl-trimethoxysilane (MTMOS) and TEOS as alkoxysilanes in 10:0, 9:1, 8:2 and 7:3 molar ratios and studied their degradation. This characterization suggested the ability to regulate the degradation of such materials by modifying their composition in order to design suitable controlled-released vehicles [14]. Another research study developed hybrid sol-gel coatings with different percentages of MTMOS and 3-glycidoxypropyl-trimethoxysilane (GPTMS) as precursors to enhance the osseointegration ability of titanium dental implants [18]. These materials showed a good *in vitro* behaviour with an improvement in the proliferation and mineralization respect to titanium, being this effect more pronounced for the 1:1 MTMOS:GPTMS ratio. However, the *in vivo* response was not as good as was expected due to the formation of a fibrous capsule, probably as a consequence of the poor degradation kinetics.

The aim of this work is the development of organic-inorganic sol-gel coatings through triple-precursor compositions based on the combination of alkoxysilanes (MTMOS, GPTMS and TEOS). The addition of TEOS into MTMOS:GPTMS coatings, which already show a good *in vitro* behaviour [18] is expected to allow the control of the degradation kinetics and hence improve the osseointegration ability of metallic implants. Simultaneously, the coating should protect the implant during the first stage post-implantation, being then necessary a balance between degradation and protection. The study of this compromise is conducted by hydrolytic degradation and electrochemical impedance spectroscopy (EIS) tests.

2.2. Materials and methods

2.2.1. Sol-gel synthesis

The synthesis process of the hybrid coatings was based in a sol-gel route employing MTMOS, TEOS and GPTMS (Sigma-Aldrich, St. Louis, MO, USA) as precursors. Different compositions of these precursors were used as shown in Table 2.1. 2-Propanol (Sigma-Aldrich) was used in the process to improve the mixing of the siloxanes in a volume ratio alcohol:siloxane 1:1. Precursor hydrolysis was performed by adding the corresponding stoichiometric amount of an acidified aqueous solution 0.1 M HNO_3 (Panreac, Barcelona, Spain) to catalyze the reaction. The solution was kept 1 h under stirring and then 1 h at rest. The samples were prepared from the corresponding sol-gel solution immediately after this time.

Table 2.1. Molar percentage of the materials under study.

	MTMOS (%)	***GPTMS (%)***	***TEOS (%)***
50M50G	50	50	0
45M45G10T	45	45	10
35M35G30T	35	35	30
25M25G50T	25	25	50
15M15G70T	15	15	70
5M5G90T	5	5	90

2.2.2. Coating preparation

Three different processes were adopted for the sample preparation as required by the different characterization methods. Firstly, AISI 316-L stainless steel plates (5 cm x 5 cm, RNSinox S.L.) were used as substrates. The surfaces of the plates were polished and then cleaned with acetone to remove impurities. After cleaning, the film deposition was performed employing a dip-coater (KSV DC; KSV NIMA, Espoo, Finland). Plates were immersed into the previously prepared sol-gel solutions at a speed of 60 cm min^{-1}, then kept immersed for one minute, and finally they were removed at a 100 cm min^{-1} speed. After the corresponding heat treatment (Table 2), the adhesion was evaluated by means of the cross-cut test (UNE EN-ISO 2409:2013). Once proved that the

highest adherence value, i.e. 0, was obtained, the thickness of the coatings prepared was measured by mechanical profilometry (Dektack 6; Veeco, NY, USA). Two distinct samples identically prepared were tested, performing 3 measurements per sample.

Secondly, glass slides were used as substrates of the coatings. The glass surfaces were previously cleaned in an ultrasonic bath (Sonoplus HD 3200) for 20 min at 30 W with nitric acid solution at 25 % volume. Then a further cleaning was carried out with distilled water under the same conditions. After being dried at 100 °C, the glass slides were coated by the flow-coating technique.

Finally, free films of materials were obtained by pouring the sol-gel solutions into non-stick Teflon molds. Samples were cured under the conditions described in Table 2.2, which shows the minimum temperatures required to obtain homogeneous and well-cured films.

Table 2. Heat treatment conditions applied to each sol-gel composition.

Composition	*50M50G*	*45M45G10T*	*35M35G30T*	*25M25G50T*	*15M15G70T*	*5M5G90T*
Curing temperature (ºC)	140	100	80	80	80	80
Curing time (min)	120	120	120	120	120	120

2.2.3. Chemical characterization

Attenuated total reflection (ATR) analysis was performed on the free film samples using a Fourier-transform infrared spectrometer (Model FTIR 6700, NICOLET) to analyse the chemical composition of the sol-gel materials. Before each measurement, a background FTIR spectrum was taken and deducted from the sample spectra. All spectra were recorded in the 600 - 4000 cm^{-1} wavelength range.

Solid-state 29Si-NMR spectroscopy was used to evaluate the crosslinking density of the silicon network after the thermal processing. Free films were used for this purpose. The spectra were obtained using a Bruker 400 AVANCE II WB Plus spectrometer, equipped with a Cross Polarization Magic Angle Spinning (CP-MAS) probe. The samples were placed inside a 4 mm rotor sample tube.

The spinning speed was 7.0 kHz. The pulse sequence employed was the Bruker standard: 79.5 MHz frequency, spectral width of 55 KHz, 2 ms contact time and 5 s delay time.

2.2.4. Physico-chemical characterization

The wettability of the sol-gel coating was determined by the measurement of the contact angle. An automatic contact angle meter Dataphysics OCA 20 (DataPhysics Instruments, Filderstadt, Germany) was used to measure this parameter. 10 µL of ultrapure water were deposited on the hybrid sol-gel coated steel plates at room temperature. The drops were formed with a dossing rate of 27.5 µL s^{-1} and the angles were determined with the aid of SCA 20 software. Reported values are the average of 60 measurements obtained at different spots of three different samples identically prepared. Roughness of the material on coated steel plates was assessed using a mechanical profilometer Dektack 6 (Veeco). Three individual measurements were performed to obtain each value.

The anticorrosive properties of the sol-gel coatings were evaluated by EIS measurements, which were carried out on the samples deposited on the steel substrates at different exposure times to 3.5 % wt. NaCl in deionized water for up to 48 h. The exposure surface area was 3.14 cm^2. A three-electrode electrochemical cell was employed. The sample without coating acted as the working electrode, a Ag/AgCl electrode was used as reference and a graphite sheet was employed as counter-electrode. Measurements were obtained using an Autolab Ecochemie PGSTAT30 potentiostat equipped with a frequency response analyser module. The tests were conducted at the free corrosion potential. A frequency ranges from 10 mHz to 100 kHz with a sinusoidal voltage perturbation of 10 mV amplitude was applied to the system. Experiments were performed inside a Faraday cage in order to minimize external interference. Measurements were carried out at 0, 1.5, 3, 4, 6, 8, 10, 24 and 48 h of exposure at room temperature. All tests were repeated at least three times in order to check reproducibility. Two equal results are considered valid and the results shown are from the most representative sample.

The hydrolytic degradation of the coatings was evaluated using the materials deposited on glass slides. The kinetics of degradation was determined by means of the weight loss in the samples before and after soaking in 100 mL distilled water at 37 ºC for periods of 7, 14, 28, 42 and 63 days.

The samples were dried in a vacuum oven at 37 ºC for 48 h before and after soaking. Each data point is the mean of three measurements performed in three different samples identically prepared.

2.3. **Results**

2.3.1. Chemical characterization

The degree of condensation of the materials synthesized from the alkoxysilanes was studied by ^{29}Si solid NMR. The nomenclature used in the analysis of the results was described in reference [23]. T^n and Q^n represents the trifunctional and tetrafunctional silicon, respectively, while the superscript n shows the number of bonded oxygens to silicon. Figure 2.1 shows the NMR spectra of the fabricated films.

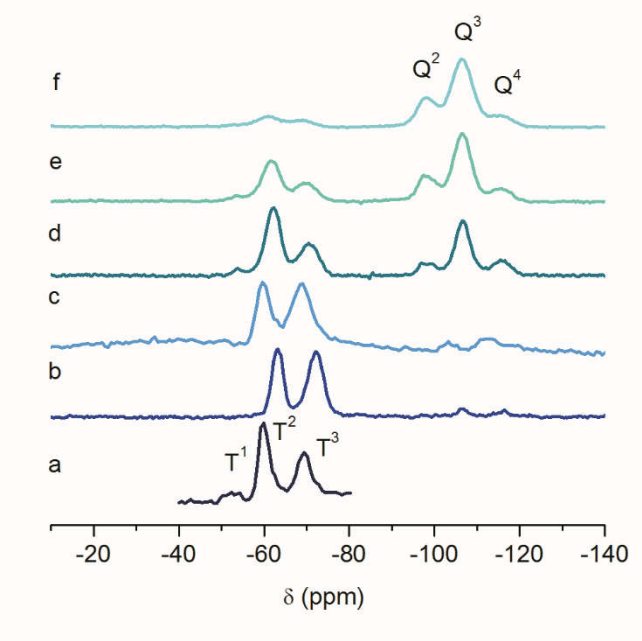

Figure 2.1. ^{29}Si solid NMR of (a) 50M50G, (b) 45M45G10T, (c) 35M35G30T, (d) 25M25G50T, (e) 15M15G70T and (f) 5M5G90T films.

For the composition 50M50G, the signal associated to T^1, T^2 and T^3 species can be observed, being the most intense and the weakest the signals with two (T^2) and only one (T^1) oxygens bonded to

the silicon atom, respectively. It should be mentioned that the recorded signal for the 50M50G spectrum only covers the -40 to -80 ppm chemical shift range since no response is usually observed for chemical shifts more negative than -80 ppm [18].

The NMR spectra when TEOS precursor is introduced in the films are also given in Figure 2.1 (spectra b to f). These spectra, apart from T^n species from MTMOS and GPTMS, show Q^2, Q^3 and Q^4 signals from TEOS. When the ratio of TEOS is increased it is observed that the signals Q^n become more intense and T^n are attenuated, due to the reduced number of MTMOS and GPTMS species in the sol-gel network. The addition of TEOS causes the almost total suppression of T^1 signal and the intensity increase of T^3 peak, especially at low TEOS content (spectra b and c). Thus, in materials 45M45G10T and 35M35G30T the intensity of the signals from T^2 species is quite similar to T^3 (spectra b and c in Figure 2.1). However, when the percentage of TEOS increases, T^2 becomes more intense than T^3 (spectra d, e and f) and Q^2 increases respect to Q^4 (spectra e and f).

Figure 2.2 shows the IR spectra of the sol-gel networks. The bands associated with the vibrational modes of the Si-O-Si chains were detected at ~780, ~1010 and ~1100 cm^{-1}, which are due to the formation of the inorganic network [24,25]. The bands related to the vibrational modes of OH groups (3200-3500 cm^{-1}) and Si-OH terminals (~890 cm^{-1}) were also observed [24,25]. The bands detected between 2870 and 2950 cm^{-1} indicate the presence of C-H bonds and the band at ~1265 cm^{-1} correspond to Si-C [25]. All these signals show the presence of organic matter introduced through the MTMOS and GPTMS precursors. These signals become less intense in those materials with the highest proportion of TEOS and nearly disappear for the 5M5G90T composition (spectrum f).

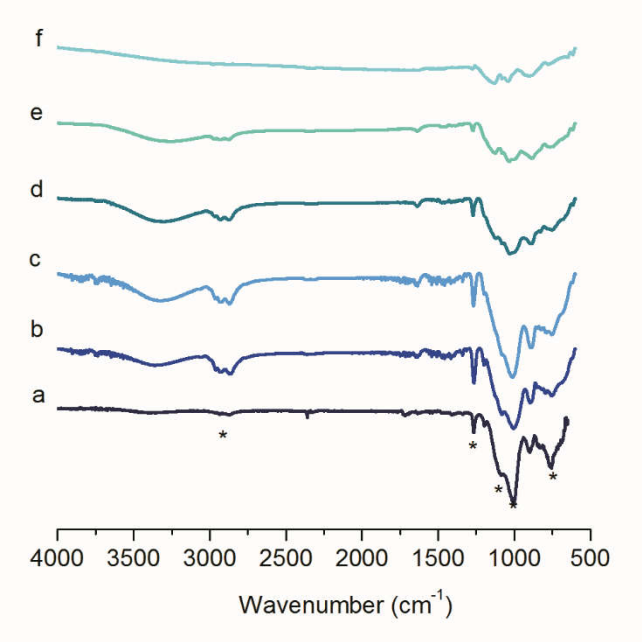

Figure 2.2. FTIR spectra of (a) 50M50G, (b) 45M45G10T, (c) 35M35G30T, (d) 25M25G50T, (e) 15M15G70T and (f) 5M5G90T films.

2.3.2. Contact angle

The wettability of the formulations was studied by means of contact angle measurements. Results are shown in Figure 2.3. It is observed that the addition of TEOS to the sol-gel network in moderate amounts decreases the contact angle, i.e., the material becomes more hydrophilic. However, the contact angle increases after reaching a minimum for the 30 % TEOS film when the TEOS percentage is increased further.

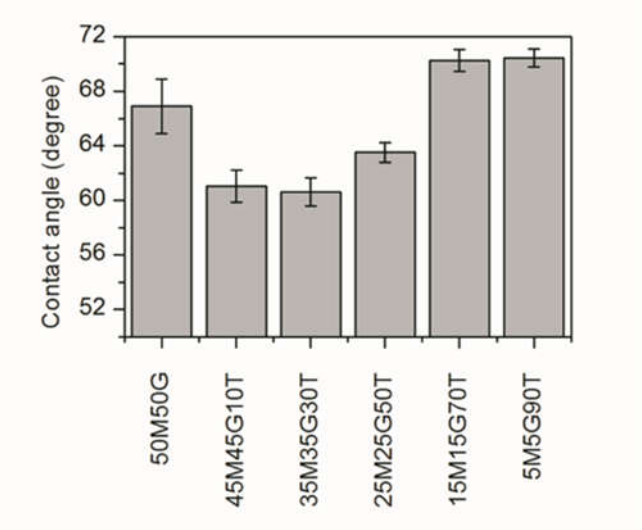

Figure 2.3. Contact angle results for films deposited on stainless steel substrates with different MTMOS:GPTMS:TEOS molar ratios. Bars indicate standard deviations.

2.3.3. Morphological characterization

Figure 2.4 shows the coating thickness measurements. When is added up to 70 % of TEOS, the coating thicknesses have a value between 0.87 – 1.18 µm without statistically significant differences between them. However, the 5M5G90T composition shows a markedly smaller thickness compared with the other materials.

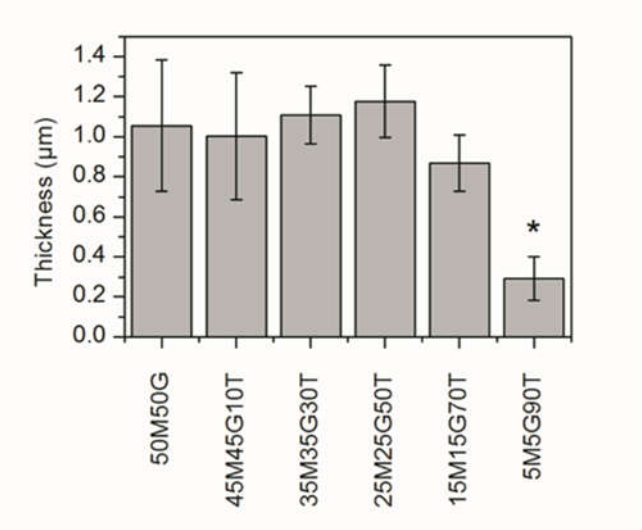

Figure 2.4. Coating thickness measured by mechanical profilometry of sol-gel coatings prepared onto stainless steel plates by dip-coating. Statistically significant differences were found in the 5M5G90T coating thickness respect the other materials (ANOVA, * $p < 0.05$). Bars indicate the standard deviations.

Table 2.3 shows the average surface roughness values (Ra) and their standard deviations. The reference material 50M50G shows a Ra value of 288.7 ± 73.1 Å. When TEOS is introduced into the structure, it is observed that Ra increases to a maximum (788.5 ± 3.5 Å) for the 35M35G30T composition. However, further TEOS addition produces a less rough surface and a value of 475.7 ± 81.7 Å is reached for 5M5G90T composition.

Table 2.3. Ra values and their standard deviations for steel plates coated with MTMOS:GPTMS:TEOS materials in different ratios.

Material	Ra (Å)
50M50G	288.7 ± 73.1
45M45G10T	659.5 ± 50.2
35M35G30T	788.5 ± 3.5
25M25G50T	646.3 ± 33.3
15M15G70T	496.7 ± 26.8
5M5G90T	475.7± 81.7

2.3.4. EIS

Stainless steel plates were coated with 50M50G, 45M45G10T, 35M35G30T, 25M25G50T, 15M15G70T and 5M5G90T materials to perform the EIS tests. After 48 h of testing, the coatings showed degradation signs, being this more significant in the case of the compositions with higher TEOS percentages (70% and 90%). Figure 2.5 shows the results obtained.

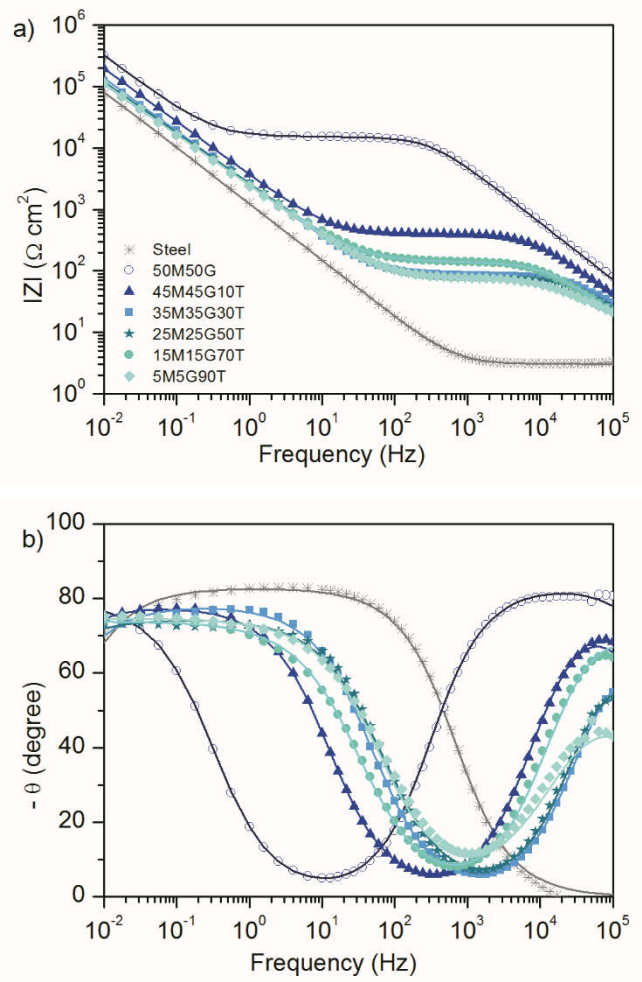

Figure 2.5. (a) Impedance modules and (b) phase angel bode plots for stainless steel, 50M50G, 45M45G10T, 35M35G30T, 25M25G50T, 15M15G70T and 5M5G90T sol-gel coatings at 8 h of immersion in the electrolyte. Fitted results are represented by the solid lines.

It is observed that the impedance values decrease when TEOS is added in the sol-gel network (Figure 2.5a). It should be noted that the variation in the impedance module values with time is less significant at the highest TEOS content, reaching nearly no variation (Figure 2.5a) for the films with the highest TEOS composition. Despite the introduction of this precursor in the sol-gel structure both impedance module and phase angle maintain a similar shape to the plot obtained for the 50M50G material, so no additional process is introduced by the presence of TEOS.

The EIS spectra were fitted to equivalent circuits using Z-view software. For the coating with bare stainless steel only the natural formation of the oxide layer in the steel was observed. However, samples with sol-gel coatings present two processes, the first one related to the coating at high frequencies and the other at low frequencies to do with the native oxide layer. Therefore, the coating free system was fitted with an equivalent circuit of one time constant (Figure 2.6a) and two time constants were employed for coated samples (Figure 2.6b). This type of equivalent circuits is widely used by many authors [9,11,14,26–28].

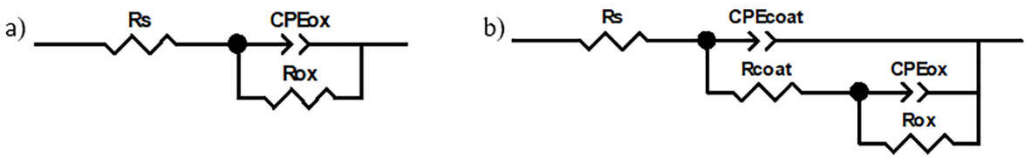

Figure 2.6. Equivalent circuits used for (a) non-coated and (b) coated stainless steel substrates. They correspond to the presence of one and two time constants, respectively.

In the model of Figure 2.6a, Rox and CPEox correspond to the oxide layer. In Figure 2.6b the coating response is added in Rcoat and CPEcoat. By fitting the EIS data to the equivalent circuits information about the corrosion properties of the system can be extracted from the parameters obtained [29–31]. Rcoat can be related to the porosity and the deterioration of the coating and allows to study the deterioration of the sol-gel materials, hence, its capability to protect the metal. The CPEcoat is related to the water absorption. Rs is the electrolyte resistance.

The CPE equivalent circuit element provides values in $s^n\ \Omega^{-1}$ units, being n an exponent which is fitted. Capacitance values, in F units, can be obtained when n is known [32]. All fittings were quite good (Chi-squared < 0.01) as observed in Figure 2.5.

It should be mentioned that in some systems with two time constants, the second time constant signal appears at such low frequencies that it is not possible to obtain all the characteristic parameters for the measured frequency range. In any case, as the aim of these measurements is to study the process of coating degradation, the attention is more focused on the representative parameters of this process (Rcoat and CPEcoat). Figures 2.7 and 2.8 show the values of Rcoat and CPEcoat from the coating and Rox and CPEox from the oxide layer, respectively.

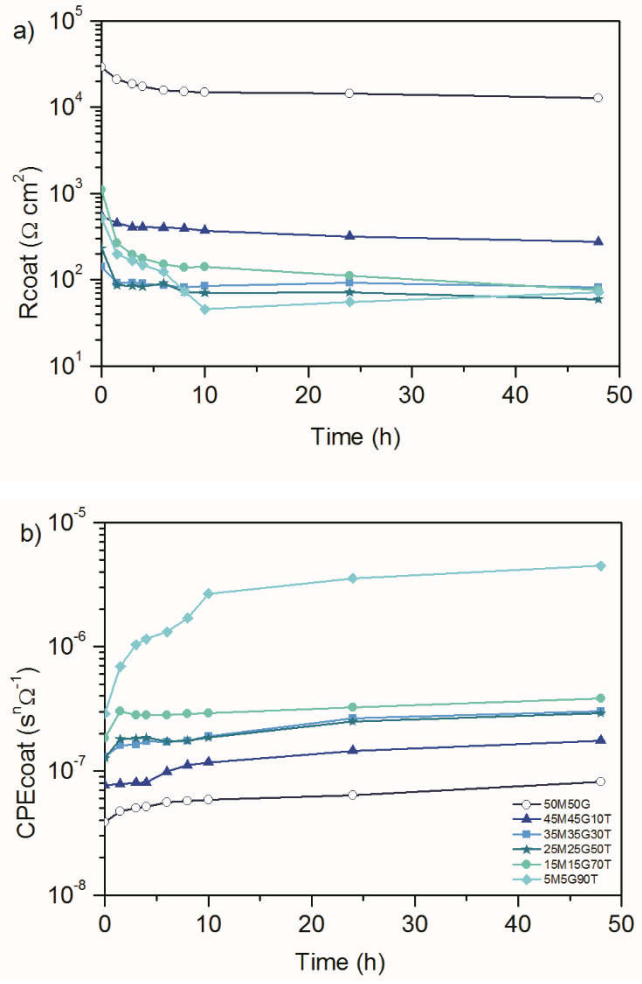

Figure 2.7. Evolution of (a) Rcoat and (b) CPEcoat along the time of contact with electrolyte (3.5 % wt. NaCl) for 50M50G, 45M45G10T, 35M35G30T, 25M25G50T, 15M15G70T and 5M5G90T coatings.

As CPE elements were used instead of pure capacitors, the values of the parameter n are given in Table 2.4.

Figure 2.7a shows the evolution of Rcoat with the exposure time. This parameter decreases with time, more significantly at shorter times, until a nearly constant value is achieved. This is due to the degradation of the coatings by hydrolysis. When TEOS is added to the coating, a significant decrease of Rcoat was observed (see Figure 2.7a). When the presence of TEOS is increased further, Rcoat continues decreasing but more monotonically. The distinct behaviour between materials may result from different initial porosity of the coatings, which can be produced by changes in the compositions. For the case of the 5M5G90T film, the different thickness could also influence. In some curves of Figure 2.7a it can be seen that the value of Rcoat increases with time, this could be due to the formation of deposits that clog the pores of the coating [31].

CPE parameters are directly related with Cc, which represents the capacitance of the coating and relates to the permeability to water penetration as [11,14].

Increasing the value of Cc can be correlated directly with the increase in permittivity by the Equation 2.1, where ε is the dielectric constant of the material, ε0 the permittivity of vacuum, A is the area of coating in contact with the electrolyte and d is the thickness.

$$Cc = \varepsilon\varepsilon_0 \, A/d \qquad \textbf{Eq. 2.1}$$

Hence, the behaviour of the capacitance allows studying water absorption by the coating. In Figure 2.7b it is shown that the CPE value increases with the exposure time to the electrolyte in all cases. In the initial stage, this increase is more intense which could be due to initial water absorption in the coating [18]. At the longest times, the higher value of CPE observed is associated to the degradation of the sol-gel network, which facilitates the penetration of water. This behaviour was also observed in MTES:TEOS coatings and was related to a decrease of organic groups that introduces a more hydrophobic character and provides more resistive capabilities to the film [5].

Figure 2.8 shows the evolution of Rox and CPEox, which are representative parameters of the dielectric properties of the oxide layer. Rox increased during the early stages of exposure (Figure 2.8a). At the same time, CPEox decreased, except for the bare substrate (Figure 2.8b). This might

be due to the passivation of steel by the formation of chrome oxides as a result of the presence of dissolved oxygen in the electrolyte [33]. At longer exposure times Rox and CPEox values remain nearly constant, showing that the oxide layer becomes quite stable. An increase of Rox and a decrease of CPEox are observed respect to the bare steel substrate when the coating is applied, showing an increase of the steel passivation.

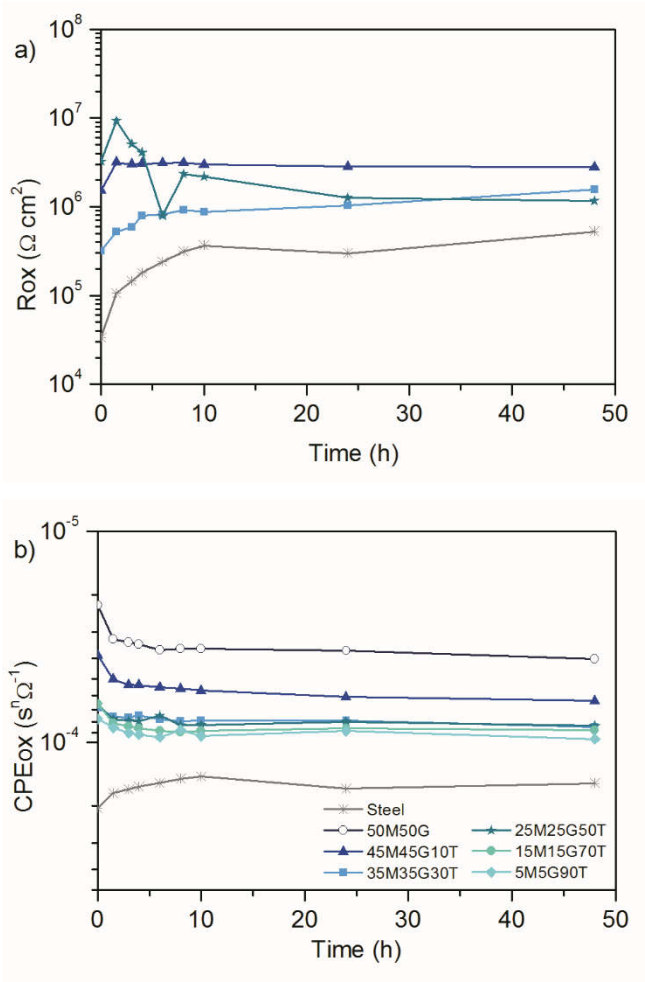

Figure 2.8. Evolution of Rox (a) and CPEox (b) versus time of contact with electrolyte (3.5 % wt. NaCl) for Stainless steel, 50M50G, 45M45G10T, 35M35G30T, 25M25G50T, 15M15G70T and 5M5G90T coatings.

Table 4. Parameters n_1 and n_2 of CPEcoat and CPEox elements, respectively, for each formulation and measuring time.

Material	*n*	*0 h*	*1.5 h*	*3 h*	*4 h*	*6 h*	*8 h*	*10 h*	*24 h*	*48 h*
Stainless steel	n_2	0.89	0.91	0.91	0.92	0.92	0.92	0.92	0.92	0.93
50M50G	n_1	0.95	0.94	0.94	0.93	0.93	0.93	0.92	0.92	0.90
	n_2	0.81	0.85	0.86	0.87	0.87	0.88	0.88	0.89	0.89
45M45G10T	n_1	0.94	0.94	0.94	0.94	0.93	0.93	0.92	0.91	0.89
	n_2	0.83	0.86	0.86	0.87	0.87	0.87	0.88	0.89	0.90
35M35G30T	n_1	0.93	0.91	0.91	0.91	0.91	0.91	0.90	0.87	0.86
	n_2	0.81	0.85	0.86	0.86	0.87	0.87	0.87	0.90	0.90
25M25G50T	n_1	0.95	0.93	0.92	0.92	0.91	0.93	0.93	0.90	0.89
	n_2	0.78	0.81	0.82	0.82	0.86	0.83	0.83	0.85	0.87
15M15G70T	n_1	0.93	0.90	0.90	0.91	0.91	0.90	0.90	0.90	0.89
	n_2	0.79	0.80	0.81	0.81	0.81	0.82	0.82	0.83	0.84
5M5G90T	n_1	0.91	0.85	0.82	0.81	0.80	0.78	0.77	0.74	0.73
	n_2	0.80	0.80	0.81	0.81	0.81	0.83	0.83	0.84	0.84

2.3.5. Hydrolytic degradation

The polysiloxane network degrades in contact with water by hydrolysis following the Reaction 2.1 [11,14]:

$$SiO_2\ (s) + 2H_2O \leftrightarrow Si(OH)_4\ (aq)$$

Reaction 2.1. SiO_2 hydrolytic degradation.

In Figure 2.9, the evolution with time of the degradation curves (weight loss) is shown. It is observed that in all cases the materials degrade, however, the kinetics of degradation depends on the composition.

Incorporating TEOS to the sol-gel network increases the number of Si-O-Si bonds, as a result, the materials present higher degree of degradation after 63 days for higher TEOS content. For the case of 25M25G50T and 35M35G30T compositions, a similar response occurs (it should be noted that error bars overlap). Coatings with a 10 % TEOS showed a 12.88 % weight loss after 62 days of exposure to water, this degree of degradation is just slightly higher than 50M50G material, which

showed a 10.22 % value, so the variation is not significant. However, both 35M35G30T and 25M25G50T coatings show a similar rate of degradation (around 20 %) after 62 days, whereas compositions 15M15G70T and 5M5G90T reached values of weight loss around 30 % after 62 days in contact with water. These higher variations respect to the 50M50G material can be more beneficial if higher release kinetics is needed.

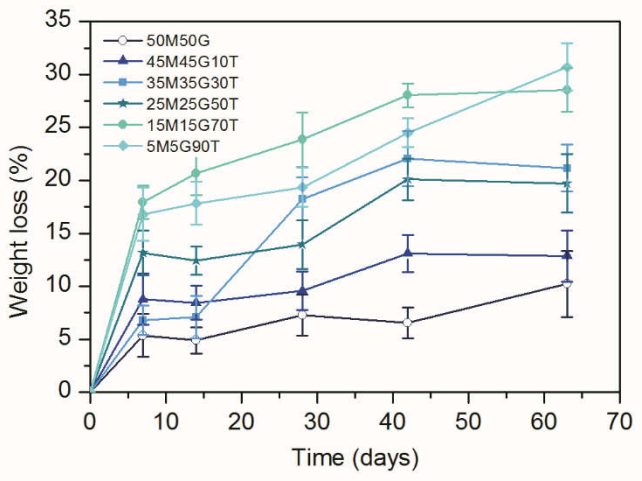

Figure 2.9. Weight loss versus time during the hydrolytic degradation for 50M50G, 45M45G10T, 35M35G30T, 25M25G50T, 15M15G70T and 5M5G90T coatings.

2.4. **Discussion**

Hybrid sol-gel materials from the triple mixture of alcoxysilanes: MTMOS, GPTMS and TEOS were successfully synthesized. Furthermore, it has been possible to obtain homogeneous, transparent and well adhered coatings to the metal substrate, showing adequate properties for implants handling requirements. Sol-gel network condensation process has been demonstrated using ^{29}Si solid NMR (Figure 2.1). Thus, the chemical characterization showed that the addition of TEOS promotes the sol-gel reticulation of MTMOS and GPTMS molecules, probably due to the small size and higher functionality of TEOS molecules, which favour the access and binding to the silicon atomic positions that do not react in the 50M50G composition. However, when the percentage of TEOS is higher than 30%, it becomes more difficult to reach these free positions for condensation and the cross-linking becomes slightly lower.

It should be mentioned that despite the lower curing temperature of 45M45G10T with respect to 50M50G (see Table 2), a higher degree of condensation is obtained for 45M45G10T. This shows that the differences observed in the NMR results have a minor dependency on the curing temperature and are more significantly influenced by composition. FT-IR results corroborate that the condensation reactions have been properly produced and the Si-O-Si network successfully formed, demonstrating the feasibility of the sol-gel process in all cases. As can be seen in Figure 2.2, the processing has been able to incorporate organic moieties in the structure, and the integrity of these functional groups has been maintained.

Contact angle results (Figure 2.3) show that the moderate addition of TEOS to the sol-gel network increases hydrophilicity, reaching the maximum hydrophilic behaviour for the 30% TEOS composition. After that, a higher percentage of TEOS in the composition supposes an increase of contact angle. This behaviour is not completely understood and further experiments should be needed for a clear understanding. However, we believe that the initial increase in hydrophilicity could be due to the opening of the GPTMS epoxy rings, which produces an increase of silanol groups in the structure [18], and is enhanced by the presence of TEOS. Nevertheless, despite the further increase of TEOS content, a decrease of hydrophility takes place due to the more dominant reduction of GPTMS species. Hydrophilicity values are important for the cells behaviour and the values found are in the optimal range (60º - 90º) for an adequate cell attachment [34,35].

Furthermore, a maximum roughness value was measured for the composition 35M35G30T.The biomaterial surface roughness is a critical parameter to obtain suitable tissue regeneration. Wirth et al. found in cell culture with rat osteoblasts that cell proliferation activity is modulated by roughness [36]. Consequently, it is possible to produce a better bone fixation with rough surfaces than employing smooth surfaces [37]. Hence, the coating with 30% TEOS is the material with the most suitable roughness.

EIS tests show that the impedance values decrease when TEOS is added in the sol-gel network (Figure 2.5). This behaviour was reported before in VTES:TEOS coatings [11] and for MTMOS:TEOS materials [14]. From the analysis of Rcoat and CPEcoat parameters (Figure 2.7), it has been clearly shown that the presence of TEOS in the material reduces its capability as a protective coating, but increases its degradability. Furthermore, weight loss results (Figure 2.9) are in agreement with the EIS results. Thus, 50M50G sol-gel network has the lowest rate of degradation from the weight loss analysis, which is in agreement with the higher pore resistance and lower capability of water absorption observed by EIS. Moreover, the higher degradability of coatings with more TEOS can be due to the increase of the porosity and the presence of higher quantities of water in the coatings. Since hydrolytic degradation of these sol-gel networks leads to the release of Si compounds with positive properties on bone regeneration [19], this behaviour is considered crucial for the purpose of these coatings.

Therefore, for applications in implants, a compromise between degradation (silicon release) and protection of the metal during the early stages of the curing process is very important. In this work, it has been demonstrated that the use of different compositions allows tuning the balance between the adequate protective character and the gradual coating degradation kinetics. Finally, considering all the results obtained, the materials with 30% and 50% TEOS show an interesting intermediate compromise between degradation and protection. Besides, as 35M35G30T coating showed the highest roughness, it could be a good candidate for being used in the proposed application too. However, in a next step, biological assessments will be needed to shed more light on what is the optimal composition as biomaterial.

2.5. Conclusions

In this study it was possible to obtain homogeneous and well bonded hybrid coatings from a triple mixture of alkoxysilanes by the sol-gel technique, achieving high degrees of condensation. Furthermore, it has been found by electrochemical impedance spectroscopy and hydrolytic degradation tests that the variation of TEOS percentage in the composition allows regulating the degradation of the material without impairing other properties such as wettability. Adding TEOS to the reference composition (50 % GTPMS and 50 % MTMOS) improved the roughness of the material. These results suggest that the increment achieved in the degradation could significantly improve the *in vivo* behaviour of the reference composition 50M50G, and coatings with this new series of materials could be used in metal implants to improve their osseointegration. As the next step in this work, testing these materials in biological assays will be very interesting to confirm their promising properties.

ACKNOWLEDGEMENTS

The financial support of MAT2014-51918-C2-2-R, P11B2014-19 and Plan de Promoción de la Investigación from the Universitat Jaume I (Predoc/2014/25) is gratefully acknowledged. J. García-Cañadas acknowledge financial support from Ramón y Cajal programme (RYC-2013-13970). The experimental support of Raquel Oliver Valls and José Ortega Herreros is also acknowledged.

REFERENCES

[1] S. Prasad, M. Ehrensberger, M.P. Gibson, H. Kim, E.A. Monaco, Biomaterial properties of titanium in dentistry, J. Oral Biosci. 57 (2015) 192–199. doi:10.1016/j.job.2015.08.001.

[2] D.G. Olmedo, D.R. Tasat, G. Duffó, M.B. Guglielmotti, R.L. Cabrini, The issue of corrosion in dental implants: a review., Acta Odontol. Latinoam. 22 (2009) 3–9. http://www.scopus.com/inward/record.url?eid=2-s2.0-70349258115&partnerID=tZOtx3y1.

[3] A. Arys, C. Philippart, N. Dourov, Y. He, Q.T. Le, J.J. Pireaux, Analysis of titanium dental implants after failure of osseointegration: combined histological, electron microscopy, and X-ray photoelectron spectroscopy approach., J. Biomed. Mater. Res. 43 (1998) 300–12. doi:10.1002/(SICI)1097-4636(199823)43:3<300::AID-JBM11>3.0.CO;2-J.

[4] S. Omar, F. Repp, P.M. Desimone, R. Weinkamer, W. Wagermaier, S. Ceré, J. Ballarre, Sol–gel hybrid coatings with strontium-doped 45S5 glass particles for enhancing the performance of stainless steel implants: Electrochemical, bioactive and in vivo response, J. Non. Cryst. Solids. 425 (2015) 1–10. doi:10.1016/j.jnoncrysol.2015.05.024.

[5] L.E. Amato, D. a. López, P.G. Galliano, S.M. Ceré, Electrochemical characterization of sol-gel hybrid coatings in cobalt-based alloys for orthopaedic implants, Mater. Lett. 59 (2005) 2026–2031. doi:10.1016/j.matlet.2005.02.010.

[6] J. Gallardo, P. Galliano, A. Durán, Bioactive and protective sol-gel coatings on metals for orthopaedic prostheses, J. Sol-Gel Sci. Technol. 21 (2001) 65–74. doi:10.1023/A:1011257516468.

[7] M. Martínez-Ibáñez, M.J. Juan-Díaz, I. Lara-Saez, A. Coso, J. Franco, M. Gurruchaga, J. Suay Antón, I. Goñi, Biological characterization of a new silicon based coating developed for dental implants., J. Mater. Sci. Mater. Med. 27 (2016) 80. doi:10.1007/s10856-016-5690-9.

[8] R.M. Pilliar, Sol–gel surface modification of biomaterials, in: C. Wen (Ed.), Surf. Coat. Modif. Met. Biomater., Elsevier, 2015: pp. 185–217. doi:10.1016/B978-1-78242-303-4.00006-5.

[9] N.C. Rosero-Navarro, S.A. Pellice, Y. Castro, M. Aparicio, A. Durán, Improved corrosion resistance of AA2024 alloys through hybrid organic-inorganic sol-gel coatings produced from sols with controlled polymerisation, Surf. Coatings Technol. 203 (2009) 1897–1903. doi:10.1016/j.surfcoat.2009.01.019.

[10] G. Schottner, Hybrid sol-gel-derived polymers: Applications of multifunctional materials, Chem. Mater. 13 (2001) 3422–3435. doi:10.1021/cm011060m.

[11] M. Hernández-Escolano, M. Juan-Díaz, M. Martínez-Ibáñez, A. Jimenez-Morales, I. Goñi, M. Gurruchaga, J. Suay, The design and characterisation of sol-gel coatings for the controlled-release of active molecules, J. Sol-Gel Sci. Technol. 64 (2012) 442–451. doi:10.1007/s10971-012-2876-6.

[12] D. Arcos, M. Vallet-Regí, Sol-gel silica-based biomaterials and bone tissue regeneration., Acta Biomater. 6 (2010) 2874–88. doi:10.1016/j.actbio.2010.02.012.

[13] M. Catauro, F. Bollino, F. Papale, C. Ferrara, P. Mustarelli, Silica–polyethylene glycol hybrids

synthesized by sol–gel: Biocompatibility improvement of titanium implants by coating, Mater. Sci. Eng. C. 55 (2015) 118–125. doi:10.1016/j.msec.2015.05.016.

[14] M.J. Juan-Díaz, M. Martínez-Ibáñez, M. Hernández-Escolano, L. Cabedo, R. Izquierdo, J. Suay, M. Gurruchaga, I. Goñi, Study of the degradation of hybrid sol–gel coatings in aqueous medium, Prog. Org. Coatings. 77 (2014) 1799–1806. doi:10.1016/j.porgcoat.2014.06.004.

[15] M. Manzano, V. Aina, C.O. Areán, F. Balas, V. Cauda, M. Colilla, M.R. Delgado, M. Vallet-Regí, Studies on MCM-41 mesoporous silica for drug delivery: Effect of particle morphology and amine functionalization, Chem. Eng. J. 137 (2008) 30–37. doi:10.1016/j.cej.2007.07.078.

[16] L. Guo, W. Feng, X. Liu, C. Lin, B. Li, Y. Qiang, Sol-gel synthesis of antibacterial Hybrid Coatings on titanium, Mater. Lett. (2015) MLBLUED1503211. doi:10.1016/j.matlet.2015.08.027.

[17] J. Hyung-Jun, Y. Sung-Chul, O. Seong-Geun, Preparation and antibacterial effects of Ag–SiO2 thin films by sol–gel method, Biomaterials. 24 (2003) 4921–4928. doi:10.1016/S0142-9612(03)00415-0.

[18] M.J. Juan-Díaz, M. Martínez-Ibáñez, I. Lara-Sáez, S. da Silva, R. Izquierdo, M. Gurruchaga, I. Goñi, J. Suay, Development of hybrid sol–gel coatings for the improvement of metallic biomaterials performance, Prog. Org. Coatings. 96 (2016) 42–51. doi:10.1016/j.porgcoat.2016.01.019.

[19] E.M. Carlisle, Silicon: A possible factor in bone calcification, Science. 167 (1970) 279–280. doi:10.1126/science.167.3916.279.

[20] A.M. Pietak, J.W. Reid, M.J. Stott, M. Sayer, Silicon substitution in the calcium phosphate bioceramics, Biomaterials. 28 (2007) 4023–4032. doi:10.1016/j.biomaterials.2007.05.003.

[21] A.F. Khan, M. Saleem, A. Afzal, A. Ali, A. Khan, A.R. Khan, Bioactive behavior of silicon substituted calcium phosphate based bioceramics for bone regeneration, Mater. Sci. Eng. C. 35 (2014) 245–252. doi:10.1016/j.msec.2013.11.013.

[22] J. Ballarre, D.A. López, W.H. Schreiner, A. Durán, S.M. Ceré, Protective hybrid sol–gel coatings containing bioactive particles on surgical grade stainless steel: Surface characterization, Appl. Surf. Sci. 253 (2007) 7260–7264. doi:10.1016/j.apsusc.2007.03.007.

[23] J. Méndez-Vivar, A. Mendoza-Bandala, Spectroscopic study on the early stages of the polymerization of hybrid TEOS–RSi (OR')3 sols, J. Non. Cryst. Solids. 261 (2000) 127–136. doi:10.1016/S0022-3093(99)00605-5.

[24] H. Aguiar, J. Serra, P. González, B. León, Structural study of sol–gel silicate glasses by IR and Raman spectroscopies, J. Non. Cryst. Solids. 355 (2009) 475–480. doi:10.1016/j.jnoncrysol.2009.01.010.

[25] L.B. Capeletti, I.M. Baibich, I.S. Butler, J.H.Z. dos Santos, Infrared and Raman spectroscopic characterization of some organic substituted hybrid silicas., Spectrochim. Acta. A. Mol. Biomol. Spectrosc. 133 (2014) 619–25. doi:10.1016/j.saa.2014.05.072.

[26] A.M. Cabral, R.G. Duarte, M.F. Montemor, M.G.S. Ferreira, A comparative study on the corrosion resistance of AA2024-T3 substrates pre-treated with different silane solutions: Composition of the films formed, Prog. Org. Coatings. 54 (2005) 322–331. doi:10.1016/j.porgcoat.2005.08.001.

[27] K. a. Yasakau, J. Carneiro, M.L. Zheludkevich, M.G.S. Ferreira, Influence of sol-gel process parameters on the protection properties of sol-gel coatings applied on AA2024, Surf. Coatings Technol. 246 (2014) 6–16. doi:10.1016/j.surfcoat.2014.02.038.

[28] J. Ballarre, D. a. López, N.C. Rosero, A. Durán, M. Aparicio, S.M. Ceré, Electrochemical evaluation of multilayer silica-metacrylate hybrid sol-gel coatings containing bioactive particles on surgical grade stainless steel, Surf. Coatings Technol. 203 (2008) 80–86. doi:10.1016/j.surfcoat.2008.08.005.

[29] M. Puig, L. Cabedo, J.J. Gracenea, A. Jiménez-Morales, J. Gámez-Pérez, J.J. Suay, Adhesion enhancement of powder coatings on galvanised steel by addition of organo-modified silica particles, Prog. Org. Coatings. 77 (2014) 1309–1315. doi:10.1016/j.porgcoat.2014.03.017.

[30] S.J. García, J. Suay, Optimization of deposition voltage of cataphoretic automotive primers assessed by EIS and AC/DC/AC, Prog. Org. Coatings. 66 (2009) 306–313. doi:10.1016/j.porgcoat.2009.08.012.

[31] S.J. García, J. Suay, Application of electrochemical techniques to study the effect on the anticorrosive properties of the addition of ytterbium and erbium triflates as catalysts on a powder epoxy network, Prog. Org. Coatings. 57 (2006) 273–281. doi:10.1016/j.porgcoat.2006.09.008.

[32] M. Puig, L. Cabedo, J.J. Gracenea, J.J. Suay, The combined role of inhibitive pigment and organo-modified silica particles on powder coatings: Mechanical and electrochemical investigation, Prog. Org. Coatings. 80 (2015) 11–19. doi:10.1016/j.porgcoat.2014.11.014.

[33] V.H.V. Sarmento, M.G. Schiavetto, P. Hammer, A.V. Benedetti, C.S. Fugivara, P.H. Suegama, S.H. Pulcinelli, C.V. Santilli, Corrosion protection of stainless steel by polysiloxane hybrid coatings prepared using the sol–gel process, Surf. Coatings Technol. 204 (2010) 2689–2701. doi:10.1016/j.surfcoat.2010.02.022.

[34] P.B. van Wachem, T. Beugeling, J. Feijen, A. Bantjes, J.P. Detmers, W.G. van Aken, Interaction of cultured human endothelial cells with polymeric surfaces of different wettabilities, Biomaterials. 6 (1985) 403–408. doi:10.1016/0142-9612(85)90101-2.

[35] C.P. Stallard, K.A. McDonnell, O.D. Onayemi, J.P. O'Gara, D.P. Dowling, Evaluation of protein adsorption on atmospheric plasma deposited coatings exhibiting superhydrophilic to superhydrophobic properties., Biointerphases. 7 (2012) 31. doi:10.1007/s13758-012-0031-0.

[36] C. Wirth, B. Grosgogeat, C. Lagneau, N. Jaffrezic-Renault, L. Ponsonnet, Biomaterial surface properties modulate in vitro rat calvaria osteoblasts response: Roughness and or chemistry?, Mater. Sci. Eng. C. 28 (2008) 990–1001. doi:10.1016/j.msec.2007.10.085.

[37] D. Buser, R.K. Schenk, S. Steinemann, J.P. Fiorellini, C.H. Fox, H. Stich, Influence of surface characteristics on bone integration of titanium implants. A histomorphometric study in miniature pigs, J. Biomed. Mater. Res. 25 (1991) 889–902. doi:doi.org/10.1002/jbm.820250708.

3. CHAPTER 2

Proteomic analysis of silica hybrid sol-gel coatings: a potential tool for predicting biocompatibility of implants *in vivo*

3. Chapter 2

Proteomic analysis of silica hybrid sol-gel coatings: a potential tool for predicting biocompatibility of implants *in vivo*

F. Romero-Gavilán[1], A.M. Sánchez-Pérez[2], N. Araújo-Gomes[1,2], M. Azkargorta[3], I. Iloro[3], F. Elortza[3], M. Gurruchaga[4], I. Goñi[4], J. Suay[1]

[1] Department of Industrial Systems and Design, Universitat Jaume I, Av. Vicent-Sos Baynat s/n. Castellón, 12071 Spain.

[2] Department of Medicine. Universitat Jaume I, Av. Vicent-Sos Baynat s/n. Castellón, 12071 Spain.

[3] Proteomics Platform, CIC bioGUNE, CIBERehd, ProteoRed-ISCIII, Bizkaia Science and Technology Park. Derio, 48160 Spain.

[4] Facultad de Ciencias Químicas. Universidad del País Vasco. P. M. de Lardizábal, 3. San Sebastián, 20018 Spain.

Biofouling (2017)

ABSTRACT

Biomaterials interact with the host organism, determining the success or failure of an implantation. *In vitro* testing is used to assess the biocompatibility of a material. Unfortunately, *in vitro* and *in vivo* results are not always concordant. New methods for biomaterial characterisation are needed for an effective prediction of *in vivo* outcome. The first layer of proteins conditions the host response. Four distinct hybrid sol-gel biomaterials were tested. No differences were observed *in vitro,* although *in vivo* show distinct material behaviour. Mass spectrometry analysis was performed to characterize the first layer of proteins adsorbed onto the different surfaces. Six of the 171 proteins adsorbed onto the surfaces were significantly more abundant on the materials with weak biocompatibility, with known relation to the complement pathway. This could indicate that protein analysis might be a suitable tool for the prediction of the *in vivo* outcome of implantations using new biomaterials.

Keywords: hemocompatibility, osteoimmunology, fibrous capsule, bone regeneration, dental implants, C-reactive protein.

Graphical abstract

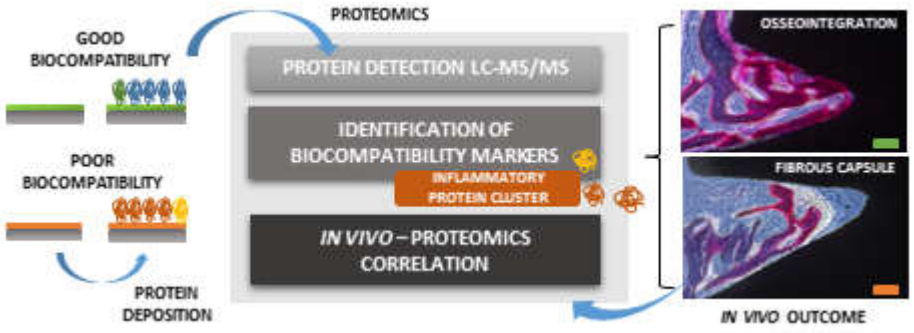

Figure 3.0. Graphical abstract of the work named "proteomic analysis of silica hybrid sol-gel coatings: a potential tool for predicting biocompatibility of implants *in vivo*".

3.1. **Introduction**

Newly developed biomaterials used in the field of medical engineering and regenerative medicine require *in vitro* testing to assess their safety and efficacy. One of the major drawbacks of implantations is the induction of foreign body reaction, which might include an acute and chronic inflammation and scar tissue formation [1,2], conditions that cannot be tested *in vitro*. Consequently, the *in vitro* outcome does not predict well the *in vivo* behaviour of a given biomaterial. It is, therefore, necessary to develop new methods for characterisation of biomaterials, with sufficient accuracy to predict the outcome of implantation [3].

Biomaterials interact with the host organism on several levels of biological organization, and this interface with the host organism might determine the success or failure of the implant. In particular, the surface properties of the implanted device (e.g., hydrophilicity, roughness or surface energy) are important for defining a path of tissue remodelling [4].

When a biomaterial interacts with the bodily fluids of the host, it triggers a natural immune response to the foreign body. The immune response starts with the activation of the innate immune system, a normal short-term reaction. However, sometimes, the implant might induce chronic inflammation and the formation of a fibrous capsule ((myo)fibroblasts, neutrophils and foreign body giant cells [5]), leading to implant rejection [1].

The understanding of the biological events after the implantation trauma is crucial in the development of new biomaterials to prevent or control blood coagulation, infections, immune response and, ultimately, implant rejection. It has been suggested that the differences between the foreign body reactions induced by different biomaterials are mostly determined by the first layer of serum proteins adsorbed onto the implant surface [6,7]. The adsorption mechanisms are not yet completely elucidated [8]; however, the first protein layer is likely to be responsible for the cell/organism response to the foreign bodies [9].

Proteomics has at its disposal powerful tools to examine the proteins adsorbed on different surfaces [10]. In a previous study, we have reported differences between the compositions of protein layers deposited onto two distinct titanium surfaces [11]. Some authors have proposed the C4/C4BP protein ratio as a predictor of biomaterial biocompatibility [9]. Other studies indicate that

binding of C3 protein onto biomaterials is correlated with their biocompatibility [12]. It is, therefore, tempting to assume a direct link between the proteins absorbed on the biomaterial surface and the elicited inflammatory response [13]. However, the mechanisms of the immune response to biomaterials remain largely unknown [14].

The hybrid sol-gel materials synthesized using alkoxysilanes have shown great potential in biomedical applications [15]. These biomaterials, during their degradation process, release silicon compounds in the $Si(OH)_4$ form [16], imparting the osteoinductive properties [17].

Our research group has been working on sol-gel biomaterials applied as coatings on dental implants. A variety of compositions based on mixtures of different alkoxysilanes had been developed and widely studied [16,18–20]. In previous studies, a poor correlation between *in vitro* and *in vivo* results has been observed for some of these biomaterials. Whereas only small differences between the two studied surfaces have been found *in vitro*, a completely diverse *in vivo* behaviour has been observed. The objective of the current study was to characterize the first protein layer adsorbed on titanium discs coated with four distinct hybrid silica sol-gel formulations. Two of the formulations induced the formation of a fibrous connective tissue surrounding the implant (poor biocompatibility), whereas the other two showed good osseointegration (good biocompatibility). The correlation between the properties of the first adsorbed protein layer with the in vivo outcome of implantation was examined for the four tested coatings.

3.2. **Materials and methods**

3.2.1. Titanium discs

Titanium (Ti) discs (12 mm in diameter, 1-mm thick) were made from commercially available, pure, grade-4 Ti bar (Ilerimplant SL, Lleida, Spain). As substrate were used sandblasted acid-etched (SAE) Ti discs, abraded with 4-µm aluminium oxide particles and acid-etched by submersion in sulphuric acid for 1 h to simulate a moderately rough implant surface. Discs were then washed in acetone, ethanol and 18.2 Ω purified water (for 20 min in each liquid) in an ultrasonic bath and dried under vacuum. Finally, all Ti discs were sterilised using UV irradiation.

3.2.2. Sol-gel synthesis and sample preparation

The silica hybrid coatings were obtained using the sol-gel route. The alkoxysilanes precursors used were methyltrimethoxysilane (MTMOS), 3-glycidoxypropyl-trimethoxysilane (GPTMS), tetraethyl orthosilicate (TEOS) and triethoxyvinylsilane (VTES) (Sigma-Aldrich, St. Louis, MO, USA). Four different compositions were synthesized with molar percentages of 70 % MTMOS and 30 % TEOS (70M30T), 35 % MTMOS, 35 % GPTMS and 30 % TEOS (35M35G30T), 50 % MTMOS and 50 % GPTMS (50M50G) and 50 % VTES and 50 % GPTMS (50V50G). The compositions to be studied are established from previous works [11,16,18,20]. 2-Propanol (Sigma-Aldrich, St. Louis, MO, USA) was used as a solvent in the alcohol-siloxane mix (volume ratio 1:1). Hydrolysis of alkoxysilanes was carried out by adding (drop s^{-1}) the corresponding stoichiometric amount of acidified aqueous solution 0.1 M HNO_3 (Panreac, Barcelona, Spain). The solution was stirred for 1 h and left to rest for 1 h; the samples were prepared immediately after this stage. SAE titanium discs were used as the substrate. The coating was performed employing a KSV DC dip-coater (Biolin Scientific, Stockholm, Sweden). The discs were introduced into the appropriate sol-gel solution at a speed of 60 cm min^{-1}, for one minute, and removed at a 100 cm min^{-1}. Finally, samples were cured for 2 h (70M30T and 35M35G30T coatings at 80 ºC, and 50M50G and 50V50G, at 140 ºC).

3.2.3. Physicochemical characterisation of coated titanium discs

The contact angle was measured using an automatic contact angle meter OCA 20 (DataPhysics Instruments, Filderstadt, Germany). An aliquot of 10 µL of ultrapure water W04 was deposited on the sol-gel coated surface at a dosing rate of 27.5 µL s^{-1} at room temperature. Contact angles were determined using SCA 20 software (http://www.dataphysics.de/startseite/produkte/software-module/). Five discs of each material were examined (two drops deposited on each). The surface topography and specific surface area of coated titanium discs was characterised using atomic force microscopy Bruker Multimode 8 (AFM; Newport Multimode, MA, USA) under dry conditions. Measurements were carried out at scan size of 60 µm, with a scan rate of 1 Hz. Three measurements were made for each coating. A mechanical profilometer Dektack 6M (Veeco, NY, USA) was used to determine the roughness. Two coated discs of each composition were tested. Three measurements were performed for each disc to obtain the average values of the Ra parameter. The coatings were studied using scanning electron Leica-Zeiss LEO microscope (SEM;

Leica, Wetzlar, Germany) under vacuum. Platinum sputtering was applied to increase conductivity for the SEM.

3.2.4. In vitro assays

3.2.4.1. Cell culture

MC3T3-E1 (mouse calvaria osteosarcoma cell line) cells were cultured on the sol-gel coated titanium discs at a concentration of 1×10^4 cells/well. We used the Dulbecco's Modified Eagle's medium (DMEM) with phenol red (Thermo Fisher Scientific, Waltham, MA, USA), 1 % 100 × penicillin/streptomycin (Biowest Inc., Riverside, KS, USA) and 10 % fetal bovine serum (FBS) (Thermo Fisher Scientific, Waltham, MA, USA). The cells were incubated for 24 h at 37 ºC in a humidified (95%) atmosphere with 5% CO_2. Then, the medium was replaced with an osteogenic medium composed of DMEM with phenol red 1 ×, 1 % penicillin/streptomycin, 10 % FBS, 1 % ascorbic acid (5 mg mL^{-1}) and 0.21 % β-glycerol phosphate, and the cells were incubated again under the same conditions. The culture medium was changed every 48 h. Wells without Ti discs were used as a control of culture conditions.

3.2.4.2. Cytotoxicity

The cytotoxicity of the biomaterials was assessed following the ISO 10993-5 norm. The 96-Cell Titter Proliferation Assay (Promega®, Madison, WI, USA) was employed to measure the cell viability after 24-h incubation of the cells with the extract. Cells not exposed to the biomaterial extract were used as a negative control. At the same time, cells incubated with latex (known to be cytotoxic) were used as a positive control; 70 % of cell viability was considered the limit below which a biomaterial was considered cytotoxic.

3.2.4.3. ALP activity

The conversion of p-nitrophenylphosphate (p-NPP) to p-nitrophenol was used to assess the ALP activity. Aliquots of 0.1 mL of cell lysate were used to conduct the assay. Lysate was obtained by adding 100 µL of lysate buffer (0.2 % Triton X-100, 10 mM Tris-HCl pH 7.2) to each well. After a period of 7 min of ice, the samples were removed from the wells, transferred to microtubes, and

sonicated for 2 min, obtaining the final lysate. Following centrifugation, 100 µL of p-NPP (1mg mL^{-1}) in substrate buffer (50 mM glycine, 1 mM $MgCl_2$, pH 10.5) was added to 100 µL of the supernatant obtained from the lysate. After a 2-h incubation in the dark (37 ºC, 5 % CO_2), the absorbance was spectrophotometrically measured using a microplate reader, at a wavelength of 405 nm. ALP activity was read from a standard curve, previously obtained using different solutions of p-nitrophenol and 0.02 mM sodium hydroxide. The results were presented as mmol p-nitrophenol per h (mM PNP h^{-1}). The ALP activity data were normalized to the total protein content (µg μL^{-1}) established using Pierce BCA assay kit (Thermo Fisher Scientific, Waltham, MA, USA), at 7 and 14 days.

3.2.5. In vivo assay

3.2.5.1. In vivo experimentation

To evaluate the histological response to the selected coatings, dental implants were surgically placed in the tibia of New Zealand rabbits (Oryctolagus cuniculus). This implantation model is widely used for examining the osseointegration of dental implants [21]. All experiments were conducted in accordance with the protocols of Ethical Committee at the University of Murcia (Spain), European guidelines, the legal conditions in R. D. 223/1988 of March 14th and the Order of October 13rd, 1988 of the Spanish Government law on the protection of experimental animals. The rabbits were kept under 12-h span darkness-light cyclic conditions; room temperature was set at 20.5 ± 0.5 °C and the relative humidity ranged between 45 and 65 %. The animals were individually caged and fed a standard diet and filtered water ad libitum. Dental implants were supplied by Ilerimplant SL (Lleida, Spain). The implants were of internal connection type, made with titanium grade-4 (trademark GMI dental implants, of 3.75-mm diameter and 8-mm length, Frontier model). They had undergone the Advanced Doubled-Grip surface treatment, a combination of white corundum micro-bubble treatment and etching with nitric acid and sulphuric acid solution. 40 implants were employed, 20 uncoated (controls) and 5 coated (test samples) with each material. The control samples and test samples were implanted under the same conditions.

20 rabbits (5 for each material) with weights between 2000 and 3000 g were used. Their age was near the physical closure, which is indicative of an adequate bone volume. The implantation period

was 2 weeks. The implants were inserted in the left and right proximal tibiae, two implants per animal (one control and one test sample). Animals were first sedated (chlorpromazine hydrochloride) and prepared for surgery, and then anesthetized (ketamine chlorhydrate). A coetaneous incision was made in the proximal tibia. The periosteum was removed, and the osteotomy was made using low revolution micromotor and drills of successive diameters of 2, 2.8 and 3.2 mm, with continuous irrigation. Implants were put in by press-fit, and the wound was sutured, washed with saline solution and covered with plastic spray dressing (Nobecutan, Inibsa Laboratories, Barcelona, Spain). At the end of each implantation period, the animals were euthanized by carbon monoxide inhalation to retrieve the screws and to study the surrounding tissues.

3.2.5.2. Histological quantification

Samples for histological examination were processed following the method described by Peris *et al.* [22]. Briefly, the samples were embedded in methyl methacrylate, and 25–30 mm thick sections were obtained using EXAKT technique (EXAKT Technologies, Inc., Oklahoma, USA). For optical microscopy examination, all the sections were stained using Gomori Trichrome solution. The region of interest was delimited using the software ImageJ (https://imagej.nih.gov/ij/, NIH, Bethesda, MD, USA). The area occupied by connective tissue surrounding the implant was measured (mm^2).

3.2.6. Statistical analysis

Data were submitted to one-way analysis of variance (ANOVA) and Newman-Keuls multiple comparison post-test, when appropriate. Differences with $p \leq 0.05$ were considered statistically significant.

3.2.7. Adsorbed protein layer

Ti discs coated with different sol-gel compositions were incubated in 24-well plates for 180 min in a humidified atmosphere (37 ºC, 5 % CO_2), after the addition of 2 mL of human blood serum from male AB plasma (Sigma-Aldrich, St. Louis, MO, USA). After the removal of the serum, the discs were rinsed five times with ddH_2O and once with 100 mM NaCl, 50 mM Tris-HCl, pH 7.0. The adsorbed

protein layer was collected by washing the discs in a 4 % SDS, 100 mM dithiothreitol (DTT), 0.5 M triethylammonium bicarbonate buffer (TEAB) solution (Sigma-Aldrich, St. Louis, MO, USA). The experimental method was adopted from a study by Kaneko et *al.* [10]. Four independent experiments were carried out for each coating (n=4), each one is the resulting elution of four coated-discs. Total protein content was quantified before the experiment (Pierce BCA assay kit; Thermo Fisher Scientific, Waltham, MA, USA), obtaining the value of 51 mg mL^{-1}.

3.2.8. Proteomic analysis

The eluted protein sample was resolved on 10 % polyacrylamide gels, using a Mini-Protean II electrophoresis cell (Bio-Rad®, Hercules, CA, USA). A constant voltage of 150 V was applied for 45 min. The gel was then stained using SYPRO Ruby stain (Bio-Rad®, Hercules, CA, USA) following the manufacturer's instructions. The gel was washed, and each lane was cut into 4 slices. Each of these slices was digested with trypsin following a standard protocol [23]. The resulting peptides were resuspended in 0.1 % formic acid, separated using online NanoLC and analysed using electrospray tandem mass spectrometry. Peptide separation was performed on a nanoACQUITY UPLC system connected to a SYNAPT G2-Si spectrometer (Waters, Milford, MA, USA). Samples were loaded onto a Symmetry 300 C18 UPLC Trap column of 5 µm, 180 µm × 20 mm (Waters, Milford, MA, USA), connected to a BEH130 C18 column of 1.7 µm, 75 µm × 200 mm (Waters, Milford, MA, USA). The column was equilibrated in 3 % acetonitrile and 0.1 % FA. Peptides were eluted at 300 nL min^{-1} using a 60-min linear gradient of 3−50 % acetonitrile.

A SYNAPT G2-Si ESI Q-Mobility-TOF spectrometer (Waters, Milford, MA, USA) equipped with an ion mobility chamber (T-Wave-IMS) for high definition data acquisition analyses was used for the analysis of the peptides. All analyses were performed using electrospray ionization in a positive ion mode. Data were post-acquisition lock-mass corrected using the double-charged monoisotopic ion of [Glu1]-fibrinopeptide B. Accurate LC-MS data were collected in HDDA (High Definition Data Dependant Analysis) mode, which enhances signal intensities using the ion mobility separation.

Progenesis LC-MS software (Nonlinear Dynamics, Newcastle-upon-Tyne, UK) was used for differential protein expression analysis. Raw files were imported into the program, and one of the samples was selected for a reference run to which the precursor masses in all the other samples

were aligned. Abundance ratio between the run to be aligned and the reference run were calculated for all features at given retention times. These values were then logarithmised and the program, based on the analysis of the distribution of all ratios, automatically calculated a global scaling factor. Once normalized, the samples were grouped into the appropriate experimental categories and compared. A peak list containing the peptides detected in all samples was searched against a Swiss-Prot database using the Mascot search engine (www.matrixscience.com). Peptide mass tolerance of 10 ppm and 0.2-Da fragment mass tolerance were used for the searches. Carbamidomethylation of cysteines was selected as the fixed modification and oxidation of methionine as a variable modification for tryptic peptides. Proteins identified with at least two peptides with an FDR < 1 % were kept for further examination. Proteins were quantified based on the intensity of their 3 most abundant peptides, when available. Proteins with ANOVA $p < 0.05$ and a ratio higher than 1.3 in either direction were considered significantly different. Each material was analysed in quadruplicate.

Finally, the data were entered in the Database for Annotation, Visualization and Integrated Discovery (DAVID) Bioinformatics Resources to classify the Progenesis differential protein list into functionally related clusters.

3.3. **Results**

3.3.1. Synthesis and physicochemical characterisation

Four different sol-gel compositions were coated onto the surface of SAE titanium discs. The coatings were homogeneous, without cracks, as can be seen on SEM micrographs (Figure 3.1). The 70M30T biomaterial conserved the initial titanium topography to a greater extent (Figure 3.1b) than 35M35G30T (c), 50M50G (d) and 50V50G (e). AFM images show that the 70M30T surface is the roughest (Figure 3.2b). The 35M35G30T, 50M50G and 50V50G coatings display a smoother topography (Figures 3.2c, d and e), covering well the initially rough titanium surface (Figure 3.2a). The specific surface area measurements showed values of 19.40 ± 2.13 %, 2.54 ± 0.43 %, 0.84 ± 0.22 %, 0.39 ± 0.16 %, and 0.36 ± 0.16 % for Ti-Control, 70M30T, 35M35G30T, 50M50G and 50V50G coatings, respectively. Mechanical profilometer measurements obtained a significantly higher Ra value for 70M30T than for 35M35G30T, 50M50G and 50V50G coatings (Figure 3.2f). This result

may be due to the GPTMS in the last three biomaterials, which might affect the coating thickness, allowing an effective masking of the initial rough features.

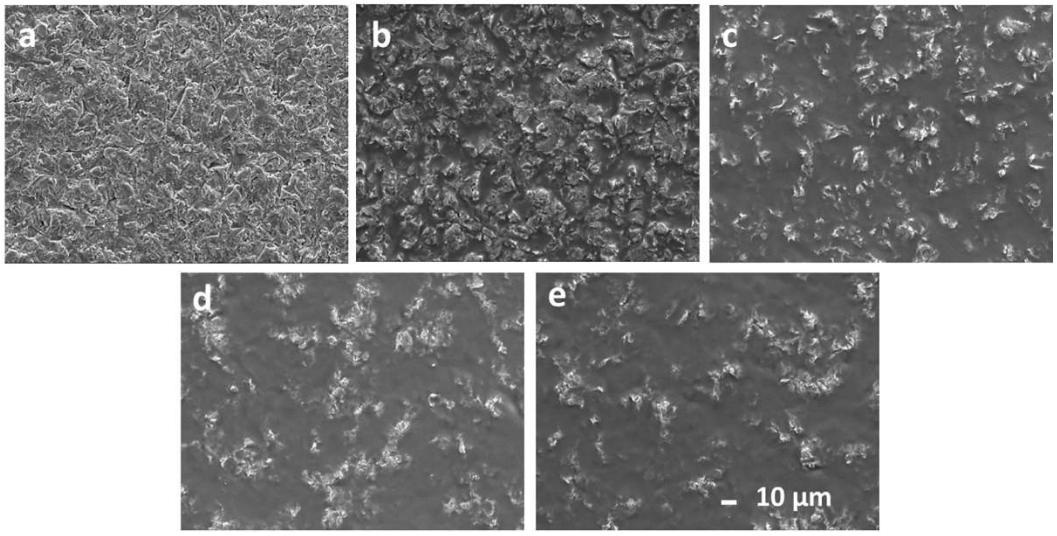

Figure 3.1. SEM micrographs of hybrid sol-gel coatings on SAE titanium discs: (a) Ti-Control, (b) 70M30T, (c) 35M35G30T, (d) 50M50G and (e) 50V50G. Calibration bar 10 µm.

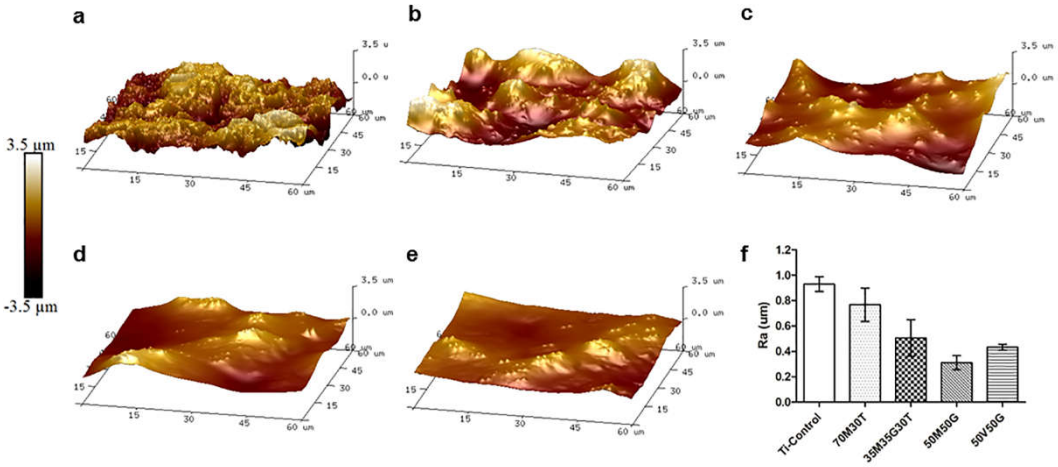

Figure 3.2. AFM images of hybrid sol-gel coatings: (a) Ti-Control, (b) 70M30T, (c) 35M35G30T, (d) 50M50G and (e) 50V50G. (f) Mechanical profilometer measures of Ra. Bars indicate standard deviations.

Contact angle measurements showed that the coatings with TEOS (non-organo-modified precursor), 70M30T and 35M35G30T, were the most hydrophilic (Figure 3.3). The 50M50G and 50V50G coatings had a larger contact angle, probably due to the higher organic matter content.

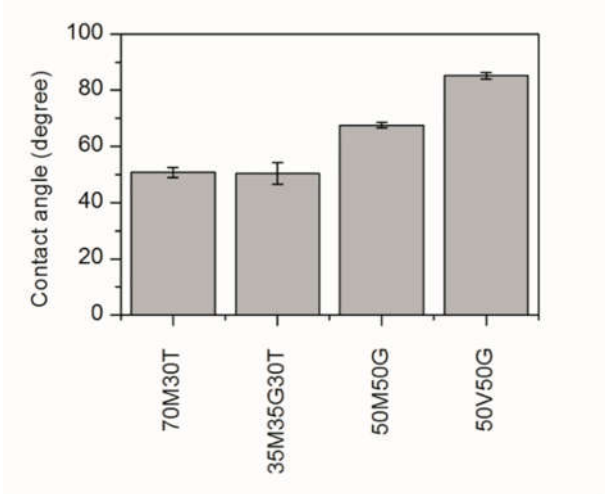

Figure 3.3. Contact angle results for sol-gel coatings on titanium discs. Bars indicate standard deviations.

3.3.2. In vitro assays

None of the biomaterials was cytotoxic (Figure 3.4a). ALP activity measurements showed no significant differences between the tested materials (Figure 3.4b). Interestingly, whereas normalized ALP activity of control cells (wells without Ti disc) seemed to decrease with time, the cells grown on Ti and coated Ti discs maintained or even increased this activity.

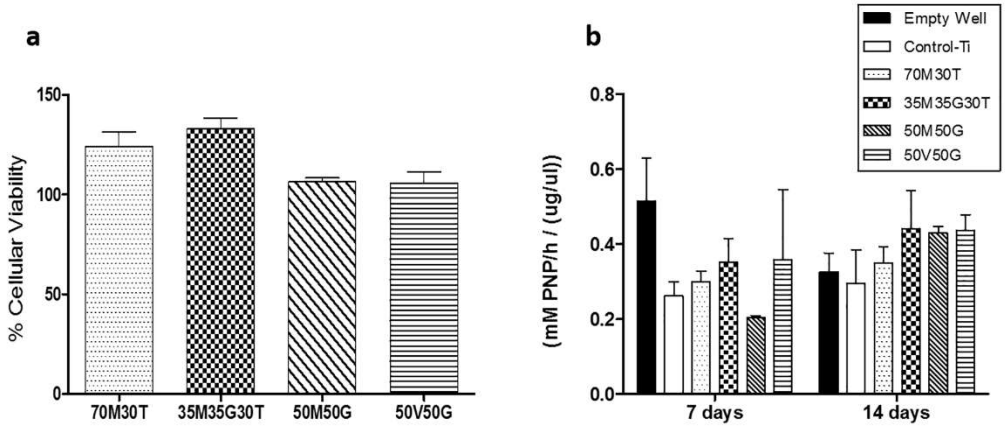

Figure 3.4. MC3T3-E1 cell viability and mineralization *in vitro*. (a) Percentage of cell survival following the norm ISO 10993-5. (b) ALP activity (mM PNP h^{-1}) normalized to the amount of total protein (µg μL^{-1}) levels of the MC3T3-E1 cells cultivated on titanium discs treated with 70M30T (dotted column), 35M35G30T (checkered column), 50M50G (diagonal striped column) and 50V50G (horizontal striped column) formulations. Cells on an empty well without disc were used as a positive control (black column), whereas uncoated titanium discs (white column) were used as a negative control. There were no statistically significant differences between the different formulations at the times measured.

3.3.3. In vivo assays

Histological analysis showed a good osseointegration pattern (it occurs on direct contact between the new bone and the implant surface) for 70M30T- and 35M35G30T-coated implants (Figure 3.5b and 3.5c). However, using 50V50G (Figure 3.5d) and 50M50G (Figure 3.5e) coatings resulted in a formation of a distinct area of fibrous connective tissue between the material and the osteoid/newly formed bone. The sizes of these areas were similar for 35M35G30T and 70M30T but were larger in the 50V50G and 50M50G samples (Figure 3.6). The materials were categorized into two groups according to the *in vivo* results. The first group, comprising 70M30T and 35M35G30T, achieved a good level of osseointegration (high biocompatibility). The coatings in the second group, composed of the 50M50G and 50V50G materials, caused the formation of fibrous connective tissue surrounding the implant surface, blocking the direct contact between the newly formed bone and the biomaterial (poor biocompatibility).

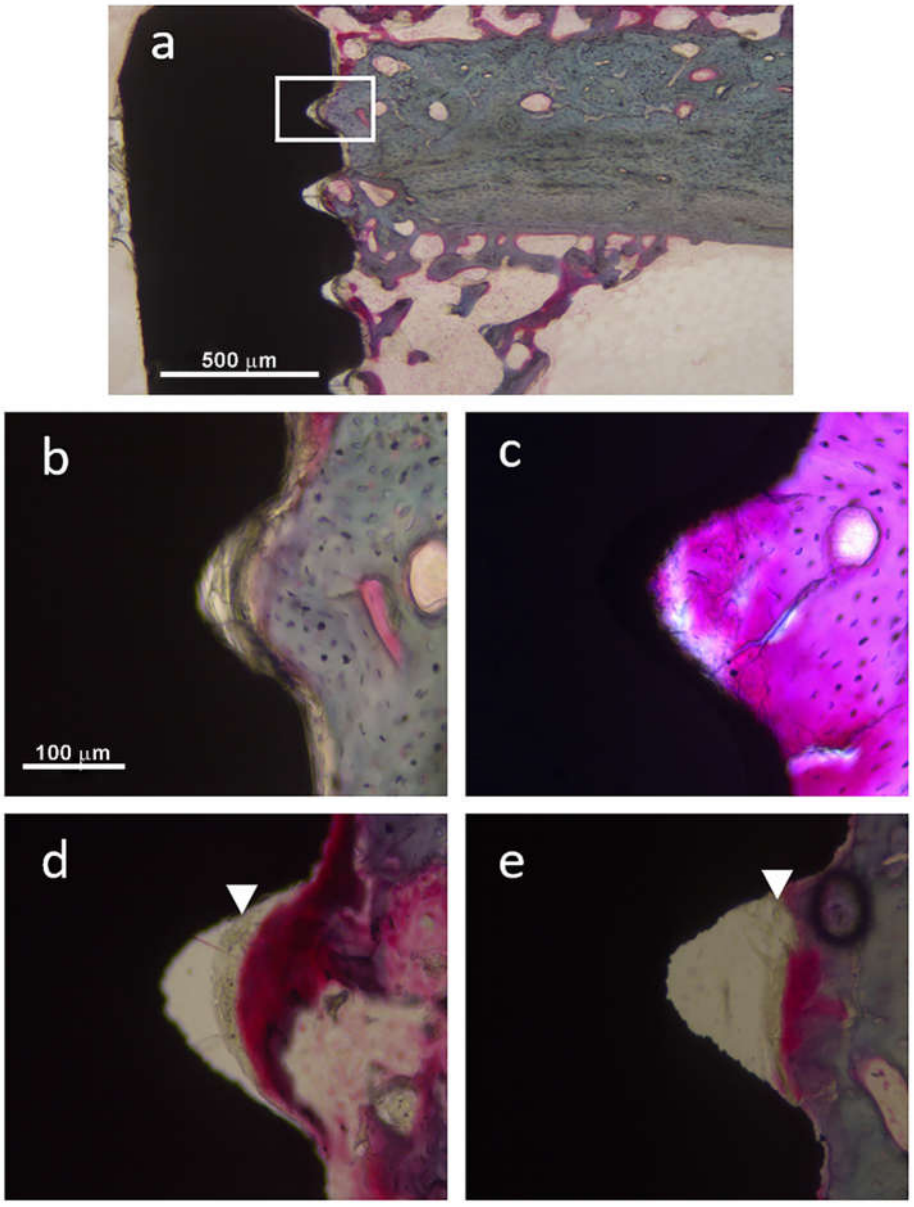

Figure 3.5. Light microscopy representative images (EXAKT® cut and Gomori Trichrome stain) *in vivo* implants 2 weeks post-implantation of: (a) representative photo of the area chosen to analyse the osseointegration state (b) 70M30T, (c) 35M35G30T, (d) 50M50G and (e) 50V50G sol-gel coated screws. The white arrows point to the area where the fibrous connective tissue was being formed.

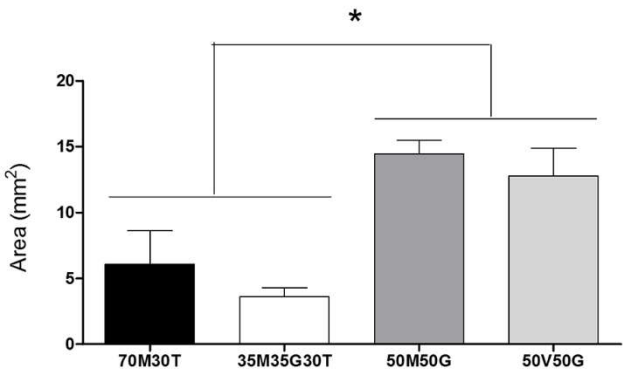

Figure 3.6. Area in mm^2 occupied by the fibrous connective tissue occupied by the four tested coatings. Significantly differences between 70M30T/35M35G30T and 50M50G/50V50G were found (ANOVA $p \leq 0.05$ with a Kruskal-Wallis post-test).

3.3.4. Proteomic analysis

The eluted proteins were analysed using LC-MS/MS. Progenesis QI software was employed to identify the proteins attached to different materials. The DAVID was used to classify according to their function. We detected and identified 171 proteins for each material. When comparing 70M30T with 35M35G30T (good biocompatibility group), 6 proteins were found to be more abundant on the 35M35G30T coating. The largest difference was observed for MYH1 protein (17.19-fold), involved in maintenance of cytoskeletal integrity. The other proteins were associated with the immune system (C1QA and FCN2) and metal-binding (HBA) functions. However, we found 3 proteins that adhered to the 70M30T coating in larger amounts than to 35M35G30T. These were the proteins involved in the protection against the inflammatory disorders (CLUS) [24], coagulation (FAXII) [25] and lipid transport and carbohydrate binding (APOA5) (Table 3.1).

It was also carried out a comparative study of proteins adhering to 50V50G and 50M50G surfaces (poor biocompatibility group, Table 3.1). Two proteins were found adhering in substantially larger amounts to the 50V50G coating, both with metal-binding functions (HORN and DSC1). The enzyme endopeptidase (LCN1) was found predominantly on 50M50G surfaces. The proteomic analysis showed few differences between the coatings in each group. On the two coatings with good

biocompatibility, we found 9 differentially predominant proteins and only 3 on the poor biocompatible materials.

Table 3.1. Proteins differentially predominant in 70M30T vs 35M35G30T (above), and 50V50G vs 50M50G (below) sol-gel coating comparatives (Progenesis method). ANOVA (p-value < 0.05). DAVID classification functions were (1) inflammatory/immune response, (2) hydroxylation, (3) blood coagulation, (4) apoptosis regulation, (5) metal binding, (6) phosphorylation, (7) carbohydrate binding, (8) peptidase activity, (9) lipid transport and (10) cytoskeleton integrity.

Description	Accession	Ratio 35M35G30T/70M30T	DAVID
Myosin-1	MYH1_HUMAN	17.19	10
L-lactate dehydrogenase B chain	LDHB_HUMAN	12.18	-
Glutamate dehydrogenase 1. mitochondrial	DHE3_HUMAN	8.65	-
Ficolin-2	FCN2_HUMAN	8.28	1-2-7-5-10
Complement C1q subcomponent subunit A	C1QA_HUMAN	3.06	1-2
Hemoglobin subunit alpha	HBA_HUMAN	1.73	5-10
Clusterin	CLUS_HUMAN	0.61	1-4-9
Coagulation factor XII	FA12_HUMAN	0.58	3-5-8
Apolipoprotein A-V	APOA5_HUMAN	0.53	7-9

Description	Accession	Ratio 50V50G/50M50G	DAVID
Hornerin	HORN_HUMAN	3.41	5-8-10
Desmocollin-1	DSC1_HUMAN	2.14	5
Lipocalin-1	LCN1_HUMAN	0.14	8

To find an explanation for the differences in the *in vivo* outcomes, we compared the proteins differentially attached to each of the materials with good biocompatibility (70M30T and 35M35G30T) with the proteins detected on one of the materials with a negative outcome (poor biocompatibility group), 50M50G (Table 3.2). Fifteen proteins were found predominantly adsorbed onto the 50M50G surface in comparison with the other two materials. They included the proteins involved in bone metabolism and regeneration (VTNC [26], APOE [27–29] and KNG1 [30,31]) and proteins related to the immune system and inflammatory response (VTNC, CRP, SAMP, C1QB,

C1QC, CO7, C1S and C4BPA). All these proteins seem to favour the complement cascade activation [32], except for C4BPA and VTNC (which might inhibit this process [33]).

Table 3.2. Proteins differentially predominant in both 70M30T vs 50M50G and 35M35G30T vs 50M50G sol-gel coating comparatives (Progenesis method), ANOVA (p-value < 0.05). DAVID classification functions were (1) inflammatory/immune response, (2) hydroxylation, (3) blood coagulation, (4) apoptosis regulation, (5) metal binding, (6) phosphorylation, (7) carbohydrate binding, (8) peptidase activity, (9) lipid transport and (10) cytoskeleton integrity.

Description	Accession	Ratio 50M50G/ 70M30T	Ratio 50M50G/ 35M35G30T	DAVID
C-reactive protein	CRP_HUMAN	7.83	5.28	1-5-8
Lipocalin-1	LCN1_HUMAN	4.28	5.37	8
Serum amyloid P-component	SAMP_HUMAN	3.48	1.93	1-5-7-8
Apolipoprotein E	APOE_HUMAN	2.40	3.09	3-4-5-6-7-9
Complement C1q subcomponent subunit C	C1QC_HUMAN	2.26	2.12	1-2
Complement C1q subcomponent subunit B	C1QB_HUMAN	2.24	2.05	1-2
Complement component C7	CO7_HUMAN	2.22	1.99	1
Vitronectin	VTNC_HUMAN	2.21	1.77	7
Ig kappa chain V-IV region Len	KV402_HUMAN	2.08	1.93	-
Complement C1s subcomponent	C1S_HUMAN	2.07	2.19	1-2-5-8
C4b-binding protein alpha chain	C4BPA_HUMAN	2.06	2.25	1
Kininogen-1	KNG1_HUMAN	2.02	1.82	1-2-3-4-5-7
Ig lambda-2 chain C regions	LAC2_HUMAN	1.73	1.57	-
Apolipoprotein A-IV	APOA4_HUMAN	1.67	2.23	5
Ig kappa chain V-II region Cum	KV201_HUMAN	1.63	1.79	-
Keratin. type II cytoskeletal 2 epidermal	K22E_HUMAN	0.63	0.62	10
Keratin. type I cytoskeletal 10	K1C10_HUMAN	0.61	0.55	10
Keratin. type II cytoskeletal 78	K2C78_HUMAN	0.60	0.56	10
Hornerin	HORN_HUMAN	0.40	0.16	5-8-10
Filaggrin-2	FILA2_HUMAN	0.35	0.35	5-8

However, 5 proteins (3 types of keratins, HORN and FILA2) adsorbed more to 70M30T and 35M35G30T than to 50M50G coatings. These proteins play a role in the cytoskeleton integrity and have a peptidase activity. The proteins on the good biocompatibility materials (70M30T and 35M35G30T) were also compared with those found on the 50V50G coating (negative outcome). Table 3.3 displays the 16 proteins with the highest difference in abundance, among which 15 adhered more to the 50V50G coating.

Table 3.3. Proteins differentially predominant in both 70M30T vs 50V50G and 35M35G30T vs 50V50G sol-gel coating comparatives (Progenesis method), ANOVA (p-value < 0.05). DAVID classification functions were (1) inflammatory/immune response, (2) hydroxylation, (3) blood coagulation, (4) apoptosis regulation, (5) metal binding, (6) phosphorylation, (7) carbohydrate binding, (8) peptidase activity, (9) lipid transport and (10) cytoskeleton integrity.

Description	Accession	Ratio 50V50G/ 70M30T	Ratio 50V50G/ 35M35G30T	DAVID
C-reactive protein	CRP_HUMAN	15.26	10.29	1-5-8
Complement C5	CO5_HUMAN	10.43	5.78	1-6
Serum amyloid P-component	SAMP_HUMAN	3.33	1.84	1-5-7-8
Complement C1q subcomponent subunit B	C1QB_HUMAN	2.45	2.24	1-2
Ig kappa chain V-IV region Len	KV402_HUMAN	2.45	2.27	-
Plasma protease C1 inhibitor	IC1_HUMAN	2.22	1.66	1-3
Complement factor H	CFAH_HUMAN	2.09	1.73	1
Complement component C7	CO7_HUMAN	2.07	1.86	1
Ig kappa chain V-III region SIE	KV302_HUMAN	2.03	1.83	-
Complement C1s subcomponent	C1S_HUMAN	1.98	2.10	1-2-5-8
Vitronectin	VTNC_HUMAN	1.98	1.58	7
Complement C3	CO3_HUMAN	1.93	1.65	1
Complement C1r subcomponent	C1R_HUMAN	1.92	1.79	1-2-5-8
Ig lambda-2 chain C regions	LAC2_HUMAN	1.72	1.57	-
Complement C1q subcomponent subunit C	C1QC_HUMAN	1.71	1.61	1-2
Serpin B3	SPB3_HUMAN	0.33	0.41	8

All the proteins characteristically associated with the 50V50G coating are directly involved in the immune response and acute inflammatory response (CRP, CO5, SAMP, C1QB, IC1, CFAH, CO7, C1S, CO3, C1R, VTNC and C1QC). Most of the proteins in this cluster are involved in the complement cascade activation [32], except for CFAH and VTNC, the important regulators/repressors of the activation of the complement system [33,34]. Only one protein, the endopeptidase SPB, was more abundant on both positive-outcome materials than on 50V50G.

To establish which proteins adhere differentially to both 50M50G and 50V50G (poor biocompatibility) in comparison with 35M35G30T and 70M30T (good biocompatibility) sol-gel coatings, the data in Tables 3.2 and 3.3 was analysed. The common proteins with increased abundance on the poor biocompatibility materials were looked for (Table 3.4). Nine such proteins were found, including VTCN, 2 immunoglobulins and 6 proteins related to the acute inflammatory response processes of the immune system (CRP, SAMP, C1QB, C1QC, C1S and CO7).

Table 3.4. Proteins differentially predominant at the same time in both 50M50G and 50V50G respect to 35M35G30T and 70M30T sol-gel coatings (Progenesis method). ANOVA (p-value < 0.05).

Description	Accession	Ref. bone metabolism or/and immune response
C-reactive protein	CRP_HUMAN	[43,50,51]
Serum amyloid P-component	SAMP_HUMAN	[52,53]
Complement C1q subcomponent subunit C	C1QC_HUMAN	[32]
Complement C1q subcomponent subunit B	C1QB_HUMAN	[32]
Complement component C7	CO7_HUMAN	[32]
Vitronectin	VTNC_HUMAN	[54]
Ig kappa chain V-IV region Len	KV402_HUMAN	-
Complement C1s subcomponent	C1S_HUMAN	[32]
Ig lambda-2 chain C regions	LAC2_HUMAN	-

These results demonstrate that the proteins related to the activation or inhibition of the complement cascade have higher affinity to 50M50G and 50V50G coatings. The complement system is a highly complex mechanism with the intricate regulation of inhibition and activation. Table 3.5 displays the abundance of adsorbed inhibitory proteins (C4BPS, CFAH and VTNC), comparing the materials with good and poor *in vivo* outcome and their respective protein ratios.

The complement-inhibiting proteins C4BPA, CFAH and VTNC and two of the principal activating proteins of the same system, CRP and SAMP, were the main differentially adhering proteins on the poor-outcome materials. Interestingly, the inhibitory proteins were more predominant in the weak biocompatibility material group. Nevertheless, the ratio of complement-system inhibitory proteins to activating proteins was higher for the biomaterials of good biocompatibility (70M30T and 35M35G30T) than for those with the poor biocompatibility (50M50G and 50V50G).

Table 3.5. Inhibitory/activator protein ratio detected in 70M30T, 35M35G30T, 50M50G and 50V50G biomaterials.

Ratios	70M30T	35M35G30T	50M50G	50V50G
CFAH/CRP	75.19	61.30	17.44	10.32
CFAH/SAMP	2.04	1.37	1.07	1.28
C4BPA/CRP	18.53	11.48	4.88	1.89
C4BPA/SAMP	0.50	0.26	0.30	0.24
VTNC/CRP	76.05	64.09	21.47	9.87
VTNC/SAMP	2.06	1.43	1.31	1.23

3.4. **Discussion**

Biomaterials and non-biological substances introduced into the human body are exposed to the blood and tissue elements. The first event after their introduction is the deposition of a monolayer of plasma proteins onto the surfaces of foreign materials. This can induce, among other processes, the activation of the complement system and coagulation cascades [35]. In extreme cases, it can result in a host reaction to the foreign body, which includes blood-material interactions, provisional matrix formation, acute and/or chronic inflammation, granulation tissue development and the formation of fibrous capsules [6,36]. The physicochemical properties of the different biomaterials used in implants such as their topography, roughness, chemistry and surface energy might affect the types and quantities of adsorbed proteins and even their conformation [14] and, consequently, the body response. This paper focuses on the characterisation of the protein layer adsorbed onto titanium coated with four distinct silica hybrid sol-gel biomaterials (70M30T, 35M35G30T, 50M50G and 50V50G). The coatings had been originally introduced to make titanium implant surface more bioactive and increase its capacity of osteogenic molecule delivery [16,18]. The different

compositions of the coatings change their physicochemical properties [37]. Thus, 70M30T formulation resulted in the highest roughness in comparison with the others (all containing GPTMS). 50V50G and 50M50G coatings were more hydrophobic than the other surfaces, probably due to their higher organic compound content. However, compositions containing TEOS (non-organo-modified alkoxysilane) displayed a more hydrophilic behaviour. Apart from dissimilarities in morphology and hydrophilicity, these coatings also differ chemically, depending on the organo-modified alkoxysilanes used in their synthesis [38]. All these variations might affect the implant biocompatibility and, therefore, the biological response.

None of the four biomaterials tested in vitro was found to be cytotoxic, and the ALP activity assay showed no significant differences. In fact, all the sol-gel compositions showed a good *in vitro* behaviour, even in comparison with the control sandblasted and acid-etched titanium (SAE-Ti), whose good properties are widely known [39,40].

Although *in vitro* experimentation is largely used to predict the host response to a biomaterial, it cannot accurately predict biocompatibility *in vivo*. This is because, in such experiments, many of the *in vivo* elements are missing (e.g., the blood and the immune system). These elements strongly affect the *in vivo* result, especially in the field of osteoregenerative materials [3,41]. During the bone regeneration process, the vascularisation, stabilisation, scaffolding, cell signalling and progenitor cells are all required [42]. Following the implantation, the material is in contact with the blood, which contains the innate immune system cells that might degrade the implanted material or induce the formation of connective tissue surrounding the implant, hampering the osseointegration. The formation of the fibrous capsule surrounding the implant is regarded a natural immune response of the host to a foreign body [43].

A fibrous connective tissue was found surrounding 50M50G and 50V50G-coated implants; this did not happen in the cases 70M30T and 35M35G30T coatings even though they showed similar *in vitro* outcomes. Hence, even though *in vitro* tests might offer some guidance, neutral or positive results of such tests do not guarantee similar outcomes *in vivo*.

The implanted biomaterials are exposed to the blood immediately after their insertion. The *in vivo* behaviour of a given biomaterial is difficult to predict; however, it has been proposed that the first

layer of adhering serum proteins might be responsible for the different responses of the host organism [44].

Employing proteomic analysis using LC/MS-MS and the Progenesis software, the first layer of proteins was studied. Following examination of the proteins predominately adhered to the biomaterials with similar *in vivo* response (Table 3.1), it was acknowledged that the differences within these groups of materials were very limited. However, when the two biomaterials with good biocompatibility were compared to either of the coatings inducing the formation of connective tissue, a significant number of differentially adhering proteins was detected. Interestingly, proteins related to the immune/inflammatory response were found predominantly on the poor biocompatibility surfaces 50M50G (Table 3.2) and 50V50G (Table 3.3), when compared simultaneously to 70M30T and 35M35G30T (good biocompatibility).

In parallel, there were also found (Table 3.4) some proteins differentially adhered to the two good biocompatibility materials (70M30T and 35M35G30T) in comparison with the poor biocompatibility coatings (50M50G and 50V50G). It is compelling that most of these proteins are associated with the immune system, including the pentraxins CRP and SAMP, as well as the complement proteins (C1QB, C1QC, C1S and CO7). The latter belong, according to the DAVID analysis, to a protein cluster related to an acute inflammatory response. Notably, CRP, an activator of the classical pathway [45] was particularly more abundant on the two materials with poor biocompatibility than on the 70M30T and 35M35G30T coatings. CRP acts by direct binding of the globular heads of C1q, the first component of the complement system [32]. It was found that the amounts of C1q adhering to 50V50G and 50G50G surfaces were larger than on the coatings that achieve a good *in vivo* osseointegration. Upon the activation of C1q, the classical inflammatory pathway follows a series of complement activations, peaking on the generation of C3 and C5 convertases, which results in the production of C3a and C5b fragments. These are chemoattractant proteins with a role in the proliferation of the elements of the innate immunity system, such as macrophages [32]. In turn, the macrophages regulate fibrogenesis by releasing the cytokines and growth factors. Furthermore, the macrophages modulate fibroblast proliferation and collagen synthesis [46]. However, the VTNC, which might participate in the regulation/repression of complement activation [33], is vital for interleukin IL-4 adhesion on biomaterial surfaces and induces the switch of the macrophages to their M2 reparative phenotype [13].

As this chain of events might lead to the formation of a fibrous capsule (a typical foreign body reaction of the host), it may seem paradoxical that the inhibitors of the complement system such as VTNC are found predominantly adhering onto 50M50G and 50V50G coatings, whose surfaces become surrounded by a layer of connective tissue after implantation. Explanation of this apparently contradictory finding might lie in the ratio of inhibitory to activator proteins on each surface. It is observed that the 70M30T and 35M35G30T biomaterials showed a higher ratio of the complement system inhibitory proteins to activator proteins in comparison with the materials of poor biocompatibility.

These results suggest that the equilibrium between the activating and inhibitory proteins regulating the complement system might determine the *in vivo* success of an implantation. Thus, a high ratio of inhibitory to activating proteins should lead to a positive outcome. A low ratio might trigger a disproportionate immune response with consequent excessive and chronic inflammation reaction, culminating in the formation of the fibrous capsule around the implant [13]. This acute inflammation response might alter the normal balance between the coagulation cascade and the natural anticoagulant pathway, possibly by suppression of the latter [47]. The anticoagulant pathway not only limits the coagulation but also modulates the inflammatory response (e.g., by reduction of cytokine expression) [48]. The lack of control in both coagulation and inflammatory pathways, a consequence of the anticoagulant system alteration, might cause a negative *in vivo* response after implantation.

This hypothesis is consistent with other reports, in which the proteins of the complement system have been associated with biocompatibility problems [35,49]. Engberg *et al.* have even proposed a method for prediction of biocompatibility by evaluating the ratio of C4/C4BP, assumed to reflect the inflammatory response of the host organism to a biomaterial [9]. However, in their study, a protein list was preselected; the CRP levels were not analysed in that publication.

The proteomic approach using the LC/MS-MS might have a significant potential for predicting the biocompatibility of biomaterials by analysing the first layer of proteins attached to the tested surfaces.

3.5. **Conclusions**

In summary, four different hybrid sol-gel biomaterials have been tested. These biomaterials have distinct physico-chemical properties, which might affect the composition of the protein layer adhered to their surfaces. The implants with different coatings had different *in vivo* outcomes. The results of the proteomic analysis suggested some causes for these differences. It was found a cluster of proteins differentially adhered to bad biocompatibility coatings, most of them related to acute inflammatory response regulation. The formation of a layer of fibrous connective structure *in vivo* surrounding the 50M50G and 50V50G materials might be correlated with the adsorption of these proteins. Regardless of the experimental limitations of this study, this correlation (proteomic analysis-*in vivo*) might be the basis for the development of a new methodology to detect biocompatibility problems and therefore reduce the number of experimental subjects *in vivo*. The proteins in this group (CRP, SAMP, C1S, C1QB, C1QC, C7 and VTN) should be useful as biomarkers in the evaluations of material biocompatibility.

ACKNOWLEDGEMENTS

This work was supported by the MAT 2014-51918-C2-2-R (MINECO), P11B2014-19, Plan de Promoción de la Investigación de la Universidad Jaume I under grant Predoc/2014/25 and Generalitat Valenciana under grant Grisolia/2014/016. Authors would like to thank Antonio Coso and Jaime Franco (GMI-Ilerimplant) for their inestimable contribution to this study, and Irene Lara, Raquel Oliver, Jose Ortega (UJI) and Iraide Escobes (CIC bioGUNE) for their valuable technical assistance.

REFERENCES

[1] R. Boehler, J. Graham, L. Shea, Tissue engineering tools for modulation of the immune response, Biotechniques. 51 (2011) 239–240. doi:10.2144/000113754.Tissue.

[2] J.S. Duffield, M. Lupher, V. Thannickal, T. Wynn, Host Responses in Tissue Repair and Fibrosis, Annu Rev Pathol. 141 (2008) 520–529. doi:10.1016/j.surg.2006.10.010.Use.

[3] G. Hulsart-Billström, J.I. Dawson, S. Hofmann, R. Müller, M.J. Stoddart, M. Alini, H. Redl, A. El Haj, R. Brown, V. Salih, J. Hilborn, S. Larsson, R.O.C. Oreffo, A surprisingly poor correlation between in vitro and in vivo testing of biomaterials for bone regeneration: Results of a multicentre analysis, Eur. Cells Mater. 31 (2016) 312–322. doi:10.22203/eCM.v031a20.

[4] P.J. Molino, M.J. Higgins, P.C. Innis, R.M.I. Kapsa, G.G. Wallace, Fibronectin and bovine serum albumin adsorption and conformational dynamics on inherently conducting polymers: A QCM-D study, Langmuir. 28 (2012) 8433–8445. doi:10.1021/la300692y.

[5] F.F.R. Damanik, T.C. Rothuizen, C. van Blitterswijk, J.I. Rotmans, L. Moroni, Towards an in vitro model mimicking the foreign body response: tailoring the surface properties of biomaterials to modulate extracellular matrix., Sci. Rep. 4 (2014) 6325. doi:10.1038/srep06325.

[6] J.M. Anderson, A. Rodriguez, D.T. Chang, Foreign body reaction to biomaterials, Semin. Immunol. 20 (2008) 86–100. doi:10.1016/j.smim.2007.11.004.

[7] J.L. Brash, P. Ten Hove, Effect of plasma dilution on adsorption of fibrinogen to solid surfaces, Thromb. Haemost. 51 (1984) 326–330.

[8] S. Arvidsson, A. Askendal, P. Tengvall, Blood plasma contact activation on silicon, titanium and aluminium, Biomaterials. 28 (2007) 1346–1354. doi:10.1016/j.biomaterials.2006.11.005.

[9] A.E. Engberg, P.H. Nilsson, S. Huang, K. Fromell, O.A. Hamad, T.E. Mollnes, J.P. Rosengren-Holmberg, K. Sandholm, Y. Teramura, I.A. Nicholls, B. Nilsson, K.N. Ekdahl, Prediction of inflammatory responses induced by biomaterials in contact with human blood using protein fingerprint from plasma, Biomaterials. 36 (2015) 55–65. doi:10.1016/j.biomaterials.2014.09.011.

[10] H. Kaneko, J. Kamiie, H. Kawakami, T. Anada, Y. Honda, N. Shiraishi, S. Kamakura, T. Terasaki, H. Shimauchi, O. Suzuki, Proteome analysis of rat serum proteins adsorbed onto synthetic octacalcium phosphate crystals, Anal. Biochem. 418 (2011) 276–285. doi:10.1016/j.ab.2011.07.022.

[11] F. Romero-Gavilán, N.C. Gomes, J. Ródenas, A. Sánchez, F. , M. Azkargorta, Ibon Iloro, F. Elortza, I. García-Arnáez, M. Gurruchaga, I. Goñi, J. Suay, Proteome analysis of human serum proteins adsorbed onto different titanium surfaces used in dental implants, Biofouling. 33 (2017) 98–111. doi:10.1080/08927014.2016.1259414.

[12] K. Nilsson-Ekdahl, B. Nilsson, C.G. Gölander, H. Elwing, B. Lassen, U.R. Nilsson, C. Golander, Gustaf, C.G. Golander, Complement activation on radio frequency plasma modified polystyrene surfaces, J. Colloid Interface Sci. 158 (1993) 121–128. doi:10.1006/jcis.1993.1236.

[13] Z. Chen, T. Klein, R.Z. Murray, R. Crawford, J. Chang, C. Wu, Y. Xiao, Osteoimmunomodulation for the development of advanced bone biomaterials, Mater. Today. 19 (2015) 304–321. doi:10.1016/j.mattod.2015.11.004.

[14] A. Vishwakarma, N.S. Bhise, M.B. Evangelista, J. Rouwkema, M.R. Dokmeci, A.M. Ghaemmaghami, N.E. Vrana, A. Khademhosseini, Engineering Immunomodulatory Biomaterials To Tune the Inflammatory Response, Trends Biotechnol. 34 (2016) 470–482. doi:10.1016/j.tibtech.2016.03.009.

[15] A. P. Chiriac, L. E. Nita, I. Neamtu, M. T. Nistor, Sol - Gel Technique Applied for Biomaterials Achievement, Recent Patents Mater. Sci. 4 (2011) 224–237. doi:10.2174/1874464811104030224.

[16] M.J. Juan-Díaz, M. Martínez-Ibáñez, I. Lara-Sáez, S. da Silva, R. Izquierdo, M. Gurruchaga, I. Goñi, J. Suay, Development of hybrid sol–gel coatings for the improvement of metallic biomaterials performance, Prog. Org. Coatings. 96 (2016) 42–51. doi:10.1016/j.porgcoat.2016.01.019.

[17] A.F. Khan, M. Saleem, A. Afzal, A. Ali, A. Khan, A.R. Khan, Bioactive behavior of silicon substituted calcium phosphate based bioceramics for bone regeneration, Mater. Sci. Eng. C. 35 (2014) 245–252. doi:10.1016/j.msec.2013.11.013.

[18] M. Martínez-Ibáñez, M.J. Juan-Díaz, I. Lara-Saez, A. Coso, J. Franco, M. Gurruchaga, J. Suay Antón, I. Goñi, Biological characterization of a new silicon based coating developed for dental implants, J. Mater. Sci. Mater. Med. 27 (2016) 80. doi:10.1007/s10856-016-5690-9.

[19] M.J. Juan-Díaz, M. Martínez-Ibáñez, M. Hernández-Escolano, L. Cabedo, R. Izquierdo, J. Suay, M. Gurruchaga, I. Goñi, Study of the degradation of hybrid sol–gel coatings in aqueous medium, Prog. Org. Coatings. 77 (2014) 1799–1806. doi:10.1016/j.porgcoat.2014.06.004.

[20] M. Hernández-Escolano, M.J. Juan-Díaz, M. Martinez-Ibáñez, J. Suay, I. Goñi, M. Gurruchaga, Synthesis of hybrid sol-gel materials and their biological evaluation with

human mesenchymal stem cells, J. Mater. Sci. Mater. Med. 24 (2013) 1491–1499. doi:10.1007/s10856-013-4900-y.

[21] H. Mori, M. Manabe, Y. Kurachi, M. Nagumo, Osseointegration of dental implants in rabbit bone with low mineral density, J. Oral Maxillofac. Surg. 55 (1997) 351–361. doi:10.1016/S0278-2391(97)90124-5.

[22] J.L. Peris, J. Prat, M. Comin, R. Dejoz, I.R.P. Vera, Técnica histológica para la inclusión en metil- metacrilato de muestras óseas no descalcificadas, Rev. Española Cirugía Osteoartic. 28 (1993) 231–238.

[23] E. Anitua, R. Prado, M. Azkargorta, E. Rodriguez-Suárez, I. Iloro, J. Casado-Vela, F. Elortza, G. Orive, High-throughput proteomic characterization of plasma rich in growth factors (PRGF-Endoret)-derived fibrin clot interactome., J. Tissue Eng. Regen. Med. 9 (2015) E1-12. doi:10.1002/term.1721.

[24] P. Cunin, C. Beauvillain, C. Miot, J. Augusto, L. Preisser, S. Blanchard, P. Pignon, M. Scotet, E. Garo, I. Fremaux, A. Chevailler, J.-F. Subra, P. Blanco, M.R. Wilson, P. Jeannin, Y. Delneste, Clusterin facilitates apoptotic cell clearance and prevents apoptotic cell-induced autoimmune responses, Cell Death Dis. 7 (2016) e2215. doi:10.1038/cddis.2016.113.

[25] S. de Maat, C. Maas, Factor XII: form determines function, J. Thromb. Haemost. 14 (2016) 1498–1506. doi:10.1111/jth.13383.

[26] R.M. Salasznyk, W.A. Williams, A. Boskey, A. Batorsky, G.E. Plopper, Adhesion to Vitronectin and Collagen I Promotes Osteogenic Differentiation of Human Mesenchymal Stem Cells., J. Biomed. Biotechnol. 2004 (2004) 24–34. doi:10.1155/S1110724304306017.

[27] A.M. Rodrigues, J. Caetano-Lopes, A.C. Vale, B. Vidal, A. Lopes, I. Aleixo, J. Polido-Pereira, A. Sepriano, I.P. Perpétuo, J. Monteiro, M.F. Vaz, J.E. Fonseca, H. Canhão, Low osteocalcin/collagen type I bone gene expression ratio is associated with hip fragility fractures., Bone. 51 (2012) 981–9. doi:10.1016/j.bone.2012.08.129.

[28] P. Newman, F. Bonello, A.S. Wierzbicki, P. Lumb, G.F. Savidge, M.J. Shearer, The uptake of lipoprotein-borne phylloquinone (vitamin K1) by osteoblasts and osteoblast-like cells: role of heparan sulfate proteoglycans and apolipoprotein E., J. Bone Miner. Res. 17 (2002) 426–33. doi:10.1359/jbmr.2002.17.3.426.

[29] M. Shiraki, Y. Shiraki, C. Aoki, T. Hosoi, S. Inoue, M. Kaneki, Y. Ouchi, Association of bone mineral density with apolipoprotein E phenotype., J. Bone Miner. Res. 12 (1997) 1438–45. doi:10.1359/jbmr.1997.12.9.1438.

[30] E. Tsuruga, D.S. Rao, J.E. Baatz, S. V. Reddy, Elevated serum kininogen in patients with

Paget's disease of bone: A role in marrow stromal/preosteoblast cell proliferation, J. Cell. Biochem. 98 (2006) 1681–1688. doi:10.1002/jcb.20874.

[31] J.I. Yamamura, Y. Morita, Y. Takada, H. Kawakami, The fragments of bovine high molecular weight kininogen promote osteoblast proliferation in vitro, J. Biochem. 140 (2006) 825–830. doi:10.1093/jb/mvj217.

[32] D. Ricklin, G. Hajishengallis, K. Yang, J.D. Lambris, Complement: a key system for immune surveillance and homeostasis., Nat. Immunol. 11 (2010) 785–97. doi:10.1038/ni.1923.

[33] T.E. Mollnes, M. Kirschfink, Strategies of therapeutic complement inhibition, Mol. Immunol. 43 (2006) 107–121. doi:10.1016/j.molimm.2005.06.014.

[34] U. Kishore, R.B. Sim, Factor H as a regulator of the classical pathway activation, Immunobiology. 217 (2012) 162–168. doi:10.1016/j.imbio.2011.07.024.

[35] J. Andersson, K.N. Ekdahl, J.D. Lambris, B. Nilsson, Binding of C3 fragments on top of adsorbed plasma proteins during complement activation on a model biomaterial surface, Biomaterials. 26 (2005) 1477–1485. doi:10.1016/j.biomaterials.2004.05.011.

[36] D.T. Luttikhuizen, M.C. Harmsen, M.J.A. Van Luyn, Cellular and molecular dynamics in the foreign body reaction., Tissue Eng. 12 (2006) 1955–70. doi:10.1089/ten.2006.12.1955.

[37] F. Romero-Gavilán, S. Barros-Silva, J. García-Cañadas, B. Palla, R. Izquierdo, M. Gurruchaga, I. Goñi, J. Suay, Control of the degradation of silica sol-gel hybrid coatings for metal implants prepared by the triple combination of alkoxysilanes, J. Non. Cryst. Solids. 453 (2016) 66–73. doi:10.1016/j.jnoncrysol.2016.09.026.

[38] G. Schottner, Hybrid sol-gel-derived polymers: Applications of multifunctional materials, Chem. Mater. 13 (2001) 3422–3435. doi:10.1021/cm011060m.

[39] A. Wennerberg, T. Albrektsson, Effects of titanium surface topography on bone integration: A systematic review, Clin. Oral Implants Res. 20 (2009) 172–184. doi:10.1111/j.1600-0501.2009.01775.x.

[40] A.M. Khorasani, M. Goldberg, E.H. Doeven, G. Littlefair, Titanium in biomedical applications—properties and fabrication: A review, J. Biomater. Tissue Eng. 5 (2015) 593–619. doi:10.1166/jbt.2015.1361.

[41] J.M. Anderson, Future challenges in the in vitro and in vivo evaluation of biomaterial biocompatibility, Regen. Biomater. 3 (2016) 73–77. doi:10.1093/rb/rbw001.

[42] P. V. Giannoudis, T.A. Einhorn, D. Marsh, Fracture healing: The diamond concept, Injury.

38 (2007). doi:10.1016/S0020-1383(08)70003-2.

[43] A.W. Varley, M.G. Coulthard, R.S. Meidell, R.D. Gerard, R.S. Munford, Inflammation-induced recombinant protein expression in vivo using promoters from acute-phase protein genes., Proc. Natl. Acad. Sci. U. S. A. 92 (1995) 5346–50. doi:10.1073/pnas.92.12.5346.

[44] K.N. Ekdahl, J. Hong, O.A. Hamad, R. Larsson, B. Nilsson, Evaluation of the blood compatibility of materials, cells, and tissues: basic concepts, test models, and practical guidelines., in: J. Lambris, V. Holers, D. Ricklin (Eds.), Complement Ther. Adv. Exp. Med. Biol., Springer, Boston, 2013: pp. 257–270.

[45] T.W. Du Clos, Pentraxins: structure, function, and role in inflammation., ISRN Inflamm. 2013 (2013) 379040. doi:10.1155/2013/379040.

[46] E. Song, N. Ouyang, M. Hörbelt, B. Antus, M. Wang, M.S. Exton, Influence of alternatively and classically activated macrophages on fibrogenic activities of human fibroblasts., Cell. Immunol. 204 (2000) 19–28. doi:10.1006/cimm.2000.1687.

[47] S.M. Opal, C.T. Esmon, Bench-to-bedside review: Functional relationships between coagulation and the innate immune response and their respective roles in the pathogenesis of sepsis, Crit. Care. 7 (2003) 23–38. doi:10.1186/cc1854.

[48] C.T. Esmon, Interactions between the innate immune and blood coagulation systems, Trends Immunol. 25 (2004) 536–542. doi:10.1016/j.it.2004.08.003.

[49] V.C.F. Mosqueira, P. Legrand, A. Gulik, O. Bourdon, R. Gref, D. Labarre, G. Barratt, Relationship between complement activation, cellular uptake and surface physicochemical aspects of novel PEG-modified nanocapsules, Biomaterials. 22 (2001) 2967–2979. doi:10.1016/S0142-9612(01)00043-6.

[50] B. Bottazzi, A. Inforzato, M. Messa, M. Barbagallo, E. Magrini, C. Garlanda, A. Mantovani, The pentraxins PTX3 and SAP in innate immunity, regulation of inflammation and tissue remodelling., J. Hepatol. 64 (2016) 1–12. doi:10.1016/j.jhep.2016.02.029.

[51] B. Ghafouri, A. Carlsson, S. Holmberg, A. Thelin, C. Tagesson, Biomarkers of systemic inflammation in farmers with musculoskeletal disorders; a plasma proteomic study, BMC Musculoskelet. Disord. 17 (2016) 1–11. doi:10.1186/s12891-016-1059-y.

[52] M. Fujimoto, S. Serada, K. Suzuki, A. Nishikawa, A. Ogata, T. Nanki, K. Hattori, H. Kohsaka, N. Miyasaka, T. Takeuchi, T. Naka, Brief Report: Leucine-Rich α 2 -Glycoprotein as a Potential Biomarker for Joint Inflammation During Anti-Interleukin-6 Biologic Therapy in Rheumatoid Arthritis, Arthritis Rheumatol. 67 (2015) 2056–2060. doi:10.1002/art.39164.

[53] R.B. Sim, G.J. Arlaud, M.G. Colomb, C1 inhibitor-dependent dissociation of human complement component C1 bound to immune complexes., Biochem. J. 179 (1979) 449–57. http://www.pubmedcentral.nih.gov/articlerender.fcgi?artid=1186649&tool=pmcentrez&rendertype=abstract.

[54] L. Mao, N. Kawao, Y. Tamura, K. Okumoto, K. Okada, M. Yano, O. Matsuo, H. Kaji, Plasminogen activator inhibitor-1 is involved in impaired bone repair associated with diabetes in female mice., PLoS One. 9 (2014) e92686. doi:10.1371/journal.pone.0092686.

4. CHAPTER 3

Proteome analysis of human serum proteins adsorbed onto different titanium surfaces used in dental implants

4. Chapter 3

Proteome analysis of human serum proteins adsorbed onto different titanium surfaces used in dental implants

F. Romero-Gavilán[1], N. Araújo-Gomes[1,2], J. Ródenas[1], A.M. Sánchez-Pérez[2], M. Azkargorta[3], I. Iloro[3], F. Elortza[3], I. García-Arnáez[4], M. Gurruchaga[4], I. Goñi[4], J. Suay[1]

[1] Department of Industrial Systems and Design, Universitat Jaume I, Av. Vicent-Sos Baynat s/n. Castellón, 12071 Spain.

[2] Department of Medicine. Universitat Jaume I, Av. Vicent-Sos Baynat s/n. Castellón, 12071 Spain.

[3] Proteomics Platform, CIC bioGUNE, CIBERehd, ProteoRed-ISCIII, Bizkaia Science and Technology Park. Derio, 48160 Spain.

[4] Facultad de Ciencias Químicas. Universidad del País Vasco. P. M. de Lardizábal, 3. San Sebastián, 20018 Spain.

Biofouling (2017)

ABSTRACT

Titanium dental implants are commonly used due to their biocompatibility and biochemical properties; blasted acid-etched Ti is used more frequently than smooth Ti surfaces. In this study, physico-chemical characterisation revealed important differences in roughness, chemical composition and hydrophilicity, but no differences were found in cellular *in vitro* studies (proliferation and mineralization). However, the deposition of proteins onto the implant surface might affect *in vivo* osseointegration. To test that hypothesis, protein layers formed on discs of both surface types after incubation with human serum were analysed. Using mass spectrometry (LC/MS/MS), 218 proteins were identified, 30 of which were associated with bone metabolism. Interestingly, Apo E, antithrombin and protein C adsorbed mostly onto blasted and acid-etched Ti, whereas the proteins of the complement system (C3) were found predominantly on smooth Ti surfaces. These results suggest that physico-chemical characteristics could be responsible for the differences observed in the adsorbed protein layer.

Keywords: titanium, surface properties, human serum, apolipoprotein E, bone regeneration, proteomics.

Graphical abstract

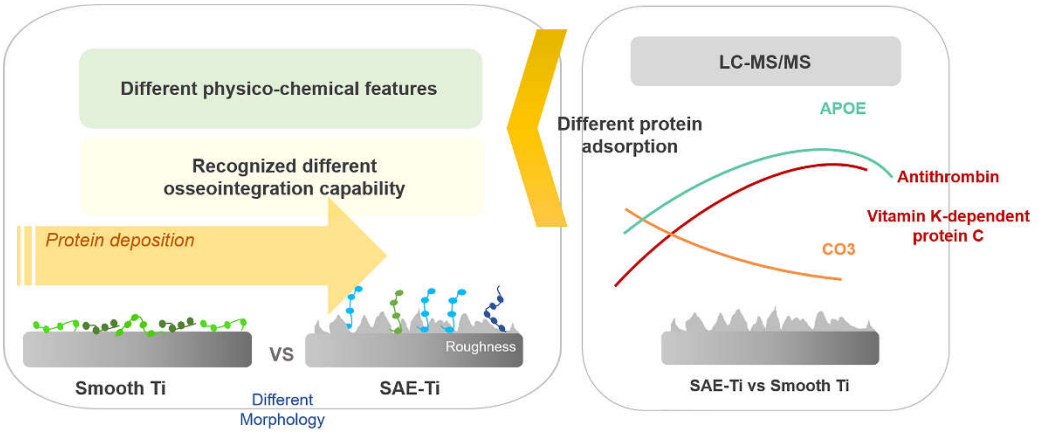

Figure 4.0. Graphical abstract of the work named "Proteome analysis of human serum proteins adsorbed onto different titanium surfaces used in dental implants".

4.1. Introduction

Titanium dental implants are commonly used due to their biocompatibility and biochemical properties [1–3]. Blood plasma is the main biological fluid interacting with these implants [4]. The first event taking place at the biomaterial–tissue interface is the interaction of water molecules and salt ions with the surface of the implant. Shortly after the formation of a hydration layer, a variety of blood proteins adsorb onto implant surfaces. This occurs within seconds or minutes after implantation [5,6]. The resulting protein film mediates all subsequent biological interactions between the material and the surrounding environment; the cells are unlikely ever to interact directly with the native material surfaces. The concentration, composition and conformation of the protein layer on a biomaterial surface may vary. These characteristics of the protein layer are important for synergistic interactions promoting either favourable or adverse cellular and tissue responses, such as attachment to material surfaces, proliferation, and phenotypic changes [7,8].

Rough and blasted acid-etched Ti have replaced smooth Ti after reports of a positive correlation between surface roughness and bone integration [9]. Moreover, rough Ti surfaces adsorb more proteins than smooth Ti due to the increased surface area [10,11]. Protein adsorption is a dynamic process involving non-covalent interactions such as hydrophobic interactions, electrostatic forces, hydrogen bonding and Van der Waals forces [12]. Non-covalent interactions are controlled by many protein parameters, such as protein size, pI and secondary and tertiary structures [13,14]. The specific physico-chemical properties of the biomaterial surface, such as its chemistry, wettability, charge and surface morphology, also affect the protein adsorption process [15].

For these reasons, the researchers have focused on the elucidation of the mechanisms governing protein interactions with various biomaterials including polymers, metals and ceramics [16]. A number of surface-sensitive techniques have been used for the quantification of protein adsorption: surface plasmon resonance, optical waveguide lightmode spectroscopy, ellipsometry, quartz crystal microbalance with dissipation and total internal reflection fluorescence spectroscopy [17].

Many studies evaluating the kinetics of protein adsorption onto Ti have been focused on the exposure of Ti to single protein solutions or protein mixtures [18–22]. However, the protein

adsorption process is a complex phenomenon depending on many parameters, some of which are not considered in these studies. For instance, in multi-protein systems such as blood plasma/serum, increasing the protein concentration or/and the number of small molecules improves their diffusion and accelerates the displacement; thus, they are the first to be adsorbed onto the surface. With time, molecules with greater affinity for the surface but slower rate of diffusion (due to their low concentration or large size) replace the smaller molecules. This is known as the Vroman effect [23,24].

A study using mass spectrometry techniques identified fibronectin, albumin, fibrinogen, IgG and complement CO3 adsorbed on a modified Ti surface incubated in human plasma for 24 h [10]. The same study showed that the adsorption of plasma proteins depends on the roughness of the surface. Recently, label-free quantitative proteomics has been used in a study of the composition and function of adsorbed protein layers [25]. Dodo *et al*. characterised the proteome of the protein layer adsorbed onto a rough Ti surface, after exposure to human blood plasma. The study has shown that the layer adsorbed on this surface is composed mainly of proteins associated with cell adhesion, molecular transportation and coagulation processes. This layer creates a polar and hydrophilic interface for subsequent interactions with host cells [26].

At present, the biological evaluation of medical devices includes a battery of standardised tests, as defined in ISO 10993, highly accepted in the biomaterials research field. Typical tests for biocompatibility of biomaterials involves cytotoxicity, cell attachment, cells proliferation and mineralization assays. However, a lack of correlation between *in vitro* and *in vivo* results has been observed in many instances. Since the first step before cells attachment on the materials surface is protein adsorption, the use of proteomics is proposed to further the understanding of material biocompatibility.

Thus the aim of the present study was to compare the protein layers adsorbed onto two types of Ti surfaces, smooth Ti and blasted acid-etched Ti, after incubation in serum. To achieve this goal, liquid chromatography-tandem mass spectrometry (LC-MS/MS) analysis was employed. Furthermore, a comparison of the more relevant results with *in vitro* tests outcomes was performed. Therefore, this work aimed to establish a correlation between protein deposition and

in vitro outcomes when testing surfaces, such as those currently used in commercial dental implants.

4.2. **Materials and methods**

4.2.1. Surface disc preparation

Ti discs (12 mm in diameter, 1-mm thick) were fabricated from a bar of commercially available, pure, grade-4 Ti (Ilerimplant SL, Lleida, Spain). Some of the discs, sandblasted-acid-etched (SAE) Ti were abraded with 4-µm aluminium oxide particles and acid-etched by submersion in sulfuric acid for 1 h to obtain a moderately rough implant surface. All discs were then washed in acetone, ethanol and 18.2 Ω purified water (for 20 min in each liquid) in an ultrasonic bath and dried under vacuum. Finally, all Ti discs were sterilised using UV radiation.

4.2.2. Physico-chemical characterisation of titanium discs

The surface topography of the Ti discs was characterized using atomic force microscopy Bruker Multimode 8 (AFM, Newport Multimode, MA, USA) under dry conditions. Images were taken at different amplitudes. Measurements at scan sizes of 60 and 1 µm, with a scan rates of 1 and 0.3 Hz, respectively, were carried out (n = 3). The results were analysed using the NanoScope Analysis software (http://nanoscaleworld.bruker-axs.com/nanoscaleworld/media/p/775.aspx). The scanning electron microscopy (SEM) coupled with energy-dispersive X-ray spectroscopy (EDX) (Leica-Zeiss LEO, Wetzlar, Germany) was used to study these surfaces under vacuum. Platinum sputtering was employed to make the samples more conductive for the SEM examination. SEM micrographs were analysed by image processing using Image J software (https://imagej.nih.gov/ij/).

The roughness of the samples was determined using a mechanical Dektak 6M profilometer (Veeco, Plainview, NY, USA). Two samples of each material were tested, with three measurements for each sample to obtain the average values of the parameters Ra and Rt.

Wettability was evaluated by measuring the contact angle using an automatic contact-angle meter DataPhysics OCA 20 (DataPhysics Instruments, Filderstadt, Germany), after depositing 10 µL of

ultrapure water W04 on the titanium surface at room temperature. The drops were formed at dosing rate of 27.5 µL s^{-1} and the angles were determined using SCA 20 software (http://www.dataphysics.de/startseite/produkte/software-module/). Five discs of each material were studied after depositing two drops on each sample.

4.2.3. In vitro assays

4.2.3.1. Cell culture

MC3T3-E1 (mouse calvaria osteosarcoma cell line) cells were cultured in DMEM with phenol red (Gibco–Life Technologies, Waltham, MA, USA), supplemented with 1 % of (100 ×) penicillin/streptomycin (Biowest Inc., Riverside, KS, USA) and 10 % of FBS (Gibco–Life Technologies) for the first 24 h. Then, the medium was replaced with differentiation medium: DMEM with phenol red (1 ×) containing 1 % of penicillin/streptomycin, 1 % of ascorbic acid (5 mg mL^{-1}) and 0.21 % of β-glycerol phosphate. Cells were cultured (at a concentration of 1 × 104 cells $well^{-1}$) with the Ti discs in 24-well culture plates (Thermo Scientific, Waltham, MA, USA) at 37 ºC in a humidified (95 %) atmosphere of 5 % CO_2. The Ti discs were not exposed to blood serum before cell culture. The culture medium was changed every 48 h. In each plate, wells with the same concentration of cells, but no Ti discs, were used as a control of culture conditions.

4.2.3.2. Cell proliferation

For measuring cell proliferation, the commercial cell viability assay alamarBlue® (Invitrogen-Thermo Fisher Scientific, Waltham, MA, USA) was used. This kit measures the cell viability based on a redox reaction with resazurin. The cells were cultured in wells with the discs (3 replicates per treatment) and examined following the manufacturer's protocol after 24, 72 and 120 h. The percentage of reduced resazurin was used to evaluate cell proliferation.

4.2.3.3. ALP activity

ALP activity was assayed by measuring the conversion from p-nitrophenyl phosphate (p-NPP) to p-nitrophenol, and the specific activity of the enzyme was calculated.

Aliquots (0.1 mL) of the solution used for measuring the protein content were assayed for ALP activity. To each aliquot, 100 µL of p-NPP (1 mg mL^{-1}) in substrate buffer (50 mM glycine, 1 mM $MgCl_2$, pH 10.5) was added. After incubation for 2 h in the dark (37 ºC, 5 % CO_2), absorbance was spectrophotometrically measured at 405 nm using a microplate reader. ALP activity was acquired from a standard curve obtained using various concentrations of p-nitrophenol in 0.02 mM sodium hydroxide. The results were calculated in mmols of p- nitrophenol h^{-1} (mM PNP h^{-1}), and data were expressed as ALP activity normalized to the total protein content after 14 and 21 days.

4.2.3.4. Total protein

Total protein content was quantified using Pierce™ BCA Protein Assay Kit (Thermo Fisher Scientific, Walham, MA, USA) for colorimetric protein quantitation based on copper reduction. The culture medium was removed from the wells, the wells were washed 3 times with 1 × DPBS, and 100 µL of lysis buffer (0. 2 % Triton X-100, 10 mM Tris-HCl pH 7.2) were added to each. After 10 min, the lysate was sonicated and centrifuged for 7 min at 13300 rpm and 4 ºC. 20 µL of the supernatant were used for colorimetric measurement of BCA at 570 nm on a microplate reader Multiskan FC® (Thermo Scientific). The total protein content was calculated from a standard curve for bovine albumin and expressed as µg $µL^{-1}$. These data were used to normalize the alkaline phosphatase (ALP) activity after 14 and 21 days.

4.2.4. Statistical analysis

Data were submitted for analysis of variance (ANOVA) and a Newman-Keuls multiple comparison test, when appropriate. Differences at $p \leq 0.05$ were considered statistically significant.

4.2.5. Formation of the protein layer

Each disc was incubated in a well of a 24-well plate (Thermo Scientific) with 2 mL of human blood serum from male AB plasma (Sigma-Aldrich, St Louis, MO, USA) for 180 min (37 ºC, 5 % CO_2). The use of blood serum may deplete some very high abundant proteins, such as fibrin-related proteins. Then, the serum was removed, and the discs were subjected to five consecutive washes with 200µL of double-distilled water and a final wash with 100 mM NaCl in 50 mM Tris-HCl, at pH 7.1, to remove unadsorbed proteins. The final eluate was obtained by submerging the discs in a solution

containing 4 % SDS, 100 mM DTT and 0.5 M TEAB. This method was based on previous studies [27]. Three elutions were performed for each surface treatment; each eluate was obtained from four separate discs. The total protein of the serum was quantified, using the method described above (Pierce™ BCA Protein Assay Kit), yielding a concentration of 51 mg mL^{-1}.

4.2.6. Proteomic analysis

Each eluted protein sample was resolved in 10 % polyacrylamide gels, using a Mini-Protean II electrophoresis cell (Bio-Rad, Hercules, CA, USA). A constant voltage of 150 V was applied for 45 min. The gel was then stained using SYPRO Ruby stain (Bio-Rad) following the manufacturer's instructions. The gel was then washed, and each lane was cut into four slices. Each of these slices was digested with trypsin following a standard protocol [28].

The resulting peptides were resuspended in 0.1 % formic acid, separated using online NanoLC and analysed using electrospray tandem mass spectrometry. Peptide separation was performed on a nanoACQUITY UPLC system connected to a SYNAPT G2-Si spectrometer (Waters, Milford, MA, USA). Samples were loaded onto a Symmetry 300 C18 UPLC Trap column (5 µm, 180 µm × 20 mm, Waters) connected to a BEH130 C18 column (1.7 µm, 75 µm × 200 mm, Waters). The column was equilibrated in 3 % acetonitrile and 0.1 % FA. Peptides were eluted at 300 nL min^{-1} using a 60-min linear gradient of 3 % - 50 % acetonitrile.

A SYNAPT G2-Si ESI Q-Mobility-TOF spectrometer (Waters) equipped with an ion mobility chamber (T-Wave-IMS) for high-definition data acquisition analysis was used for the analysis of the peptides. All analyses were performed using electrospray ionization (ESI) in a positive ion mode. Data were post-acquisition lock-mass corrected using the double charged monoisotopic ion of [Glu^1]-fibrinopeptide B. Accurate LC-MS data were collected in HDDA mode, which enhances signal intensities using the ion mobility separation. Searches were performed using Mascot search engine (Matrix Science, London, UK) in Proteome Discoverer v.1.4 software (Thermo Scientific). Mascot generic files (MGF) files were generated from the original SYNAPT RAW files using ProteinLynx Global Server 3.0.2 (PLGS, Waters) and further processed using the Proteome Discoverer. A peptide mass tolerance of 10 ppm and a fragment mass tolerance of 0.2 Da were used as parameters for the searches. Carbamidomethylation of cysteines was selected as the fixed modification and

oxidation of methionine as a variable modification for tryptic peptides. Proteins identified with at least one peptide with an FDR < 1 % were kept for further examination.

Progenesis LC-MS software (Nonlinear Dynamics, Newcastle-upon-Tyne, UK) was used for differential protein expression analysis. Raw files were imported into the programme, and one of the samples was selected for a reference run to which the precursor masses in all the other samples were aligned. The abundance ratio between the run to be aligned and the reference run were calculated for all features at given retention times. These values were then logarithmised and the programme, based on the analysis of the distribution of all ratios, automatically calculated a global scaling factor. Once normalised, the samples were grouped into the appropriate experimental categories and compared. Differences between groups were only considered for peptide abundances with an ANOVA p-value < 0.05 and a ratio > 1.5 in either direction. A peak list containing the differing peptides was generated for each comparison and searched against a Swiss Prot database using the Mascot Search engine (www.matrixscience.com). Proteins with ANOVA p < 0.05 and a ratio higher than 1.3 in either direction were considered different.

4.3. **Results**

4.3.1. Physico-chemical characterisation of Ti discs

Figure 4.1 shows SEM images of smooth Ti and SAE-Ti surfaces. The different topographies can be clearly seen. The particles on the titanium surface (Figure 4.1b) are visible in the image. EDX results indicated that these were alumina (Al_2O_3) particles that may have been encrusted in the material after the sandblasting process (Figure 4.2). The area of the disc covered by alumina particles comprises around 13.84 % of the disc surface area. AFM images in Figure 4.3, with a scan size of 60 µm, were analysed and an increase on the surface area was detected after aluminium oxide blasting acid-etching treatment. The untreated discs showed a specific surface area of 0.69 ± 0.16 %, while that of the blasted acid-etched discs was of 19.97 ± 1.40 %.

Untreated titanium discs, with smoother topography (Figures 4.3a and c), showed a series of grooves due to the machining process. The change in the topography of Ti after the surface blasting and acid-etching treatment is clearly visible in Figure 4.3b and d. Machining grooves disappeared as a result of sandblasting, and the roughness increased significantly ($p < 0.05$) when the surface

was marked by alumina powder. As it can be seen in Figures 4.3c and d, blasting and acid-etching resulted in larger irregularities but the surface was smoother in comparison with the untreated Ti. This can be attributed to the acid-etching treatment.

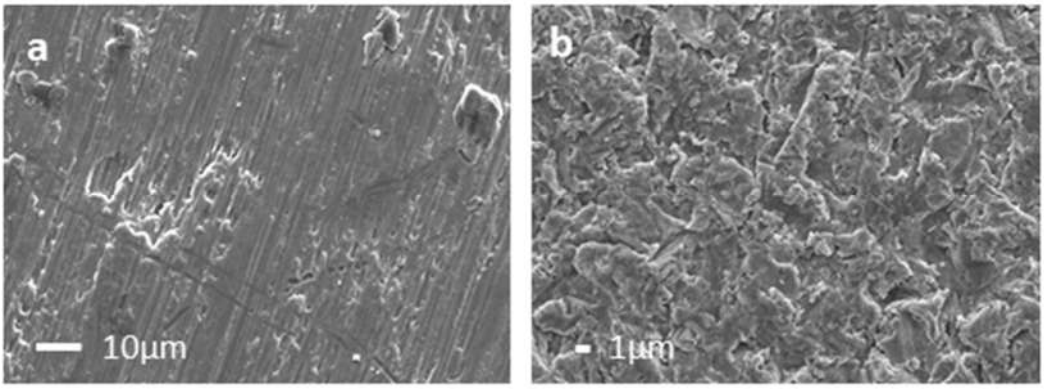

Figure 4.1. SEM images of disc surface: (a) smooth-Ti and (b) SAE-Ti (x1000).

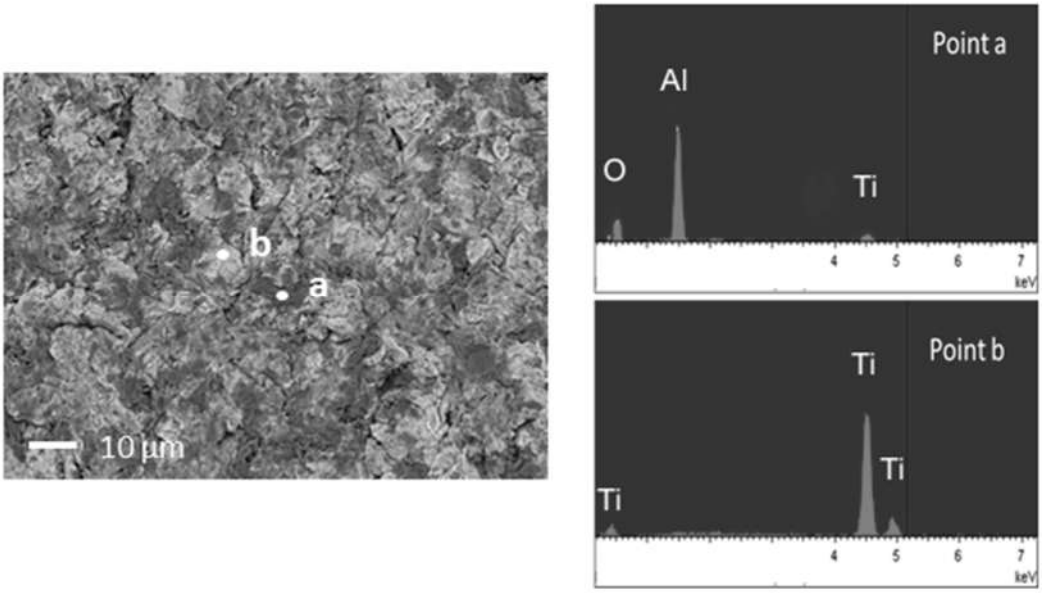

Figure 4.2. SEM/EDX images of titanium sandblasted and acid-etched disc for Al_2O_3 particles identification.

The mechanical profilometer revealed that for the smooth Ti surface, Ra and Rt parameters were 0.14 ± 0.04 and 1.28 ± 0.40 µm, respectively. After blasting and acid-etching, Ra and Rt were 0.93 ± 0.06 and 8.38 ± 0.99 µm, respectively. Thus, the surface roughness of the treated discs was significantly higher than the roughness of the untreated samples.

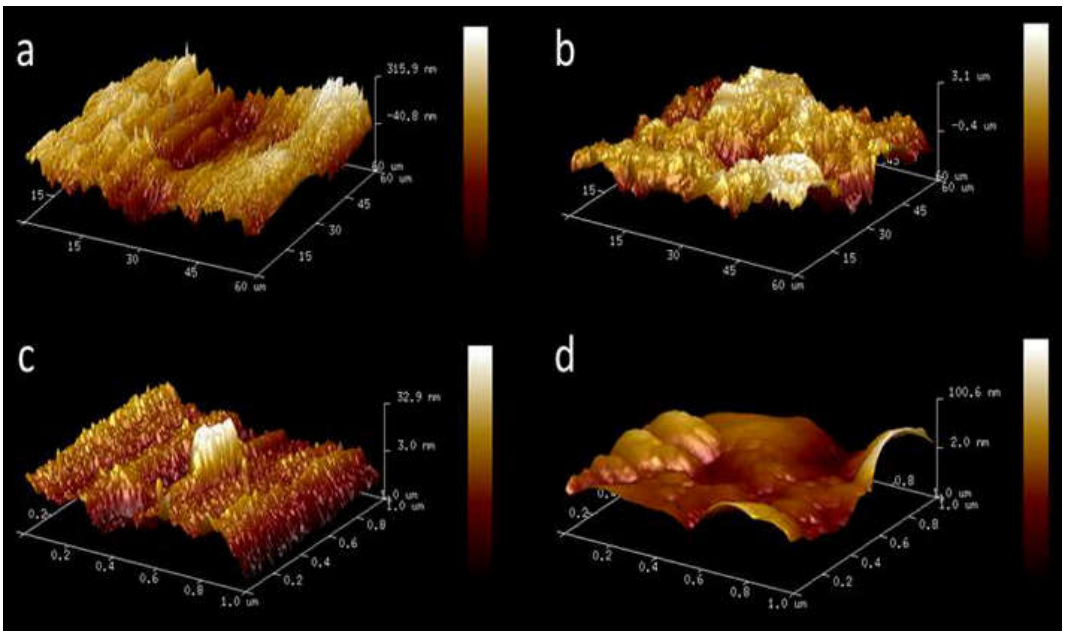

Figure 4.3. AFM images at scan size 60 µm: (a) untreated titanium and (b) SAE treated Ti; and 1 µm: (c) untreated titanium and (d) SAE treated titanium. The z-axis could not be normalized to the same scale due to the height difference between treatments.

Contact angle measurements were carried out to determine the wettability of the surface. Significantly ($p < 0.05$) lower contact angles were observed for blasted acid-etched Ti surfaces than for the untreated discs, namely, 85.70 ± 2.83° and 94.53 ± 2.59°, respectively. Thus, the treated discs showed greater hydrophilicity.

4.3.2. In vitro cultures

Analysis of cell proliferation (Figure 4.4) clearly showed that disc treatment had no significant effect on the cellular growth. Cells proliferated at equal rates on both types of discs during the five-day protocol. A threefold increase in cell numbers was observed between 24 h and 3 days in culture. Proliferation slowed down between 3 and 5 days of incubation, showing a plateau and a reduction in proliferation.

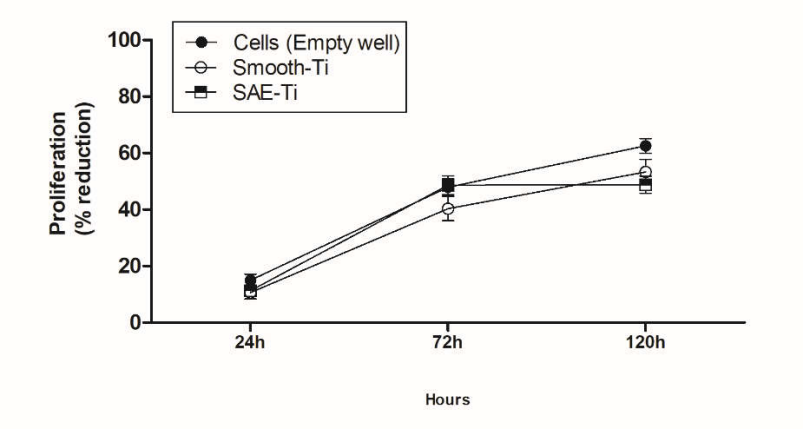

Figure 4.4. MC3T3-E1 cell proliferation on different treated discs: Smooth-Ti (white circle), SAE-Ti (black semi-square with dotted line). Cells, on an empty well, without disc was used as a control (white circle). No statistically significant differences were found between treatments.

ALP enzyme activity (Figure 4.5) was not affected by disc topography after 14 and 21 days (ANOVA, $p > 0.05$). Moreover, between these time points, there was a slight decrease in the ALP activity, as expected. These *in vitro* data indicate that the disc topographies examined in this study do not affect the metabolic and division processes of MC3T3-E1 cells, related to mineralization.

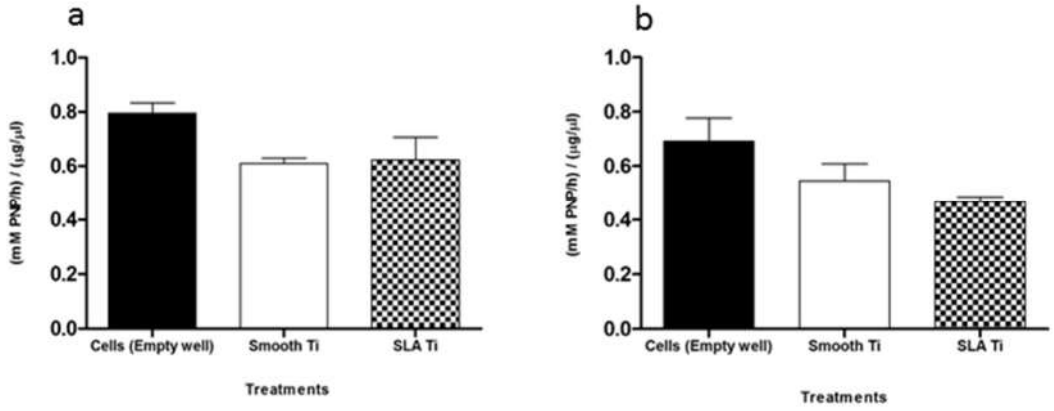

Figure 4.5. MC3T3-E1 cells ALP activity normalized to the total protein (BCA) levels (mM PNP h^{-1}) / (µg μL^{-1}) on different treated discs at (a) 14 and (b) 21 days; Smooth-Ti (white column); SAE-Ti (squared/dotted column). Cells, on an empty well, without disc was used as a control (black column). No statistically significant differences were found between treatments.

4.3.3. Proteomic analysis

4.3.3.1. Identification of proteins adsorbed onto the SAE-Ti and smooth Ti

LC-MS/MS analysis of the protein layers adsorbed to both Ti surfaces resulted in the identification of 218 different proteins, 30 of which related with bone metabolism (Table 4.1). Serum proteins involved in cell adhesion and extracellular matrix, important for implant integration, were also found: vitronectin [29–31] and proteoglycan 4 [32]. Intriguingly, cellular/cytoplasmic components of cell adhesion and cell junction adsorbed to the Ti surfaces were found: integrin alpha-V [33–35], junction plakoglobin [36], gelsolin [37–39] and actin cytoplasmic 1 [40]. LC MS/MS analysis also revealed cellular and secreted proteins associated with bone homeostasis: peptidyl-prolyl cis-trans isomerase B [41] and lysozyme C [42,43]. Serum proteins involved in bone formation were also found to a certain degree, serum paraoxonase/arylesterase 1 [44], vitamin D binding protein [45–47] and pigment epithelium-derived factor [48,49].

Table 4.1. Plasma proteins adsorbed on SAE-Ti and Smooth Ti as identified by LC-MS/MS. Spectral counts indicates number of MS/MS spectra obtained for each protein.

		Spectral counts						
		Smooth			SLA-treated			
Description	**Accession**	**B1**	**B2**	**B3**	**A1**	**A2**	**A3**	**Ref. related to bone**
Beta-2-glycoprotein 1	APOH_HUMAN	5	2	1	2	0	1	[50]
Complement component C8 beta chain	CO8B_HUMAN	2	0	0	0	0	0	[51,52]
Metal transporter CNNM2	CNNM2_HUMAN	0	1	0	0	3	1	[53]
Junction plakoglobin	PLAK_HUMAN	1	0	23	4	0	0	[36]
Vitronectin	VTNC_HUMAN	14	3	6	15	10	12	[29–31]
Serum paraoxonase/arylesterase 1	PON1_HUMAN	2	0	8	7	0	0	[44]
Plasminogen	PLMN_HUMAN	7	0	2	3	3	7	[54–56]
Coagulation factor XII	FA12_HUMAN	3	0	1	0	0	0	[57]
Gelsolin	GELS_HUMAN	12	2	6	6	6	6	[37,39]
Integrin alpha-V	ITAV_HUMAN	0	2	1	0	0	1	[33,35]
Alpha-2-macroglobulin	A2MG_HUMAN	15	0	23	17	8	6	[58]
Complement C3	CO3_HUMAN	135	31	115	88	58	75	[59,60]
Tetranectin	TETN_HUMAN	2	2	2	4	0	2	[61,62]
Pigment epithelium-derived factor	PEDF_HUMAN	5	0	2	2	0	0	[48,49]
Complement C4-A	CO4A_HUMAN	54	14	37	34	17	14	[63]
Alpha-1-acid glycoprotein 2	A1AG2_HUMAN	1	0	3	3	0	0	[64]
Apolipoprotein E	APOE_HUMAN	57	20	55	64	43	65	[65–68]
Proteoglycan 4	PRG4_HUMAN	1	0	3	2	0	3	[32]
Alpha-1-acid glycoprotein 1	A1AG1_HUMAN	0	0	2	2	0	0	[69]
Peptidyl-prolyl cis-trans isomerase B	PPIB_HUMAN	0	0	0	1	0	1	[41]
Complement component C6	CO6_HUMAN	0	0	1	1	0	2	[70,71]
Haptoglobin-related protein	HPTR_HUMAN	3	0	9	5	3	0	[72]
Vitamin D-binding protein	VTDB_HUMAN	2	0	4	1	0	0	[45–47]

Actin, cytoplasmic 1	ACTB_HUMAN	10	5	11	19	53	22	[40]
Lysozyme C	LYSC_HUMAN	0	0	2	2	0	1	[42,43]
Hemoglobin subunit beta	HBB_HUMAN	1	0	2	2	0	0	[73]
Apolipoprotein C-I	APOC1_HUMAN	1	0	0	2	0	1	[74]
Kininogen-1	KNG1_HUMAN	4	0	4	0	0	0	[75]
Serotransferrin	TRFE_HUMAN	15	4	22	12	1	5	[76,77]

4.3.3.2. Gene ontology analysis of the identified proteins

Proteomic analysis led to the identification of 181 and 162 proteins on smooth Ti and blasted acid-etched surfaces, respectively. Adsorbed proteins were classified using the PANTHER (Protein ANalysis THrough Evolutionary Relationships) classification system (Figures 4.6 and 4.7). The results of protein classification according to biological processes were almost identical for the two types of surfaces (Figure 4.6a and b).

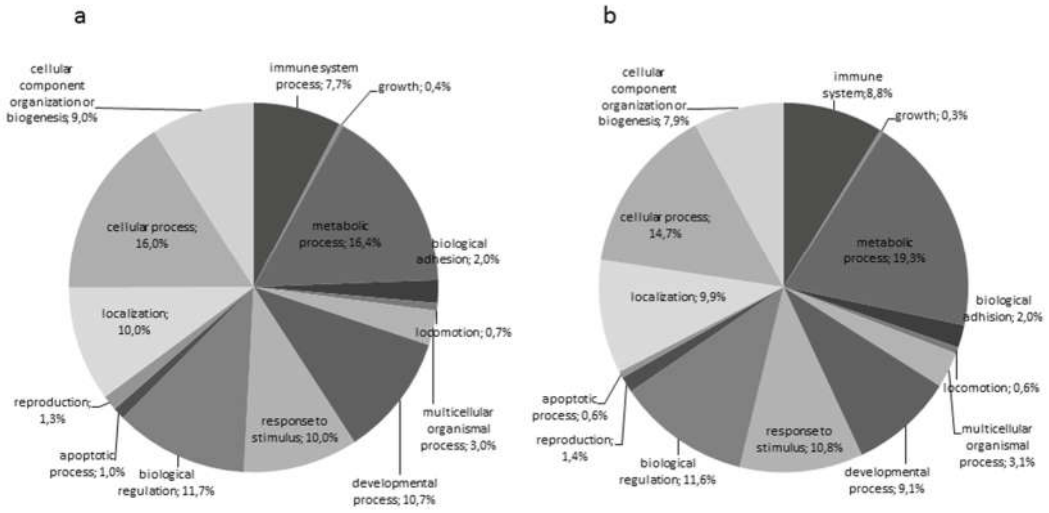

Figure 4.6. PieCharts showing the biological processes of the proteins adhered to (a) SAE-Ti and (b) Smooth-Ti.

However, classification of proteins according to the pathways in which they are involved revealed differences between the two types of surfaces (Figure 4.7a and b). Interestingly, smooth Ti-adsorbed proteins were observed to participate in a wider range of pathways than those found on the blasted acid-etched Ti. Blood coagulation (43.35 %), inflammation mediated by cytokines (17.34 %) and integrin signalling (13.29 %) were the three major process-classified protein categories found on the treated (SAE) Ti. For smooth Ti, blood coagulation (28.52 %) and inflammation (11.91 %) were the most significant categories. However, a major group of proteins related to glycolysis (11.91 %) was adsorbed on smooth Ti, which is absent on SAE surfaces. Integrin signalling was only represented by a relatively minor proportion of proteins on the smooth Ti (4.69 %) in comparison with the treated Ti surfaces. Proteins related to diseases such as Parkinson's and Alzheimer's and proteins related to CCKR signalling pathways were found on both disc types (a very small proportion of the total protein). In addition to these categories, smooth Ti surfaces adsorbed a small percentage of proteins involved in apoptotic and plasminogen signalling pathways.

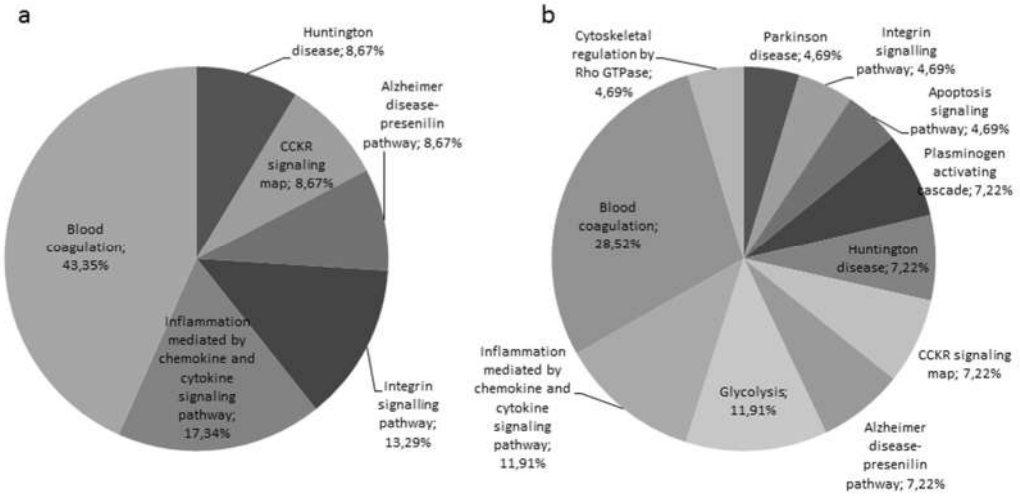

Figure 4.7. PieCharts pathways of the proteins adhered to (c) SAE-Ti and (d) Smooth-Ti.

4.3.3.3. Specifically enriched proteins

To find the specifically enriched proteins adsorbed onto the two surface types that might reflect their different osteoinduction capabilities, a differential analysis was performed (in triplicate) using the Progenesis QI software. This method identified nine proteins differentially enriched/associated with each surface (Table 4.2).

Proteins enriched on the blasted acid-etched Ti were apolipoproteins ApoA-I, ApoE, ApoA-IV, plectin, antithrombin III and Vitamin K-dependent protein. The largest difference between the two surface types was found for ApoA-IV and plectin. It was also found that complement CO3 and some immunoglobulins (Ig gamma and lambda chains) were significantly enriched on the smooth Ti but not on the blasted and acid-etched Ti discs.

Table 4.2. Specific proteins (Progenesis method).

Accession	Description	Confidence score	Anova (p)	Average SLA	Average Smooth	Ratio SLA / Smooth
PLEC_HUMAN	Plectin	56.31	2.76E-03	871.54	3.02	288.22
ANT3_HUMAN	Antithrombin-III	75.68	5.92E-04	2613.27	13.25	197.22
PROC_HUMAN	Vitamin K-dependent protein C	87.11	1.39E-02	3106.36	158.53	19.59
APOA4_HUMAN	Apolipoprotein A-IV	247.55	4.48E-03	1326.02	499.46	2.65
APOA1_HUMAN	Apolipoprotein A-I	197.75	3.27E-02	21111.07	12019.28	1.76
APOE_HUMAN	Apolipoprotein E	438.34	1.97E-02	7706.64	4798.73	1.61
LV301_HUMAN	Ig lambda chain V-III region SH	37.01	1.21E-02	1040.84	1522.40	0.68
CO3_HUMAN	Complement C3	205.15	1.23E-02	2030.88	4398.04	0.46
IGHG1_HUMAN	Ig gamma-1 chain C region	49.04	2.20E-02	506.02	2040.67	0.25

4.4. Discussion

The main part of this study characterised the protein layer adsorbed onto Ti discs with two different surface types: a SAE-Ti and an untreated, smooth Ti. It is reasonable to assume that different surface characteristics will affect the adsorption of proteins.

Roughness is a key parameter in the assessment of the osseointegrative properties of material [78]. The two surface types studied in this work have different topography, i.e. SAE-Ti is rougher than the untreated Ti surface. These results are consistent with previous studies [79]. Moreover, the presence of alumina is also associated with a good bone response [80] and a change in hydrophilicity affecting both chemical and physical composition of the surface. All these physico-chemical features will affect the affinity of the protein layer formed on the material.

Ti surfaces are widely used in implants; techniques advancing the osteogenesis are needed to improve the quality of health care and patient recovery. The surface types described here have been extensively used in orthopaedic implants with overall similar outcomes [81].

The *in vitro* experiments, using an osteosarcoma cell line, showed no differences between both samples either in proliferation or mineralization. Both surfaces showed very similar cell proliferation results with time, increasing gradually throughout the test period. Mineralization in cells, measured by ALP activity, an enzyme that becomes very active during osteoblast differentiation, decreased on both Ti surfaces with time with no statistically significant differences. In similar studies, no significant differences in either proliferation or mineralization were found [82]. These results are supported by proteomic analysis of proteins adsorbed onto the different discs since the majority of proteins attach on similar way to both surfaces. The extensive list of adsorbed proteins shows that at least 30 of these proteins are involved in bone homeostasis in a direct or indirect way (Table 4.1).

However, the blasted and acid-etched Ti surfaces and smooth Ti surfaces showed different osteogenic properties in *in vivo* models [83]. Furthermore, Aparicio *et al.* [84] showed that high Ra values favour osseointegration of dental implants in comparison with smoother surfaces. This effect is attributed to a higher implant-bone contact interface as a consequence of increased roughness. Nevertheless, in this study chemical differences between treatments were also found.

To test this premise a detailed analysis of the proteins adsorbed to the two surface types was performed. In order to isolate and identify these surface adsorbed proteins, a protocol was established where, following serum incubation, discs were washed and final protein elution was obtained with an SDS-containing buffer. This approach permitted washing of the surfaces thoroughly and getting a good protein yield for the characterisation of the differences between both surfaces. The procedure indicates that under the same regime of washes and the same elution strength, a number of different proteins bound more consistently to each of the surfaces at statistically significant different concentrations, revealing differences in surface-protein interactions. Although other approaches cannot be discarded, the present method has been shown to be useful for the intended purpose. One the other hand, the use of a harsher buffer could release proteins that might have remained attached after the SDS wash. However, it is believed that although the total list of proteins could increase, it should not affect the differential analysis results. There was an average of 181 proteins identified in the smooth Ti surface discs, and 162 proteins on the blasted and acid-etched Ti surface. This suggests that the differences observed between the surfaces is a result of differential binding of certain proteins and not from the total amount of protein.

The proteomics differential quantification analysis performed by Progenesis found some significant differences for plectin, antithrombin-III and several other apolipoproteins. Plectin is a cytoskeleton protein that links intermediate filaments to other cytoskeletal systems and anchors them to the membrane junction sites. It binds mostly to vimentin and is very important for preserving the mechanical integrity of the tissue [85]. Plectin is not a typical serum protein; therefore, its presence in the protein layer formed by incubation of Ti discs with the serum was unexpected. Antithrombin (AT) is a glycoprotein that inactivates several enzymes of the coagulation system. Specifically, AT-III inactivates thrombin, which catalyses the formation of fibrin from fibrinogen. Fibrin architecture at the clot affects bone healing [86]. However, apolipoproteins are important serum proteins involved in lipid transport; different isoforms have different properties and activities. Apolipoprotein A-IV has antioxidant-like activity and is involved in the inhibition of lipid oxidation [87]. It has been reported that patients with osteonecrosis, a skeletal pathology with intense bone degeneration, have lower levels of ApoA-IV in comparison with healthy individuals [88]. Lipid metabolism and oxidative injury are important processes in the pathophysiology of the disease.

Apo A-IV mutations are linked to corticosterone-induced osteonecrosis in patients with renal transplants [89]. In the present study, Apo A-IV level was significantly higher on the blasted acid-etched Ti than on the smooth Ti. This observation might account for a favourable osseointegration environment created by the treated discs as the protein acts as an antioxidant. Another important apolipoprotein, ApoA1, adsorbed to treated Ti at higher concentrations than to smooth Ti. ApoA1 is the main component of the high-density cholesterol complex, but it has not been associated with bone formation or resorption. Interestingly, ApoE, which is involved in the regulation of bone metabolism, was also adsorbed to the SAE-Ti in larger amounts than to smooth Ti. Although still somewhat controversial, ApoE has been extensively reported to be involved in bone homeostasis [65], possibly via promotion of vitamin K uptake into the osteoblasts [66]. However, various ApoE alleles behave very differently in this process. ApoƐ2 is the allele with the lowest involvement in the transport of vitamin K [90]. The ApoƐ4 allele has been associated with a low bone mass in several studies in postmenopausal women [68,91]. More recently, epidemiological studies have confirmed that ApoƐ2 represents an increased risk for trabecular bone fracture [67]. The most frequent ApoE allele is ApoƐ3, found with a frequency of 79 %. ApoƐ2 is present in approximately 7 % of the population, and ApoƐ4 in 14 %. ApoƐ3 is also called the neutral allele because it is not associated with any of the human diseases. ApoƐ2 and 4 have been associated with increased probability of developing arthrosclerosis and Alzheimer's disease [92].

The method used to characterise the protein layer on Ti surfaces did not allow for the determination of the type of ApoE allele adsorbed. Moreover, is not clear whether physico-chemical properties of the surface discriminate between the allele types. It is tempting to hypothesize that SAE-Ti has the ability to enrich the microenvironment of the implant with ApoE. However, this could only improve the osseointegration outcome if the patient carried the ApoƐ3 alleles. Following this line of thought might help to determine the mechanisms of the variability in the outcomes of the same implant type in different patients.

Kaneko *et al.* [27] published a similar study using different surfaces, octacalcium phosphate (OCP) and hydroxyapatite crystals (HA). They have found that ApoE and complement component 3 (CO3) were among the proteins differentially associated with these surfaces. They observed that HA adsorbed more CO3 than OCP, whereas OCP adsorbed more ApoE.

Interestingly, in the present study, CO3 was enriched on smooth Ti discs. CO3 belongs to a family of proteins involved in immune and inflammatory responses [93]. Osteoclasts are bone macrophages derived from the myeloid lineage that requires complement CO3 and CO5 for optimal differentiation [52]. Osteoclasts are necessary for bone resorption and the optimal balance between osteoblast and osteoclast differentiation must be reached to achieve healthy bone formation. It is not clear whether increased CO3 adsorption onto smooth Ti surfaces alters this balance.

4.5. **Conclusions**

To summarise, two types of surfaces smooth and SAE, were studied by physico-chemical, *in vitro* and proteomic analysis. Al_2O_3 was found in the SAE surface and only Ti in the smooth sample. Roughness and hydrophilicity were increased by SAE treatment. In this study, in accordance with published literature, no differences in *in vitro* tests (proliferation and mineralization) were found. Proteomic analysis of the proteins adsorbed onto both surfaces showed the presence of proteins related to bone generation. Proteins enriched on the SAE-Ti were apolipoproteins ApoA-I, ApoE, ApoA-I, plectin, antithrombin III and Vitamin K-dependent protein C. The largest difference between the two surface types was found for ApoA-IV and plectin. It was also found that complement CO3 and some immunoglobulins (Ig gamma and lambda chains) were significantly enriched on smooth Ti but not on the blasted and acid-etched Ti discs. Although significant physico-chemical differences were found between samples (chemical composition, roughness and hydrophilicity), *in vitro* test did not show any differences. Further work is needed to demonstrate that proteomic analysis can correlate with *in vivo* behaviour.

ACKNOWLEDGEMENTS

This work was supported by Ministerio de Economia y Competitividad (MINECO) via MAT 2014-51918-C2-2-R, Universitat Jaume I through P11B2014-19 and under grant Predoc/2014/25; Generalitat Valenciana under grant Grisolia/2014/016. Authors would like to thank Antonio Coso and Jaime Franco (GMI-Ilerimplant) for their inestimable contribution in this study, and Raquel Oliver, José Ortega (UJI) and Iraide Escobés (CIC bioGUNE) for their valuable technical assistance.

REFERENCES

[1] J.E. Lemons, L.C. Lucas, Properties of biomaterials, J. Arthroplasty. 1 (1986) 143–147. doi:10.1016/S0883-5403(86)80053-5.

[2] H. Nakajima, T. Okabe, Titanium in Dentistry: Development and Research in the U.S.A., Dent. Mater. J. 15 (1996) 77–90. doi:10.4012/dmj.15.77.

[3] D.C. Smith, Dental implants: materials and design considerations., Int. J. Prosthodont. 6 (1993) 106–117.

[4] J.Y. Park, J.E. Davies, Red blood cell and platelet interactions with titanium implant surfaces, Clin. Oral Implants Res. 11 (2000) 530–539. doi:10.1034/j.1600-0501.2000.011006530.x.

[5] D. Puleo, Understanding and controlling the bone–implant interface, Biomaterials. 20 (1999) 2311–2321. doi:10.1016/S0142-9612(99)00160-X.

[6] D. MacDonald, N. Deo, B. Markovic, M. Stranick, P. Somasundaran, Adsorption and dissolution behavior of human plasma fibronectin on thermally and chemically modified titanium dioxide particles, Biomaterials. 23 (2002) 1269–1279. doi:10.1016/S0142-9612(01)00317-9.

[7] P.J. Molino, M.J. Higgins, P.C. Innis, R.M.I. Kapsa, G.G. Wallace, Fibronectin and bovine serum albumin adsorption and conformational dynamics on inherently conducting polymers: a QCM-D study., Langmuir. 28 (2012) 8433–45. doi:10.1021/la300692y.

[8] B. Fernández-Montes Moraleda, J. San Román, L.M. Rodríguez-Lorenzo, Influence of surface features of hydroxyapatite on the adsorption of proteins relevant to bone regeneration., J. Biomed. Mater. Res. A. 101 (2013) 2332–9. doi:10.1002/jbm.a.34528.

[9] A. Wennerberg, T. Albrektsson, On implant surfaces: a review of current knowledge and opinions., Int. J. Oral Maxillofac. Implants. 25 (2010) 63–74.

[10] M.N. Sela, L. Badihi, G. Rosen, D. Steinberg, D. Kohavi, Adsorption of human plasma proteins to modified titanium surfaces., Clin. Oral Implants Res. 18 (2007) 630–8. doi:10.1111/j.1600-0501.2007.01373.x.

[11] G.P. Rockwell, L.B. Lohstreter, J.R. Dahn, Fibrinogen and albumin adsorption on titanium nanoroughness gradients., Colloids Surf. B. Biointerfaces. 91 (2012) 90–6. doi:10.1016/j.colsurfb.2011.10.045.

[12] J.D. Andrade, V. Hlady, Protein adsortion and materials biocompatibility: a tutorial review

and suggested hypotheses., in: Biopolym. HPLC. Adv. Polym. Sci., Springer-Nature, Berlin, 1987: pp. 1–63. doi:10.1007/3-540-16422-7_6.

[13] M. Rabe, D. Verdes, S. Seeger, Understanding protein adsorption phenomena at solid surfaces., Adv. Colloid Interface Sci. 162 (2011) 87–106. doi:10.1016/j.cis.2010.12.007.

[14] C.A. Haynes, W. Norde, Globular proteins at solid/liquid interfaces, Colloids Surfaces B Biointerfaces. 2 (1994) 517–566. doi:10.1016/0927-7765(94)80066-9.

[15] W.J. Schmidt, D.R., Waldeck, H., Kao, Protein adsorption to biomaterials, in: D. Puleo, R. Bizios (Eds.), Biol. Interact. Mater. Surfaces Underst. Control. Protein, Cell, Tissue, Springer, New York, 2009: pp. 1–18. doi:10.1007/978-0-387-98161-1_1.

[16] J.L. Wehmeyer, R. Synowicki, R. Bizios, C.D. García, Dynamic Adsorption of Albumin on Nanostructured TiO2Thin Films., Mater. Sci. Eng. C. Mater. Biol. Appl. 30 (2010) 277–282. doi:10.1016/j.msec.2009.11.002.

[17] J. Malmström, H. Agheli, P. Kingshott, D.S. Sutherland, Viscoelastic modeling of highly hydrated laminin layers at homogeneous and nanostructured surfaces: quantification of protein layer properties using QCM-D and SPR., Langmuir. 23 (2007) 9760–8. doi:10.1021/la701233y.

[18] M. Pegueroles, C. Tonda-Turo, J.A. Planell, F.-J. Gil, C. Aparicio, Adsorption of fibronectin, fibrinogen, and albumin on TiO2: time-resolved kinetics, structural changes, and competition study., Biointerphases. 7 (2012) 1–13. doi:10.1007/s13758-012-0048-4.

[19] K. Imamura, M. Shimomura, S. Nagai, M. Akamatsu, K. Nakanishi, Adsorption characteristics of various proteins to a titanium surface., J. Biosci. Bioeng. 106 (2008) 273–8. doi:10.1263/jbb.106.273.

[20] S.R. Sousa, M. Lamghari, P. Sampaio, P. Moradas-Ferreira, M.A. Barbosa, Osteoblast adhesion and morphology on TiO2 depends on the competitive preadsorption of albumin and fibronectin., J. Biomed. Mater. Res. A. 84 (2008) 281–90. doi:10.1002/jbm.a.31201.

[21] J. Pei, H. Hall, N.D. Spencer, The role of plasma proteins in cell adhesion to PEG surface-density-gradient-modified titanium oxide., Biomaterials. 32 (2011) 8968–78. doi:10.1016/j.biomaterials.2011.08.034.

[22] D. Kohavi, L. Badihi Hauslich, G. Rosen, D. Steinberg, M.N. Sela, Wettability versus electrostatic forces in fibronectin and albumin adsorption to titanium surfaces., Clin. Oral Implants Res. 24 (2013) 1002–8. doi:10.1111/j.1600-0501.2012.02508.x.

[23] K.C. Dee, D. Puleo, R. Bizios, An Introduction To Tissue-Biomaterial Interactions, Wiley &

Sons, New Jersey, 2003. doi:10.1002/0471270598.

[24] K. Wang, C. Zhou, Y. Hong, X. Zhang, A review of protein adsorption on bioceramics., Interface Focus. 2 (2012) 259–77. doi:10.1098/rsfs.2012.0012.

[25] A. Montoya, L. Beltran, P. Casado, J.C. Rodríguez-Prados, P.R. Cutillas, Characterization of a TiO_2 enrichment method for label-free quantitative phosphoproteomics., Methods. 54 (2011) 370–8. doi:10.1016/j.ymeth.2011.02.004.

[26] C.G. Dodo, P.M. Senna, W. Custodio, A.F. Paes Leme, A.A. Del Bel Cury, Proteome analysis of the plasma protein layer adsorbed to a rough titanium surface., Biofouling. 29 (2013) 549–57. doi:10.1080/08927014.2013.787416.

[27] H. Kaneko, J. Kamiie, H. Kawakami, T. Anada, Y. Honda, N. Shiraishi, S. Kamakura, T. Terasaki, H. Shimauchi, O. Suzuki, Proteome analysis of rat serum proteins adsorbed onto synthetic octacalcium phosphate crystals., Anal. Biochem. 418 (2011) 276–85. doi:10.1016/j.ab.2011.07.022.

[28] E. Anitua, R. Prado, M. Azkargorta, E. Rodriguez-Suárez, I. Iloro, J. Casado-Vela, F. Elortza, G. Orive, High-throughput proteomic characterization of plasma rich in growth factors (PRGF-Endoret)-derived fibrin clot interactome., J. Tissue Eng. Regen. Med. 9 (2015) E1-12. doi:10.1002/term.1721.

[29] A. Di Benedetto, G. Brunetti, F. Posa, A. Ballini, F.R. Grassi, G. Colaianni, S. Colucci, E. Rossi, E.A. Cavalcanti-Adam, L. Lo Muzio, M. Grano, G. Mori, Osteogenic differentiation of mesenchymal stem cells from dental bud: Role of integrins and cadherins., Stem Cell Res. 15 (2015) 618–28. doi:10.1016/j.scr.2015.09.011.

[30] A.K. Kundu, A.J. Putnam, Vitronectin and collagen I differentially regulate osteogenesis in mesenchymal stem cells., Biochem. Biophys. Res. Commun. 347 (2006) 347–57. doi:10.1016/j.bbrc.2006.06.110.

[31] R.M. Salasznyk, W.A. Williams, A. Boskey, A. Batorsky, G.E. Plopper, Adhesion to Vitronectin and Collagen I Promotes Osteogenic Differentiation of Human Mesenchymal Stem Cells., J. Biomed. Biotechnol. 2004 (2004) 24–34. doi:10.1155/S1110724304306017.

[32] C.M. Novince, M.N. Michalski, A.J. Koh, B.P. Sinder, P. Entezami, M.R. Eber, G.J. Pettway, T.J. Rosol, T.J. Wronski, K.M. Kozloff, L.K. McCauley, Proteoglycan 4: a dynamic regulator of skeletogenesis and parathyroid hormone skeletal anabolism., J. Bone Miner. Res. 27 (2012) 11–25. doi:10.1002/jbmr.508.

[33] K. Kaneko, M. Ito, Y. Naoe, A. Lacy-Hulbert, K. Ikeda, Integrin αv in the mechanical response of osteoblast lineage cells., Biochem. Biophys. Res. Commun. 447 (2014) 352–7.

doi:10.1016/j.bbrc.2014.04.006.

[34] S. Roux, New treatment targets in osteoporosis., Jt. Bone Spine. 77 (2010) 222–8. doi:10.1016/j.jbspin.2010.02.004.

[35] C. Kumar, Integrin αvβ3 as a Therapeutic Target for Blocking Tumor-Induced Angiogenesis, Curr. Drug Targets. 4 (2003) 123–131. doi:10.2174/1389450033346830.

[36] I. D'Alimonte, A. Lannutti, C. Pipino, P. Di Tomo, L. Pierdomenico, E. Cianci, I. Antonucci, M. Marchisio, M. Romano, L. Stuppia, F. Caciagli, A. Pandolfi, R. Ciccarelli, Wnt signaling behaves as a "master regulator" in the osteogenic and adipogenic commitment of human amniotic fluid mesenchymal stem cells., Stem Cell Rev. 9 (2013) 642–54. doi:10.1007/s12015-013-9436-5.

[37] D.J. Kwiatkowski, P.A. Janmey, H.L. Yin, Identification of critical functional and regulatory domains in gelsolin, J. Cell Biol. 108 (1989) 1717–1726. doi:10.1083/jcb.108.5.1717.

[38] J.M. Kim, J. Kim, Y.H. Kim, K.T. Kim, S.H. Ryu, T.G. Lee, P.G. Suh, Comparative secretome analysis of human bone marrow-derived mesenchymal stem cells during osteogenesis., J. Cell. Physiol. 228 (2013) 216–24. doi:10.1002/jcp.24123.

[39] C. Thouverey, A. Malinowska, M. Balcerzak, A. Strzelecka-Kiliszek, R. Buchet, M. Dadlez, S. Pikula, Proteomic characterization of biogenesis and functions of matrix vesicles released from mineralizing human osteoblast-like cells., J. Proteomics. 74 (2011) 1123–34. doi:10.1016/j.jprot.2011.04.005.

[40] B. Sen, Z. Xie, G. Uzer, W.R. Thompson, M. Styner, X. Wu, J. Rubin, Intranuclear Actin Regulates Osteogenesis., Stem Cells. 33 (2015) 3065–76. doi:10.1002/stem.2090.

[41] S.M. Pyott, U. Schwarze, H.E. Christiansen, M.G. Pepin, D.F. Leistritz, R. Dineen, C. Harris, B.K. Burton, B. Angle, K. Kim, M.D. Sussman, M. Weis, D.R. Eyre, D.W. Russell, K.J. McCarthy, R.D. Steiner, P.H. Byers, Mutations in PPIB (cyclophilin B) delay type I procollagen chain association and result in perinatal lethal to moderate osteogenesis imperfecta phenotypes., Hum. Mol. Genet. 20 (2011) 1595–609. doi:10.1093/hmg/ddr037.

[42] H. Siebert, N. Treber, P. Konold, A. Pannike, Zur Rolle des Lysozyms bei der Mineralisation von Callusgewebe, Langenbecks Arch. Chir. 346 (1978) 193–199. doi:10.1007/BF01261242.

[43] T. Briggs, T.L. Arinzeh, Examining the formulation of emulsion electrospinning for improving the release of bioactive proteins from electrospun fibers., J. Biomed. Mater. Res. A. 102 (2014) 674–84. doi:10.1002/jbm.a.34730.

[44] P. Dowling, C. Hayes, K.R. Ting, A. Hameed, J. Meiller, C. Mitsiades, K.C. Anderson, M.

Clynes, C. Clarke, P. Richardson, P. O'Gorman, Identification of proteins found to be significantly altered when comparing the serum proteome from Multiple Myeloma patients with varying degrees of bone disease., BMC Genomics. 15 (2014) 904. doi:10.1186/1471-2164-15-904.

[45] K.A. Benis, G.B. Schneider, The effects of vitamin D binding protein-macrophage activating factor and colony-stimulating factor-1 on hematopoietic cells in normal and osteopetrotic rats, Blood. 88 (1996) 2898–2905.

[46] N. Swamy, S. Ghosh, G.B. Schneider, R. Ray, Baculovirus-expressed vitamin D-binding protein-macrophage activating factor (DBP-maf) activates osteoclasts and binding of 25-hydroxyvitamin D(3) does not influence this activity., J. Cell. Biochem. 81 (2001) 535–46. doi:10.1002/1097-4644(20010601)81:3<535::AID-JCB1067>3.0.CO;2-6.

[47] P.S.N. Schneider G.B., Grecco K.J., Safadi F.F., The anabolic effects of vitamin D-binding protein-macrophage activating factor (DBP-MAF) and a novel small peptide on bone, Crit. Rev. Eukaryot. Gene Expr. 13 (2003) 277–284. doi:10.1615/CritRevEukaryotGeneExpr.v13.i24.180.

[48] F. Li, N. Song, J. Tombran-Tink, C. Niyibizi, Pigment epithelium-derived factor enhances differentiation and mineral deposition of human mesenchymal stem cells., Stem Cells. 31 (2013) 2714–23. doi:10.1002/stem.1505.

[49] F. Li, N. Song, J. Tombran-Tink, C. Niyibizi, Pigment epithelium derived factor suppresses expression of Sost/Sclerostin by osteocytes: implication for its role in bone matrix mineralization., J. Cell. Physiol. 230 (2015) 1243–9. doi:10.1002/jcp.24859.

[50] Y. Adachi, K. Sugimoto, A.K. Sato, K.J. Mori, Identification of Negative Regulator of Interleukin-3 (NIL-3) in Bone Marrow, Cell Struct. Funct. 27 (2002) 81–89. doi:10.1247/csf.27.81.

[51] J.A. Andrades, M.E. Nimni, J. Becerra, R. Eisenstein, M. Davis, N. Sorgente, Complement proteins are present in developing endochondral bone and may mediate cartilage cell death and vascularization., Exp. Cell Res. 227 (1996) 208–13. doi:10.1006/excr.1996.0269.

[52] Z. Tu, H. Bu, J.E. Dennis, F. Lin, Efficient osteoclast differentiation requires local complement activation., Blood. 116 (2010) 4456–63. doi:10.1182/blood-2010-01-263590.

[53] J.H.F. de Baaij, J.G.J. Hoenderop, R.J.M. Bindels, Magnesium in man: implications for health and disease., Physiol. Rev. 95 (2015) 1–46. doi:10.1152/physrev.00012.2014.

[54] L. Mao, N. Kawao, Y. Tamura, K. Okumoto, K. Okada, M. Yano, O. Matsuo, H. Kaji, Plasminogen activator inhibitor-1 is involved in impaired bone repair associated with

diabetes in female mice., PLoS One. 9 (2014) e92686. doi:10.1371/journal.pone.0092686.

[55] L.H. Engelholm, B.S. Nielsen, S. Netzel-Arnett, H. Solberg, X.D. Chen, J.M. Lopez Garcia, C. Lopez-Otin, M.F. Young, H. Birkedal-Hansen, K. Danø, L.R. Lund, N. Behrendt, T.H. Bugge, The urokinase plasminogen activator receptor - Associated protein/Endo180 is coexpressed with its interaction partners urokinase plasminogen activator receptor and matrix metalloprotease-13 during osteogenesis, Lab. Investig. 81 (2001) 1403–1414. doi:10.1038/labinvest.3780354.

[56] E. Daci, V. Everts, S. Torrekens, E. Van Herck, W. Tigchelaar-Gutterr, R. Bouillon, G. Carmeliet, Increased bone formation in mice lacking plasminogen activators., J. Bone Miner. Res. 18 (2003) 1167–76. doi:10.1359/jbmr.2003.18.7.1167.

[57] J. Hong, J. Andersson, K.N. Ekdahl, G. Elgue, N. Axén, R. Larsson, B. Nilsson, Titanium is a highly thrombogenic biomaterial: Possible implications for osteogenesis, Thromb. Haemost. 82 (1999) 58–64. doi:10.1055/s-0037-1614630.

[58] M.A. Kerachian, D. Cournoyer, E.J. Harvey, T.Y. Chow, L.R. Bégin, A. Nahal, C. Séguin, New insights into the pathogenesis of glucocorticoid-induced avascular necrosis: microarray analysis of gene expression in a rat model., Arthritis Res. Ther. 12 (2010) R124. doi:10.1186/ar3062.

[59] S.J. Kuo, F.S. Wang, J.M. Sheen, H.R. Yu, S.L. Wu, J.Y. Ko, Complement component C3: Serologic signature for osteogenesis imperfecta. Analysis of a comparative proteomic study., J. Formos. Med. Assoc. 114 (2015) 943–9. doi:10.1016/j.jfma.2014.01.016.

[60] K. Matsuoka, K.-A. Park, M. Ito, K. Ikeda, S. Takeshita, Osteoclast-derived complement component 3a stimulates osteoblast differentiation., J. Bone Miner. Res. 29 (2014) 1522–30. doi:10.1002/jbmr.2187.

[61] U.M. Wewer, A potential role for tetranectin in mineralization during osteogenesis, J. Cell Biol. 127 (1994) 1767–1775. doi:10.1083/jcb.127.6.1767.

[62] K. Driller, A. Pagenstecher, M. Uhl, H. Omran, A. Berlis, A. Gründer, A.E. Sippel, Nuclear factor I X deficiency causes brain malformation and severe skeletal defects., Mol. Cell. Biol. 27 (2007) 3855–3867. doi:10.1128/MCB.02293-06.

[63] P. Májek, Z. Reicheltová, J. Suttnar, J. Cermák, J.E. Dyr, Plasma proteome changes associated with refractory cytopenia with multilineage dysplasia., Proteome Sci. 9 (2011) 64. doi:10.1186/1477-5956-9-64.

[64] F.M. Moussa, I.A. Hisijara, G.R. Sondag, E.M. Scott, N. Frara, S.M. Abdelmagid, F.F. Safadi, Osteoactivin promotes osteoblast adhesion through HSPG and αvβ1 integrin., J. Cell.

Biochem. 115 (2014) 1243–53. doi:10.1002/jcb.24760.

[65] A. Niemeier, T. Schinke, J. Heeren, M. Amling, The role of apolipoprotein E in bone metabolism., Bone. 50 (2012) 518–24. doi:10.1016/j.bone.2011.07.015.

[66] P. Newman, F. Bonello, A.S. Wierzbicki, P. Lumb, G.F. Savidge, M.J. Shearer, The uptake of lipoprotein-borne phylloquinone (vitamin K1) by osteoblasts and osteoblast-like cells: Role of heparan sulfate proteoglycans and apolipoprotein E, J. Bone Miner. Res. 17 (2002) 426–433. doi:10.1359/jbmr.2002.17.3.426.

[67] M. Dieckmann, F.T. Beil, B. Mueller, A. Bartelt, R.P. Marshall, T. Koehne, M. Amling, W. Ruether, J.A. Cooper, S.E. Humphries, J. Herz, A. Niemeier, Human apolipoprotein E isoforms differentially affect bone mass and turnover in vivo., J. Bone Miner. Res. 28 (2013) 236–45. doi:10.1002/jbmr.1757.

[68] M. Shiraki, Y. Shiraki, C. Aoki, T. Hosoi, S. Inoue, M. Kaneki, Y. Ouchi, Association of bone mineral density with apolipoprotein E phenotype., J. Bone Miner. Res. 12 (1997) 1438–45. doi:10.1359/jbmr.1997.12.9.1438.

[69] C. Puel, A. Quintin, A. Agalias, J. Mathey, C. Obled, A. Mazur, M.J. Davicco, P. Lebecque, A.L. Skaltsounis, V. Coxam, Olive oil and its main phenolic micronutrient (oleuropein) prevent inflammation-induced bone loss in the ovariectomised rat., Br. J. Nutr. 92 (2004) 119–27. doi:10.1079/BJN20041181.

[70] L.G. Raisz, A.L. Sandberg, J.M. Goodson, H.A. Simmons, S.E. Mergenhagen, Complement dependent stimulation of prostaglandin synthesis and bone resorption, Science (80-.). 185 (1974) 789–791. doi:10.1126/science.185.4153.789.

[71] A.L. Sandberg, L.G. Raisz, L.M. Wahl, H.A. Simmons, Enhancement of complement-mediated prostaglandin synthesis and bone resorption by arachidonic acid and inhibition by cortisol, Prostaglandins Leukot. Med. 8 (1982) 419–427.

[72] A. Rusińska, M. Świątkowska, W. Koziołkiewicz, S. Skurzyński, J. Golec, D. Chlebna-Sokół, Proteomic analysis of plasma profiles in children with recurrent bone fractures, Acta Biochim. Pol. 58 (2011) 553–561.

[73] K. Thongchote, S. Svasti, M. Sa-ardrit, N. Krishnamra, S. Fucharoen, N. Charoenphandhu, Impaired bone formation and osteopenia in heterozygous β(IVSII-654) knockin thalassemic mice., Histochem. Cell Biol. 136 (2011) 47–56. doi:10.1007/s00418-011-0823-1.

[74] Y. Wang, W.-H. Li, Z. Li, W. Liu, L. Zhou, J.-F. Gui, BMP and RA signaling cooperate to regulate Apolipoprotein C1 expression during embryonic development., Gene. 554 (2015) 196–204. doi:10.1016/j.gene.2014.10.047.

[75] J. Yamamura, Y. Morita, Y. Takada, H. Kawakami, The fragments of bovine high molecular weight kininogen promote osteoblast proliferation in vitro., J. Biochem. 140 (2006) 825–30. doi:10.1093/jb/mvj217.

[76] M.F. Carlevaro, A. Albini, D. Ribatti, C. Gentili, R. Benelli, S. Cermelli, R. Cancedda, F.D. Cancedda, Transferrin Promotes Endothelial Cell Migration and Invasion: Implication in Cartilage Neovascularization, J. Cell Biol. 136 (1997) 1375–1384. doi:10.1083/jcb.136.6.1375.

[77] C. Gentili, R. Doliana, P. Bet, G. Campanile, A. Colombatti, F.D. Cancedda, R. Cancedda, Ovotransferrin and ovotransferrin receptor expression during chondrogenesis and endochondral bone formation in developing chick embryo, J. Cell Biol. 124 (1994) 579–588. doi:10.1083/jcb.124.4.579.

[78] D. Buser, R.K. Schenk, S. Steinemann, J.P. Fiorellini, C.H. Fox, H. Stich, Influence of surface characteristics on bone integration of titanium implants. A histomorphometric study in miniature pigs, J. Biomed. Mater. Res. 25 (1991) 889–902. doi:doi.org/10.1002/jbm.820250708.

[79] S. Grassi, A. Piattelli, L.C. de Figueiredo, M. Feres, L. de Melo, G. Iezzi, R.C. Alba, J.A. Shibli, Histologic Evaluation of Early Human Bone Response to Different Implant Surfaces, J. Periodontol. 77 (2006) 1736–1743. doi:10.1902/jop.2006.050325.

[80] A. Wennerberg, T. Albrektsson, B. Andersson, J.J. Krol, A histomorphometric and removal torque study of screw-shaped titanium implants with three different surface topographies., Clin. Oral Implants Res. 6 (1995) 24–30. doi:10.1034/j.1600-0501.1995.060103.x.

[81] Z. Schwartz, P. Raz, G. Zhao, Y. Barak, M. Tauber, H. Yao, B.D. Boyan, Effect of micrometer-scale roughness of the surface of Ti6Al4V pedicle screws in vitro and in vivo., J. Bone Joint Surg. Am. 90 (2008) 2485–98. doi:10.2106/JBJS.G.00499.

[82] E. Yoshida, Y. Yoshimura, M. Uo, M. Yoshinari, T. Hayakawa, Influence of nanometer smoothness and fibronectin immobilization of titanium surface on MC3T3-E1 cell behavior, J. Biomed. Mater. Res. - Part A. 100 A (2012) 1556–1564. doi:10.1002/jbm.a.34084.

[83] A. Wennerberg, T. Albrektsson, Effects of titanium surface topography on bone integration: a systematic review, Clin. Oral Implants Res. 20 (2009) 172–184. doi:10.1111/j.1600-0501.2009.01775.x.

[84] C. Aparicio, A. Padrós, F.J. Gil, In vivo evaluation of micro-rough and bioactive titanium dental implants using histometry and pull-out tests, J. Mech. Behav. Biomed. Mater. 4 (2011) 1672–1682. doi:10.1016/j.jmbbm.2011.05.005.

[85] G. Burgstaller, M. Gregor, L. Winter, G. Wiche, Keeping the vimentin network under control: cell-matrix adhesion-associated plectin 1f affects cell shape and polarity of fibroblasts., Mol. Biol. Cell. 21 (2010) 3362–75. doi:10.1091/mbc.E10-02-0094.

[86] H.T. Shiu, B. Goss, C. Lutton, R. Crawford, Y. Xiao, Formation of blood clot on biomaterial implants influences bone healing, Tissue Eng. - Part B Rev. 20 (2014). doi:10.1089/ten.teb.2013.0709.

[87] H.L. Spaulding, F. Saijo, R.H. Turnage, J.S. Alexander, T.Y. Aw, T.J. Kalogeris, Apolipoprotein A-IV attenuates oxidant-induced apoptosis in mitotic competent, undifferentiated cells by modulating intracellular glutathione redox balance., Am. J. Physiol. Cell Physiol. 290 (2006) C95–C103. doi:10.1152/ajpcell.00388.2005.

[88] R.W. Wu, F.S. Wang, J.Y. Ko, C.J. Wang, S.L. Wu, Comparative serum proteome expression of osteonecrosis of the femoral head in adults., Bone. 43 (2008) 561–6. doi:10.1016/j.bone.2008.04.019.

[89] T. Hirata, M. Fujioka, K.A. Takahashi, A. Takeshi, M. Ishida, K. Akioka, M. Okamoto, N. Yoshimura, Y. Satomi, H. Nishino, Y. Hirota, S. Nakajima, S. Kato, T. Kubo, Low molecular weight phenotype of apolipoprotein(a) is a risk factor of corticosteroid-induced osteonecrosis of the femoral head after renal transplant, J. Rheumatol. 34 (2007) 516–522.

[90] J. Saupe, M.J. Shearer, M. Kohlmeier, Phylloquinone transport and its influence on γ-carboxyglutamate residues of osteocalcin in patients on maintenance hemodialysis, Am. J. Clin. Nutr. 58 (1993) 204–208. doi:10.1093/ajcn/58.2.204.

[91] M. Sanada, H. Nakagawa, I. Kodama, T. Sakasita, K. Ohama, Apolipoprotein E phenotype associations with plasma lipoproteins and bone mass in postmenopausal women, Climacteric. 1 (1998) 188–195. doi:10.3109/13697139809085540.

[92] D.T.A. Eisenberg, C.W. Kuzawa, M.G. Hayes, Worldwide allele frequencies of the human apolipoprotein E gene: climate, local adaptations, and evolutionary history., Am. J. Phys. Anthropol. 143 (2010) 100–11. doi:10.1002/ajpa.21298.

[93] A. Sahu, J.D. Lambris, Structure and biology of complement protein C3, a connecting link between innate and acquired immunity, Immunol. Rev. 180 (2001) 35–48. doi:10.1034/j.1600-065X.2001.1800103.x.

5. CHAPTER 4

Bioactive potential of silica coatings and its effect on the adhesion of proteins to titanium implant

5. Chapter 4

Bioactive potential of silica coatings and its effect on the adhesion of proteins to titanium implants

F. Romero-Gavilán[1], N. Araújo-Gomes[1,2], A.M. Sánchez-Pérez[2], I. García-Arnáez[2], F. Elortza[4], M Azkargorta[4], J.J. Martín de Llano[5], C. Carda[5], M. Gurruchaga[3], J. Suay[1], I. Goñi[3]

[1] Department of Industrial Systems and Design, Universitat Jaume I, Av. Vicent-Sos Baynat s/n. Castellón, 12071 Spain.

[2] Department of Medicine. Universitat Jaume I, Av. Vicent-Sos Baynat s/n. Castellón 12071. Spain.

[3] Facultad de Ciencias Químicas. Universidad del País Vasco. P. M. de Lardizábal, 3. San Sebastián 20018. Spain.

[4] Proteomics Platform, CIC bioGUNE, CIBERehd, ProteoRed-ISCIII, Bizkaia Science and Technology Park, 48160 Derio, Spain.

[5] Department of Pathology and Health Research Institute of the Hospital Clínico (INCLIVA), Faculty of Medicine and Dentistry, University of Valencia, 46010 Valencia, Spain.

Colloids and Surfaces B: Biointerfaces, 2018

ABSTRACT

There is an ever-increasing need to develop dental implants with ideal characteristics to achieve specific and desired biological response in the scope of improve the healing process post-implantation. Following that premise, enhancing and optimizing titanium implants through superficial treatments, like silica sol-gel hybrid coatings, are regarded as a route of future research in this area. These coatings change the physico-chemical properties of the implant, ultimately affecting its biological characteristics. Sandblasted acid-etched titanium (SAE-Ti) and a silica hybrid sol-gel coating (35M35G30T) applied onto the Ti substrate were examined. The results of *in vitro* and *in vivo* tests and the analysis of the protein layer adsorbed to each surface were compared and discussed. *In vitro* analysis with MC3T3-E1 osteoblastic cells, showed that the sol-gel coating raised the osteogenic activity potential of the implants (the expression of osteogenic markers, the alkaline phosphatase (ALP) and IL-6 mRNAs, increased). In the *in vivo* experiments using as model rabbit tibiae, both types of surfaces promoted osseointegration. However, the coated implants demonstrated a clear increase in the inflammatory activity in comparison with SAE-Ti. Mass spectrometry (LC-MS/MS) analysis showed differences in the composition of protein layers formed on the two tested surfaces. Large quantities of apolipoproteins were found attached predominantly to SAE-Ti. The 35M35G30T coating adsorbed a significant quantity of complement proteins, which might be related to the material intrinsic bioactivity, following an associated, natural and controlled immune response. The correlation between the proteomic data and the *in vitro* and *in vivo* outcomes is discussed on this experimental work.

Keywords: dental implants, apolipoproteins, osteoimmunology, osteogenesis, bone regeneration, proteomics

Graphical abstract

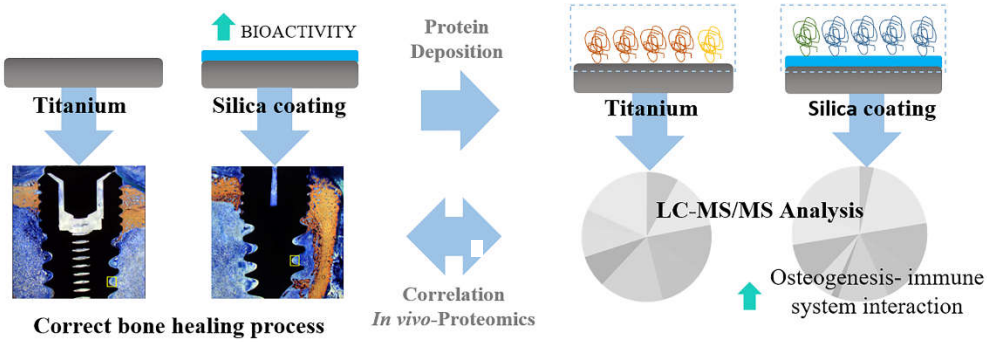

Figure 5.0. Graphical abstract of the work named "Bioactive potential of silica coatings and its effect on the adhesion of proteins to titanium implants".

5.1. Introduction

Titanium is a material often used in dental implants due to its high biocompatibility, resistance to corrosion and good mechanical properties, such as its strength and relatively low modulus of elasticity [1]. These are excellent characteristics for biomedical purposes. However, specific surface treatments might enhance the bioactivity of titanium devices, leading to the desired biological response [2]. Such surface modifications are designed to boost osseointegration in dental implants, improving tissue healing [3].

The degree of integration of a biomaterial in a living organism depends on the interaction of many factors in the microenvironment formed after the implantation. The first layer of proteins adsorbed onto the biomaterial surface might have a strong effect on the development and activation of several biological processes. The success of implantation might depend on these proteins, spreading and adsorbing on the surface by competitive displacement (Vroman effect) [4].

Coagulation cascades, complement system pathways, platelets and immune cells are activated and become involved immediately in the microenvironment formed after the surgical procedure, starting the process of inflammation [5]. The deposition of the proteins activating these processes depends on distinct features of the surfaces. The preferential adsorption of certain types of proteins might be associated with the specific physical and chemical properties of these materials [6]. Hence, controlling the amount, type and the conformation of the adhering proteins is of the utmost importance in promoting the correct, fast tissue regeneration. It is vital to obtain a moderate and natural immune response (not a chronic inflammation) to the biomaterial. Such a response should favour the regeneration and good osseointegration, thus contributing to the success of the implantation [7].

The use of silica sol-gel hybrid materials in biomedical applications is becoming increasingly widespread [8–10]. The versatility of the sol-gel techniques allows tuning the final physico-chemical properties of a biomaterial by selection of appropriate precursors and optimisation of synthesis parameters [11]. The hybrid silica sol-gel materials can be applied easily as a coating onto titanium, bioactivating the surface and conferring the desired properties to the implants. These coatings are biocompatible and biodegradable, with osteoinductive properties due to the release

of silicon compounds during their hydrolytic degradation [8–10]. Silicon is an essential element in bone metabolism and it is involved in the formation and mineralisation of this tissue [12].

The behaviour of sandblasted, acid-etched titanium (SAE-Ti) and a hybrid silica sol-gel coating applied onto this substrate was compared using *in vitro* and *in vivo* tests. The pattern of proteins adsorbed onto these two surface types was analysed. Then, the results of the proteomic study of protein–biomaterial interactions were compared with the outcomes of *in vitro* and *in vivo* studies.

5.2. **Materials and methods**

5.2.1. Titanium discs

Ti discs (12 mm in diameter, 1-mm thick) were made from a bar of commercially available, pure, grade-4 Ti (Ilerimplant-GMI S.L., Lleida, Spain). To obtain the sandblasted, acid-etched (SAE) Ti, the discs were abraded with 4-µm aluminium oxide particles and acid-etched by submersion in sulfuric acid for 1 h, to simulate a moderately rough implant surface. Discs were then washed with acetone, ethanol and 18.2-Ω purified water (for 20 min in each liquid) in an ultrasonic bath and dried under vacuum. Finally, all Ti discs were sterilised using UV radiation.

5.2.2. Sol-gel synthesis and sample preparation

The silica hybrid material was obtained through the sol-gel route. The precursors used were the alkoxysilanes: methyltrimethoxysilane, 3-(glycidoxypropyl)-trimethoxysilane and tetraethyl orthosilicate (Sigma-Aldrich, St. Louis, MO, USA) in molar percentages of 35 %, 35 % and 30 %, respectively. This composition, 35M35G30T, was chosen based on previous studies [8]. 2-Propanol (Sigma-Aldrich, St. Louis, MO, USA) was used as a solvent in the synthesis at a volume ratio (alcohol:siloxane) of 1:1. Hydrolysis of alkoxysilanes was carried out by adding (at a rate of 1 drop s^{-1}) the corresponding stoichiometric amount of acidified aqueous solution of 0.1M HNO_3 (Panreac, Barcelona, Spain). The mixture was kept for 1 h under stirring and then 1 h at rest. The samples were prepared immediately afterwards. SAE-Ti was used as the substrate for the sol-gel coating. The coating was performed employing a dip-coater (KSV DC; KSV NIMA, Espoo, Finland). Discs and implants were immersed in the sol-gel solution at a speed of 60 cm min^{-1}, left immersed for one minute, and removed at a 100 cm min^{-1}. Finally, the samples were cured for 2 h at 80 ºC.

5.2.3. Physico-chemical characterisation of coated titanium discs

The surface topography of samples was characterised using scanning electron microscopy (SEM) employing the Leica-Zeiss LEO equipment under vacuum (Leica, Wetzlar, Germany). Platinum sputtering was applied to make the materials more conductive for the SEM observations. An optical profilometer (interferometric and confocal) PLm2300 (Sensofar, Barcelona, Spain) was used to determine the roughness. Three discs of each type were tested. Three measurements were performed for each disc to obtain the arithmetic average values of roughness (Ra). An atomic force microscope (AFM; Bruker Multimode, Billerica, MA, USA) was employed to evaluate the nanocomponents of roughness. Measurements were carried out at scan size of 1 µm and at scan rate of 0.3 Hz (n = 3). The results were analysed using the NanoScope Analysis software (http://nanoscaleworld.bruker-axs.com/nanoscaleworld/media/p/775.aspx). The contact angle was measured using an automatic contact angle meter OCA 20 (Dataphysics Instruments, Filderstadt, Germany). Ten µL of ultrapure water were deposited on the disc surfaces at a dosing rate of 27.5 µL s^{-1} at room temperature. Contact angles were determined using SCA 20 software (Dataphysics Instruments, Filderstadt, Germany). Six discs of each material were studied, after depositing two drops on each disc.

5.2.4. In vitro assays

5.2.4.1. Cell culture

MC3T3-E1 (mouse calvaria osteosarcoma cell line) cells were cultured on the 35M35G30T-coated and uncoated Ti discs at a concentration of 1 × 104 cells $well^{-1}$, in 24-well culture NUNC plates (Thermo Fisher Scientific, Waltham, MA, USA). The medium contained Dulbecco Modified Eagle Medium (DMEM) with phenol red (Gibco-Life Technologies, Grand Island, NY, USA), 1 % 100× penicillin/streptomycin (Biowest Inc., Riverside, KS, USA) and 10 % fetal bovine serum (FBS; Gibco-Life Technologies, Grand Island, NY, USA). After incubation for 24 hours at 37 ºC in a humidified (95 %) atmosphere of 5 % CO_2, the medium was replaced with an osteogenic medium composed of DMEM with phenol red 1×, 1 % penicillin/streptomycin, 10 % FBS, 1 % ascorbic acid (5 mg mL^{-1}) and 0.21 % β glycerol phosphate, and incubated again under the same conditions. The culture medium was changed every 48 hours. In each plate, a well with cells at the same concentration

(1×10^4 cells) was used as a control of culture conditions. In parallel, cells were allowed to differentiate for 7, 14 and 21 days before being harvested for RNA isolation.

5.2.4.2. Cytotoxicity

The biomaterial cytotoxicity was assessed following the ISO 10993-5 specifications, measured by spectrophotometry, after contact of the material extract with the cell line. The 96-Cell Titter Proliferation Assay (Promega®, Madison, WI, USA) was employed to measure the cell viability after 24-h incubation of the cells with the extract. One negative control (empty well) and a positive control with latex, known to be toxic to the cells were used. Seventy-percent cell viability was the limit below which a biomaterial was considered cytotoxic.

5.2.4.3. Cell Proliferation

For measuring cell proliferation, the commercial cell-viability assay AlamarBlue® (Invitrogen-Thermo Fisher Scientific, Waltham, MA, USA) was used. This kit measures the cell viability on the basis of a redox reaction with resazurin. The cells were cultured in wells with the discs (3 replicates per treatment) and examined following the manufacturer's protocol after 1, 3, 5 and 7 days of culture. The percentage of reduced resazurin was used to evaluate cell proliferation.

5.2.4.4. ALP activity

The conversion of p-nitrophenylphosphate (p-NPP) to p-nitrophenol was used to assess the ALP activity. The culture medium was removed from the wells, the wells were washed 3 times with 1 × Dulbecco's Phosphate Buffered Saline (DPBS), and 100 µL of lysis buffer (0.2 % Triton X-100, 10 mM Tris-HCl pH 7.2) was added to each. The sample aliquots of 0.1 mL were used to carry out the assay. One hundred µL of p-NPP (1 mg mL^{-1}) in substrate buffer (50 mM glycine, 1mM $MgCl_2$, pH 10.5) was added to 100 µL of the supernatant obtained from the lysate. After two hours of incubation in the dark (37 ºC, 5 % CO_2), absorbance was measured using a microplate reader at a wavelength of 405 nm. ALP activity was obtained from a standard curve obtained using different solutions of p-nitrophenol and 0.02 mM sodium hydroxide. Results were presented as mmol of p-nitrophenol $hour^{-1}$ (mmol PNP h^{-1}). The data were expressed as ALP activity normalised by the total

protein content (µg μL^{-1}) obtained using Pierce BCA assay kit (Thermo Fisher Scientific, Waltham, MA, USA) after 7 and 14 days.

5.2.4.5. RNA isolation and cDNA synthesis

Total RNA was prepared from the cells grown on the sol-gel coated titanium discs, using Qiagen RNeasy Mini kit (Qiagen, Hilden, Germany), following digestion with DNaseI (Qiagen), according to the manufacturer's instructions. The quantity, integrity and quality of the resulting RNA were measured using NanoVue® Plus Spectrophotometer (GE Healthcare Life Sciences, Litlle Chafont, United Kingdom). For each sample, about 1 µg of total RNA was converted to cDNA using PrimeScript RT Reagent Kit (Perfect Real Time) (TAKARA Bio Inc., Shiga, Japan). The resulting cDNA was diluted in DNase free water to a concentration suitable for reliable RT-PCR analysis.

5.2.4.6. Quantitative Real-time PCR

Prior to the RT-qPCR reaction, primers for ALP and IL6 genes were designed from specific DNA sequences for these genes available from NCBI (https://www.ncbi.nlm.nih.gov/nuccore) using PRIMER3plus software tool (http://www.bioinformatics.nl/cgi-bin/primer3plus/primer3plus.cgi). Expression levels were measured using primers purchased from Life Technologies S.A. (Gaithersburg, MD), GADPH sense TGCCCCCATGTTTGTGATG; GADPH antisense TGGTGGTGCAGGATGCATT; ALP sense CCAGCAGGTTTCTCTCTTGG; ALP antisense CTGGGAGTCTCATCCTGAGC; IL-6 sense AGTTGCCTTCTTGGGACTGA and IL-6 antisense TCCACGATTTCCCAGAGAAC. All primers are listed from 5' to 3' and GADPH was used as a housekeeping gene to normalise the data obtained from the RT qPCR and calculate the relative fold-change between conditions. qPCR reactions were carried out using SYBR PREMIX Ex Taq (Tli RNase H Plus) (TAKARA Bio Inc., Shiga, Japan), in an Applied Biosystems StepOne Plus™ Real-Time PCR System (Foster City, California, USA). The cycling parameters were as follows: an initial denaturation step at 95 ºC for 30 s followed by 95 ºC for 5 s and 60 ºC for 34 s for 40 cycles. The final melt curve stage comprised a cycle at 95 ºC for 15 s and at 60 ºC, for 60 s.

5.2.5. Statistical analysis

Data were submitted to one-way analysis of variance (ANOVA) and to a Newman-Keuls multiple comparison post-test, when appropriate. Differences with $p \leq 0.05$ were considered statistically significant.

5.2.6. In vivo experimentation

To assess the *in vivo* behaviour of the two biomaterials, the bare and coated dental implants were surgically placed in the tibia of New Zealand rabbits (Oryctolagus cuniculus). This implantation model is widely used to study the osseointegration of dental implants [13]. All the experiments were conducted in accordance with the protocols of Ethical Committee of the Valencia Polytechnic University (Spain), the European guidelines and legal conditions laid in R. D. 223/1988 of March 14th, and the Order of October 13rd, 1988, of the Spanish Government on the protection of animals used for experimentation and other scientific purposes. The rabbits were kept under 12-h span darkness-light cycle; room temperature was set at 20.5 ± 0.5 ºC, and the relative humidity ranged between 45 and 65 %. The animals were individually caged and fed a standard diet and filtered water ad libitum. Dental implants were supplied by Ilerimplant S.L. (Lleida, Spain). These were internal-connection dental implants, made with titanium grade 4 (trademark GMI), of 3.75-mm diameter and 8-mm length, Frontier model with SAE surface treatment. Overall, 10 implants were used, 5 uncoated (SAE-Ti) and 5 coated with the 35M35G30T sol-gel composition. They were all implanted under the same conditions.

5 rabbits were employed to carry out the assay, all of them weighing between 2000 and 3000 g, aging near the physeal closure (indicative of an adequate bone volume). The implantation period for the experimental model was 2 weeks. Implants were inserted in both left and right proximal tibiae, each animal receiving two implants (one SAE-Ti sample and one sol-gel coated sample). Animals were sedated (chlorpromazine hydrochloride) and prepared for surgery, and then anaesthetized (ketamine hydrochloride). A coetaneous incision was made to the implantation site in the proximal tibia. The periosteum was removed, and the osteotomy was performed using a low revolution micromotor and drills of successive diameters of 2, 2.8 and 3.2 mm, with continuous irrigation. Implants were placed by press-fit, and surgical wound was sutured by tissue planes,

washed with saline water and covered with plastic spray dressing (Nobecutan, Inibsa Laboratories, Barcelona, Spain). After the implantation period, animals were euthanized by carbon monoxide inhalation, and the implant screws were retrieved to study the surrounding tissues. The samples were embedded in methyl methacrylate, and 25–30 µm sections were obtained using EXAKT Technique (EXAKT Technologies, Inc., Oklahoma, USA). Slides were sequentially stained with Stevenel's blue and van Gieson's picro-fuchsin following the procedure described by Maniatopoulos et al. [14]. Digital images of the tissues surrounding the implant threads were recorded with a bright field Leica DM4000 B microscope and a DFC420 digital camera using 1.6, 5, 10, 20 and 100x objectives. The bone–implant contact in the cortical region of the implant and the length of osteoclast-like and foreign body giant cells in contact with the implant surface of threads in the medullar bone cavity were evaluated using the image-processing program ImageJ 1.48 (National Institutes of Health, USA, http://imagej.nih.gov/ij).

5.2.7. Adsorbed protein layer

Sol-gel-coated and uncoated titanium discs were incubated in a 24-well plate for 180 min in a humidified atmosphere (37 ºC, 5 % CO_2), after the addition of 1 mL of human blood serum from male AB plasma (Sigma-Aldrich, St. Louis, MO, USA).

The serum was removed, and, to eliminate the non-adsorbed proteins, the discs were rinsed five times with ddH_2O and once with 100 mM NaCl, 50 mM Tris-HCl, pH 7.0. The adsorbed protein layer was collected by washing the discs in 0.5 M triethylammonium bicarbonate buffer (TEAB) with 4 % of sodium dodecyl sulphate and 100 mM of dithiothreitol (DTT). Four independent experiments were carried out for each type of surface; in each experiment, four discs for each material were processed. The protein content was quantified before the experiment (Pierce BCA assay kit; Thermo Fisher Scientific, Waltham, MA, USA), obtaining a value of 51 mg mL^{-1}.

5.2.8. Proteomic analysis

Proteomic analysis was performed as described by Romero-Gavilán *et al.* [6], with minor variations. Briefly, the eluted protein was in solution digested following the FASP protocol established by Wisnewski *et al.* [15] loaded onto a nanoACQUITYUPLC system connected online to an SYNAPT G2-Si MS System (Waters, Milford, MA, USA). Each material was analysed in quadruplicate. Differential

protein analysis was carried out using Progenesis software (Nonlinear Dynamics, Newcastle, UK) as described before [6], and the functional annotation of the proteins was performed using PANTHER (www.pantherdb.org/) and DAVID Go annotation programmes (https://david.ncifcrf.gov/).

5.3. **Results**

5.3.1. Synthesis and physicochemical characterisation

The sol-gel synthesis was carried out, and a well-adhering and homogenous coating was obtained on SAE-Ti discs. SEM micrographs showed substantial morphological differences between the bare and coated titanium discs (Figure 5.1a-d). The sol-gel material partly covered the initial roughness (shown by the data obtained using optical profilometer). After the 35M35G30T sol-gel treatment, Ra decreased to 0.79 ± 0.09 µm from its original value of 1.15 ± 0.10 µm for SAE-Ti surfaces. AFM images display the morphological properties of both surfaces on a lower scale (Figure 5.1e and f). The uncoated surface showed a Ra value of 19.00 ± 2.05 nm, while the sol-gel coating involved a reduction of the roughness nanocomponents displaying a Ra value of 1.75 ± 0.94 nm. The contact angle measurements revealed a significant increase in wettability as a consequence of coating. Uncoated and coated discs presented angles of 79.55 ± 7.51º and 50.39 ± 3.78º, respectively. Thus, the sol-gel-coated material was more hydrophilic than the initial SAE-Ti, possibly due to its hydroxyl group content [8].

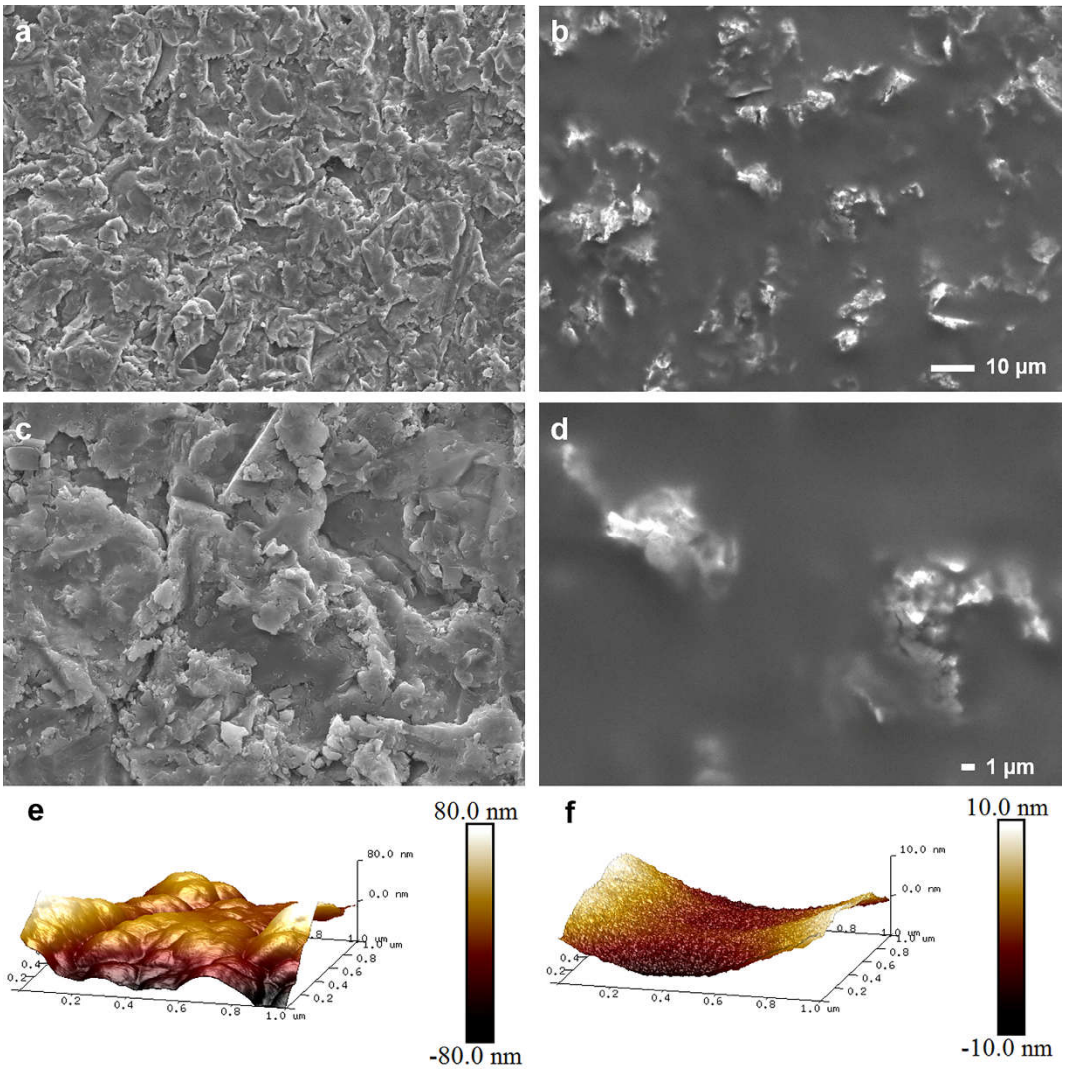

Figure 5.1. SEM micrographs of (a) and (c) SAE-Ti and (b) and (d) 35M35G30T coating. Scale bars: (a) and (b), 10 µm and (c) and (d), 1 µm. AFM images of (e) SAE-Ti and (f) 35M35G30T coating.

5.3.2. In vitro assays

5.3.2.1. Cell cytotoxicity, proliferation and ALP activity

Neither of the examined materials was cytotoxic (data not shown). The proliferation and ALP activity assays do not show significant differences between the two materials at most of the time points, except for the proliferation assay at 3-day period, in which the 35M35G30T boosts higher values of proliferation (Figure 5.2).

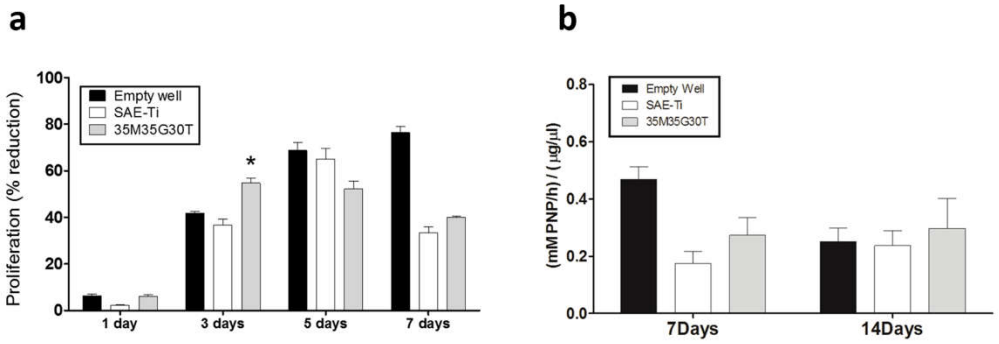

Figure 5.2. MC3T3-E1 *in vitro* assays: a) MC3T3-E1 cell proliferation after 1, 3, 5 and 7 days of cell culture with SAE-Ti (white bar) and 35M35G30T (grey bar); b) ALP activity (mM PNP h^{-1}), normalised to the amount of total protein (µg μL^{-1}), in the MC3T3-E1 cells cultivated on SAE-Ti (white bar) and 35M35G30T formulation (grey bar). Cells in an empty well were used as a positive control (black bar). Statistical analysis was performed using one-way ANOVA with a Kruskal-Wallis post- test (*, $p \leq 0.05$).

5.3.2.2. mRNA expression levels

After 14 days of incubation, there were found large and statistically significant differences ($p < 0.001$) between mRNA expression levels for ALP and IL-6 in the cells cultivated on 35M35G30T discs and those grown on SAE-Ti and the blank controls (Figure 5.3), showing the bioactive potential of this coating formulation.

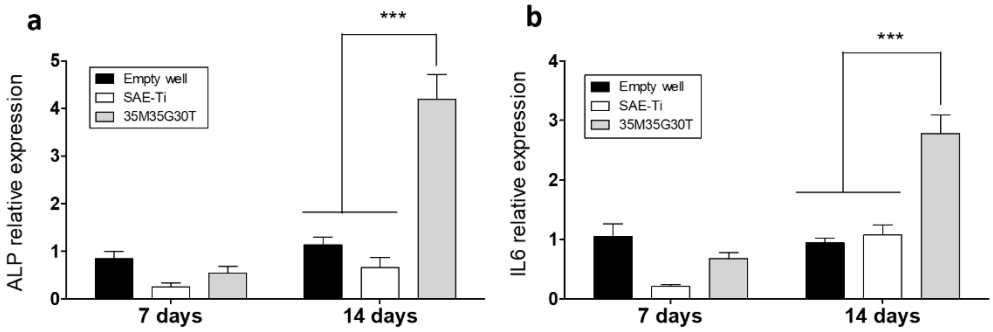

Figure 5.3. Gene expression of osteogenic markers (a) ALP and (b) I-L6 on MC3T3-E1 osteoblastic cells cultured on SAE-Ti (white bar) and 35M35G30T (grey bar). Cells in an empty well were used as a positive control (black bar). The relative mRNA expression was determined by RT-PCR after 7 and 14 days of cell culture. Statistical analysis was performed using one-way ANOVA with a Kruskal-Wallis post-test (***, $p \leq 0.001$).

5.3.3. In vivo experimentation

No statistically significant differences were found between osseointegration levels for the uncoated (SAE-Ti) and sol-gel-coated implants during the studied period (Figure 5.4, A-B). On the coated implants, transparent layers of undegraded material (Figure 5.4, B and D) were observed in the deep areas of the screw grooves. This coating layer was thinner or absent in the threads in contact with or next to the bone tissue. It was more evident in the grooves of the implant located in the medullary cavity of the bone and away from the trabeculae of bone tissue. Along this medullary zone, in the implant–tissue interface (SAE-Ti samples) or coating–tissue interface (35M35G30T samples), were observed connective tissue, inflammatory components and two types of multinucleated cells. One of these cell types had the size and morphological characteristics similar to osteoclasts, and the other was composed of larger cells, similar to foreign body giant cells (Figure 5.4, C-D and insets). The length of that interface and the length of the osteoclast-like and giant cells were measured. The cells shorter than 100 µm were considered osteoclast-like cells and the larger cells were classified as giant cells. Osteoclastic cells from the uncoated and coated implants were of similar length (44.4 ± 21.6 µm, N = 272 and 40.4 ± 27.9 µm, N = 50, respectively). The giant cells were smaller in the SAE-Ti than in 35M35G30T samples (cell length 162.0 ± 73.6 µm, N = 66 and 268.0 ± 140.0 µm, N = 46, respectively). The difference was statistically significant ($p < 0.001$, non-parametric Mann–Whitney test). In the coated implants, the areas of bone

regeneration showed fewer giant cells, and fibrous capsules between the bone tissue and implant were not observed.

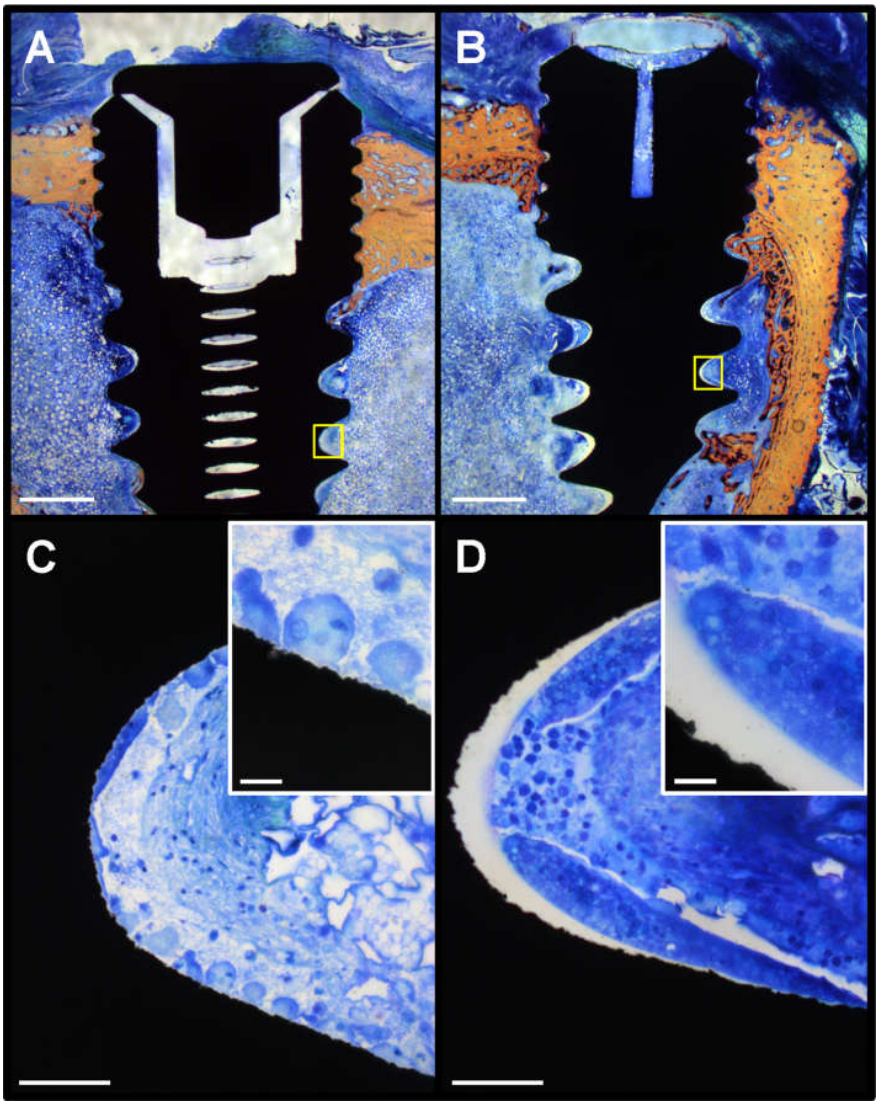

Figure 5.4. Microphotographs of SAE-Ti and 35M35G30T samples. Panoramic images of (A) SAE-Ti and (B) 35M35G30T samples show the implant regions close to the cortical bone and in the medullary cavity. The regions enclosed in white-edged squares in A and B are shown in panels C and D, respectively. In the panel C, several rounded and elongated osteoclast-like and giant cells touch the surface of the implant. In the D panel, two giant cells, flanking a region with inflammatory cells, are in contact with the transparent coating of the

implant surface. Lower regions of the C and D images are shown magnified in the corresponding insets. Stevenel's blue and van Gieson's picro-fuchsin staining was used. Scale bars: A and B, 1 mm; C and D, 0.1 mm; insets, 0.02 mm.

5.3.4. Proteomic analysis

LC-MS/MS analysis detected and identified 133 proteins for each material. Progenesis QI software was employed to study differences between protein adsorption on the SAE-Ti and hybrid silica-treated surfaces. DAVID and PANTHER tools were used to classify these proteins according to their function.

The comparison of the characteristic proteins attached to the two biomaterials showed that 16 proteins were more abundant on the SAE-Ti than on the coated surfaces (Table 5.1).

The list in Table 5.1 shows some proteins related to blood coagulation processes, such as FA11, THRB and PROC. Notably, a large number of apolipoproteins adsorbed preferentially to the titanium surface in comparison with the sol-gel material (APOA, APOA1, APOA4, APOA5, APOC1, APOC2, APOC4 and APOE), as well as SAA4, classified as high-density lipoprotein by DAVID. PF4V, KCRM, VTNC and SEPP1 were also identified as more abundant in SAE-Ti elutions.

PANTHER chart in Figure 5.5a displays the classification of biological processes in which the proteins characteristic for titanium surfaces are involved. Among the identified processes, the most significant were the cellular (14 %) and metabolic (16 %) processes and the response to stimulus (16 %). Molecules with functions related to the immune system were also detected although they constituted only 2 % of the proteins.

Table 5.2 shows the 20 proteins more predominant on the 35M35G30T biomaterial than on untreated surfaces. A large proportion of these proteins is related to the immune response and the complement system, such as C1R, CO5, CO6, CO7, CO8A and CO8B proteins and the immunoglobulins IGJ, IGHA1 and IGHM. The proteins AFAM, HPT, A1AT and A2MG were also detected.

For the 35M35G30T samples, PANTHER analysis identified, among others, protein functions associated with cellular (19 %) and metabolic (10 %) processes, in similarity to the titanium-only results. However, in this case, the proportion of proteins related to immune system processes reached 17 % (Figure 5.5b).

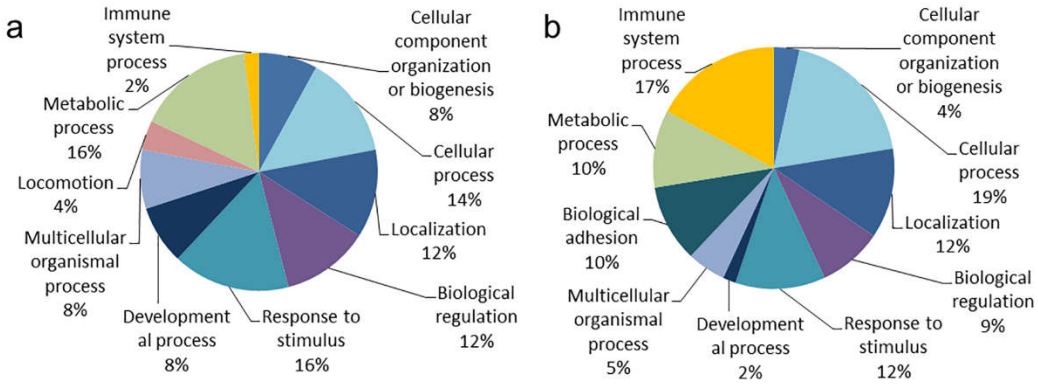

Figure 5.5. PANTHER pie chart of the biological processes associated with the proteins differentially adhering to (a) SAE-Ti and (b) 35M35G30T.

Table 5.1. Progenesis analysis of proteins differentially attached to SAE-Ti.

Description	Accession	Confidence score	Average SAE-Ti	Average 35M35G30T	ANOVA (p)	Ratio SAE-Ti / 35M35G30T
Platelet factor 4 variant	PF4V_HUMAN	106.83	2.05E+05	3.95E+03	6.62E-04	52.00
Coagulation factor XI	FA11_HUMAN	337.82	2.21E+05	9.18E+03	4.67E-02	24.06
Apolipoprotein C-IV	APOC4_HUMAN	80.60	1.18E+05	5.39E+03	3.91E-05	21.81
Vitamin K-dependent protein C	PROC_HUMAN	124.64	2.08E+05	1.36E+04	4.21E-03	15.27
Serum amyloid A-4 protein	SAA4_HUMAN	150.29	2.24E+06	2.11E+05	1.09E-04	10.60
Creatine kinase M-type	KCRM_HUMAN	104.21	1.58E+04	1.74E+03	1.66E-03	9.06
Prothrombin	THRB_HUMAN	375.17	1.91E+06	2.72E+05	1.15E-03	7.02
Apolipoprotein E	APOE_HUMAN	1836.86	2.54E+07	4.62E+06	9.73E-03	5.51
Vitronectin	VTNC_HUMAN	430.96	1.03E+07	2.06E+06	3.53E-04	4.98
Apolipoprotein C-I	APOC1_HUMAN	163.40	3.22E+06	6.53E+05	9.19E-03	4.94
Apolipoprotein A-V	APOA5_HUMAN	134.27	4.82E+04	1.03E+04	2.61E-04	4.67
Selenoprotein P	SEPP1_HUMAN	242.92	1.99E+05	6.33E+04	4.35E-03	3.14
Apolipoprotein(a)	APOA_HUMAN	108.16	8.15E+04	3.90E+04	3.74E-02	2.09
Apolipoprotein A-IV	APOA4_HUMAN	1044.44	1.36E+06	7.07E+05	2.24E-02	1.92
Apolipoprotein A-I	APOA1_HUMAN	1051.15	1.25E+07	6.68E+06	1.19E-03	1.87
Apolipoprotein C-II	APOC2_HUMAN	133.73	3.20E+05	1.85E+05	4.09E-02	1.73

Table 5.2. Progenesis analysis of proteins differentially attached to silica sol-gel coating.

Description	Accession	Confidence score	Average SAE-Ti	Average 35M35G30T	ANOVA (p)	Ratio 35M35G30T / SAE-Ti
Complement component C6	CO6_HUMAN	100.06	1.02E+04	3.02E+04	5.20E-03	2.97
Complement factor H-related protein 2	FHR2_HUMAN	253.29	3.93E+04	1.07E+05	4.31E-03	2.72
Immunoglobulin J chain	IGJ_HUMAN	123.70	1.30E+05	3.41E+05	1.29E-02	2.62
Ceruloplasmin	CERU_HUMAN	338.22	5.49E+04	1.36E+05	8.43E-03	2.48
Alpha-1-antitrypsin	A1AT_HUMAN	466.15	4.73E+05	1.15E+06	6.21E-04	2.44
Alpha-1-acid glycoprotein 1	A1AG1_HUMAN	171.81	4.74E+04	1.14E+05	1.41E-02	2.41
Complement component C7	CO7_HUMAN	358.70	7.98E+04	1.85E+05	1.78E-02	2.32
Ig mu chain C region	IGHM_HUMAN	262.24	1.92E+05	4.32E+05	2.25E-02	2.25
Alpha-1-antichymotrypsin	AACT_HUMAN	490.40	7.31E+04	1.63E+05	4.01E-03	2.23
Serotransferrin	TRFE_HUMAN	1935.92	2.56E+06	5.58E+06	1.26E-02	2.18
Complement C5	CO5_HUMAN	620.04	4.90E+04	1.07E+05	2.10E-02	2.18
Haptoglobin	HPT_HUMAN	755.00	5.13E+05	1.09E+06	7.85E-03	2.13
Serum albumin	ALBU_HUMAN	2067.21	2.34E+07	4.96E+07	1.70E-02	2.12
Complement component C8 alpha chain	CO8A_HUMAN	193.83	8.99E+04	1.88E+05	1.43E-02	2.09
Complement component C8 beta chain	CO8B_HUMAN	96.20	1.45E+04	3.01E+04	8.01E-03	2.08
Ig alpha-1 chain C region	IGHA1_HUMAN	386.53	7.00E+05	1.44E+06	7.20E-03	2.06
Complement C1r subcomponent	C1R_HUMAN	306.85	1.33E+05	2.52E+05	4.79E-03	1.90
Retinol-binding protein 4	RET4_HUMAN	79.55	7.64E+04	1.42E+05	3.37E-02	1.85
Alpha-2-macroglobulin	A2MG_HUMAN	669.00	1.91E+05	3.45E+05	1.81E-02	1.81
Afamin	AFAM_HUMAN	188.26	3.52E+04	6.32E+04	1.68E-02	1.80

5.4. **Discussion**

There is an ever-increasing interest and research on the biomaterial science industry for the development of implants with bioactive properties in the scope of decreasing the recovery times following the post-implantation procedure. Chemical and physical surface modifications of the implants are state-of-the-art areas in which researchers focus their attention, due to the fact that these modifications can ultimately influence cell behaviour [16]. To a large extent, this behaviour is affected by the proteins attached to the surface of the implant, representing a microenvironment whose characteristics determine the success of the implantation [17]. It is widely known that the titanium is not, by itself, bioactive; even though it has osteoconductive properties, it is not osteoinductive [2]. To confer osteoinductive characteristics to the titanium devices, imply the modification of the physicochemical properties of their surfaces. This alters the conformation, quantity and type of proteins that attach to the implant in contact with biological fluids [18].

This experimental study was designed to compare and characterise two distinct surfaces, one an uncoated sandblasted acid-etched titanium (SAE-Ti), and the other coated with a silica sol-gel hybrid 35M35G30T biomaterial, regarding their physico-chemical properties, *in vitro* and *in vivo* behaviour and the characterization of the protein layer adsorption onto each surface.

Apart from the obvious chemical differences between the titanium surfaces and silicon coatings, their morphological characterisation revealed specific properties of these surfaces, showing that the application of the sol-gel coating decreases surface roughness at micro and nano-level and increases hydrophilicity. These distinct characteristics might ultimately affect both the protein adsorption and the biological behaviour of the biomaterial. Indeed, *in vitro* results demonstrated an increase in the bioactive potential of the sol-gel-coated implant in comparison with the uncoated titanium. In particular, it was observed changes in the mRNA expression levels, as it was found an almost 4-fold increase in the expression of the ALP mRNA and at least 2-fold increase in the expression of the mRNA for IL-6 (Figure 5.3). ALP is expressed early in the development of the bone and during cartilage calcification [19] and is a well-known biomarker for osteoblastic differentiation. This marker has been used for the assessment of fracture healing [20]. IL-6 is a regulator of the differentiation of pre-osteoblastic cells and initiates apoptosis in the mature

osteoblasts. Moreover, the expression of its receptor is high during differentiation of osteoblasts *in vitro* [21]. It has also been reported as a direct stimulator of RANKL and OPG mRNA expression in the mouse bone tissue [22], promoting prostaglandin production and, thus, modulating the inflammatory potential [23]. Interestingly, IL-6 can act as an ALP induction factor during the inflammatory phase of wound repair in the skin [24] and even in bone tissue remodelling [25]. Therefore, the 35M35G30T material might have a role in promoting osteoblastic activity.

In vivo results for the two examined surfaces did not show clear differences in bone repair during the tested period even though the *in vitro* experiments demonstrated higher bioactivity in the coated samples. Nevertheless, there was a significant increase in the immune complex activation on the sol-gel-coated implants. This was demonstrated by the higher abundance of the foreign body giant cells (FBGC) surrounding the residual areas of non-degraded material, in comparison with the SAE-Ti (Figure 5.4). The presence of FBGCs in degradable materials is quite common as their activity is needed for the recovery of the implanted tissue. Without it, immune structures like thick fibrous capsules might be formed around the material, with all the associated disadvantages [26]. In fact, for the coated surfaces, in the areas of bone regeneration, it occurs a clear decrease in the number of giant cells and no presence of fibrotic tissue.

The comparison between the composition of protein layers on SAE-Ti and 35M35G30T coating revealed many proteins differentially attached to these surfaces. This distinct affinity of some proteins to these materials could be attributed to their different physico-chemical properties such surface chemistry, wettability or roughness [27,28]. In this sense, for example, an increase in surface roughness could be involved with changes in the adsorption of specific proteins [29].

Interestingly, among the protein group characteristic for titanium, the PF4V protein was the most abundant (52-fold increase in comparison with the sol-gel treated samples). This protein is a platelet chemokine inhibiting both angiogenesis and tumour growth [30]. However, its specific role in bone regeneration processes remains unclear. Remarkably, a large number of apolipoproteins were attached predominantly to the SAE-Ti surface. Cho *et al.* [31] have reported that apolipoproteins might prevent the activation of innate immunity response, and have an anti-inflammatory potential. These results indicate that the high biocompatibility of titanium might be related to the preferential adsorption of this family of proteins onto its surface. Other studies

suggest that the immunomodulatory role of apolipoproteins might be associated with the polarisation of macrophages in their anti-inflammatory phenotype [32,33]. Similarly, VTNC has been identified as an inhibitor of the complement cascade activation [34]. This protein has an important role in the interleukin IL-4 adhesion to biomaterials, leading the macrophage polarisation to their M2 reparative phenotype [16]. VTNC also interacts with the coagulation cascades, contributing to thrombus formation, and participates in the establishment of vascular homoeostasis, wound repair and tissue regeneration [35]. This protein promotes the osteogenesis by boosting the osteoblast differentiation [36]. APOE protein was also found predominantly on the SAE-Ti surfaces. This protein is involved in the regulation of bone metabolism; its role in the bone tissue is probably related to its effect on vitamin K uptake into osteoblasts [37]. Proteins FA11, THRB and PROC play an important role in blood clotting. FA11 and THBR participate in the activation of the blood coagulation pathway. PROC is involved in the regulation of this pathway, through the inactivation of Va and VIIIa factors in the presence of phospholipids [38,39].

At the same time, proteomic analysis to the proteins more predominantly found in the silica sol-gel material (in comparison with the SAE-Ti) revealed a prevalence of proteins belonging to the complement system, namely CO5, CO8B, CO8A, CO7, C1R and CO6 [40], as well as the immunoglobulins IGJ, IGHM and IGHA1. This result was supported by the PANTHER analysis, which found a pronounced increase in the attachment of proteins related to immune system, from 2 % on the uncoated SAE-Ti to 17 % on the sol-gel coating (Figure 5.5). Interestingly, there was not found C-reactive protein adsorption, which, in a previous study, has been reported as related to acute/chronic inflammation processes and put forward as a bad biocompatibility biomarker [41].

This data unveils the relationship that an increment in immune response can suppose an increase on the activity of osteogenic markers (ALP and IL-6) observed in the *in vitro* assays. This augmented immune system activation was also seen *in vivo* (Figure 5.4).

The implantation of biomedical devices entails a natural and significant immune response to the foreign material. The migration of white blood cells to the implantation site is caused by complement cascade proteins adsorbed on the surface of the implant. The consequent immune response is guided by cytokines that are activated and released by white blood cells, e.g., macrophages [42]. These cytokines can be responsible for producing a natural inflammatory

reaction, giving the kick-start to the healing processes in the damaged tissue. An interaction between the host and the implant surface will result in the release of such molecules and trigger the activation of a series of cascades, determining the outcome of the implantation. The results obtained here show that an increase in the immune response to the implanted material might affect its bioactive potential, as a result of the interactions between the immune and skeletal systems [43]. Such interactions, as long as the release of the immune product is controlled, might help to modulate the bioactivity of material towards the bone cells [44].

5.5. **Conclusion**

In summary, this study shows the importance of the adsorbed layer of proteins in the bioactivation of the material. The proteins from these layers, whose composition depends on the intrinsic characteristics of the material, might trigger the bioactivation process. Indeed, it has been found a significant deposition of complement-related proteins. These proteins intervene in processes such as the maintenance of cellular turnover, healing, proliferation and regeneration, apart from their role in the immune processes. This assumes a prolonged presence of the FBCGs on the regenerating tissue, and at the same time, a boost in the osteogenic potential, even though no effect on the *in vivo* regenerative potential is found.

ACKNOWLEDGEMENTS

This work was supported by the MAT 2014-51918-C2-2-R (MINECO), P11B2014-19, Universidad Jaume I under grant Predoc/2014/25, Generalitat Valenciana under grant Grisolia/2014/016 and Basque Government under grant Predoct/2016/1/0141. Authors would like to thank Antonio Coso and Jaime Franco (GMI-Ilerimplant) for their inestimable contribution to this study, and Raquel Oliver, Jose Ortega (UJI), Iraide Escobes (CIC bioGUNE), and Víctor Primo (IBV) for their valuable technical assistance.

REFERENCES

[1] M. Özcan, C. Hämmerle, Titanium as a reconstruction and implant material in dentistry: Advantages and pitfalls, Materials. 5 (2012) 1528–1545. doi:10.3390/ma5091528.

[2] X. Liu, P.K. Chu, C. Ding, Surface modification of titanium, titanium alloys, and related materials for biomedical applications, Mater. Sci. Eng. R Reports. 47 (2004) 49–121. doi:10.1016/j.mser.2004.11.001.

[3] A. Jemat, M.J. Ghazali, M. Razali, Y. Otsuka, Surface modifications and their effects on titanium dental implants, Biomed Res. Int. 2015 (2015) ID 791725. doi:10.1155/2015/791725.

[4] S.L. Hirsh, D.R. McKenzie, N.J. Nosworthy, J.A. Denman, O.U. Sezerman, M.M.M. Bilek, The Vroman effect: Competitive protein exchange with dynamic multilayer protein aggregates, Colloids Surfaces B Biointerfaces. 103 (2013) 395–404. doi:10.1016/j.colsurfb.2012.10.039.

[5] D.F. Williams, On the mechanisms of biocompatibility, Biomaterials. 29 (2008) 2941–2953. doi:10.1016/j.biomaterials.2008.04.023.

[6] F. Romero-Gavilán, N.C. Gomes, J. Ródenas, A. Sánchez, M. Azkargorta, I. Iloro, F. Elortza, I. García-Arnáez, M. Gurruchaga, I. Goñi, J. Suay, Proteome analysis of human serum proteins adsorbed onto different titanium surfaces used in dental implants, Biofouling. 33 (2017) 98–111. doi:10.1080/08927014.2016.1259414.

[7] S.N. Christo, K.R. Diener, A. Bachhuka, K. Vasilev, J.D. Hayball, Innate Immunity and Biomaterials at the Nexus: Friends or Foes, Biomed Res. Int. 2015 (2015) Article ID 342304. doi:10.1155/2015/342304.

[8] F. Romero-Gavilán, S. Barros-Silva, J. García-Cañadas, B. Palla, R. Izquierdo, M. Gurruchaga, I. Goñi, J. Suay, Control of the degradation of silica sol-gel hybrid coatings for metal implants prepared by the triple combination of alkoxysilanes, J. Non. Cryst. Solids. 453 (2016) 66–73. doi:10.1016/j.jnoncrysol.2016.09.026.

[9] M. Martínez-Ibáñez, M.J. Juan-Díaz, I. Lara-Saez, A. Coso, J. Franco, M. Gurruchaga, J. Suay Antón, I. Goñi, Biological characterization of a new silicon based coating developed for dental implants, J. Mater. Sci. Mater. Med. 27 (2016) 80. doi:10.1007/s10856-016-5690-9.

[10] M.J. Juan-Díaz, M. Martínez-Ibáñez, I. Lara-Sáez, S. da Silva, R. Izquierdo, M. Gurruchaga, I.

Goñi, J. Suay, Development of hybrid sol–gel coatings for the improvement of metallic biomaterials performance, Prog. Org. Coatings. 96 (2016) 42–51. doi:10.1016/j.porgcoat.2016.01.019.

[11] D. Arcos, M. Vallet-Regí, Sol-gel silica-based biomaterials and bone tissue regeneration., Acta Biomater. 6 (2010) 2874–88. doi:10.1016/j.actbio.2010.02.012.

[12] E.M. Carlisle, Silicon: A possible factor in bone calcification, Science. 167 (1970) 279–280. doi:10.1126/science.167.3916.279.

[13] H. Mori, M. Manabe, Y. Kurachi, M. Nagumo, Osseointegration of dental implants in rabbit bone with low mineral density, J. Oral Maxillofac. Surg. 55 (1997) 351–361. doi:10.1016/S0278-2391(97)90124-5.

[14] C. Maniatopoulos, A. Rodriguez, D.A. Deporter, A.H. Melcher, An improved method for preparing histological sections of metallic implants., Int. J. Oral Maxillofac. Implant. 1 (1986) 31–37.

[15] J.R. Wisniewski, A. Zougman, N. Nagaraj, M. Mann, Universal sample preparation method for proteome analysis, 6 (2009) 3–8. doi:10.1038/NMETH.1322.

[16] Z. Chen, T. Klein, R.Z. Murray, R. Crawford, J. Chang, C. Wu, Y. Xiao, Osteoimmunomodulation for the development of advanced bone biomaterials, Mater. Today. 19 (2015) 304–321. doi:10.1016/j.mattod.2015.11.004.

[17] A.E. Engberg, P.H. Nilsson, S. Huang, K. Fromell, O.A. Hamad, T.E. Mollnes, J.P. Rosengren-Holmberg, K. Sandholm, Y. Teramura, I.A. Nicholls, B. Nilsson, K.N. Ekdahl, Prediction of inflammatory responses induced by biomaterials in contact with human blood using protein fingerprint from plasma, Biomaterials. 36 (2015) 55–65. doi:10.1016/j.biomaterials.2014.09.011.

[18] R. Latour, Biomaterials: protein-surface interactions, in: G.E. Wnek, G.L. Bowlin (Eds.), Encycl. Biomater. Biomed. Eng., Informa Healthcar, 2008: pp. 270–284. doi:10.3171/PED/2008/1/4/270.

[19] E.E. Golub, K. Boesze-Battaglia, The role of alkaline phosphatase in mineralization, Curr. Opin. Orthop. 18 (2007) 444–448. doi:10.1097/BCO.0b013e3282630851.

[20] S. Ajai, A. Sabir, Evaluation of Serum Alkaline Phosphatase as a Biomarker of Healing Process Progression of Simple Diaphyseal Fractures in Adult Patients, Int. Res. J. Biol. Sci. Int. Res. J. Biol. Sci. 2 (2013) 40–43.

[21] Y. Li, C.-M. Bäckesjö, L.-A. Haldosén, U. Lindgren, IL-6 receptor expression and IL-6 effects

change during osteoblast differentiation., Cytokine. 43 (2008) 165–173. doi:10.1016/j.cyto.2008.05.007.

[22] P. Palmqvist, E. Persson, H.H. Conaway, U.H. Lerner, IL-6, Leukemia Inhibitory Factor, and Oncostatin M Stimulate Bone Resorption and Regulate the Expression of Receptor Activator of NF- B Ligand, Osteoprotegerin, and Receptor Activator of NF- B in Mouse Calvariae, J. Immunol. 169 (2002) 3353–3362. doi:10.4049/jimmunol.169.6.3353.

[23] X.H. Liu, A. Kirschenbaum, S. Yao, A.C. Levine, Cross-talk between the interleukin-6 and prostaglandin E2 signaling systems results in enhancement of osteoclastogenesis through effects on the osteoprotegerin/receptor activator of nuclear factor-??B (RANK) ligand/RANK system, Endocrinology. 146 (2005) 1991–1998. doi:10.1210/en.2004-1167.

[24] R.L. Gallo, R.A. Dorschner, S. Takashima, M. Klagsbrun, E. Eriksson, M. Bernfield, Endothelial cell surface alkaline phosphatase activity is induced by IL-6 released during wound repair, J Invest Dermatol. 109 (1997) 597–603. doi:10.1111/1523-1747.ep12337529.

[25] F. Blanchard, L. Duplomb, M. Baud'huin, B. Brounais, The dual role of IL-6-type cytokines on bone remodeling and bone tumors, Cytokine Growth Factor Rev. 20 (2009) 19–28. doi:10.1016/j.cytogfr.2008.11.004.

[26] K.M.R. Nuss, B. von Rechenberg, Biocompatibility issues with modern implants in bone - a review for clinical orthopedics., Open Orthop. J. 2 (2008) 66–78. doi:10.2174/1874325000802010066.

[27] S. Spriano, V. Sarath Chandra, A. Cochis, F. Uberti, L. Rimondini, E. Bertone, A. Vitale, C. Scolaro, M. Ferrari, F. Cirisano, G. Gautier di Confiengo, S. Ferraris, How do wettability, zeta potential and hydroxylation degree affect the biological response of biomaterials?, Mater. Sci. Eng. C. 74 (2017) 542–555. doi:10.1016/j.msec.2016.12.107.

[28] K. Rechendorff, M.B. Hovgaard, M. Foss, V.P. Zhdanov, F. Besenbacher, Enhancement of protein adsorption induced by surface roughness, Langmuir. 22 (2006) 10885–10888. doi:10.1021/la0621923.

[29] D. Deligianni, N. Katsala, S. Ladas, D. Sotiropoulou, J. Amedee, Y. Missirlis, Effect of surface roughness of the titanium alloy Ti-6Al-4V on human bone marrow cell response and on protein adsorption., Biomaterials. 22 (2001) 1241–51. doi:10.1016/S0142-9612(00)00274-X.

[30] J. Vandercappellen, J. Van Damme, S. Struyf, The role of the CXC chemokines platelet factor-4 (CXCL4/PF-4) and its variant (CXCL4L1/PF-4var) in inflammation, angiogenesis and cancer, Cytokine Growth Factor Rev. 22 (2011) 1–18. doi:10.1016/j.cytogfr.2010.10.011.

[31] N.H. Cho, S.Y. Seong, Apolipoproteins inhibit the innate immunity activated by necrotic cells or bacterial endotoxin, Immunology. 128 (2009) 479–486. doi:10.1111/j.1365-2567.2008.03002.x.

[32] Q. Li, Z. Zhai, W. Ma, Z. Qian, Anti-inflammatory effects of apoprotein AI are mediated via modulating macrophage polarity, Chinese J. Cardiol. 42 (2014) 132–135. doi:10.3760/cma.j.issn.0253-3758.2014.02.007.

[33] D. Baitsch, H.H. Bock, T. Engel, R. Telgmann, C. Müller-Tidow, G. Varga, M. Bot, J. Herz, H. Robenek, A. Von Eckardstein, J.-R. Nofer, Apolipoprotein e induces antiinflammatory phenotype in macrophages, Arterioscler. Thromb. Vasc. Biol. 31 (2011) 1160–1168. doi:10.1161/ATVBAHA.111.222745.

[34] T.E. Mollnes, M. Kirschfink, Strategies of therapeutic complement inhibition, Mol. Immunol. 43 (2006) 107–121. doi:10.1016/j.molimm.2005.06.014.

[35] D.I. Leavesley, A.S. Kashyap, T. Croll, M. Sivaramakrishnan, A. Shokoohmand, B.G. Hollier, Z. Upton, Vitronectin - Master controller or micromanager?, IUBMB Life. 65 (2013) 807–818. doi:10.1002/iub.1203.

[36] R.M. Salasznyk, W.A. Williams, A. Boskey, A. Batorsky, G.E. Plopper, Adhesion to Vitronectin and Collagen I Promotes Osteogenic Differentiation of Human Mesenchymal Stem Cells., J. Biomed. Biotechnol. 2004 (2004) 24–34. doi:10.1155/S1110724304306017.

[37] A. Niemeier, T. Schinke, J. Heeren, M. Amling, The role of Apolipoprotein E in bone metabolism, Bone. 50 (2012) 518–524. doi:10.1016/j.bone.2011.07.015.

[38] P.N. Walsh, Roles of platelets and factor XI in the initiation of blood coagulation by thrombin, Thromb. Haemost. 86 (2001) 75–82.

[39] D. Josic, L. Hoffer, A. Buchacher, Preparation of vitamin K-dependent proteins, such as clotting factors II, VII, IX and X and clotting inhibitor Protein C, J. Chromatogr. B Anal. Technol. Biomed. Life Sci. 790 (2003) 183–197. doi:10.1016/S1570-0232(03)00082-5.

[40] K. Murphy, P. Travers, M. Walport, The complement system and innate immunity., Janeway's Immunobiol. 7 (2008) 61–81. doi:10.1086/596249.

[41] N. Araújo-Gomes, F. Romero-Gavilán, A.M. Sanchez-Pérez, M. Gurruchaga, M. Azkargorta, F. Elortza, M. Martínez-Ibáñez, I. Iloro, J. Suay, I. Goñi, Characterization of serum proteins attached to distinct sol – gel hybrid surfaces, J. Biomed. Mater. Res. - Part B Appl. Biomater. 106 (2017) 1477–1485. doi:10.1002/jbm.b.33954.

[42] G.S.A. Boersema, N. Grotenhuis, Y. Bayon, J.F. Lange, Y.M. Bastiaansen-Jenniskens, The

Effect of Biomaterials Used for Tissue Regeneration Purposes on Polarization of Macrophages., Biores. Open Access. 5 (2016) 6–14. doi:10.1089/biores.2015.0041.

[43] F. Romero-Gavilán, A.M. Sanchez-Pérez, N. Araújo-Gomes, M. Azkargorta, I. Iloro, F. Elortza, M. Gurruchaga, I. Goñi, J. Suay, Proteomic analysis of silica hybrid sol-gel coatings: a potential tool for predicting the biocompatibility of implants in vivo, Biofouling. 33 (2017) 676–689. doi:10.1080/08927014.2017.1356289.

[44] J. Lorenzo, M. Horowitz, Y. Choi, Osteoimmunology: Interactions of the bone and immune system, Endocr. Rev. 29 (2008) 403–440. doi:10.1210/er.2007-0038.

8. GENERAL DISCUSSION

8. General discussion

The progressive aging in the population and the appearance of pathologies associated with a lower capacity for bone tissue regeneration, such as diabetes or osteoporosis, involve a greater demand for dental substitutions, not only in healthy individuals.

As consequence, the design of new biomaterials for dental implantology able to accomplish better results is crucial. However, the development methodologies of these biomaterials show a low efficiency because of surprising poor correlation between *in vitro* and *in vivo* testing. This fact highlights the need to stablish new *in vitro* techniques which guarantee a better prediction of the material *in vivo* response.

In this regard, the layer of proteins adsorbed onto biomaterials after their implantation could mark the initiation and development of the successive events that take place during tissue healing, and therefore the implant success or failure.

On this basis, this work aims the identification of proteomic biomarkers useful to provide more information about the future biomaterial behaviour *in vivo*, which could support the establishment of new *in vitro* methodologies with better performances.

To attain this goal, the first step was the design of biomaterials with controlled biological responses. For that, a base sol-gel material which can be applied as coating onto implants and, at the same time, can be used as controlled release vehicle of different compounds was developed. The modelled sol-gel synthesis method allowed design materials with the ability to provoke different biological responses. Then, the next step was the physico-chemical, biological and proteomic characterization of these compositions. Hence, the comparative analysis of materials with specific properties allowed the identification of distinct protein biomarkers.

For this reason, in **chapter 1**, a silica hybrid sol-gel synthesis procedure was developed. A triple mixture of MTMOS, GPTMS and TEOS alkoxysilanes allowed to obtain homogeneous and well-adhered coatings, which could be used to bioactivate metallic dental implants. Additionally, both the electrochemical and the hydrolytic degradation assays revealed that the composition

35M35G30T has an interesting degradation kinetic in order to employ this sol-gel network as delivery vehicle of osteogenic compounds.

Then, building on this previous sol-gel development work, the biological behaviour of a variety of treatments were systematically characterized. As well as, the composition of the serum protein layer adsorbed onto their surfaces.

In this way, the results obtained with the comparative analysis of both biocompatible and non-biocompatible treatments are described in **chapter 2**. Following the sol-gel synthesis method, different materials were obtained altering their chemical composition with the intent to provoke distinct biological responses. The 35M35G30T coating together another silica hybrid sol-gel composition, 70M30T, showed a good *in vivo* outcome despite of having distinct physico-chemical properties. Similarly, 50M50G and 50V50G materials showed analogous outcomes, but in this case the implantation of this materials results in the formation of connective fibrous tissue, fact related to a poor biocompatibility. Interestingly, traditional *in vitro* cell culture did not reveal differences between these four material, being all them supposedly biocompatible. So this study underlines the poor correlation between *in vitro* testing and the subsequent *in vivo* experimentation. The LC-MS/MS allowed the identification of 171 different proteins adsorbed onto the sol-gel coatings, fact that emphasizes the potential of this technique to approach the study of protein adsorption on biointerfaces. Moreover, the Progenesis comparative analysis found a cluster of proteins differentially adhered to the both non-biocompatible compositions respect to the biocompatible ones (CRP, SAMP, C1S, C1QB, C1QC, CO7 and VTNC). This cluster was mainly formed by proteins related to an acute inflammatory/immune response, which could explain the implant failure. Notably, the pentraxin CRP was found as the protein differentially more adhered to the non-biocompatible materials in all cases. This acute-phase protein is directly associated with the complement system activation via the classical pathway, involving proinflammatory effects. Nevertheless, VTNC, which was also found more adhered to non-biocompatible compositions, inhibits the complement system activation and thus contributes to the inflammatory response regulation. This is not as contradictory as it may seem, since the ratio between activating / inhibitory proteins shows a proportionally greater affinity of activating proteins to both 50M50G and 50V50G. This higher activating / inhibitory ratio could result in a disproportionate complement system activation, culminating in the formation of the fibrous tissue observed *in vivo*. Then, these

results suggest that the ratio between the activating and inhibitory proteins regulating the complement system such as CRP / VTNC might constitute a useful biomarker to predict biocompatibility problems *in vivo*.

In parallel, it would be interesting to identify biomarkers associated to an improved osseointegration capability. For this reason, **chapter 3** describes the proteomic characterization carried out to two distinct titanium surfaces commonly employed in implants: a sand-blasted acid-etched Ti (SAE-Ti) respect to non-treated one. It is widely accepted the benefits of SAE surfaces for dental implantology purposes due to their better osseointegrative properties. Apart from the greater roughness they possess other variables that can condition positively cell behaviour, such as its possible distinct surface chemistry and wettability. The LC-MS/MS analysis allowed the detection of 218 distinct adsorbed proteins, being 37 of those related to bone regenerative processes and dental implant integration. It is remarkable the great affinity of both Ti surfaces for key proteins related to the coagulation (FA12, PROC, THBR, ANT and KNG1) and fibrinolysis (PLMN) systems, as well as, proteins with tissue regenerative potential (TENT, PRG4, ACTB and VTNC). The comparative analysis between the proteomic results obtained with each of the Ti surfaces found that SAE-Ti, in comparison with non-treated Ti, have a greater affinity to APOE, ANT3 and PROC proteins. At the same time, SAE-Ti showed lower affinity to CO3, protein related to an acute inflammatory response, and IGHG1, IGHM, LV301 immunoglobulins. Thus, this better osseointegration potential associated to the SAE treatment could be related to the increased adsorption of osteogenic protein APOE, the higher presence of coagulation inhibitors (PROC and ANT3), combined with a lower adsorption of some proteins related to the immune response such as CO3.

Chapter 4 was focused on the comparison between SAE-Ti and the 35M35G30T silica hybrid sol-gel composition applied as coating onto that Ti surface in order to bioactivate it. At the first sight, qRT-PCR assays show a greater gene expression of osteogenic markers when the Ti is treated with the sol-gel material, which could be related to a higher osteogenic activity. However, both 35M30G30T and the non-coated SAE-Ti materials displayed a successful *in vivo* outcome, without significant differences among them. The LC-MS/MS proteomic characterization identified 133 proteins for each material. A comparative analysis using Progenesis QI software was performed, detecting patterns of proteins differentially adsorbed onto each material. Indeed, osteogenic

proteins such as APOE and VTNC, as well as proteins related to blood coagulation process were found more adhered onto SAE-Ti. Whereas 35M35G30T treatment showed a greater adsorption of proteins related to immune system processes. Then, in view of the similar *in vivo* outcome showed by both biomaterials, the proteomic results suggest that their different protein adsorption patterns could suppose the regeneration process development through distinct mechanisms. SAE-Ti has a greater affinity to proteins described in literature to promote osteoblastogenesis (APOE and VTNC), while 35M35G30T coating displayed a higher, although no disproportioned, immune activity which could be associated to the osteogenesis boosting, following the subject of osteoimmunology.

Since, it is widely recognized the osteogenic capability of Ca^{2+} and Sr^{2+} cations when they are introduced into biomaterials such as bioglasses. The next step was the addition of osteogenic salts ($SrCl_2$ and $CaCl_2$) into this 35M35G30T silica hybrid sol-gel material, aiming the enhancement of their osseointegration potential.

In **chapter 5**, the incorporation of $SrCl_2$ into the sol-gel network provokes physico-chemical changes, resulting in a distinct *in vitro* cell responses in a dose-dependent manner. In this sense, it was found an increase in the gene expression of ALP and TGF-β in MC3T3-E1 cells. At the same time, the macrophage gene expressions of inflammatory marker TNF-α decreases and the anti-inflammatory marker IL-10 increases when Sr was added to the coating. LC-MS/MS analysis identified 136 different proteins, detecting variations in the protein patterns adhered onto the coatings as the Sr was incorporated. In fact, it is remarkable the higher adsorption of APOE and VTNC as result of the increasing amount of $SrCl_2$ incorporated in the sol-gel material. These proteins are not only related to osteogenic functions, but also described as promotors of macrophage shift to an anti-inflammatory phenotype. Thus, it is tempting to think that a greater attachment of proteins such as APOE and VTNC can affect the cellular response to the biomaterial, resulting in increased osteogenic and anti-inflammatory potential *in vitro* for Sr-coatings.

Similarly, **chapter 6** shows as the addition of $CaCl_2$ to 35M35G30T supposes physico-chemical changes. Regarding the biological responses to these biomaterials, the higher osteoblastic gene expression of ALP marker infers that the incorporation of Ca^{2+} increases the 35M35G30T osteogenic potential in a dose-dependent manner. However, in this case, the higher macrophage

gene expression of TNF-α and IL1-β markers reveals an increased inflammatory potential depending on the $CaCl_2$ concentration. Otherwise, the proteomic characterization found 113 different proteins adhered to these Ca-coatings. Additionally, important differences in the adsorption protein patterns were detected through the Progenesis comparative analysis, as consequence of the $CaCl_2$ incorporation into the sol-gel network. Ca-coatings showed a greater attachment of APOE and VTNC onto their surfaces, signalling an osteogenic potential which is consistent with the *in vitro* results. These biomaterials also revealed, in turn, a clear higher affinity to proteins related to blood coagulation, which is not surprising considering the role of Ca^{2+} during blood clotting. It should be highlighted that this likely greater clotting activity, associated to the higher adsorption of coagulation system proteins, seems to be tightly regulated. Thereby, despite the greater attachment of pro-coagulating proteins such THRB, the differentially higher adoption of inhibitory proteins as ANT3, PROC and PROS could ensure there is no a disproportionate clotting reaction. However, more studies in this line would be necessary to stablish what coagulation patterns are the most suitable for implant osseointegration. Regarding to the elevated inflammatory gene expression detected mainly in compositions with around 2.5 % molar of $CaCl_2$, it is difficult to stablish a correlation between these signals and the adhered protein patterns. In this sense, this inflammatory potential could be associated to the increasing adhesion of inflammatory proteins (SAMP) or even to the interactions of coagulation system molecules in the immune response *in vitro* of these biomaterials. Despite this higher inflammatory potential, the addition of $CaCl_2$ did no suppose an increase of proteins related to an acute inflammatory response as CRP, which could indicate their adequate biocompatibility. Nevertheless, it would be necessary to know the *in vivo* outcome of these Ca-treatments in order to obtain conclusive result in regard to their biological response and thus, verify these hypotheses.

Considering together the results obtained in the studies that have been carried out systematically to different biomaterials, it seems ambitious to establish a general biomarker to identify their osseointegration effectiveness. This fact is consequence of the multitude systems interfering in this process. However, it was successively detected a common protein pattern associated to an increased osteogenic potential. Then, this protein pattern that consist in the greater affinity to APOE and VTNC proteins could be useful as biomarker, since their detection onto biomaterials for bone regeneration might be correlated to a higher osteogenic behaviour.

9. CONCLUSIONS

9. Conclusions

The **partial conclusions** of each study carried out are detailed below:

- **Chapter 1** - A general sol-gel synthesis procedure was developed, by which biomaterials able to lead different biological responses were designed. The sol-gel technique allowed to obtain homogeneous and well-adhered coatings from the mixture of three alkoxysilanes (MTMOS, GPTMS and TEOS), being the composition 35M35G30T the one that presents the most interesting degradation kinetics to be used as release vehicle in dental implants.

- **Chapter 2** - The proteomic analysis of different hybrid sol-gel formulations, which result in two differentiated *in vivo* responses (implant osseointegration and no osseointegration) showed that the biocompatibility problems observed *in vivo* could be associated with the adsorption of a protein cluster related to an acute immune / inflammatory reaction.

- **Chapter 3** - The comparative proteomic analysis of sand-blasted acid-etched Ti (SAE-Ti), respect to the untreated Ti, resulted in the identification of proteins APOE, ANT3 and PROC as more adsorbed on SAE-Ti, which could be associated with the greater osseointegration capability of this surface treatment.

- **Chapter 4** - The comparative proteomic analysis between both SAE-Ti and 35M35G30T coating resulted in the identification of important differences on the proteomic adsorption patterns. The sol-gel material showed greater affinity for proteins associated to the immune system, while the SAE-Ti showed more affinity for proteins related to both coagulation and bone regeneration (APOE and VTNC). As both materials display succesful *in vivo* outcomes, the detected proteomic differences could indicate relevant information regarding the regeneration mechanisms associated to each biomaterial.

- **Chapter 5** - The addition of $SrCl_2$ into the sol-gel network supposed an increase in its osteogenic and anti-inflammatory potential *in vitro* in a dose-dependent manner, which was correlated with the greater adsorption of proteins related to both osteogenic functions and the regulation / inhibition of the immune system.

- **Chapter 6** - The addition of $CaCl_2$ to the sol-gel network resulted in an increase in its osteogenic potential, as well as a greater inflammatory potential *in vitro* at determinated concentrations. The proteomic analysis showed that the presence of Ca resulted in higher affinity for proteins associated to the coagulation cascade, as well as APOE and VTNC, fact that could be correlated with the greater osteogenic potential *in vitro*.

In this way, the **general conclusions** that can be drawn from the presented experimental work are:

- The sol-gel technique allows the design of coatings to superficially modify the properties of dental implants, thus enabling the control of their biological response.

- Proteomics can be used as tool to predict the *in vivo* response of biomaterials, being able to provide more reliable results than traditional *in vitro* studies. The systematic characterization of the serum proteins adsorption onto the surface of different materials used in dental implantology has allowed the detection of protein patterns that would indicate the best or worst osseointegration capacity of a given biomaterial.

- Problems related to poor biocompatibility could be associated with a disproportionate adsorption of proteins that trigger to an acute inflammatory reaction, such as CRP. Thus, the proportion of proteins that activate the immune response in regard of proteins capable of regulating and inhibiting this response seems to play a key role on this reaction. Based on the results, CRP / VTNC protein ratio is proposed as biomarker for the prediction of biocompatibility problems in this type of materials.

- In turn, the biomaterial regenerative efficiency seems to be a much more complex objective since a multitude of systems can participate during bone healing. Additionally, this process can be carried out through different mechanisms. Despite this complexity, the results show that a greater adsorption of proteins related to the immune system that result in a non-disproportionate and well-regulated reaction could be indicative of greater material bioactivity and may have positive effects during implant osseointegration. On the other hand, the higher affinity to proteins such as VTNC and APOE could mark a greater osseointegration capacity and might be regarded as efficiency biomarkers.

Conclusiones

Las **conclusiones parciales** de cada uno de los estudios llevados a cabo se detallan a continuación:

- **Capítulo 1** – Se desarrolló un proceso de síntesis sol-gel por el cual se han diseñado biomateriales capaces de der lugar a diferentes respuestas biológicas. Así, la técnica sol-gel permitió la obtención de recubrimientos homogéneos y bien adheridos a partir de la mezcla de tres alcoxisilanos (MTMOS, GPTMS y TEOS), siendo la composición 35M35G30T la que presenta una cinética de degradación interesante para ser empleada como vehículo de liberación en implantes dentales.

- **Capítulo 2** - El análisis proteómico a distintas formulaciones híbridas sol-gel que dan lugar a dos respuestas *in vivo* diferenciadas, oseointegración y no oseointegración del implante, mostró que los problemas de biocompatibilidad observados *in vivo* podrían estar asociados a la adsorción de un clúster de proteínas asociadas a una fuerte reacción inmune / inflamatoria.

- **Capítulo 3** - El análisis proteómico comparativo de una superficie de titanio granallado con ataque acido (SAE), respecto al mismo material sin tratar, resultó en la identificación de las proteínas APOE, ANT3 y PROC como más adsorbidas en el SAE-Ti, pudiendo estar éstas asociadas a la mayor capacidad de osteointegración de este tratamiento superficial.

- **Capítulo 4** – El análisis proteómico comparativo del material SAE-Ti respecto al recubrimiento 35M35G30T resultó en la identificación de importantes diferencias en los perfiles de proteómica adsorbidos. La superficie sol-gel mostró mayor afinidad por proteínas asociadas al sistema inmune, mientras que el SAE-Ti mostró más afinidad por proteínas asociadas a la coagulación y a la regeneración ósea (APOE y VTNC). El hecho de que ambos materiales den lugar a buenos resultados *in vivo*, podría suponer que la proteómica está aportando información relevante al mecanismo de regeneración asociado a cada biomaterial.

- **Capítulo 5** – La adición de $SrCl_2$ a la red sol-gel supuso un incremento de su potencial osteogénico y antiinflamatorio *in vitro* de un modo dependiente de la concentración, que se correlacionó con la detección de patrones de adsorción de proteínas relacionadas con la osteogenesis y la regulación / inhibición de la respuesta inmune.

- **Capítulo 6** – La adición de $CaCl_2$ a la red sol-gel supuso un incremento de su potencial osteogénico, así como un mayor potencial inflamatorio *in vitro* a determinadas concentraciones. El análisis proteómico de estas superficies mostró que la presencia del Ca supuso una mayor afinidad por proteínas asociadas a la cascada de coagulación, así como por las proteínas APOE y VTNC, hecho que podría estar correlacionado con el mayor potencial osteogénico observado *in vitro*.

De este modo, las **conclusiones generales** que pueden extraerse del trabajo experimental presentado son:

- La técnica sol-gel permite el diseño de recubrimientos para modificar superficialmente las propiedades de implantes dentales y así controlar su respuesta biológica.

- La proteómica puede emplearse como herramienta predictiva de la respuesta *in vivo* de biomateriales, pudiendo llegar a dar resultados más fiables que los estudios *in vitro* tradicionales. Así, la caracterización sistemática de la adsorción de proteínas séricas a la superficie de diferentes materiales empleados en implantologia dental ha permitido la detección de patrones proteicos que indicarían la mejor o peor capacidad de osteointegración de un determinado biomaterial.

- La falta de biocompatibilidad podría estar asociada a una desproporcionada adsorción de proteínas que dan lugar a una fuerte reacción inflamatoria, como por ejemplo la CRP. Así la proporción de proteínas activadoras de la respuesta inmune respecto a la de proteínas capaz de regular e inhibir esta respuesta parece tener un papel clave. En base a los resultados se propone el biomarcador proteico CRP / VTNC para la predicción de problemas de biocompatibilidad en este tipo de materiales.

- A su vez, la eficiencia regenerativa de un biomaterial parece ser un objetivo mucho más complejo al poder entrar en juego multitud de procesos y poder ser llevado a cabo

mediante distintos mecanismos. A pesar de esta complejidad, los resultados muestran que una mayor adsorción de proteínas asociadas al sistema inmune que den lugar a una reacción no desproporcionada y bien regulada podría ser indicativo de una mayor bioactivación por parte del material y tener efectos positivos en la regeneración ósea. Por otro lado, la mayor afinidad de un implante hacía proteínas como VTNC y APOE podría señalar una mayor capacidad de osteointegración. En este sentido, la VTNC y APOE podrían ser empleadas como biomarcadores de eficiencia.

Conclusions

Les **conclusions parcials** de cada un dels estudis duts a terme es detallen a continuació:

- **Capítol 1** - Es va desenvolupar un procés de síntesi sol-gel pel qual s'han dissenyat biomaterials capaços de donar lloc a diferents respostes biològiques. Així, la tècnica sol-gel va permetre l'obtenció de recobriments homogenis i ben adherits a partir de la mescla de tres alcoxisilans (MTMOS, GPTMS i TEOS), sent la composició 35M35G30T la que presenta una cinètica de degradació interessant per a ser empleada com a vehicle d'alliberament en implants dentals.

- **Capítol 2** - L'anàlisi proteòmica a distintes formulacions híbrides sol-gel que donen lloc a dos respostes *in vivo* diferenciades, oseointegració i no oseointegració de l'implant, va mostrar que els problemes de biocompatibilitat observats *in vivo* podrien estar associats a l'adsorció d'un clúster de proteïnes associades a una forta reacció immune / inflamatòria.

- **Capítol 3** - L'anàlisi proteòmica comparatiu d'una superfície de titani granallat amb atac àcid (SAE), respecte al mateix material sense tractar, va resultar en la identificació de les proteïnes APOE, ANT3 i PROC com més adsorbides en el SAE-Ti, podent estar estes associades a la major capacitat d'osteointegració d'aquest tractament superficial.

- **Capítol 4** - L'anàlisi proteòmica comparatiu del material SAE-Ti respecte al recobriment 35M35G30T va resultar en la identificació d'importants diferències en els perfils de proteòmica adsorbits. La superfície sol-gel va mostrar major afinitat per proteïnes associades al sistema immune, mentres que el SAE-Ti va mostrar més afinitat per proteïnes associades a la coagulació i a la regeneració òssia (APOE i VTNC). El fet de que ambdós materials donen lloc a bons resultats *in vivo*, podria suposar que la proteòmica està aportant informació rellevant al mecanisme de regeneració associat a cada biomaterial.

- **Capítol 5** - L'addició de $SrCl_2$ a la xarxa sol-gel va suposar un increment del seu potencial osteogènic i antiinflamatori *in vitro* d'una manera dependent de la concentració, que es

va correlacionar amb la detecció de patrons d'adsorció de proteïnes relacionades amb l'osteogènesi i la regulació / inhibició de la resposta immune.

- **Capítol 6** - L'addició de $CaCl_2$ a la xarxa sol-gel va suposar un increment del seu potencial osteogènic, així com un major potencial inflamatori *in vitro* a determinades concentracions. L'anàlisi proteòmica d'aquestes superfícies va mostrar que la presència del Ca va suposar una major afinitat per proteïnes associades a la cascada de coagulació, així com per les proteïnes APOE i VTNC, fet que podria estar correlacionat amb el major potencial osteogènic observat *in vitro*.

D'esta manera, les **conclusions generals** que es poden extraure del treball experimental presentat són:

- La tècnica sol-gel permet el disseny de recobriments per a modificar superficialment les propietats d'implants dentals i així controlar la seua resposta biològica.

- La proteòmica pot emprar-se com a ferramenta predictiva de la resposta *in vivo* de biomaterials, podent arribar a donar resultats més fiables que els estudis *in vitro* tradicionals. Així, la caracterització sistemàtica de l'adsorció de proteïnes sèriques a la superfície de diversos materials empleats en implantologia dental ha permès la detecció de patrons proteics que indicarien la millor o pitjor capacitat d'osteointegració d'un determinat biomaterial.

- La manca de biocompatibilitat podria estar associada a una desproporcionada adsorció de proteïnes que donen lloc a una forta reacció inflamatòria, com ara la CRP. Així la proporció de proteïnes activadores de la resposta immune respecte a la de proteïnes que són capaços de regular i inhibir esta resposta sembla tenir un paper clau. En base als resultats es proposa el biomarcador proteic CRP / VTNC per a la predicció de problemes de biocompatibilitat en aquest tipus de materials.

- Al seu torn, l'eficiència regenerativa d'un biomaterial sembla ser un objectiu molt més complex al poder entrar en joc multitud de processos i poder ser dut a terme mitjançant diferents mecanismes. Malgrat aquesta complexitat, els resultats mostren que una major

adsorció de proteïnes associades al sistema immune que donin lloc a una reacció no desproporcionada i ben regulada podria ser indicatiu d'una major bioactivació per part del material i tenir efectes positius en la regeneració òssia. D'altra banda, la major afinitat d'un implant per proteïnes com VTNC i APOE podria assenyalar una major capacitat d'osteointegració. En aquest sentit, VTNC i APOE podrien ser emprades com a biomarcadors d'eficiència.

10. FUTURE LINES OF RESEARCH

10. Future lines of research

The future lines of research based on the biomaterial proteomic studies, as well as the development of new *in vitro* methodologies for their biological evaluation are detailed in this chapter. Some of these research lines would constitute the continuation of the studies presented in the doctoral thesis.

After the development of new sol-gel coatings doped with $CaCl_2$ and $SrCl_2$ and their subsequent biological characterization through *in vitro* and proteomic analyses, these materials are being tested *in vivo* in order to evaluate their potential enhancing the osseointegration capability of dental implants. These tests will be useful to check the osteogenic *in vivo* potential of these materials, allowing a more robust discussion in regard of their proteomic characterization.

In parallel, following the outlined strategy, it is of great importance for this research line to evaluate new compositions in order to obtain more information about the protein-biomaterial interactions, as well as the effect of the adsorption of these proteins in the biomaterial *in vivo* response. In this sense, we are already carrying out the analysis, through proteomics, of the effect that the addition of different compounds such as $MgCl_2$, $ZnCl_2$, boron, melatonin and gelatin can have on the adhesion of proteins on the biomaterial surface. This battery of tests would allow to identify new patterns of adsorption of key proteins associated with processes, such as angiogenesis, not detected with the design of materials carried out so far; as well as obtaining more conclusive results in reference to coagulation and verifying the reproducibility of the patterns associated with osteogenesis.

In this line, the next step would be to carry out an escalation of this proteomic methodology and evaluate biomaterials widely recognized and with very diverse properties: calcium phosphates, bioglasses, hydrogels, polyethylene, stainless steel etc. The coherence between the results obtained with the sol-gel materials and those obtained with this future experimentation would validate the use of proteomics as a tool to predict the *in vivo* response of biomaterials.

Likewise, based on the results obtained in chapter 2, which shows the relationship between the adsorption of proteins associated with an acute immune reaction with the lack of biocompatibility *in vivo* shown by some compositions. A new line of work has been initiated based on the study of

macrophage polarization on biomaterials, as a complementary methodology to the traditional *in vitro* studies using osteoblasts.

On the other hand, in the included studies the protein source composition has been kept constant, using a commercial human serum. However, this parameter, in reality, is not constant, but can vary depending on the metabolism of each person. For this reason, one of the future research lines is based on conducting comparative proteomic studies using serum from different population groups associated with pathologies related to a lower capacity for bone regeneration, such as diabetes or osteoporosis, compared to a healthy population group, keeping the biomaterial parameter as constant. From this research we could extract very useful information to be able to offer personalized medicine to future patients associated with this type of risk factors.

In this line, another parameter that has been kept constant is the serum incubation time, which was established in 3 hours based on preliminary studies and bibliography. However, a future research line would be the proteomic study of biomaterials using different incubation times, which could help to improve the Vroman effect understanding, as well as the evolution of key protein patterns over time.

The conformation that proteins acquire on the material is another factor to take into account during the study of biosurface - protein interactions. In this sense, this type of characterization is extremely complex when the studies are carried out with multiprotein media. However, being aware of its importance, studies based on the characterization of standard proteins adsorption kinetics have been carried out on the sol-gel coatings. These studies have been performed using the QCM-D technique during a doctoral stay in the Biomaterial Department of the University of Oslo. Thus, it would be interesting to evaluate the adsorption kinetics and conformation of proteins that are detected as key in the carried out studies (CRP, VTNC, APOE), in order to achieve a better understanding of their interaction with biomaterials.

From the biomaterial design point of view, once the key protein patterns to ensure a good implant osseointegration process have been established, it would be necessary to optimize the superficial characteristics of implants. In other words, a possible line of work would be opened based on evaluating for each biomaterial physical-chemical parameter which values would favour the adhesion of key proteins with positive effects and which values would reduce the adhesion of key

proteins related to biocompatibility problems; thus we would be able to design biomaterials with ideal properties from the proteomic point of view.

Another line of future research would be based on the correlation of proteomics results carried out on the biomaterial surfaces with more complex models such as carrying out proteomic studies with cells or *in vivo*. This type of experimentation would allow us to obtain a more global view of the phenomena associated to the osseointegration process and the protein pivotal role during it.

11. ANNEXES

11. Annexes

11.1. List of publications

The list of works published in indexed international journals, which are the result of the experimental work carried out during the PhD period, is detailed below:

- F. Romero-Gavilán, S. Barros-Silva, J. García-Cañadas, B. Palla, R. Izquierdo, M. Gurruchaga, I. Goñi, J. Suay, Control of the degradation of silica sol-gel hybrid coatings for metal implants prepared by the triple combination of alkoxysilanes, J. Non. Cryst. Solids. 453 (2016) 66–73. doi:10.1016/j.jnoncrysol.2016.09.026.

- F. Romero-Gavilán, N.C. Gomes, J. Ródenas, A. Sánchez, M. Azkargorta, I. Iloro, F. Elortza, I. García Arnáez, M. Gurruchaga, I. Goñi, J. Suay, Proteome analysis of human serum proteins adsorbed onto different titanium surfaces used in dental implants, Biofouling. 33 (2017) 98–111. doi:10.1080/08927014.2016.1259414.

- F. Romero-Gavilán, A.M. Sanchez-Pérez, N. Araújo-Gomes, M. Azkargorta, I. Iloro, F. Elortza, M. Gurruchaga, I. Goñi, J. Suay, Proteomic analysis of silica hybrid sol-gel coatings: a potential tool for predicting the biocompatibility of implants in vivo, Biofouling. 33 (2017) 676–689. doi:10.1080/08927014.2017.1356289.

- F. Romero-Gavilan, N. Araújo-Gomes, A.M. Sánchez-Pérez, I. García-Arnáez, F. Elortza, M. Azkargorta, J.J.M. de Llano, C. Carda, M. Gurruchaga, J. Suay, I. Goñi, Bioactive potential of silica coatings and its effect on the adhesion of proteins to titanium implants, Colloids Surfaces B Biointerfaces. 162 (2017) 316–325. doi:10.1016/j.colsurfb.2017.11.072.

- M. Martinez-Ibañez, I. Aldalur, F. Romero-Gavilán, J. Suay, I. Goñi, M. Gurruchaga, Design of nanostructured siloxane-gelatin coatings: Immobilization strategies and dissolution properties, J. Non. Cryst. Solids. 481 (2018) 368–374. doi:10.1016/j.jnoncrysol.2017.11.010.

- N. Araújo-Gomes, F. Romero-Gavilán, A.M. Sánchez-Pérez, M. Gurruchaga, M. Azkargorta, F. Elortza, M. Martinez-Ibañez, I. Iloro, J. Suay, I. Goñi, Characterization of serum proteins

attached to distinct sol–gel hybrid surfaces, J. Biomed. Mater. Res. - Part B Appl. Biomater. 106 (2018) 1477–1485. doi:10.1002/jbm.b.33954.

- N. Araújo-Gomes, F. Romero-Gavilán, I. García-Arnáez, C. Martínez-Ramos, A.M. Sánchez-Pérez, M. Azkargorta, F. Elortza, J.J.M. de Llano, M. Gurruchaga, I. Goñi, J. Suay, Osseointegration mechanisms: a proteomic approach, J. Biol. Inorg. Chem. 23 (2018) 459–470. doi:10.1007/s00775-018-1553-9.

- N. Araújo-Gomes, F. Romero-Gavilán, I. Lara-Sáez, F. Elortza, M. Azkargorta, I. Iloro, M. Martínez-Ibañez, J.J. Martín de Llano, M. Gurruchaga, I. Goñi, J. Suay, A.M. Sánchez-Pérez, Silica-gelatin hybrid sol-gel coatings: a proteomic study with biocompatibility implications, J. Tissue Eng. Regen. Med. (2018) 1–11. doi:10.1002/term.2708.

- I. García-Arnáez, B. Palla, J. Suay, F. Romero-Gavilán, M. Fernández, L. García-Fernández, I. Goñi, M. Gurruchaga, A single coating with antibacterial and osteogenic properties for bone implants, Thin Solid Films. Under review, March 2018.

- F. Romero-Gavilán, N. Araújo-Gomes, I. García-Arnáez, C. Martínez-Ramos, F. Elortza, M. Azkargorta, I. Iloro, M. Gurruchaga, J. Suay, I. Goñi, The effect of strontium incorporation into sol-gel biomaterials on their protein adsorption and cell interactions, Colloids Surfaces B Biointerfaces. Under review, May 2018.

- F. Romero-Gavilán, N. Araújo-Gomes, I. García-Arnáez, C. Martínez-Ramos, F. Elortza, M. Azkargorta, I. Iloro, M. Gurruchaga, J. Suay, I. Goñi, Proteomic analysis of calcium enriched sol-gel biomaterials. In process, 2018.

- N. Araújo-Gomes, F. Romero-Gavilán, Y. Zhang, C. Martinez-Ramos, A.M. Sánchez-Pérez, F. Elortza, M. Azkargorta, J.J. Martín de Llano, M. Gurruchaga, I. Goñi, J.J.J.P. van den Beucken, J. Suay, Complement pathways and macrophage polarization regulation: proteomic interfaces. In process, 2018.

11.2. First page of the published articles presented as thesis results

Chapter 1

Journal of Non-Crystalline Solids 453 (2016) 66–73

Contents lists available at ScienceDirect

Journal of Non-Crystalline Solids

journal homepage: www.elsevier.com/locate/jnoncrysol

Control of the degradation of silica sol-gel hybrid coatings for metal implants prepared by the triple combination of alkoxysilanes

F. Romero-Gavilán [a], S. Barros-Silva [a], J. García-Cañadas [a,*], B. Palla [b], R. Izquierdo [a], M. Gurruchaga [b], I. Goñi [b], J. Suay [a]

[a] Departamento de Ingeniería de Sistemas Industriales y Diseño, Universitat Jaume I, Av. Vicent Sos Baynat s/n, Castellón 12071, Spain
[b] Facultad de Ciencias Químicas, Universidad del País Vasco, P. M. de Lardizábal, 3, San Sebastián 20018, Spain

ARTICLE INFO

Article history:
Received 2 August 2016
Received in revised form 20 September 2016
Accepted 23 September 2016
Available online 30 September 2016

Keywords:
Si release
Corrosion resistance
TEOS
Biomaterials
Coatings

ABSTRACT

Hybrid materials obtained by sol-gel process are able to degrade and release Si compounds that are useful in regenerative medicine due to their osteoinductive properties. The present work studies the behavior of new organic-inorganic sol-gel coatings based on triple mixtures of alkoxysilanes in different molar ratios. The precursors employed are methyl-trimethoxysilane (MTMOS), 3-glycidoxypropyl-trimethoxysilane (GPTMS) and tetraethyl-orthosilicate (TEOS). After optimization of the synthesis conditions, the coatings were characterized using ^{29}Si nuclear magnetic resonance (^{29}Si-MNR), Fourier transform infrared spectrometry (FT-IR), contact angle measurements, hydrolytic degradation assays, electrochemical impedance spectroscopy (EIS) and mechanical profilometry. The degradation and EIS results show that by controlling the amount of TEOS precursor in the coating it is possible to tune its degradation by hydrolysis, while keeping properties such as wettability at their optimum values for biomaterials application. The corrosion properties of the new coatings were also evaluated when applied to stainless steel substrate. The coatings showed an improvement of the anticorrosive properties of the steel which is important to protect the metal implants at the early stages of the regeneration process.

Chapter 2

BIOFOULING, 2017
VOL. 33, NO. 8, 676–689
https://doi.org/10.1080/08927014.2017.1356289

Proteomic analysis of silica hybrid sol-gel coatings: a potential tool for predicting the biocompatibility of implants *in vivo*

F. Romero-Gavilan[a#], A. M. Sánchez-Pérez[b#], N. Araújo-Gomes[a,b], M. Azkargorta[d], I. Iloro[d], F. Elortza[d], M. Gurruchaga[c], I. Goñi[c] and J. Suay[a]

[a]Department of Industrial Systems and Design, Universitat Jaume I, Castellón, Spain; [b]Department of Medicine, Universitat Jaume I, Castellón, Spain; [c]Facultad de Ciencias Químicas, Universidad del País Vasco, San Sebastián, Spain; [d]Proteomics Platform, CIC bioGUNE, CIBERehd, ProteoRed-ISCIII, Derio, Spain

ABSTRACT

The interactions of implanted biomaterials with the host organism determine the success or failure of an implantation. Normally, their biocompatibility is assessed using *in vitro* tests. Unfortunately, *in vitro* and *in vivo* results are not always concordant; new, effective methods of biomaterial characterisation are urgently needed to predict the *in vivo* outcome. As the first layer of proteins adsorbed onto the biomaterial surfaces might condition the host response, mass spectrometry analysis was performed to characterise these proteins. Four distinct hybrid sol-gel biomaterials were tested. The *in vitro* results were similar for all the materials examined here. However, *in vivo*, the materials behaved differently. Six of the 171 adsorbed proteins were significantly more abundant on the materials with weak biocompatibility; these proteins are associated with the complement pathway. Thus, protein analysis might be a suitable tool to predict the *in vivo* outcomes of implantations using newly formulated biomaterials.

ARTICLE HISTORY
Received 1 February 2017
Accepted 11 July 2017

KEYWORDS
Haemocompatibility; osteoimmunology; fibrous capsule; bone regeneration; dental implants; C-reactive protein

Chapter 3

BIOFOULING, 2017
VOL. 33, NO. 1, 98–111
http://dx.doi.org/10.1080/08927014.2016.1259414

Taylor & Francis
Taylor & Francis Group

Proteome analysis of human serum proteins adsorbed onto different titanium surfaces used in dental implants

Francisco Romero-Gavilán[a], N. C. Gomes[b], Joaquin Ródenas[a], Ana Sánchez[b], Mikel Azkargorta[c], Ibon Iloro[c], Felix Elortza[c], Iñaki García Arnáez[d], Mariló Gurruchaga[d], Isabel Goñi[d] and Julio Suay[a]

[a]Department of Industrial Systems and Design Engineering, University of Castellón, Castellón de la Plana, Spain; [b]Department of Medicine, University of Castellón, Castellón de la Plana, Spain; [c]Proteomics Platform, CIC bioGUNE, CIBERehd, ProteoRed-ISCIII, Derio, Spain; [d]Department of Polymer Science and Technology, University of Basque Country, San Sebastián, Spain

ABSTRACT

Titanium dental implants are commonly used due to their biocompatibility and biochemical properties; blasted acid-etched Ti is used more frequently than smooth Ti surfaces. In this study, physico-chemical characterisation revealed important differences in roughness, chemical composition and hydrophilicity, but no differences were found in cellular *in vitro* studies (proliferation and mineralization). However, the deposition of proteins onto the implant surface might affect *in vivo* osseointegration. To test that hypothesis, protein layers formed on discs of both surface type after incubation with human serum were analysed. Using mass spectrometry (LC/MS/MS), 218 proteins were identified, 30 of which were associated with bone metabolism. Interestingly, Apo E, antithrombin and protein C adsorbed mostly onto blasted and acid-etched Ti, whereas the proteins of the complement system (C3) were found predominantly on smooth Ti surfaces. These results suggest that physico-chemical characteristics could be responsible for the differences observed in the adsorbed protein layer.

ARTICLE HISTORY
Received 9 May 2016
Accepted 31 October 2016

KEYWORDS
Titanium; surface properties; human serum; apolipoprotein E; bone regeneration; proteomics

Chapter 4

Colloids and Surfaces B: Biointerfaces 162 (2018) 316–325

Contents lists available at ScienceDirect

Colloids and Surfaces B: Biointerfaces

journal homepage: www.elsevier.com/locate/colsurfb

Bioactive potential of silica coatings and its effect on the adhesion of proteins to titanium implants

F. Romero-Gavilan[a,1], N. Araújo-Gomes[a,b,*,1], A.M. Sánchez-Pérez[b], I. García-Arnáez[b], F. Elortza[d], M Azkargorta[d], J.J. Martín de Llano[e], C. Carda[e], M. Gurruchaga[c], J. Suay[a], I. Goñi[c]

[a] Departamento de Ingeniería de Sistemas Industriales y Diseño, Universitat Jaume I, Av. Vicent-Sos Baynat s/n, Castellón 12071, Spain
[b] Department of Medicine, Universitat Jaume I, Av. Vicent-Sos Baynat s/n, Castellón 12071, Spain
[c] Facultad de Ciencias Químicas, Universidad del País Vasco, P. M. de Lardizábal, 3, San Sebastián 20018, Spain
[d] Proteomics Platform, CIC bioGUNE, CIBERehd, ProteoRed-ISCIII, Bizkaia Science and Technology Park, 48160 Derio, Spain
[e] Department of Pathology and Health Research Institute of the Hospital Clínico (INCLIVA), Faculty of Medicine and Dentistry, University of Valencia, 46010 Valencia, Spain

ARTICLE INFO

Article history:
Received 1 August 2017
Received in revised form
14 November 2017
Accepted 30 November 2017

Keywords:
Dental implants
Apolipoproteins
Osteoimmunology
Osteogenesis
Bone regeneration
Proteomics

ABSTRACT

There is an ever-increasing need to develop dental implants with ideal characteristics to achieve specific and desired biological response in the scope of improve the healing process post-implantation. Following that premise, enhancing and optimizing titanium implants through superficial treatments, like silica sol-gel hybrid coatings, are regarded as a route of future research in this area. These coatings change the physicochemical properties of the implant, ultimately affecting its biological characteristics. Sand-blasted acid-etched titanium (SAE-Ti) and a silica hybrid sol-gel coating (35M35G30T) applied onto the Ti substrate were examined. The results of *in vitro* and *in vivo* tests and the analysis of the protein layer adsorbed to each surface were compared and discussed.

In vitro analysis with MC3T3-E1 osteoblastic cells, showed that the sol-gel coating raised the osteogenic activity potential of the implants (the expression of osteogenic markers, the alkaline phosphatase (ALP) and IL-6 mRNAs, increased). In the *in vivo* experiments using as model rabbit tibiae, both types of surfaces promoted osseointegration. However, the coated implants demonstrated a clear increase in the inflammatory activity in comparison with SAE-Ti. Mass spectrometry (LC–MS/MS) analysis showed differences in the composition of protein layers formed on the two tested surfaces. Large quantities of apolipoproteins were found attached predominantly to SAE-Ti. The 35M35G30T coating adsorbed a significant quantity of complement proteins, which might be related to the material intrinsic bioactivity, following an associated, natural and controlled immune response.

The correlation between the proteomic data and the *in vitro* and *in vivo* outcomes is discussed on this experimental work.

11.3. Works presented at national and international conferences

The list of works presented at national and international conferences, which are the result of the experimental work carried out during the phD period, is detailed below:

F. Romero-Gavilán; M. Azkargorta; I. Iloro; A.M. Sánchez-Pérez; N. Araújo-Gomes; I. Escobes; M. Gurruchaga; I. Goñi; F. Elortza; J. Suay; Proteomic analysis of silica hybrid sol-gel coatings: a potential tool for predicting the biocompatibility of implants in vivo. XII EUPA Congress, Translating genomes into biological functions, 16-20 June 2018, Santiago de Compostela, Spain.

N. Araújo-Gomes; F. Romero-Gavilán; A.M. Sánchez-Pérez; F. Elortza; M. Gurruchaga; I. Goñi; J. Suay; Estudio de la biocompatibilidad de biomateriales mediante marcadores de inflamación. XL Congreso Sociedad Ibérica de Biomecánica y Biomateriales (SIBB2017), 10-11 November 2017, Barcelona, Spain. In: pp 22 - 24, 2017. ISBN 9788469796283.

F. Romero-Gavilán; N. Araújo-Gomes; A.M. Sánchez-Pérez; F. Elortza; M. Gurruchaga; I. Goñi; J. Suay; Identificación de marcadores relacionados con problemas de biocompatibilidad mediante proteómica. XL Congreso Sociedad Ibérica de Biomecánica y Biomateriales (SIBB2017), 10-11 November 2017, Barcelona, Spain. In: pp 18 - 21, 2017. ISBN 9788469796283.

J. Suay; F. Romero-Gavilán; N. Araújo-Gomes; A.M. Sánchez-Pérez; F. Elortza; I. Goñi; M. Gurruchaga; J. Franco; Predictive markers associated with dental implants biocompatibility using proteomic analysis. 26 th Annual Scientific Meeting of the European Association for Osseointegration (EAO2017), 5-7 October 2017, Madrid, Spain. In: Clin Oral Impl Res. 2017, 28 (14) pp. 67. ISSN 0905-7161. doi:10.1111/clr.66_13042.

J. J. Martín de Llano; N. Araújo-Gomes; F. Romero-Gavilán; A.M. Sánchez-Pérez; M. Azkargorta; F. Elortza; M. Gurruchaga; I. Goñi; R. Salvador-Clavell; L. Milián; J. Suay; C. Carda; Tissue response to titanium implants coated with a hybrid silica sol-gel in a rabbit tibia model. XIX Congreso de la Sociedad Española de Histología e Ingeniería Tisular. IV Congreso Iberoamericano de Histología. VII International Congress of Histology and Tissue Engineering (SEHIT2107), 5-8 September 2017, Santiago de Compostela, Spain. In: pp. 155 – 155, 2017. ISSN 0213-3911. doi: 10.14670/HH-sehit17.

N. Araújo-Gomes; F. Romero-Gavilán; A.M. Sánchez-Pérez; F. Elortza; I. Goñi; M. Gurruchaga; J. Suay; The Role of Proteomics in Prediction of Biomaterials Biocompatibility. 28 th Annual Conference of the European Society for Biomaterials (ESB2017), 4-8 September 2017, Athens, Greece.

F. Romero-Gavilán; N. Araújo-Gomes; A.M. Sánchez Pérez; F. Elortza; M. Gurruchaga; I. Goñi; J. Suay; Proteomic identification of predictive markers related with biocompatibility problems. 10th annual meeting for Scandinavian Society for Biomaterials (ScSB), 15-17 March 2017, Hafjell, Norway. In: European Cells and Materials. 33 (1) pp. 26 - 26. 2017. ISSN 1473-2262.

N. Araújo-Gomes; F. Romero-Gavilán; A.M. Sánchez Pérez; F. Elortza; M. Gurruchaga; I. Goñi; J. Suay; Biocompatibility problems: an alternative method to approach in vitro testing?. 10th annual meeting for Scandinavian Society for Biomaterials (ScSB), 15-17 March 2017, Hafjell, Norway. In: European Cells and Materials. 33 (1) pp. 26 - 26. 2017. ISSN 1473-2262.

F. Romero-Gavilán; N. Araújo-Gomes; A.M. Sánchez-Pérez; F. Elortza; M. Gurruchaga; I. Goñi; J. Suay; Proteomic analysis as a biocompatibility predictor on hybrid sol-gel biomaterials. 5th International Conference on Multifunctional, Hybrid and Nanomaterials, 6-10 March 2017, Lisbon, Portugal.

F. Romero-Gavilán; A.M. Sánchez-Pérez; N. Araújo-Gomes; M. Azkargorta; I. Iloro; F. Elortza; M. Gurruchaga; I. Goñi; J. Suay; Análisis proteómico de recubrimientos híbridos sol-gel: Predicción de la respuesta in vivo. XV Jornadas sobre Biomateriales y el Entorno Celular, 23 February 2017, Ávila, Spain.

J. Suay; F. Romero-Gavilán; N. Araújo-Gomes; J. Rodenas; I. García; M. Gurruchaga; I. Goñi; A. Sánchez; Proteome analysis of human serum proteins adsorbed onto different titanium surfaces used in dental implants. 9th meeting of Scandinavian Society for Biomaterials (ScSB), 1-3 June 2016, Reykjavik, Iceland.

B. Palla; F. Romero-Gavilán; M. Fernández; J. Suay; M. Gurruchaga; l. Goñi; Osteoinductive and antibacterial coatings for dental implants. 27th European Conference on Biomaterials (ESB2015), 30 August – 3 September 2015, Kraków, Poland. ISBN 9788363663636.

B. Palla; I. Aladalur; M. Gurruchaga; F. Romero-Gavilán; J. Suay; M. Fernández; B. Vazquez; I. Goñi; Antibacterial coatings for dental implants. Fourth International Conference on Multifuncional, Hybrid and Nanomaterials, 9-13 March 2015, Sitges, Spain.

S. Da Silva-Barros; F. Romero-Gavilán; I. Lara-Sáez; M. Juan-Díaz; I. Goñi; M. Gurruchaga; J. Suay; Estudio de la degradación de recubrimientos bioactivos. I Congreso Biomedicina Predocs de Valencia, 27-28 November 2014, Valencia, Spain.

I. Lara-Sáez; M. Martínez-Ibáñez; B. Pallá-Rubio; I. Aldalur; F. Romero-Gavilán; A. Coso; J. Franco; M. Gurruchaga; I. Goñi; J. Suay; In vivo study of gelatine functionalized hybrid sol-gel coatings for titanium implants. 23rd Annual Scientific meeting EAO-European association for Osseointegration, 25-27 September 2014, Rome, Italy. In: Clin. Oral Impl. Res. 25 (10), pp. 270 - 270. ISSN 0905-7161. doi:10.1111/clr.12458_255.

I. Lara-Sáez; M. J. Juan-Díaz; M. Martínez-Ibáñez; F. Romero-Gavilán; S. Da Silva; A. Coso; J. Franco; M. Gurruchaga; I. Goñi; J. Suay; "In vivo" evaluation of Titanium implants coated with hybrid sol-gel materials. 7th Annual Meeting Scandinavian Society for Biomaterials, 26-28 March 2014, Aarhus, Denmark.

11.4. List of abbreviations and acronyms

General

A	Area of coating
AFM	Atomic force microscopy
ALP	Alkaline-phosphatase
ANG-1	Angiopoietin-1
Apo	Apolipoprotein
AT	Antithrombin
ATR	Attenuated total reflection
BMP	Bone morphogenetic protein
C4BP	C4b-binding protein
CaSR	Calcium-sensing receptor
Cc	Coating capacitance
CP-MAS	Cross Polarization Magic Angle Spinning
d	Coating thickness
DAVID	Database for Annotation, Visualization and Integrated Discovery
DMEM	Dulbecco's Modified Eagle's medium
DTT	Dithiothreitol
ECM	Extracellular matrix
EDX	Energy-dispersive X-ray spectroscopy
EGF	Epidermal growth factor
EIS	Electrochemical impedance spectroscopy
ESI	Electrospray ionization
FBGC	Foreign body giant cells
FBS	Fetal bovine serum
FGF	Fibroblast growth factor
FTICR	Fourier transform ion cyclotron resonance
FT-IR	Fourier transform infrared spectrometry
FVIIa	Factor VIIa
GPTMS	3-glycidoxypropyl-trimethoxysilane
HA	Hydroxyapatite
HDDA	High Definition Data Dependant Analysis
HIF-1α	Hypoxia inducible factor 1-α protein
IGF	Insulin-like growth factor
IL	Interleukin
LC	Liquid chromatography
LC-MS/MS	Liquid chromatography-tandem mass spectrometry
MALDI	Matrix assisted laser desorption ionization
MAPK	Mitogen-activated protein kinase
MGF	Mascot generic files
MS	Mass spectrometry
MSC	Mesenchymal stem cell

MTMOS	Methyl-trimethoxysilane
OCN	Osteocalcin
OCP	Octacalcium phosphate
OPN	Osteopontin
PAGE	Polyacrylamide gel electrophoresis
PAI	Plasminogen activator inhibitor
PCL	Polycaprolactone
PDGF	Platelet-derived growth factor
PDLLA	Poly(D,L-lactic acid)
PEG	Polyethylene glycol
PHEMA	Poly(2-hydroxyethyl methacrylate)
PMMA	Poly(methyl methacrylate)
p-NPP	p-nitrophenylphosphate
PolyNaSS	Poly sodium styrene sulfonate
QCM-D	Quartz crystal microbalance with dissipation
Ra	Average surface roughness
RT-qPCR	Quantitative Real-time PCR
RUNX2	Runt-related transcription factor 2
SAE	Sandblasted acid-etched
SDS	Sodium dodecyl sulfate
SEM	Scanning electron microscope
29Si-NMR	29Si nuclear magnetic resonance
TAFI	Thrombin-activatable fibrinolysis inhibitor
TEAB	Triethylammonium bicarbonate buffer
TEOS	Tetraethyl-orthosilicate
TF	Tissue factor protein
TGF-β	Transforming growth factor- β
Ti	Titanium
TNF-α	Tumor necrosis factor-α
TOF	Time-of-flight
t-PA	Tissue-type plasminogen activator
u-PA	Urokinase-type plasminogen activator
VEGF	Vascular endothelial growth factor
ε	Dielectric constant
ε_0	Vacuum permittivity

Protein abbreviations

A1AG1	Alpha-1-acid glycoprotein 1
A1AG2	Alpha-1-acid glycoprotein 2
A1AT	Alpha-1-antitrypsin
A2AP	Alpha-2-antiplasmin
A2GL	Leucine-rich alpha-2-glycoprotein
A2MG	Alpha-2-macroglobulin
A2AP	α2-antiplasmin
AACT	Alpha-1-antichymotrypsin
AFAM	Afamin
ALBU	Serum albumin
ANGT	Angiotensinogen
ANT3	Antithrombin-III
ANXA2	Annexin A2
APOA	Apolipoprotein(a)
APOA1	Apolipoprotein A-I
APOA2	Apolipoprotein A-II
APOA4	Apolipoprotein A-IV
APOA5	Apolipoprotein A-V
APOB	Apolipoprotein B-100
APOC1	Apolipoprotein C-I
APOC2	Apolipoprotein C-II
APOC3	Apolipoprotein C-III
APOC4	Apolipoprotein C-IV
APOD	Apolipoprotein D
APOE	Apolipoprotein E
APOL1	Apolipoprotein L1
C1QA	Complement C1q subcomponent subunit A
C1QB	Complement C1q subcomponent subunit B
C1QC	Complement C1q subcomponent subunit C
C1R	Complement C1r subcomponent
C1S	Complement C1s subcomponent
C4BPA	C4b-binding protein alpha chain
CERU	Ceruloplasmin
CFAH	Complement factor H
CLUS	Clusterin
CO3	Complement C3
CO5	Complement C5
CO6	Complement component C6
CO7	Complement component C7
CO8A	Complement component C8 alpha chain
CO8B	Complement component C8 beta chain
CRP	C-reactive protein
DHE3	Glutamate dehydrogenase 1. mitochondrial
DSC1	Desmocollin-1
FA11	Coagulation factor XI
FA12	Coagulation factor XII
FA5	Coagulation factor V
FCN2	Ficolin-2

FHR2	Complement factor H-related protein 2
FIBA	Fibrinogen alpha chain
FILA2	Filaggrin-2
GELS	Gelsolin
H4	Histone H4
HBA	Hemoglobin subunit alpha
HBB	Hemoglobin subunit beta
HEMO	Hemopexin
HORN	Hornerin
HPT	Haptoglobin
IC1	Plasma protease C1 inhibitor
IGHA1	Ig alpha-1 chain C region
IGHA2	Ig alpha-2 chain C region
IGHG4	Ig gamma-4 chain C region
IGHM	Ig mu chain C region
IGJ	Immunoglobulin J chain
IGLL5	Immunoglobulin lambda-like polypeptide 5
ITIH4	Inter-alpha-trypsin inhibitor heavy chain H4
K1C10	Keratin. type I cytoskeletal 10
K22E	Keratin. type II cytoskeletal 2 epidermal
K2C78	Keratin. type II cytoskeletal 78
KCRM	Creatine kinase M-type
KNG1	Kininogen-1
KV201	Ig kappa chain V-II region Cum
KV302	Ig kappa chain V-III region SIE
KV402	Ig kappa chain V-IV region Len
LAC2	Ig lambda-2 chain C regions
LCN1	Lipocalin-1
LDHB	L-lactate dehydrogenase B chain
LV301	Ig lambda chain V-III region SH
MYH1	Myosin-1
PF4V	Platelet factor 4 variant
PROC	Vitamin K-dependent protein C
PROS	Vitamin K-dependent protein S
RET4	Retinol-binding protein 4
S10A7	Protein S100-A7
SAA4	Serum amyloid A-4 protein
SAMP	Serum amyloid P-component
SEPP1	Selenoprotein P
SPB3	Serpin B3
TGM3	Protein-glutamine gamma-glutamyltransferase E
THRB	Prothrombin
TRFE	Serotransferrin
VTDB	Vitamin D-binding protein
VTNC	Vitronectin

11.5. List of figures

Introduction

Figure 1.1. Bone remodelling process.

Figure 1.2. Biomaterial properties affecting protein adsorption.

Figure 1.3. Biological implication of the protein layer formed onto implants during the osseointegration process.

Figure 1.4. Coagulation cascade diagram.

Figure 1.5. Scheme of the fibrinolysis process. Red items represent the inhibitory mechanism of this system.

Figure 1.6. Complement system activation mechanisms. Diamonds display the inhibitory proteins, which belong to this system, in their possible action sites.

Figure 1.7. Sol-gel route scheme: chemical reactions and coating formation.

Figure 1.8. Thesis approach.

Figure 1.9. Approach for the identification of biomarkers related to biocompatibility problems.

Chapter 1

Figure 2.0. Graphical abstract of the work named “Control of the degradation of silica sol-gel hybrid coatings for metal implants prepared by the triple combination of alkoxysilanes”.

Figure 2.1. ^{29}Si solid NMR of (a) 50M50G, (b) 45M45G10T, (c) 35M35G30T, (d) 25M25G50T, (e) 15M15G70T and (f) 5M5G90T films.

Figure 2.2. FT-IR spectra of (a) 50M50G, (b) 45M45G10T, (c) 35M35G30T, (d) 25M25G50T, (e) 15M15G70T and (f) 5M5G90T films.

Figure 2.3. Contact angle results for films deposited on stainless steel substrates with different MTMOS:GPTMS:TEOS molar ratios. Bars indicate standard deviations.

Figure 2.4. Coating thickness measured by mechanical profilometry of sol-gel coatings prepared onto stainless steel plates by dip-coating. Statistically significant differences were found in the 5M5G90T coating thickness respect the other materials (ANOVA, * $p<0.05$). Bars indicate the standard deviations.

Figure 2.5. (a) Impedance modules and (b) phase angel bode plots for stainless steel, 50M50G, 45M45G10T, 35M35G30T, 25M25G50T, 15M15G70T and 5M5G90T sol-gel coatings at 8 h of immersion in the electrolyte. Fitted results are represented by the solid lines.

Figure 2.6. Equivalent circuits used for (a) non-coated and (b) coated stainless steel substrates. They correspond to the presence of one and two time constants, respectively.

Figure 2.7. Evolution of (a) Rcoat and (b) CPEcoat along the time of contact with electrolyte (3.5 % wt. NaCl) for 50M50G, 45M45G10T, 35M35G30T, 25M25G50T, 15M15G70T and 5M5G90T coatings.

Figure 2.8. Evolution of Rox (a) and CPEox (b) versus time of contact with electrolyte (3.5 % wt. NaCl) for Stainless steel, 50M50G, 45M45G10T, 35M35G30T, 25M25G50T, 15M15G70T and 5M5G90T coatings.

Figure 2.9. Weight loss versus time during the hydrolytic degradation for 50M50G, 45M45G10T, 35M35G30T, 25M25G50T, 15M15G70T and 5M5G90T coatings.

Chapter 2

Figure 3.0. Graphical abstract of the work named “proteomic analysis of silica hybrid sol-gel coatings: a potential tool for predicting biocompatibility of implants *in vivo*”.

Figure 3.1. SEM micrographs of hybrid sol-gel coatings on SAE titanium discs: (a) Ti-Control, (b) 70M30T, (c) 35M35G30T, (d) 50M50G and (e) 50V50G. Calibration bar 10 µm.

Figure 3.2. AFM images of hybrid sol-gel coatings: (a) Ti-Control, (b) 70M30T, (c) 35M35G30T, (d) 50M50G and (e) 50V50G. (f) Mechanical profilometer measures of Ra. Bars indicate standard deviations.

Figure 3.3. Contact angle results for sol-gel coatings on titanium discs. Bars indicate standard deviations.

Figure 3.4. MC3T3-E1 cell viability and mineralization *in vitro*. (a) Percentage of cell survival following the norm ISO 10993-5. (b) ALP activity (mM PNP h^{-1}) normalized to the amount of total protein (µg μL^{-1}) levels of the MC3T3-E1 cells cultivated on titanium discs treated with 70M30T (dotted column), 35M35G30T (checkered column), 50M50G (diagonal striped column) and 50V50G (horizontal striped column) formulations. Cells on an empty well without disc were used as a positive control (black column), whereas uncoated titanium discs (white column) were used as a negative control. There were no statistically significant differences between the different formulations at the times measured.

Figure 3.5. Light microscopy representative images (EXAKT® cut and Gomori Trichrome stain) in vivo implants 2 weeks post-implantation of: (a) representative photo of the area chosen to analyse the osseointegration state (b) 70M30T, (c) 35M35G30T, (d) 50M50G and (e) 50V50G sol-gel coated screws. The white arrows point to the area where the fibrous connective tissue was being formed.

Figure 3.6. Area in mm^2 occupied by the fibrous connective tissue occupied by the four tested coatings. Significantly differences between 70M30T/35M35G30T and 50M50G/50V50G were found (ANOVA $p \leq 0.05$ with a Kruskal-Wallis post-test).

Chapter 3

Figure 4.0. Graphical abstract of the work named “Proteome analysis of human serum proteins adsorbed onto different titanium surfaces used in dental implants”.

Figure 4.1. SEM images of disc surface: (a) smooth-Ti and (b) SAE-Ti (x1000).

Figure 4.2. SEM/EDX images of titanium sandblasted and acid-etched disc for Al_2O_3 particles identification.

Figure 4.3. AFM images at scan size 60 µm: (a) untreated titanium and (b) SAE treated Ti; and 1 µm: (c) untreated titanium and (d) SAE treated titanium. The z-axis could not be normalized to the same scale due to the height difference between treatments.

Figure 4.4. MC3T3-E1 cell proliferation on different treated discs: Smooth-Ti (white circle), SAE-Ti (black semi-square with dotted line). Cells, on an empty well, without disc was used as a control (white circle). No statistically significant differences were found between treatments.

Figure 4.5. MC3T3-E1 cells ALP activity normalized to the total protein (BCA) levels (mM PNP h^{-1}) / (µg μL^{-1}) on different treated discs at (a) 14 and (b) 21 days; Smooth-Ti (white column); SAE-Ti (squared/dotted column). Cells, on an empty well, without disc was used as a control (black column). No statistically significant differences were found between treatments.

Figure 4.6. PieCharts showing the biological processes of the proteins adhered to (a) SAE-Ti and (b) Smooth-Ti.

Figure 4.7. PieCharts pathways of the proteins adhered to (c) SAE-Ti and (d) Smooth-Ti.

Chapter 4

Figure 5.0. Graphical abstract of the work named "Bioactive potential of silica coatings and its effect on the adhesion of proteins to titanium implants".

Figure 5.1. SEM micrographs of (a) and (c) SAE-Ti and (b) and (d) 35M35G30T coating. Scale bars: (a) and (b), 10 µm and (c) and (d), 1 µm. AFM images of (e) SAE-Ti and (f) 35M35G30T coating.

Figure 5.2. MC3T3-E1 *in vitro* assays: a) MC3T3-E1 cell proliferation after 1, 3, 5 and 7 days of cell culture with SAE-Ti (white bar) and 35M35G30T (grey bar); b) ALP activity (mM PNP h^{-1}), normalised to the amount of total protein (µg μL^{-1}), in the MC3T3-E1 cells cultivated on SAE-Ti (white bar) and 35M35G30T formulation (grey bar). Cells in an empty well were used as a positive control (black bar). Statistical analysis was performed using one-way ANOVA with a Kruskal-Wallis post- test (*, $p \leq 0.05$).

Figure 5.3. Gene expression of osteogenic markers (a) ALP and (b) IL-6 on MC3T3-E1 osteoblastic cells cultured on SAE-Ti (white bar) and 35M35G30T (grey bar). Cells in an empty well were used

as a positive control (black bar). The relative mRNA expression was determined by RT-PCR after 7 and 14 days of cell culture. Statistical analysis was performed using one-way ANOVA with a Kruskal-Wallis post-test (***, $p \leq 0.001$).

Figure 5.4. Microphotographs of SAE-Ti and 35M35G30T samples. Panoramic images of (A) SAE-Ti and (B) 35M35G30T samples show the implant regions close to the cortical bone and in the medullary cavity. The regions enclosed in white-edged squares in A and B are shown in panels C and D, respectively. In the panel C, several rounded and elongated osteoclast-like and giant cells touch the surface of the implant. In the D panel, two giant cells, flanking a region with inflammatory cells, are in contact with the transparent coating of the implant surface. Lower regions of the C and D images are shown magnified in the corresponding insets. Stevenel's blue and van Gieson's picro-fuchsin staining was used. Scale bars: A and B, 1 mm; C and D, 0.1 mm; insets, 0.02 mm.

Figure 5.5. PANTHER pie chart of the biological processes associated with the proteins differentially adhering to (a) SAE-Ti and (b) 35M35G30T.

Chapter 5

Figure 6.0. Graphical abstract of the work named "The effect of strontium incorporation into sol-gel biomaterials on their protein adsorption and cell interactions".

Figure 6.1. SEM micrograph of (a) SAE-Ti, (b) 0Sr, (c) 0.25Sr, (d) 0.5Sr, (e) 1Sr and (f) 1.5Sr. Scale bar: a-f: 10 µm.

Figure 6.2. (a) Roughness and (b) contact angle results. Bars indicate standard deviations. Statistical analysis was performed using one-way ANOVA with a Kruskal-Wallis post-hoc test (***, $p < 0.001$), showing significant differences in comparison with the 35M35G30T base material.

Figure 6.3. Relative gene expression levels of the osteogenic markers (a) ALP and (b) TGF-β in the MC3T3-E1 cells cultured on the different Sr-containing coatings. The dotted black line represents the control (the well containing cells only, no disc), assigned the value of 1 as a reference. The relative mRNA expression was determined by RT-PCR after 7 and 14 days of culture. Statistical analysis was performed using one-way ANOVA with Kruskal-Wallis post-hoc test (*, $p < 0.05$; **, p

< 0.01). Significant differences in expression were found between the cultures grown on Sr-discs and the base material (35M35G30T).

Figure 6.4. Relative gene expression levels of the inflammatory markers (a) TNF-α and (b) IL-10 in the RAW 264.7 cells cultured on the different tested formulations. The dotted black line represents the control (cells only, no disc), assigned the value of 1 as a reference. The relative mRNA expression was determined by RT-PCR after 7 and 14 days of cell culture. Statistical analysis was performed using one-way ANOVA with a Kruskal-Wallis post-hoc test (*, $p < 0.05$; **, $p < 0.01$; ***, $p < 0.001$). Significant differences were found for the comparisons with the non-supplemented base material (35M35G30T).

Chapter 6

Figure 7.0. Graphical abstract of the work named "Proteomic analysis of calcium enriched sol-gel biomaterials".

Figure 7.1. Bone healing processes and protein interactions around implant surfaces.

Figure 7.2. SEM micrograph of (a) SAE-Ti, (b) 0Ca, (c) 0.5Ca, (d) 1Ca, (e) 2.5Ca, (f) 5Ca and (g) 7.5Ca. Scale bar, 10 μm

Figure 7.3. (a) Roughness and (b) contact angle results. Bars indicate standard deviations. One-way ANOVA with a Kruskal-Wallis post-test was used to accomplish the statistical analysis (***, $p<0.001$). Significant values are represented regarding the 35M35G30T base material.

Figure 7.4. Relative gene expression levels of the osteogenic markers a) ALP and b) IL-6 on the MC3T3-E1 cells cultured onto the different tested Ca formulations. And relative gene expression levels of the inflammatory markers c) TNF-α and d) IL-1β on the RAW 264.7 cells cultured onto the different tested formulations The black column represents the level of the control (well only with cells), which has the value of 1 as a reference. The relative mRNA expression was determined by RT-PCR after 7 and 14 days of cell culture. Statistical analysis was performed using one-way ANOVA with a Kruskal-Wallis post-test (*, $p<0.05$; **, $p<0.01$; ***, $p<0.001$). Significant values are represented regarding the base material (35M35G30T).

Figure 7.5. PANTHER diagram with the biological process functions of the proteins more and less differentially adhered onto 0.5Ca and 7.5Ca respect the reference sample (0Ca).

Figure 7.6. PANTHER diagram with the pathway functions of the proteins more differentially adhered onto Ca-enriched sol-gel coatings respect the reference sample (0Ca).

11.6. List of tables

Introduction

Table 1.1. LC-MS/MS proteomic studies focusing on the characterization of protein adsorption onto biomaterials used in implantology.

Chapter 1

Table 2.1. Molar percentage of the materials under study.

Table 2.2. Heat treatment conditions applied to each sol-gel composition.

Table 2.3. Ra values and their standard deviations for steel plates coated with MTMOS:GPTMS:TEOS materials in different ratios.

Table 2.4. Parameters n_1 and n_2 of CPEcoat and CPEox elements, respectively, for each formulation and measuring time

Chapter 2

Table 3.1. Proteins differentially predominant in 70M30T vs 35M35G30T (above), and 50V50G vs 50M50G (below) sol-gel coating comparatives (Progenesis method). ANOVA (p-value < 0.05). DAVID classification functions were (1) inflammatory/immune response, (2) hydroxylation, (3) blood coagulation, (4) apoptosis regulation, (5) metal binding, (6) phosphorylation, (7) carbohydrate binding, (8) peptidase activity, (9) lipid transport and (10) cytoskeleton integrity.

Table 3.2. Proteins differentially predominant in both 70M30T vs 50M50G and 35M35G30T vs 50M50G sol-gel coating comparatives (Progenesis method), ANOVA (p-value < 0.05). DAVID classification functions were (1) inflammatory/immune response, (2) hydroxylation, (3) blood coagulation, (4) apoptosis regulation, (5) metal binding, (6) phosphorylation, (7) carbohydrate binding, (8) peptidase activity, (9) lipid transport and (10) cytoskeleton integrity.

Table 3.3. Proteins differentially predominant in both 70M30T vs 50V50G and 35M35G30T vs 50V50G sol-gel coating comparatives (Progenesis method), ANOVA (p-value < 0.05). DAVID

classification functions were (1) inflammatory/immune response, (2) hydroxylation, (3) blood coagulation, (4) apoptosis regulation, (5) metal binding, (6) phosphorylation, (7) carbohydrate binding, (8) peptidase activity, (9) lipid transport and (10) cytoskeleton integrity.

Table 3.4. Proteins differentially predominant at the same time in both 50M50G and 50V50G respect to 35M35G30T and 70M30T sol-gel coatings (Progenesis method). ANOVA (p-value < 0.05).

Table 3.5. Inhibitory/activator protein ratio detected in 70M30T. 35M35G30T. 50M50G and 50V50G biomaterials.

Chapter 3

Table 4.1. Plasma proteins adsorbed on SAE-Ti and Smooth Ti as identified by LC-MS/MS. Spectral counts indicates number of MS/MS spectra obtained for each protein.

Table 4.2. Specific proteins (Progenesis method).

Chapter 4

Table 5.1. Progenesis analysis of proteins differentially attached to SAE-Ti.

Table 5.2. Progenesis analysis of proteins differentially attached to silica sol-gel coating.

Chapter 5

Table 6.1. Chemical compositions of Sr-doped coatings expressed as $SrCl_2$ weight percentage.

Table 6.2. Progenesis comparative analysis of proteins differentially more adsorbed onto Sr-enriched coatings (025Sr, 05Sr, 1Sr and 1.5Sr) respect 35M35G30T base material (0Sr). Detected proteins with ANOVA p < 0.05 and a ratio higher than 1.3 in either direction were considered as significantly different (*).

Table 6.3. Progenesis comparative analysis of proteins differentially less adsorbed onto Sr-enriched coatings (025Sr, 05Sr, 1Sr and 1.5Sr) respect 35M35G30T base material (0Sr). Detected proteins with ANOVA p < 0.05 and a ratio higher than 1.3 in either direction were considered as significantly different (*).

Chapter 6

Table 7.1. Chemical compositions of Ca-enriched materials expressed as $CaCl_2$ weight percentage.

Table 7.2. Progenesis comparative analysis of proteins differentially more adsorbed onto Ca-enriched coatings (05Ca, 1Ca, 2.5Ca, 5Ca and 7.5Ca) respect 35M35G30T base material (0Ca). Detected proteins with ANOVA $p < 0.05$ and a ratio higher than 1.3 in either direction were considered as significantly different (*).

Table 7.3. Progenesis comparative analysis of proteins differentially less adsorbed onto Ca-enriched coatings (05Ca, 1Ca, 2.5Ca, 5Ca and 7.5Ca) respect 35M35G30T base material (0Ca). Detected proteins with ANOVA $p < 0.05$ and a ratio higher than 1.3 in either direction were considered as significantly different (*).